Characterization of the fatty acid beta-oxidation system in *Debaryomyces hansenii*

Selva Turkolmez, MSc Biotechnology

This thesis is submitted to the University of Sheffield for the degree of Doctor of Philosophy

The University Of Sheffield.

Faculty of Science

Department of Biosciences

Cluster of Molecular and Cellular Biology

September 2022

Abstract

Production of fatty acids for industry has started shifting from petrochemical production to sustainable production which relies on genetic engineering of micro-organisms. However, sustainable lipid production is still not highly-efficient. Some organisms with potential to produce high levels of lipid derived compounds are pathogenic or difficult to culture. Safe organisms that are amenable to metabolic engineering such as *Saccharomyces cerevisiae* only produce low level of fatty acids. In order to overcome this drawback, more advanced techniques are required to increase the lipid production at higher yield, as well as finding new microorganisms that could offer as a better host. *Debaryomyces hansenii* has been recently attracting the attention of biotechnologists for many aspects, but the most importantly by being a highly oleaginous yeast, which can store naturally very high amount of lipids compared to other yeasts. However, since it has been neglected in the past, very little is known about this organism. In addition, the molecular biology and genetics tools are very scarce for this organism.

In this study, we first aimed to develop a genetic toolbox to study with *D. hansenii*, that includes development of different selectable markers for single and multiple gene deletions and creating different fluorescent markers to tag proteins. Secondly, we tried to understand how the fatty acids are degraded via peroxisomal beta-oxidation pathway in *D. hansenii*, so that this pathway could be blocked to accumulate fatty acids.

Hydroxy acyl-CoA esters accumulate in *Saccharomyces cerevisiae* upon lowering NAD^+ availability inside peroxisomes that is required for the beta-oxidation. This was previously achieved through the simultaneous disruption of two redox shuttles that regenerate NAD^+. In this study, we investigated the contribution of the same two shuttles in *D. hansenii*. In contrast to what was observed in *S. cerevisiae*, disruption of the redox shuttles did not severely affect cells' ability to grow on a fatty acid-based medium and to breakdown fatty acids through beta-oxidation. This observation led us to investigate alternative routes for providing NAD^+ for beta-oxidation in *D. hansenii*. We identified Pmp47 in *D. hansenii*, which is not present in *S. cerevisiae*. Its further characterization suggested that this protein is a potential peroxisomal NAD^+ transporter, which is also playing a role in beta-oxidation in *D. hansenii*.

Acknowledgements

Firstly, I would like to express my utmost gratitude to my supervisor Dr Ewald Hettema, for all his support, guidance, help, care, encouragement and patience throughout this journey. He has been always the most caring supervisor and a friend of us. I also would like to thank him for introducing me to his other colleagues from outside the university for collaborating, which helped me to extend my scientific network and also for giving me the responsibility to order the lab equipment and reagents after he retired, which has been a massive experience for my future career even if it is sometimes overwhelming. My second sincere gratitude goes to Dr Donald Watts, who has always shared his invaluable experience and suggestions with me, helped me to sort out technical problems, always supported me and reassured me when things were going wrong.

I would also like to thank the former E28 Lab members Dr Lakhan Ekal, Dr Georgia Hulmes and Dr Vijayendran Raghavendran for all their help, teaching, support and patience during my first and second years of the PhD. Special thanks to Eleanor Stiles who helped me with my research by handling some of D. hansenii experiments as her final year project, as well as her friendship. I would also like to thank all the current E28 Lab members Sondos Alhajouj, Quentin Levicky, Tarad Abalkhail, Abdulaziz Alqahtani, Ibrahim Sumaily, Nourah Nayef, Yousef Alhammad and Afroza Begum for all their friendship, help, suggestions, chat and patience.

Special thanks to Dr Carlo van Roermund and all his lab members in Amsterdam, especially Serhii Chornyi, for their invaluable help in the beta-oxidation activity measurements of this study, as well as great advices, brainstorming and collaboration on our upcoming paper.

I would also like to express my deepest gratitude to my family members including Haluk Turkolmez, Peris Mehvar Turkolmez, Soner Turkolmez, Esin Capa Turkolmez, my other beloved relatives as well as my life partner Mohamed Bill Tibourtine for their unconditional love, endless encouragement, support in every possible way, care and patience throughout my entire journey and always. I sincerely would not have been able to make it until the end without them.

Table of Contents

List of Figures

Chapter 1

Chapter 2

Chapter 3

Chapter 4

Chapter 5

Chapter 6

List of Tables

Abbreviations

°C: degrees Celsius
ABC: ATP-Binding Cassette
ABCD: ATP-Binding Cassette Subfamily D
ACT1: Actin 1
ALD: Adrenoleukodystrophy
AMP: Adenosine Monophosphate
ARG1: Argininosuccinate synthetase
A. oryzae: *Aspergillus oryzae*
A. thaliana: *Arabidopsis thaliana*
ATP: Adenosine Triphosphate
bp: base pair
C. boidinii (*Cb*): *Candida boidinii*
C-terminal: Carboxyl-Terminal
CoA: Coenzyme A
D. hansenii (*Dh*): *Debaryomyces hansenii*
DHAP: Dihydroxyacetone Phosphate
DNA: Deoxyribonucleic Acid
dNTP: Deoxynucleotide Triphosphate
DTT: Dithiothreitol
E.coli: *Escherichia coli*
ECL: Enhanced Chemiluminescence
EDTA: Ethylenediaminetetraacetic acid
ER: Endoplasmic Reticulum
FA: Fatty Acid
FAAs: Fatty Acid Activators
FAD: Flavin Adenine Dinucleotide
$(Gly\text{-}Ala)_3$ linker (or alternatively GAGAGA linker): Glycine-Alanine-Glycine-Alanine-Glycine-Alanine linker
GET: Guided Entry of Tail-Anchors
GFP: Green Fluorescent Protein
G3P: Glycerol-3-Phosphate
Gpd1: Glyercol-3-Phosphate Dehydrogenase 1
H. polymorphae: *Hansenula polymorpha*
H_2O_2: Hydrogen Peroxide
kb: kilobase
KO: knock-out
Kpi: Potassium Phosphate
kV: kilo Volts
Leu: Leucine
LiAc: Lithium Acetate
Lys: Lysine
Inp1: Inheritance of Peroxisomes 1
M: molar
MCS: Multiple Cloning Site
Mdh3: Malate Dehydrogenase 3
M. guilliermondii (*Mg*): *Meyerozyma guilliermondii*
min: minutes
ml: milliliter
mM: millimolar
mPTS: Peroxisomal Membrane Protein Targeting Signal
mRFP: Monomeric red fluorescent protein
N-terminal: Amino-terminal
NAD: *Nicotinamide Adenine Dinucleotide*
NADH: Nicotinamide Adenine Dinucleotide (NAD) + Hydrogen (H)
NCYC: National Culture of Yeast Collection
ng: nanograms

nt: nucleotide
OAF1: Oleate-Activated Transcription Factor 1
OD_{600}: Optical density at 600 nm
ORF: Open reading frame
OAA: Oxaloacetate
PCR: Polymerase chain reaction
PEG: Polyethylene Glycol
Pex: Peroxin Protein
pexΔ: peroxin mutant
PGK1: Phospho Glycerate Kinase 1
PIP2: Peroxisome Induction Pathway 2
pLDH: Peroxisomal Lactate Dehydrogenase
P-L-H-S-K-L: Proline-Leucine-Histidine-Serine-Lysine-Leucine
PMP: Peroxisomal Membrane Protein
Pnc1: Pyrazinamidase/Nicotinamidase 1
PTS: Peroxisome Targeting Signal
PTS1: Peroxisomal Targeting Signal Type 1
PTS2: Peroxisomal Targeting Signal Type 2
rpm: Revolutions Per Minute
rcf: Relative Centrifugal Force
S. cerevisiae (*Sc*): *Saccharomyces cerevisiae*
SDS: Sodium Dodecyl Sulphate
SDS-PAGE: Sodium Dodecyl Sulphate-Polyacrylamide Gel Electroporesis
SLC25: Solute Carrier Family 25
ssDNA: Single-Stranded DNA
S. stipitis (*Ss*): *Schefferomyces stipitis*
TCA: Trichloroacetic Acid
TE: Tris-EDTA
TEF1: Translation Elongation Factor 1
TEMED: N, N, N-Tetramethylethlenediamine
TFs: Transcription Factors
TPI1: Triose-Phosphate Isomerase 1
U. maydis (*Um*): *Ustilago maydis*
UMC: University Medical Centers
Ura: Uracil
UV: Ultraviolet
v/v: volume per volume
w/v: weight per volume
WT: Wild-type
Y. lipolytica: Yarrowia lipolytica
YM1: Yeast Minimal Medium 1
YM2 - Yeast Minimal Medium 2
α: alpha
Δ: delta
µg: microgram
µl: microliter
µm: micrometer
µM: micromolar
~: approximately

Chapter 1- Introduction

1.1-Peroxisomes

1.1.1- Peroxisomes: Definition, history and functions

Peroxisomes are small, single membrane-bound organelles present in almost every eukaryote including animals, humans, plants, fungi and protozoa (Schulz, 1996). They were identified for the first time by a PhD student J. Rhodin in 1954, in mouse kidney cells by electron microscopy (Rhodin, 1954; reviewed in Schrader and Fahimi, 2008) and named as microbodies because of the lack of knowledge in subcellular organelles (Reviewed in van den Bosch *et al.*, 1992). Later on, De Duve *et al.* biochemically characterised the same organelle isolated from the rat liver, which revealed the presence of some enzymes in the matrix such as H_2O_2-forming oxidases and the H_2O_2-degrading enzyme catalase. As a result of their studies, the name microbodies was changed to peroxisomes (Baudhuin, Beaufay and De Duve, 1965; De Duve and Baudhuin, 1966; reviewed in Schrader and Fahimi, 2008).

The earlier studies showed that peroxisomes are DNA-free organelles (Leighton *et al.*, 1968; Douglass, Criddle and Breidenbach, 1973; Kamiryo *et al.*, 1982) with diameter of 0.1 to 1 µm. (De Duve, 1983; reviewed in van den Bosch *et al.*, 1992). These organelles contain various enzymes for multiple important biochemical pathways, whose number can change based on different conditions (Reviewed in van den Bosch *et al.*, 1992). In humans, the disruption of peroxisome biogenesis or some peroxisomal proteins lead to various severe diseases (Reviewed in Fujiki, 1997; reviewed in Schrader and Fahimi, 2008; reviewed in Thoms, Gronborg and Gartner, 2009). It was also claimed that the peroxisomes were the densest organelles by having the highest protein concentration compared to other organelles (De Duve and Baudhuin, 1966).

The most common biochemical events that take place in peroxisomes are the degradation of fatty acids via beta-oxidation and detoxification of hydrogen peroxide that was formed during beta-oxidation. Lysine metabolism, the glyoxylate cycle (Reviewed in Sibirny, 2016) as well as the metabolism of purines, alkanes and methanol in fungi (Reviewed in Bartoszewska *et al.*, 2011) also take place in peroxisomes. Peroxisomes also play a role in the formation of ether lipids in mammals (Hajra, Burke and Jones, 1979). On the other hand, it was reported that peroxisomes are also involved in other rare metabolic events in some plants and fungi. For example, in some filamentous fungi, the synthesis of some secondary metabolites such as penicillin occurs in peroxisomes (Reviewed in Bartoszewska *et al.*, 2011). Moreover, in some filamentous fungi, the formation of specialised peroxisomes called Woronin bodies was identified (Jedd and Chua, 2000). Woronin bodies reportedly plug the septal pores in case of a hyphal injury, hence prevent the cytoplasmic leakage (Reviewed in Jedd, 2011). In some fungi and plants, one step of biotin biosynthesis was also associated with the peroxisomes (Tanabe *et al.*, 2011). Additionally, it was reported that glycolysis in kinetoplastida takes place in peroxisomes (Reviewed in Opperdoes, 1987; Hannaert and Michels, 1994; Michels, Hannert and Bringaud, 2000).

The proteins that are responsible for peroxisome biogenesis are called peroxins (PEX) (Reviewed in Kim and Hettema, 2015). There are many different PEX proteins that are conserved amongst

different species. They are involved in peroxisome formation, proliferation, peroxisomal matrix and membrane protein import (Reviewed in Kiel, Veenhuis and van der Klei, 2006).

1.1.2- Formation of the peroxisomes

There have been different ideas about how peroxisomes form. The current consensus is that peroxisomes form by growth and division, in which the Endoplasmic Reticulum (ER) is thought to supply membrane lipids. However, they can also form *de novo* under some certain conditions (Reviewed in Islinger and Schrader, 2011), such as when peroxisome biogenesis mutants are complemented with the WT copy of the correspondent protein (South and Gould, 1999; Hoepfner *et al.*, 2005).

Three peroxins, that are Pex3, Pex16 and Pex19, were found to play a very important role in peroxisome biogenesis (in *S. cerevisiae*, Pex16 was not detected) (Hettema at al., 2000; van der Zand, Braakman and Tabak, 2010). They play a role in formation of the peroxisomal membrane. Earlier studies reported that the absence of these proteins leads to cells being deficient in the functional peroxisomal membranes, hence lacking functional peroxisomes. They also reported that in the peroxisomal biogenesis factor mutants, some PMPs mislocalize to the cytosol and broken down, whereas others may end up in other organelles such as ER (Hohfeld, Veenhuis and Kunau, 1991; Gotte *et al.*, 1998; Matsuzono *et al.*, 1999; Hettema at al., 2000; reviewed in Kunau, 2005; van der Zand, Braakman and Tabak, 2010). However, this has been updated with more recent study which revealed that in peroxisome biogenesis factor deficient *pex3Δ* cells, some peroxisomal membrane proteins can actually localize in pre-peroxisomal membrane structures (Wroblewska *et al.*, 2017).

1.2- The import of peroxisomal proteins

1.2.1- The import of peroxisomal matrix proteins

The mRNAs encoding the peroxisomal matrix proteins are synthesised by free polyribosomes (Reviewed in Lazarow and Fujiki, 1985). The proteins are folded in the cytosol and undergo post-translational modifications before being imported into the peroxisomes (Reviewed in Leon *et al.*, 2006).

Most of the peroxisomal matrix proteins are identified and recognised by distinct few amino acid long tags, that are Peroxisomal Targeting Signal (PTS) (Gould, Keller and Subramani, 1987). There are 2 types of PTSs, which are Peroxisomal Targeting Signal Type 1 (PTS1) and Peroxisomal Targeting Signal Type 2 (PTS2). The PTS1 is located at the Carboxy-terminus (C-terminus) of the protein (Elgersma *et al.*, 1996). It was first discovered in firefly luciferase enzyme (Gould, Keller and Subramani, 1987). The PTS1 consists of 3 amino acids, with the consensus sequence of (S/A/C)-

(K/R/H)-(L/M) (Gould, Keller and Subramani, 1988; Gould *et al.*, 1989). On the other hand, PTS2 is located at the N-terminus of the protein, which was first discovered in Thiolase protein from the rat liver (Swinkels *et al.*, 1991). It consists of 9 amino acids with consensus sequence of (R/K)-(L/V/I/Q)-X-X-(L/V/I/H/Q)-(L/S/G/A/K)-X-(H/Q)-(L/A/F) (Petriv *et al.*, 2004).

The import of peroxisomal matrix proteins first start with the recognition of the PTS1 or PTS2 of the proteins by the receptors in the cytosol (Reviewed in Kim and Hettema, 2014). The proteins with PTS1 are recognised by Pex5 which is a PTS1 receptor (Stanley *et al.*, 2006), and the recognition of the proteins with PTS2 are recognised initially by Pex7 which is a PTS2 receptor (Marzioch *et al.*, 1994; Rehling *et al.*, 1996; Elgersma *et al.*, 1998). However, Pex7 in many organisms, requires the recruitment of different co-receptors. Hence, in humans, both Pex7 and longer isoform of Pex5 (Pex5pL) are required for PTS2-dependent import (Otera *et al.*, 2000; Dodt *et al.*, 2001). In many fungi including *Yarrowia lipolytica* and *Hansenula polymorpha*, Pex20 acts as a co-receptor (Einwachter *et al.*, 2001; Otzen *et al.*, 2005). In *S. cerevisiae*, instead of Pex20, 2 different paralogues Pex18 and Pex21, that are similar to Pex20, act as co-receptors (Purdue, Yang and Lazarow, 1998).

Not all the peroxisomal matrix proteins have distinct targeting signals, hence they do not directly follow PTS1 or PTS2-dependent recognition. In this case, some of the proteins lacking PTSs get imported by piggybacking on other proteins with PTS1 or PTS2 (Reviewed in Kim and Hettema, 2014). One example of such protein is Pyrazinamidase/Nicotinamidase 1 (Pnc1) in *S. cerevisiae*, which converts nicotinamide to nicotine as part of NAD^+ salvage pathway. It does not have PTS1 or PTS2, and gets imported into the peroxisomes by piggybacking on Gpd1 (Effelsberg *et al.*, 2015; Kumar *et al.*, 2016; Al-Saryi *et al.*, 2017b). The other example is Cu/Zn Superoxide Dismutase 1 in mammals, which gets imported by piggybacking on copper chaperone for Superoxide Dismutase (Islinger *et al.*, 2009). Additionally, in *S. cerevisiae*, the exceptional import of protein, that is lacking PTS1 and PTS2, was detected via PTS1-dependent pathway. The beta-oxidation protein Acyl-CoA Oxidase (Pox1), does not have a PTS1 or PTS2. However, an internal recognition site was observed in Pox1, that is recognised via Pex5 which imports the protein into peroxisomes (Klein *et al.*, 2002).

Most of the matrix proteins are imported into the peroxisomes via either the PTS1 or PTS2-dependent import pathway (Figure 1.1). Once the receptors recognise the PTS1 or PTS2 in the cytosol, the complex dock onto the cargo complex on the peroxisomal membrane. The receptors become part of a transient pore through which cargo proteins are released into the peroxisomal matrix. Then, the PTS1 and PTS2 receptors are recycled back to the cytosol for another round of import (Reviewed in Hettema *et al.*, 2014; reviewed in Kim and Hettema, 2015).

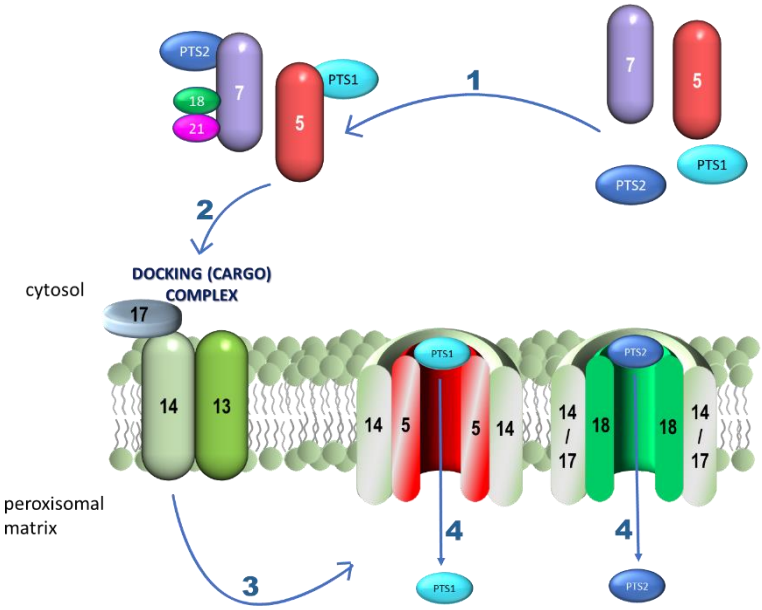

Figure 1.1: The import of peroxisomal matrix proteins via the PTS1 and PTS2-dependent pathway in yeast, as described in Mortilla-Martinez *et al.* (2015). 1) Firstly, proteins with a PTS1 or PTS2 (labelled with dark and light blue colour, respectively) are recognised in the cytosol, by PTS1 and PTS2 receptors Pex5 and Pex7, respectively. 2) After the recognition, the ''cargo-receptor'' complexes associate with the peroxisomal membrane, by binding to the docking complex. 3) Docking of these complexes leads to the formation of transient pores. 4) Subsequently, PTS1- or PTS2-containing proteins are released into the peroxisomal matrix through this pore. The diagram was adapted from Mortilla-Martinez *et al.* (2015).

1.2.2- The import of PMPs

Most of the peroxisomal matrix proteins get imported into the peroxisomes via PTS1 and PTS2-dependent pathway after recognition of their PTS1 or PTS2 sequences and most of the targeting signals fit into the consensus sequences mentioned in the previous section (Elgersma *et al.*, 1996; Gould *et al.*, 1987; Gould *et al.*, 1988; Gould *et al.*, 1989; Petriv *et al.*, 2004). Thus, these targeting signals can be easily identified by bioinformatics or non-consensus sequences could be predicted based on the similarity to the consensus at either N- or C-termini. However, peroxisomal membrane proteins do not have PTS1 or PTS2 signals, hence their import is not dependent on PTS1 or PTS2-dependent import pathways (Hettema *et al.*, 2000). Besides, there is not a very well defined consensus for targeting signals for peroxisomal membrane proteins (mPTS) (Jones, Morrell and Gould, 2001), that can be used to robustly identify peroxisomal membrane proteins via bioinformatics.

There are 2 different pathways to translocate PMPs into the peroxisomes. In the first pathway, the PMPs are imported directly from the cytosol. The transport starts by the recognition of the

membrane-PTS sequence of PMP (mPTS) by Pex19 (Dyer, McNew and Goodman, 1996). Then, Pex19 brings the membrane protein to the peroxisomal lumen (Jones, Morrell and Gould, 2004), and docks it on Pex3 (Sacksteder *et al.*, 2000; Muntau *et al.*, 2003; Fang *et al.*, 2004) which results in the release of PMP (Reviewed in Kim and Hettema, 2014). In mammals, Pex16 is also involved in the biogenesis and transport of the PMPs, (Honsho *et al.*, 1998; Honsho, Hiroshige and Fujiki, 2002) whose ortholog was not identified in *S. cerevisiae* (Hettema *et al.*, 2000).

The second PMP import pathway takes place during de-novo formation of the peroxisomes from the ER. In this model, PMPs are targeted into the ER either via Sec61 complex (Thoms *et al.*, 2012) with additional Sec62, Sec63, Sec71 and Sec72 (Rapoport, 2007) or via Guided Entry of Tail-anchors (GET) complex, consisting of Get1, Get2 and Get3 (Schuldiner *et al.*, 2008). Then, they are sorted into the pre-mature peroxisomes via Pex19 as a chaperone (van der Zand, Braakman and Tabak, 2010). Both PMP targeting pathways in *S. cerevisiae* could be seen in Figure 1.2.

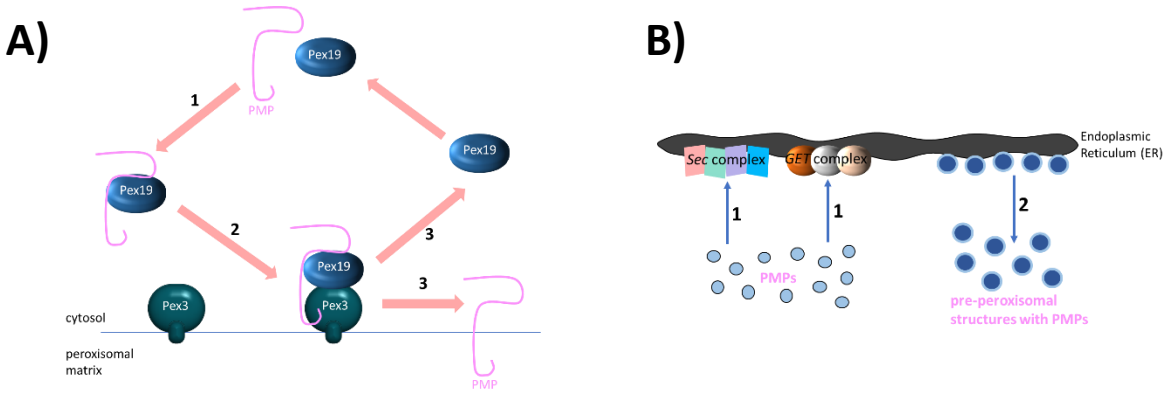

Figure 1.2: The import of PMPs in *S. cerevisiae*. A) The direct import pathway from cytosol. 1) The recognition of PMP by Pex19, followed by binding. 2) The docking of Pex19-bound PMP on Pex3. 3) The insertion of the PMP onto the peroxisomal membrane, followed by the release of Pex19 back to the cytosol. The diagram was adapted from Nuttall *et al.* (2011). B) The import via targeting into ER. 1) The targeting of PMPs into the ER via Sec or GET complex. 2) The formation of pre-peroxisomal structures carrying the PMPs that were targeted in previous step, followed by budding off.

1.3- Beta-oxidation

1.3.1- Beta-oxidation: General Characteristics

In mammals, some algae and some filamentous fungi, fatty acid beta-oxidation occurs in both peroxisomes and mitochondria (Stabenau, Winkler and Saftel, 1984; reviewed in Kunau *et al.*, 1995, reviewed in Wanders and Waterham, 2006; Camoes *et al.*, 2015; reviewed in Kong *et al.*, 2018). In mammals, the beta-oxidation of short chain (C2-C6) and medium chain fatty acids (C8-C14) take place solely in mitochondria and the oxidation of long chain fatty acids (C16-C24) is dominantly mitochondrial. In contrast, very long chain fatty acids (C24 and longer), are first chain-shortened in peroxisomes, which are further oxidised in mitochondria (Reviewed in Hettema and Tabak, 2000; reviewed in Wanders and Waterham, 2006; Wanders *et al.*, 2010). However, in yeast cells, the beta-oxidation pathway is only limited to peroxisomes (Reviewed in Kunau *et al.*, 1995). Hence, yeasts are a good model organisms to understand this process. In *S. cerevisiae*, this pathway is well-characterised and the enzymes involved are known (Reviewed in van Roermund *et al.*, 2003).

Both unsaturated and saturated fatty acids can be processed via beta-oxidation in yeasts (Dommes *et al.*, 1981) in the form of short, medium, long and very long fatty acids (Reviewed in van Roermund *et al.*, 2003). In *S. cerevisiae*, the process is triggered by collaboration of 2 different transcription factors (TFs) that form a heterodimer and start activation of beta-oxidation genes when the cells are grown on long chain fatty acid oleate. These TFs are *PIP2* and *OAF1* (Rottensteiner *et al.* 1996; Karpichev *et al.*, 1997; Karpichev and Small, 1998). After induction of beta-oxidation genes, fatty acids are transported across the peroxisomal membrane and oxidised via a multistep process (Figure 1.4).

1.3.2- Transport and activation of fatty acids before beta-oxidation

Before the fatty acid beta-oxidation starts, fatty acid molecules need to be transported across the peroxisomal membrane and they also need to be activated to Acyl-CoA. Their transport route and activation site depend on their chain length (Figure 1.3). Medium chain fatty acids (MCFA) can move across the peroxisomes as free fatty acids. Once they are in peroxisomes, they get activated to fatty acid-CoA by Faa2 (Hettema *et al.*, 1996). This step requires ATP as a co-factor, which is provided by the peroxisomal Adenine Nucleotide Transporter protein Ant1 (Palmieri *et al.*, 2001), in an exchange of AMP. This protein is a peroxisomal membrane protein that belongs to the mitochondrial carrier family, which transports ATP across the peroxisomes from the cytosol. It was reported that the deletion of *ANT1* has resulted in the disruption in the beta-oxidation of medium chain fatty acids (van Roermund *et al.*, 2001). Additionally, a recent study has revealed that the mitochondrial ATP/ADP exchanger protein Aac2 (Kolarov and Nelson, 1990; Bamber *et al.*, 2007; Klingenberg, 2008) is also localized to peroxisomes in *S. cerevisiae*, and contributes to ATP uptake into peroxisomes (van Roermund *et al.*, 2022). In addition to medium chain fatty acid activator Faa2, other FAAs such as Faa1, Faa3 and Faa4 were identified in *S. cerevisiae* that are acting as Acyl-CoA synthetase (Johnson *et al.*, 1994). The activation of fatty acids inside the peroxisomes requires the presence of peroxisomal CoA (Reviewed in Rottensteiner and Theodoulou, 2006). There are different

examples of CoA provision mechanisms observed in peroxisomes of different organisms. For example, in plants, it was suggested that a plant ortholog of the ABC transporter called Comatose (CTS), (Reviewed in Theodoulou, Holdsworth and Baker, 2006), which is the ortholog of human ALD protein, contributes to CoA uptake into the peroxisomes (Footitt *et al.*, 2002). CTS has thiolytic activity, and this activity is required for function. This suggests that transport of Acyl-CoAs across the peroxisomal membrane by CTS is coupled to cleavage of the fatty acid and CoA thiol bond (De Marcos Lousa *et al.*, 2013). However, these initial studies did not solve the question as to where the cleaved CoA is released. A more recent study revealed that the same mechanism of CoA transport applies to *S. cerevisiae*. It reported that Pxa1/Pxa2 complex imports CoA as part of ''Fatty Acid-CoA'' and similarly to CTS, Pxa1/Pxa2 complex cleaves the thiol bond between the fatty acid moiety and CoA. More importantly, this was the first study to show that after being cleaved off, free CoA is released into the peroxisomal lumen (van Roermund *et al.*, 2021). In humans, a peroxisomal transporter SLC25A17 was reported to be transporting CoA across the peroxisomal membrane (Agrimi *et al.*, 2012b). Similarly, a potential peroxisomal CoA transporter was identified in *Arabidopsis thaliana* (Haferkamp and Schmits-Esser, 2012), which was suggested to be similar to mitochondrial CoA transporter Leu5 in *S. cerevisiae* (Prohl *et al.*, 2001) (Zallot *et al.*, 2013). Taken together, there are different mechanisms that supply peroxisomes with CoA.

Long chain fatty acids are activated in the cytosol (Mannaerts *et al.*, 1982) and then transported across the membrane by Pxa1/Pxa2 complex in *S. cerevisiae*, that belongs to ATP-Binding Cassette (ABC) transporter family (Hettema, *et al.*, 1996). Recent studies revealed that some medium chain fatty acids can be also transported to the peroxisomes via Pxa1/Pxa2 complex (van Roermund *et al.*, 2021). It was reported that Pxa1 and Pxa2 act collaboratively upon forming a heterodimer complex, hence they are half-transporters (Shani and Valle, 1996). In humans, there are 3 different peroxisomal proteins that are responsible for the activation of long and very long chain fatty acids, that belong to ATP binding cassette subfamily D (ABCD proteins). These proteins are reportedly the most similar proteins to Pxa1 and Pxa2 of *S. cerevisiae* (van Roermund *et al.*, 2008). These proteins are Adrenaleukodystrophy protein (ALDp) protein (Mosser *et al.*, 1993), ALD-related protein (ALDR) (Lombard-Platet *et al.*, 1996) and Pmp70 (Kamijo *et al.*, 1990). These are ABCD1, ABCD2 and ABCD3 respectively (van Roermund *et al.*, 2008). Earlier studies claimed that there is an additional membrane protein Pmp69 (Holzinger, Kammerer and Roscher, 1997) that is also ABCD protein. However, later studies revealed that this protein is localized in ER, rather than in peroxisomes (Kashiwayama *et al.*, 2009). The expression of both ABCD1 and ABCD2 in *S. cerevisiae pxa1/pxa2Δ* mutant, either separately or together, resulted in partial complementation of the growth deficiency on oleate as well as the beta-oxidation activity (van Roermund *et al.*, 2008; van Roermund *et al.*, 2011). Similarly to Pxa1 and Pxa2 of *S. cerevisiae*, ALD protein and Pmp70 reportedly form dimers. They reportedly can both homodimerize and heterodimerize (Hillebrand *et al.*, 2007). The dimerization between ALDp and ALDR was also suggested (Genin *et al.*, 2011). Moreover, mutation in the ALD protein results in X-linked Adrenaleukodystrophy (X-ALD) which results in accumulation of very long chain acids and this leads to neurodegeneration (Mosser *et al.*, 1993).

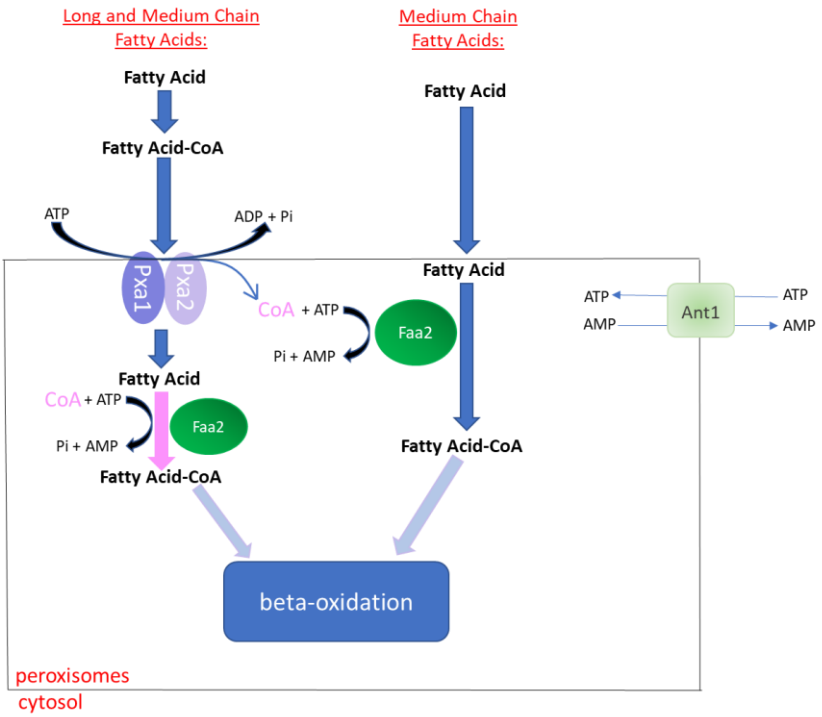

Figure 1.3: The models of transport and activation of long and medium chain fatty acids prior to beta-oxidation in *S. cerevisiae*. Medium chain fatty acids can pass the peroxisomal membrane as free fatty acids. Once they are in peroxisomes, they are activated to ''Fatty Acid-CoA'' via ATP-dependent enzyme Faa2. The ATP is provided by ATP/AMP exchanger protein Ant1. Aac2 was also identified as another ATP transporter (not shown). CoA, that is cleaved during the transport of ''Fatty Acid-CoA'' via Pxa1/Pxa2 complex, is also used by Faa2. Long chain and some medium chain fatty acids are activated to ''Fatty Acid-CoA'' in the cytosol. Activated ''Fatty Acid-CoA'' is then transported into the peroxisomes by Pxa1/Pxa2 complex, which hydrolyses ATP. During this transport, CoA is cleaved from the fatty acid and released into the peroxisomes as free CoA molecule. Then, fatty acid is ligated with CoA again within the peroxisomes by Faa2 (or another acyl-CoA synthase Fat1, not shown). Fatty acid-CoA is then ready for the beta-oxidation. The diagram was adapted from Hiltunen *et al.* (2003) and van Roermund *et al.* (2021).

1.3.3- The classical peroxisomal beta-oxidation pathway

After the fatty acid molecules are transported into the peroxisomes and activated to Acyl-CoA (fatty acid-CoA), beta-oxidation starts by the conversion of Acyl-CoA to Enoyl-CoA (Figure 1.4) by Acyl-CoA oxidase (Fox1 or Pox1 in yeast) (Kamiryo and Okazaki, 1984; Dmochowska *et al.*, 1990). This step requires FAD^+ as a cofactor (Reviewed in Rottensteiner and Theodoulou, 2006) and in *Yarrowia lipolytica*, FAD^+ reportedly gets imported into the peroxisomes by binding to Acyl-CoA oxidase enzyme in the cytosol (Titorenko *et al.*, 2002). There are 5 different Pox1 enzymes identified in *Y. lipolytica* and each enzyme is involved in the degradation of fatty acids with different chain lengths (Wang *et al.*, 1999a; Wang *et al.*, 1999b), whereas in *S. cerevisiae*, there is only one Pox1 which involves in the degradation of long, medium and short chain fatty acids (Reviewed in Hiltunen *et al.*, 2003; reviewed in van Roermund, *et al.*, 2003). The conversion of Acyl-CoA to Enoyl-CoA results in

the generation of hydrogen peroxide (H_2O_2) which is a harmful reactive oxygen species molecule. Hence, the hydrogen peroxide is converted to oxygen and water by peroxisomal Catalase 1 (Cta1) enzyme (Cohen, Rapatz and Ruis, 1988; reviewed in Jamieson, 1998).

The first step of beta-oxidation is followed the conversion of Enoyl-CoA to 3-Hydroxyacyl-CoA by bi-functional enzyme Enoyl-CoA Hydratase (Fox2 in yeast). Afterwards, 3-Hydroxyacyl-CoA is converted to 3-Ketoacyl-CoA by Fox2 again (Figure 1.4) that acts as an NAD^+ dependent 3-hydroxyacyl-CoA Dehydrogenase at this step (Hiltunen, *et al.*, 1992; reviewed in Hettema and Tabak, 2000; reviewed in Hiltunen *et al.*, 2003). However, it was discovered that the peroxisomal membrane is impermeable to NAD(H). In this case, peroxisomes require shuttles to generate NAD^+ and NADH molecules in and out of the peroxisomes (van Roermund *et al.*, 1995), which will be described further in Section 1.4.5. Alternatively, in some organisms such as plants, the NAD^+ could be transported across peroxisomes via the transporter protein located at the peroxisomal membrane (Agrimi *et al.*, 2012a; Agrimi *et al.*, 2012b; van Roermund *et al.*, 2016) which will be discussed further in Section 1.4.6.

At the final step of the beta-oxidation, the formed 3-Ketoacyl-CoA is cleaved by 3-Ketoacyl-CoA Thiolase (Fox3p/Pox3/Pot1 in yeast) which results in formation of Acetyl-CoA and C2-shortened Acyl-CoA (Igual *et al.*, 1991; reviewed in van Roermund *et al.*, 2003).

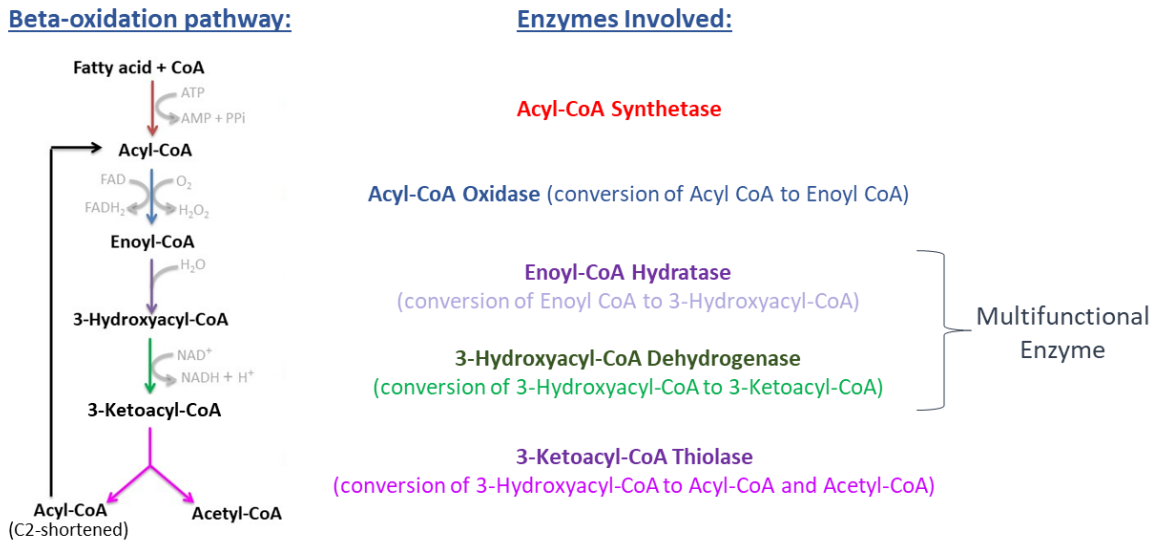

Figure 1.4: The classical peroxisomal beta-oxidation pathway with the involving enzymes at each step. After the activation of both medium chain and long chain fatty acids (in peroxisomes and in cytosol respectively) to Acyl-CoA, it is processed further via beta-oxidation pathway as shown in the figure, by corresponding enzymes. In *S. cerevisiae*, Acyl-CoA oxidase is called Pox1 (alternatively Fox1), Multifunctional Enzyme is called Fox2 and 3-Ketoacyl-CoA thiolase is called Fox3 (or alternatively Pox3 or Pot1). The diagram was adapted from Hiltunen *et al.* (2003).

1.3.4- The export of Acetyl-CoA at the end of peroxisomal beta-oxidation (based on studies in *S. cerevisiae*)

After the beta-oxidation is completed, Acetyl-CoA, which is the end product of fatty acid beta-oxidation, can be exported via 2 different shuttles in yeast (Figure 1.6), because the peroxisomal membrane is not permeable to Acetyl-CoA (van Roermund *et al.*, 1995). The first possible way is called Acetylcarnitine shuttle, which is catalysed by Carnitine Acetyltransferase (Cat2) enzyme (van Roermund *et al.*, 1995). It was discovered that Cat2 has both peroxisomal and mitochondrial targeting signal, therefore is dual localised in both peroxisomes and mitochondria (Elgersma *et al.*, 1995). In the Acetylcarnitine shuttle, Acetyl-CoA is converted to Acetyl-carnitine by peroxisomal Cat2. Acetyl-carnitine then enters the cytosol and is imported into mitochondria by mitochondrial membrane protein Carnitine Acylcarnitine Translocase (Crc1) (van Roermund *et al.*, 1999). Once in mitochondria, Acetyl-carnitine is then converted back to Acetyl-CoA by mitochondrial Cat2 (in the opposite way as what happens in the peroxisomes). Acetyl-CoA is used in the Krebs cycle (Reviewed in Hiltunen *et al.*, 2003).

The disruption of *CAT2* alone did not result in the disruption of the beta-oxidation, which suggested that there might be alternative way in which Acetyl-CoA leaves the peroxisomes (Elgersma *et al.*, 1995). This is indeed due to the presence of a second way via the glyoxylate cycle (Duntze *et al.*, 1969) (Figure 1.5), in which Citrate Synthase and Malate Synthase Mls1 (Hartig *et al.*, 1992) use Acetyl-CoA as substrate. The glyoxylate cycle starts by the conversion of Acetyl-CoA + Oxaloacetate to Citrate (van Roermund *et al.*, 1995), by the peroxisomal Citrate Synthase Cit2 (Lewin, Hines and Small, 1990). Citrate is then exported to the cytosol, converted to isocitrate by Aconitase (van Roermund *et al.*, 1995). Isocitrate in cytosol is converted to Succinate and Glyoxylate by Isocitrate Lysase Icl1 (Fernandez, Moreno and Rodicio, 1992; van Roermund *et al.*, 1995). Succinate then migrates to the mitochondria and goes into the Krebs cycle, whereas glyoxylate moves back to the peroxisomes and together with the Acetyl-CoA as a substrate, and it is converted to malate (Reviewed in Hettema and Tabak, 2000) by Malate Synthase Mls1 (Hartig *et al.*, 1992). Mls1 is located in peroxisomes upon the oleate induction (Kunze *et al.*, 2002).

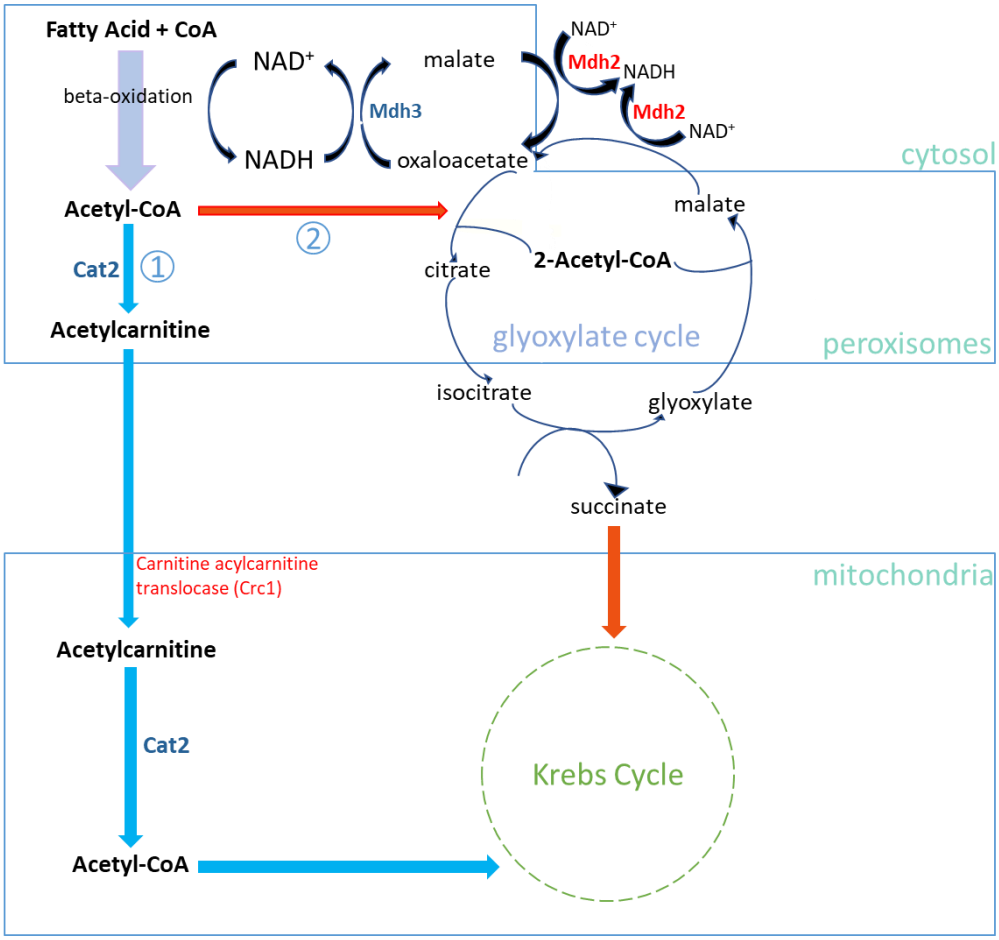

Figure 1.5: The export of Acetyl-CoA from peroxisomes in yeast via Acetylcarnitine shuttle (shown as pathway ''1'' on the figure with blue arrows) and glyoxylate cycle (shown as pathway ''2'' on the figure with orange arrows). Cat2: Catalase 2, Mdh2: cytosolic Malate Dehydrogenase 2, Mdh3: peroxisomal Malate Dehydrogenase 3. The figure was adapted from van Roermund *et al.* (1995) and Gabriel *et al.* (2014).

1.4- Different redox shuttles that are involved in the regeneration of NAD^+ for beta-oxidation

The beta-oxidation is an NAD^+-dependent process and hence requires the reduction of NAD^+ to NADH during the third step (Reviewed in Elgersma and Tabak, 1996). However, as mentioned above, the peroxisomal membrane is impermeable to NAD(H) (van Roermund *et al.*, 1995) hence the requirement for shuttles to circulate NAD^+ and NADH molecules in and out of the peroxisomes (Reviewed in Hiltunen *et al.*, 2003).

One shuttle which helps the maintenance of NAD^+/NADH balance in yeast peroxisomes is malate-oxaloacetate Shuttle (Figure 1.6A) which is catalysed by Malate Dehydrogenases 3 and 2 (Mdh3 and Mdh2). In the peroxisomes, oxaloacetate is converted to malate by peroxisomal Mdh3, which regenerates NAD^+ from NADH (Reviewed in van Roermund *et al.*, 2003). This NAD^+ generated from this step is then used in the third step of the beta-oxidation. After the conversion of oxaloacetate to

malate, it moves to the cytosol, where it is converted back to oxaloacetate by cytosolic Mdh2 (Minard and McAlister-Henn, 1991), and malate moves into the peroxisomes for the next rounds of the malate-oxaloacetate shuttle (Reviewed in Hettema and Tabak, 2000).

Supporting evidence to the malate-oxaloacetate shuttle in yeast is that Mdh3 is localized in the peroxisomes, and the disruption of *MDH3* results in remarkably impaired growth of oleate in *S. cerevisiae* as well as the accumulation of 3-Hydroxyacyl-CoA (van Roermund *et al.*, 1995). The similar case was detected in *Arabidopsis thaliana*, in which the disruption of peroxisomal Malate Dehydrogenase gene *PMDH* resulted in beta-oxidation defect (Pracharoenwattana, Cornah and Smith, 2007). Early studies suggested that in contrast to *S. cerevisiae* and *A. thaliana*, peroxisomal Malate Dehydrogenase is not found in mammals including humans, which suggested that malate-oxaloacetate shuttle does not maintain the peroxisomal NAD^+/NADH redox balance mammalians (Reviewed in McGroarty and Tolbert, 1973; Gee *et al.*, 1974). However, further studies revealed that there is a peroxisomal Malate Dehydrogenase in mice (Wiese *et al.*, 2007), as well as in humans (Gronemeyer *et al.*, 2013). It was also found that human Malate Dehydrogenase is targeted to the peroxisomes by a PTS1, that is created as a result of an C-terminal extension of the protein as a consequence of translational readthrough (Hofhuis *et al.*, 2016). As translational readthrough is not efficient, the same gene can encode for both Mdh with and Mdh without PTS1, thereby achieving dual localisation of this protein. Even though it has not been demonstrated yet, the detection of peroxisomal Malate Dehydrogenase suggested that malate-oxaloacetate shuttle might also take place in mammals (Reviewed by Chornyi *et al.*, 2021).

There is an additional malate-aspartate shuttle similar to malate-oxaloacetate shuttle, which supposedly circulates the NAD^+ in between the cytosol and mitochondria (Figure 1.6C). In this shuttle, after the conversion of oxaloacetate to malate in cytosol by cytosolic Malate Dehydrogenase, malate moves into the mitochondria where it is converted back to oxaloacetate. Since the mitochondrial membrane is impermeable to oxaloacetate, the oxaloacetate that was generated previously is converted to aspartate by Aspartate Aminotransferase enzyme (Aat). During this event, α-ketoglutarate is also converted to glutamate. Newly-generated aspartate then moves to the cytosol and it is converted to oxaloacetate by cytosolic Aat, in which case the reaction proceeds towards the opposite direction as previous step (Reviewed in Visser *et al.*, 2007). There is an evidence that such shuttle operates also for peroxisomes in some plants (Mettler and Beevers, 1980) and yeast (Verleur *et al.*, 1997). The studies of Verleur *et al.* (1997) investigated whether such shuttle is present in the yeast peroxisomes as well. By using *S. cerevisiae*, they identified an Aspartate Aminotransferase (Aat2) with a PTS1 showed that Aat2 is localised in peroxisomes. However, the disruption of *AAT2* did not result in growth defect on oleate and the beta-oxidation activity did not decrease in *aat2Δ* cells. Their findings suggest that even if there is a malate-aspartate shuttle in peroxisomes, the NAD^+ generated during this shuttle is not necessarily required for the beta-oxidation in *S. cerevisiae* (Verleur *et al.*, 1997).

Apart from the previous shuttles mentioned above, NAD^+ can also be regenerated in peroxisomes by Glycerol-3-Phosphate shuttle (Figure 1.6B), which is facilitated by Glycerol-3-Phosphate Dehydrogenase 1 and 2 (Gpd1 and Gpd2). In this shuttle, the conversion of Dihydroxyacetone Phosphate (DHAP) to Glycerol-3-Phosphate (G3P) by Gpd1 generates NAD^+. G3P then moves to cytosol and the opposite reaction as previous step takes place, which is mediated by both Gpd1 and Gpd2 (Al-Saryi *et al.*, 2017a). Earlier in *S. cerevisiae*, the Gpd1 was identified which localises in both peroxisomes and cytosol. Hence, it was hypothesised that this shuttle contributes to the NAD^+ regeneration which is used in peroxisomal beta-oxidation (Valadi *et al.*, 2004; Jung *et al.*, 2010). Further studies showed that disruption of *GPD1* in *S. cerevisiae* resulted in slight growth defect on

oleate as well as slight reduction in the beta-oxidation activity compared to when *MDH3* was disrupted. The disruption of both *MDH3* and *GPD1* resulted in further reduction in growth on oleate and beta-oxidation which was an additive effect. These results suggested that in *S. cerevisiae*, the peroxisomal Glycerol-3-Phosphate shuttle is contributing to the regeneration of NAD^+ for the beta-oxidation, although it does not seem to be as much as Malate-Oxaloacetate shuttle mediated by Mdh3 (Al-Saryi *et al.*, 2017a). On the other hand, peroxisomal Gpd1 was also detected in mammals (Gee *et al.*, 1974; reviewed in Chornyi *et al.*, 2021). Lastly, in mammals, the lactate shuttle was also suggested, that reportedly contributes to the NAD^+/NADH redox balance in peroxisomes (Baumgart *et al.*, 1996). It was also supported by the detection of peroxisomal Lactate Dehydrogenase (pLDH) in mammals (Baumgart *et al.*, 1996; McClelland *et al.*, 2003; Schueren *et al.*, 2014). In analogy to peroxisomal MDH, peroxisomal LDH is a consequence of translational readthrough (Schueren *et al.*, 2014). The peroxisomal part of the shuttle involves the conversion of pyruvate to lactate by pLDH, which regenerates NAD+ from NADH (Reviewed in Gladden, 2004).

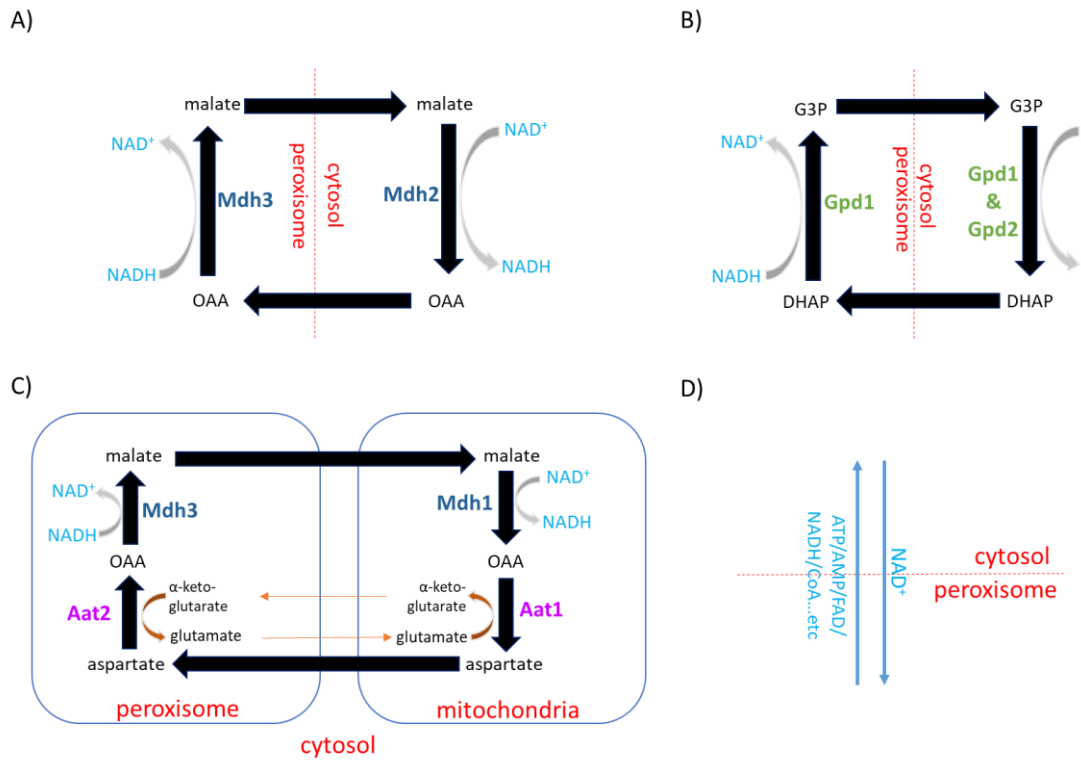

Figure 1.6- Different shuttles (and alternative way) to maintain NAD^+/NADH flux in peroxisomes. A) Malate-Oxaloacetate shuttle. OAA: oxaloacetate, Mdh3: peroxisomal Malate Dehydrogenase, Mdh2: cytosolic Malate Dehydrogenase. B) Glycerol-3-Phophate shuttle. G3P: Glycerol-3-Phosphate, DHAP: Dihydroxyacetone Phosphate, Gpd1: both peroxisomal and cytosolic Glycerol-3-Phosphate Dehydrogenase, Gpd2: cytosolic Glycerol-3-Phosphate Dehydrogenase. C) Malate-Aspartate shuttle. Aat1 and Aat2: Mitochondrial and Peroxisomal Aspartate Aminotransferase respectively. D) Direct transportation of NAD^+ from the cytosol via NAD^+ transporter protein, in an exchange of other co-factors. The diagrams were adapted from Visser *et al.* (2007) and Al-Saryi *et al.* (2017a).

1.5- The direct transport of NAD^+ into peroxisomes via transport mechanism

Apart from the regeneration of NAD^+ in peroxisomes via shuttle mechanisms, there is evidence that some organisms use direct transportation of NAD^+ through the transporter proteins located at the peroxisomal membrane (Figure 1.6D) (van Veldhoven, Just and Mannaerts, 1987; reviewed in Visser *et al.*, 2007). Peroxisomal Membrane Protein 47 from *Candida boidinii* (*C. boidinii*) and its orthologs in some other organisms are one distinct example. *Pmp47* is an integral membrane protein which was first identified in *C. boidinii* (McCammon *et al.*, 1990). It was suggested that this protein has a homology to mitochondrial solute carrier of transporters. Earlier studies revealed the structural similarity between *Pmp47* and other mitochondrial solute carrier proteins (Jank *et al.*, 1993), which is supportive to the idea of *Pmp47* being classified as part of mitochondrial carrier family SLC25 (Nakagawa et al;. 2000; reviewed in Kunji *et al.*, 2020). The ortholog of *Pmp47* is not present in *S. cerevisiae*, but it hypothetically exists in smut fungus *Ustilago maydis* based on bioinformatics research (Camoes *et al.*, 2015).

Earlier study has shown that the heterologous expression of *Pmp47* of *C. boidinii* in *S. cerevisiae* and *Hansenula polymorpha* resulted in peroxisomal membrane localization, especially upon the oleate inducing conditions (McCammon *et al.*, 1990; McCammon *et al.*, 1994; Sulter *et al.*; 1993). A plant ortholog of Pmp47 from *Arabidopsis thaliana*, named as *PXN*, has also been identified and its heterologous expression also led to targeting into the peroxisomes (Bernhardt *et al.*, 2012; van Roermund *et al.*, 2016). Additionally, the pumpkin ortholog Pmp38 was reported to be localised in peroxisomal membrane (Fukao *et al.*, 2001). The human protein SLC25A17 (alternatively Pmp34), that is also part of mitochondrial solute carrier family, was also suggested to be similar to Pmp47 and it also showed peroxisomal localization upon transfection into human and rat cells (Wylin *et al.*, 1998).

Apart from the peroxisomal localization of Pmp47 orthologs in different organisms, there is also evidence that it has a role in the lipid breakdown process (Nakagawa *et al.*, 2000; Fukao *et al.*, 2001). In *C. boinii*, the deletion of *PMP47* resulted in growth defect on middle chain fatty acid laurate-based media (Nakagawa *et al.*, 2000). Additionally, the disruption of *PXN* resulted in beta-oxidation defect and delayed the lipid breakdown in *Arabidopsis thaliana* (Bernhardt *et al.*, 2012). The pumpkin ortholog Pmp38 was also suggested as a candidate beta-oxidation protein (Fukao *et al.*, 2001).

There have been various studies with different opinions about what co-factor Pmp47 is transporting across peroxisomes (Reviewed in Linka and Esser, 2012). Earlier studies suggested that it might be transporting ATP (Nakagawa *et al.*, 2000; Fukao *et al.*, 2001; van Roermund *et al.*, 2001; Visser *et al.*, 2002). This was due to the close similarity between Pmp47 orthologs and mitochondrial solute carrier proteins, especially the ATP transporters (Fukao *et al.*, 2001), as well as some preliminary data related to reconstitution of *Hs*Pmp34 in liposomes (Visser *et al.*, 2002). However, more recent studies suggested that Pmp47 (and its orthologs) is a potential NAD^+ transporter. Linka *et al.* expressed the pumpkin Pmp38 in the *S. cerevisiae ant1Δ* mutant in which the ATP transport was disrupted. However, this expression did not rescue the growth defect of *ant1Δ* cells (Linka *et al.*, 2008). Early studies based on reconstitution of purified PXN into liposomes also suggested that PXN has NAD^+ transport activity (Agrimi *et al.*, 2012a). Additionally, the disruption of the *PXN* caused beta-oxidation deficiency (Bernhardt *et al.*, 2012) and a more recent study has shown that the expression of *PXN* in *S. cerevisiae mdh3Δ* cells (with severely disrupted NAD^+ regeneration in peroxisomes) rescued both growth defect on oleate and beta-oxidation activity. The same study clearly indicates that PXN is transporting NAD^+ in an exchange of AMP (van Roermund *et al.*, 2016).

Earlier *in vitro* studies, in which purified human Pmp34 (SLC25A17) was reconstituted in liposomes followed by transport assays, also suggested that *Hs*Pmp34 has NAD^+ uptake activity, as well as some other co-factors such as CoA and FAD (Agrimi *et al.*, 2012b). However, more recent *in vivo* studies, which focused on zebrafish orthologs of SLC25A17 (that also showed peroxisomal localization), revealed that SLC25A17 proteins of zebrafish are CoA transporters instead of NAD^+ (Kim *et al.*, 2020), which suggests that HsPmp34 might also be a CoA transporter. In this case, HsPmp34 might not be the human equivalent to the other Pmp47 orthologs described above, in terms of its transport activity.

1.6- Lysine biosynthesis in *Saccharomyces cerevisiae*

In *S. cerevisiae*, the lysine biosynthesis occurs via α-aminoadipate pathway (Figure 1.7) (Reviewed in Zabriskie and Jackson, 2000) that is specific to fungi (Reviewed in Xu *et al.*, 2006). It takes place in 3 different places in the cell that are mitochondria, cytosol as well as peroxisomes (Al-Saryi *et al.*, 2017a). It was found that that the genes involved in lysine metabolism are upregulated in peroxisomes deficient cells, which suggested that peroxisomes play role in this process (Breitling *et al.*, 2002).

The last part of lysine biosynthesis, that takes place in peroxisomes in *S. cerevisiae*, is the conversion of Saccharopine to L-lysine, which requires NAD^+ as a co-factor (Saunders and Broquist, 1966). This is achieved by Saccharopine Dehydrogenase (Lys1 in *S. cerevisiae*) (Fujioka and Nakatani, 1970; Al-Saryi *et al.*, 2017a), which is peroxisomal (Yofe *et al.*, 2016) with a targeting signal PTS1 (Al-Saryi *et al.*, 2017a). However, the peroxisomal localization of Lys1 is not essential for the lysine biosynthesis since *pex3Δ* cells, that are lacking peroxisomes, are not showing slow-growth on lysine deficient media (Breitling *et al.*, 2002). Using *S. cerevisiae*, Al-Saryi *et al.* (2017a) have found that the NAD^+ required for the last step of the pathway is provided by the Malate-Oxaloacetate and Glycerol-3-Phosphate shuttles. Hence, the disruption of *MDH3/GPD1* resulted in slow growth on lysine-deficient media as well as remarkable increase of Saccharopine/Lysine ratio. The growth deficiency was restored upon re-expression of Gpd1 in *mdh3/gpd1Δ* cells. In conclusion, besides regenerating NAD^+ for beta-oxidation, the Malate-Oxaloacetate and Glycerol-3-Phosphate shuttles also contribute to the regeneration of NAD^+ for lysine biosynthesis in *S. cerevisiae* (Al-Saryi *et al.*, 2017a).

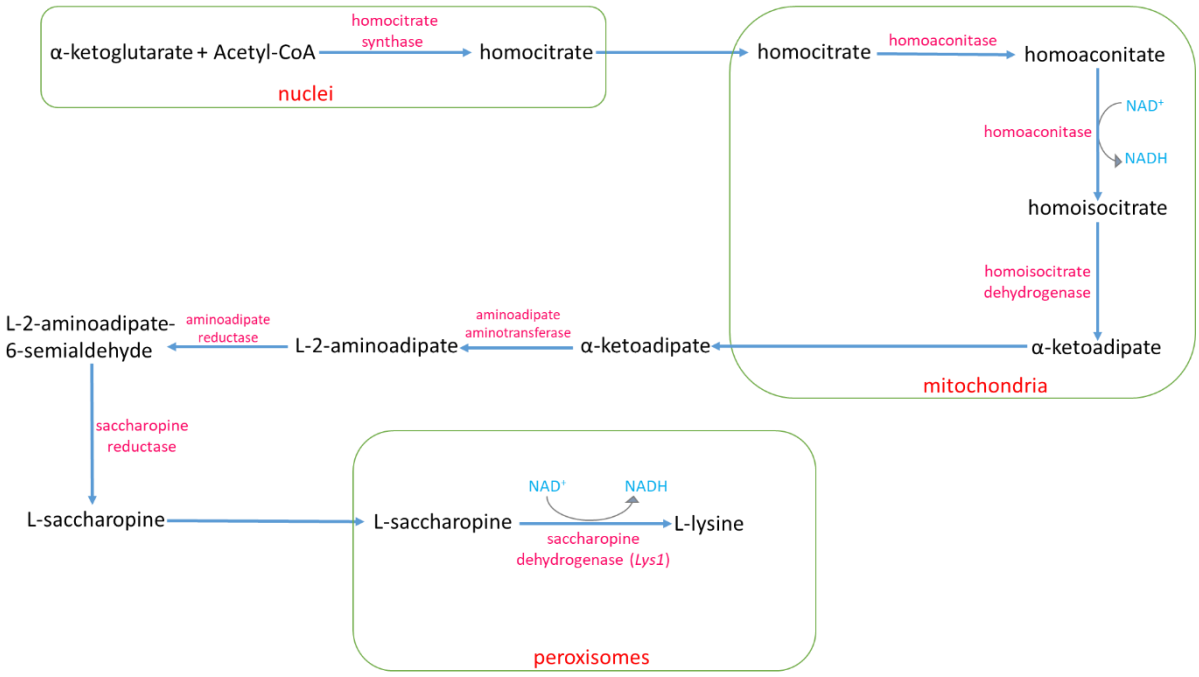

Figure 1.7: L-lysine biosynthesis via the α-aminoadipate pathway. The specific parts of pathway that take place in nucleus, mitochondrion and peroxisome were indicated by green squares. The diagram was adapted from Zabriskie and Jackson (2000) and Al-Saryi *et al.* (2017a).

1.7-*Debaryomyces hansenii* as a rising non-conventional yeast

1.7.1- *Debaryomyces hansenii*- General characteristics

D. hansenii is a non-conventional yeast, which has recently gained interest as a potential a new production host for industrial biotechnology. It is a hemiascomycetes yeast (Reviewed in Breuer and Harms, 2006; reviewed in Prista *et al.*, 2016) that is found in various environments such as marine (Norkrans, 1966), salty food such as sausage (Saldanha-da-Gama, Malfeito-Ferreira and Loureiro, 1997), cheese (Seiler and Busse, 1990) and meat (Dalton, Board and Davenport, 1984). Even though some clinical studies have reported the presence of *D. hansenii* in various human infections (Wagner *et al.*, 2005) (Desnos-Ollivier *et al.*, 2008) (Jain *et al.*, 2021), it has been usually considered as non-pathogenic yeast. It has also been considered as a haploid yeast (Reviewed in Breuer and Harms, 2006), but previous studies challenge this by suggesting that some *D. hansenii* strains can diploidize. Somatogamous autogamy (van der Walt, Taylor and Liebenberg, 1977), in which 2 haploid nuclei fuse together in one cell without the fusion of cytoplasmic content (Breitenbach, Crameri and Lehrer, 2002), conjugation between mother cell and bud (Kreger-Van Rij and Veenhuis, 1975) or mating of 2 different strains (Jacques, Mallet and Casaregola, 2009) have been reported in *D. hansenii* which allows diploidization. However, diploid state is not considered stable and it is thought that random chromosomes are lost when cells become haploid over time (Forrest *et al.*, 1987).

There are many aspects of this organism that attracted the attention of biotechnologists. Firstly, *D. hansenii* is remarkably halotolerant compared to other yeasts including *S. cerevisiae* (Norkrans,

1966; Norkrans, 1968). Two genes were reported that makes *D. hansenii* salt resistance. One of them is called Hal2, that is protecting the cells from high salt stress and playing an important in halotolerance (Aggarwal and Mondal, 2006). It reportedly protects the cells from the toxicity of sodium and lithium ions (Aggarwal, Bansal and Mondal, 2005). The homolog of Hal2 is present in *S. cerevisiae* as well as some other yeasts. However, Hal2 in *D. hansenii* is reported to provide the highest tolerance (Aggarwal and Mondal, 2006). As part of its halotolerance, *D. hansenii* is able to accumulate the osmolytes arabitol (Adler and Gustafsson, 1980) and glycerol to higher levels than *S. cerevisiae*. Moreover, it can also produce xylitol (Parajó, Domínguez and Domínguez, 1995) which is an important chemical for food industry.

Apart from its osmotolerance, *D. hansenii* was reported to be resistant to chemical stress as well as some of the toxins produced by other microorganisms (Reviewed in Breuer and Harms, 2006) and biocides such as chlorine dioxide (Ramírez-Orozco, Hernández-Saavedra and Ochoa, 2001).

1.7.2- The existing biotechnology applications using *Debaryomyces hansenii*

Firstly, *D. hansenii* has already been being used commonly in food biotechnology. It is being used in the ripening of cheese (Bonaiti *et al.*, 2004) and meat products (Cano-García, Belloch and Flores, 2014). Moreover, *D. hansenii* contributes to development of flavour in some cheeses and meats (Ferreira and Viljoen, 2003; Durá, Flores and Toldrá, 2004). Finally, it was suggested that this organism is producing enzymes that can metabolize milk proteins, therefore playing a role in metabolism of milk and milk fat (Reviewed in Breuer and Harms, 2006).

Besides these aspects related to food industry, *D. hansenii* is able to synthesise some chemicals that could have high impact in various areas of biotechnology, especially medical and industrial biotechnology. Firstly, it was discovered that *D. hansenii* was able to produce enzymes with hydrolytic activity, which can be used in industrial biotechnology. For example, the activity of beta-glucosidase (that can degrade cellobiose to glucose, which can be exploited for fuel alcohol production), was examined in some yeast species that belong to *Debaryomyces*, *Pichia*, *Kluyveromyces* and *Candida* genera. The enzymatic activity observed in *D. hansenii* was remarkably lower amongst all other tested strains, but beta-glucosidase enzyme from this organism was able to function without being inhibited by glucose which is limiting factor for beta-glucosidase activity (Saha and Bothast, 1996). Moreover, in another study, xylitol, which has a great usage in food industry as a sweetening, was produced by using *D. hansenii* (Parajó, Domínguez and Domínguez, 1995). Additionally, when glucose is present, ethanol is generated in *D. hansenii* (Gírio *et al.*, 2000). In addition, it was also reported that *D. hansenii* can generate some of the polysaccharides, such as chitin-like glucans that are both soluble and not soluble in alkali. Those molecules have great importance in industrial and medical biotechnology or cosmetics (Reviewed in Breuer and Harms, 2006). Finally, *D. hansenii* has an ability of generating pyruvic acid when thiamine is limiting. Pyruvic acid is another compound that is of great importance to industrial biotechnology, as it is a precursor of pharmaceuticals or agrochemicals used in crop protection (Reviewed in Li, Chen and Lun, 2001).

1.7.3- The aspects of *D. hansenii* that make it a suitable for biotechnology applications as well as molecular and cell biology studies

Whereas *D. hansenii* is being used for a variety of biotechnological applications already, there is scope for it to become a major biotechnological production host in the future. First, its halo and osmotolerance allow it to survive under a range of growth conditions that other organisms cannot tolerate. Furthermore, it displays strong growth on a variety of carbon sources. Therefore, it could be using complex mixtures or even wastes as feedstock for growth. Secondly, its high stress tolerance may give it an advantage over other production hosts during the stressful conditions of manufacturing chemicals. For example, since it is highly tolerant to chemical stress, they can be easily used in research with many chemical agents or stress factors (Reviewed in Breuer and Harms, 2006). On the other hand, *D. hansenii* is also able to produce a toxin that can kill invading species (Marquina *et al.*, 2001). Thus, this organism could be used in medical biotechnology to produce drugs that are killing other pathogens, as well as controlling agents in specific media to destroy unwanted microorganisms (Reviewed in Breuer and Harms, 2006).

On the other hand, *D. hansenii* has one specific characteristic that has is highly promising for biotechnology. It is considered as oleaginous organism, which means that it accumulates high amount of lipids. In fact, the ability to accumulate high amount of lipids is very rare characteristic amongst other yeast species, such that only less than 30 yeast species can do it amongst 600 yeast species (Reviewed in Ratledge, 2002). When those lipids were analysed, it was found out that they are mainly phospholipids or neutral lipids (Merdinger and Devine, 1965). This indicates that *D. hansenii* has metabolic pathways that are related to lipid metabolism, as well as genes that are controlling those pathways (Reviewed in Breuer and Harms, 2006). *D. hansenii* genome also contains the genes necessary for beta-oxidation of fatty acids (Reviewed in Prista *et al.*, 2016). Thus, potentially, beta-oxidation could be genetically modified to accumulate higher amounts of lipids. Pathway engineering of peroxisomal beta-oxidation has been tried with *S. cerevisiae* and those studies reported increased production of fatty acids (Chen, Zhang and Chen, 2014). However, although the presence of lipid accumulation and lipid degradation machinery was reported in *D. hansenii,* pathway engineering of lipids has never been tried in this organism. Thus, regarding all those aspects, if new pathway engineering methods can be developed and can be applied to modification of lipid degradation in *D. hansenii*, it could have great impact in industrial biotechnology.

Apart from being a good candidate in biotechnology to accumulate lipids, *D. hansenii* could serve as a good potential model organism for molecular and cell biology studies in the future. Traditionally, *S. cerevisiae* is used as a model organism to study human diseases or metabolic pathways (Sherman, 1991; Altmann, Durr and Westermann, 2007). This study has revealed that *D. hansenii* shares proteins that are conserved with humans but do not exist in many other yeasts, including *S.cerevisiae*. Hence, *D. hansenii* could serve as a good model organism to study certain aspects of lipid metabolism.

In this respect, *D. hansenii* is similar to the smut fungus Ustilago maydis (*U. maydis)*, which is also considered to be a good model organism because it also has proteins that exist in humans but are not present in many other yeasts (Munsterkotter and Steinberg, 2007; Steinberg and Perez-Martin, 2008), including peroxisomal proteins that are related to lipid metabolism. Homologues to these proteins were also detected in *D. hansenii*.

1.7.4- Potential challenges of working with *D. hansenii*

Although *D. hansenii* could be a good model organism with many useful aspects that can be used in molecular biology and biotechnology, there are few challenges that should be taken into account. Firstly, since this organism has been neglected in the past, there is a lack of fundamental genetic, physiological and biochemical knowledge (Reviewed in Breuer and Harms, 2006). Most importantly, there are limited existing tools for genetic modifications in *D. hansenii* (Reviewed in Prista *et al.*, 2016). Although in recent years, some progress has been attempted to develop useful genetic tools *D. hansenii* such as CRISPR/Cas9 system (Spasskaya *et al.*, 2021) (Strucko *et al.*, 2021) and different markers (Defosse *et al.*, 2018), lots of other tools are still poorly-identified and need to be developed.

Secondly, *D. hansenii* is classified as a CTG-clade organism, which means that it translates the CTG codon (which normally codes leucine) into serine in contrast to most other organisms (Miranda, Silva and Santos, 2006). As a result, many molecular biology applications which require the heterologous gene expression (such as selectable markers, fluorescence protein markers, Cre-recombinase, CRISPR-Cas9…etc) need codon optimization to change CTG codons into other leucine-coding sequences to allow their expression in *D. hansenii*.

Thirdly, studies in our lab involving *D. hansenii*, revealed that there is a variable ploidy in some strains. For example, Sondos Alhajouj found that NCYC102 strain had 2 copies of *ARG1* gene, whereas the NCYC3363 isolate turned out to have only 1 copy of the same gene. The same situation was observed for *FOX2* and potential candidates that might be encoding Acyl-CoA Oxidase in NCYC102 isolate, although further analyses are still required to clearly demonstrate the second copy of these genes in this strain. The presence of partial ploidy in some isolates might be a challenge in gene deletion studies. In these strains, more than 1 deletion is required to delete the specific gene that have more than 1 copy in the genome, which requires the usage of more than 1 deletion marker (which we are already limited for in our lab) and it is time consuming.

The advantageous aspects and challenges of working with *D. hansenii* are listed in Table 1.1.

Table 1.1: The positive aspects and challenges of working with *D. hansenii.*

D. hansenii- Advantages	*D. hansenii-* Potential Challenges
Oleaginous- accumulates high amounts of lipids	Underexplored- lack of enough literature information
Halotolerant and osmotolerant	CTG clade organism: the genes to be expressed always need to be CTG-optimised
Accumulates glycerol, arabitol and xylitol (that are widely used in industry)	Lacking molecular toolbox, even some progress has been made
Has been already been used widely in food industry	Variable ploidy that might challenge gene deletion studies
Generally considered as non-pathogenic	
Synthesises killer toxin	
Established production of some chemicals	
Could serve as a good model organism	

1.8- Aims and Objectives

In this research, our first aim was to develop a genetic toolbox for various molecular biology applications in *D. hansenii*, to develop it as a good candidate for molecular biology and genetics studies. To achieve this, our first objective was to develop different antibiotics resistance marker cassettes (ClonNat, Hygromycin B and G418 resistance markers) and their optimization for different *D. hansenii* strains, to be able to perform gene deletions as well as heterologous gene expression. Our second objective was to develop different fluorescence marker cassettes using green and red fluorescence marker protein expression, to be able to tag different genes and see the intracellular localization of their corresponding proteins.

The second aim of this research was to understand how the peroxisomal beta-oxidation works in *D. hansenii* so that the lipid breakdown process could be disrupted which would result in accumulation of fatty acids. To achieve this, our first objective was to identify the potential beta-oxidation related proteins in *D. hansenii*, by bioinformatics research. Our second objective was to understand and slow down the NAD^+-dependent step, as partial blocking the beta-oxidation at the third step could lead to accumulation of 3-Hydroxy-Fatty acids that are used in industry. The Mdh3 gene deletion was our starting point as Mdh3 is the main enzyme required for NAD^+ regeneration in peroxisomes of *S. cerevisiae* and in *D. hansenii*, Mdh3 seemed to be encoded by only one gene. As no phenotype was observed, Gpd1 and other proteins were investigated for their potential role in peroxisomal NAD^+ homeostasis. This identified a role for Pmp47 as a potential NAD^+ transporter.

The last aim was to characterise Pmp47. To achieve this, our first objective was to express it in *S. cerevisiae* (a heterologous host that lacks PMP47) to see its localization, followed by tagging it in *D. hansenii*. Our second objective was to investigate whether Pmp47 contributes to the beta-oxidation in *D. hansenii*, by gene deletion followed by growth assay using fatty acid media (oleate) as well as fatty acid oxidation activity assays. Our third objective was to determine whether Pmp47 contributes to NAD^+ availability in beta-oxidation, by expressing it in *S. cerevisiae* mutants that are beta-oxidation deficient (due to the unavailability of NAD^+ in peroxisomes), followed by growth assays using oleate. Our last objective was to investigate whether Pmp47 is exchanging the NAD^+ with AMP (as suggested for its plant homolog) by expressing it in various *S. cerevisiae* mutants (that exhibit lower fatty acid oxidation activity) followed by beta-oxidation activity assays.

Chapter 2- Materials and Methods

2.1- Strains and plasmids

2.1.1- Strains

All *D. hansenii, S. cerevisiae* and *E. coli* strains, that were used in this study, are listed in Table 2.1. Both *D. hansenii* WT strains (NCYC102 and NCYC3363), that were purchased from Natural Collection of Yeast Cultures (NCYC), can be accessed via https://www.ncyc.co.uk/. *S. cerevisiae* BY4741, *pex3Δ*, *pex5Δ* and *pex7Δ* strains are also available on http://www.euroscarf.de.

Table 2.1: The list of yeast and *E. coli* strains that were used in this research.

Strain Name	Genotype	Type of Organism	Source
NCYC 102 (YEH750 WT)	WT	*D. hansenii*	NCYC
NCYC 3363 (soy WT)	WT	*D. hansenii*	NCYC
pex3Δ	NCYC102, *pex3::SAT1*	*D. hansenii*	Hettema Lab
pex3Δ (soy)	NCYC3363, *pex3::SAT1*	*D. hansenii*	Hettema Lab
mdh3Δ	NCYC3363, *mdh3::hygB^r*	*D. hansenii*	This study
gpd1Δ	NCYC3363, *gpd1::SAT1*	*D. hansenii*	This study
gpd1/mdh3	NCYC3363, *gpd1::SAT1, mdh3::hygB^r*	*D. hansenii*	This study
pmp47Δ	NCYC3363, *pmp47::hygB^r*	*D. hansenii*	This study
npy1Δ	NCYC3363, *npy1::G418^r*	*D. hansenii*	This study
gpd1/mdh3/pmp47Δ	NCYC3363, *gpd1::SAT1, mdh3::hygB^r, pmp47::G418^r*	*D. hansenii*	This study
pmp47bΔ	NCYC3363, *pmp47b::G418^r*	*D. hansenii*	This study
pmp47a/pmp47bΔ	NCYC3363, *pmp47::hygB^r, pmp47b:: G418^r*	*D. hansenii*	This study
gpd1/mdh3/pmp47bΔ	NCYC3363, *gpd1::SAT1, mdh3::hygB^r, pmp47b::G418^r*	*D. hansenii*	This study
gpd1/mdh3/npy1Δ	NCYC3363, *mdh3::hygB^r, gpd1::SAT1, npy1::G418^r*	*D. hansenii*	This study
fox2Δ	NCYC3363, *fox2::hygB^r*	*D. hansenii*	This study
YEH750, *mCherry-SKL*	NCYC102, *yemCherry-SKL::G418^r*	*D. hansenii*	This study
pex3Δ, *mCherry-SKL*	NCYC102, *pex3::SAT1*, *yemCherry-SKL::G418^r*	*D. hansenii*	This study
YEH750, GFP-*MDH3*	NCYC102, GFP-*MDH3::hygB^r*	*D. hansenii*	This study
pex3Δ, GFP-*MDH3*	NCYC102, *pex3::SAT1*, GFP-*MDH3::hygB^r*	*D. hansenii*	This study
YEH750, *GPD1*-GFP	NCYC102, *GPD1*-GFP*::hygB^r*	*D. hansenii*	This study

pex3Δ, GPD1-GFP	NCYC102, *pex3::SAT1*, *GPD1*-GFP*::hygB*^{r}	*D. hansenii*	This study
YEH750, GFP-*MDH3, mCherry-SKL*	NCYC102, GFP-*MDH3::hygB*^{r}, *yemCherry-SKL::G418*^{r}	*D. hansenii*	This study
pex3Δ, GFP-*MDH3,* mCherry-*SKL*	NCYC102, *pex3::SAT1*, GFP-*MDH3::hygB*^{r}, *yemCherry-SKL::G418*^{r}	*D. hansenii*	This study
YEH750, GPD1-GFP, mCherry-*SKL*	NCYC102, *GPD1*-GFP*::hygB*^{r}, *yemCherry-SKL::G418*^{r}	*D. hansenii*	This study
pex3Δ, GPD1-GFP, mCherry-*SKL*	NCYC102, *pex3::SAT1*, *GPD1*-GFP*::hygB*^{r}, *yemCherry-SKL::G418*^{r}	*D. hansenii*	This study
YEH750*, PMP47a*-GFP	NCYC102, *PMP47*-GFP*::hygB*^{r}	*D. hansenii*	This study
YEH750*, PMP47a*-GFP, mCherry-*SKL*	NCYC102, *PMP47*-GFP*::hygB*^{r}, *yemCherry-SKL::G418*^{r}	*D. hansenii*	This study
BY4741 (YEH703 WT)	*MATA his3-1 leu2-0 met15-0 ura3-0*	*S. cerevisiae*	Euroscarf
pex3Δ	*MATA his3-1 leu2-0 met15-0 ura3-0 pex3::KanMX*	*S. cerevisiae*	Euroscarf
pex5Δ	*MATA his3-1 leu2-0 met15-0 ura3-0 pex5::KanMX*	*S. cerevisiae*	Euroscarf
pex7Δ	*MATA his3-1 leu2-0 met15-0 ura3-0 pex7::KanMX*	*S. cerevisiae*	Euroscarf
mdh3Δ	*MATA his3-1 leu2-0 met15-0 ura3-0 mdh3::SpHIS5*	*S. cerevisiae*	(Al-Saryi *et al.*, 2017a)
gpd1/mdh3Δ	*MATA his3-1 leu2-0 met15-0 ura3-0 gpd1::KanMX , mdh3::SpHIS5*	*S. cerevisiae*	(Al-Saryi *et al.*, 2017a)
DH5α	*supE44 ΔlacU169 (Φ80 lacZ ΔM15) hsdR17 recA1 endA1gyrA96 thi-1 relA1*	*E. coli*	Hettema Lab

2.1.2- Plasmids

All the plasmids that were used in this study were listed in Table 2.2. The maps of each toolbox plasmid, that were designed for gene deletions and tagging in the genome for (*D. hansenii*), can be seen on Appendix 1. The plasmids pDh1 and pDh2 were developed and synthesised artificially, that is described in Section 3.3.1.

The gene deletion and tagging plasmids, that were used in *D. hansenii,* were created by classical cloning method. Finally, the *S. cerevisiae* expression plasmids were constructed via either homologous recombination or classical cloning.

After being constructed, each newly-made plasmid sequence was confirmed by Sanger sequencing analysis.

Table 2.2: The list of plasmids used in this study.

Plasmid Name	Restriction sites	Insert	Parental vector	Purpose	Source
pDh1	Spe1-Not1	*SsTEF1* promoter-CTG adapted *hygB*^{r} ORF-*SsTEF1* terminator	pUC19	To generate gene deletions/modifications in *D. hansenii* using *hygB*^{r} as a marker	GenScript
pDh2	Spe1-Not1	*SsACT1* promoter-CTG adapted *G418*^{r} ORF-*SsACT1* terminator	pUC19	To generate gene deletions/modifications in *D. hansenii* using *G418*^{r} as a marker	GenScript
pZA1	BamH1-Pst1	*CaACT1* promoter-CTG adapted *SAT1* ORF-*CaURA3* terminator	pBlueSkript KS(+)	To generate gene deletions/modifications in *D. hansenii* using *SAT1* as a marker	Hettema Lab
pSLV3	Kpn1-BamH1	1 kb upstream of *DhMDH3*	pDh1	To delete *MDH3* in *D. hansenii*	This study
pSLV4	Xba1-Sph1	1 kb downstream of *DhMDH3*	pSLV3		
pSLV13	Kpn1-Spe1	1 kb upstream of *DhFOX2*	pDh1	To delete *FOX2* in *D. hansenii*	This study
pSLV14	Sal1-Hind3	1 kb downstream of *DhFOX2*	pSLV13		
pSLV18	Kpn1-Hind3	1 kb upstream of *DhGPD1*	pDh1	To delete *GPD1* in *D. hansenii*	This study
pSLV19	Not1-Sal1	1 kb downstream of *DhGPD1*	pSLV18		
YCplac33	-	-	-	Empty yeast expression plasmid with *URA3* marker to be used in *S. cerevisiae*.	Hettema Lab
YCplac111	-	-	-	Empty yeast expression plasmid with *LEU2* marker to be used in *S. cerevisiae*.	Hettema Lab
pEH116	EcoR1-Hind3*	*TPI1* promoter-MCS-GAGAGA linker-GFP-MCS-*PGK1 terminator*	YCplac33	C-terminal tagging vector with *URA3* marker to be used in *S. cerevisiae*. Asterisk means that *PGK* terminator was recombined into the vector via single digest using Hind3.	Hettema Lab
pEH117	EcoR1-Hind3*	*TPI1* promoter-MCS-GAGAGA linker-GFP-MCS-*PGK1 terminator*	YCplac111	C-terminal tagging vector with *LEU2* marker to be used in *S. cerevisiae*. Asterisk means that *PGK* terminator was recombined into the vector via single digest using Hind3.	Hettema Lab
pSLV24	Sac1-Pst1	*DhPMP47* ORF	pEH117	To express *DhPMP47*-GFP in *S. cerevisiae*, behind *TPI1* promoter	This study
pEH008	EcoR1-Hind3*	*HIS3* promoter-*PEX11*-GFP	YCplac111	Used for replacing ''PEX11-GFP'' with ''*DhPMP47*-GAGAGA linker-GFP'' (from pSLV24). Asterisk means that GFP was recombined into the vector via single digest using Hind3.	Hettema Lab
pSLV25	Sac1-Hind3	*DhPMP47*-GAGAGA linker-GFP	pEH008	Final vector to express *DhPMP47*-GFP in *S. cerevisiae*, behind *HIS3* promoter	This study
pSLV26	BamH1-Pst1	*DhLYS1*	pEH117	To tag *DhLYS1* in *S.cerevisiae* with GFP at the C-terminus	This study
pEW332	EcoR1-Hind3*	*TPI1* promoter-GFP-MCS-*PGK1 terminator*	YCplac111	N-terminal tagging vector with *LEU2* marker to be used in *S. cerevisiae*. Asterisk means that *PGK1* terminator was	Hettema Lab

				recombined into the vector via single digest using Hind3.	
pSLV27	BamH1-Pst1	*DhLYS1*	pEW332	To tag *DhLYS1* in *S.cerevisiae* with GFP at the N-terminus	This study
pNC1	Sac1-Sal1	*DhPNC1*	pUC19	The vector that has *DhPNC1* ORF that was synthesised.	GenScript
pGH113	EcoR1-Hind3	*INP1* promoter-truncated *INP1*-GAGAGA linker-mCherry	YCplac33	*S. cerevisiae* vector with ''GAGAGAGA linker-mCherry''. Used as a backbone to do C-terminal tagging with red fluorescent marker.	Hettema Lab
pSLV28	Sac1-Sal1	*DhPNC1*	pGH113	To fuse *DhPNC1* with GAGAGA linker-mCherry in pGH113 (to tag *PNC1* at the C-terminus). Made by replacing truncated *INP1* in pGH113 with *DhPNC1* ORF	This study
pSLV29	Sac1-Hind3	*DhPNC1*-GAGAGA linker-mCherry	pSLV26	To clone ''*DhPNC1*-GAGAGA linker-mCherry'' (in pSLV28) into pSLV26 behind *TPI1* promoter	This study
pSA4	EcoR1-BamH1 (for upstream) & Pst1-Sph1 (for downstream)	~1 kb of upstream & ~1 kb of downstream sequences of *DhARG1*	pDh2	To target desired cassettes into *DhARG1* locus in *D. hansenii*	Hettema Lab
pSA5	Not1-Spe1 (for *hygB*^{r} expression cassette) & Kpn1-Sal1 (for GFP-SKL)	*hygB*^{r} expression cassette from pDh1 & *MgACT1* promoter-CTG adapted GFP ORF-P-L-H-S-K-L	pSA4	Plasmid with green peroxisomal marker with *hygB*^{r} selectable marker. ''*MgACT1* promoter-CTG adapted GFP'' was used to generate N-terminal tagging construct in *D. hansenii*.	Hettema Lab
pSLV35	Not1-Sal1	*MgACT1* promoter-CTG-adapted *yemCherry* ORF-SKL	pSA4	To generate red peroxisomal marker construct (*mCherry*-SKL) behind *MgACT1* promoter to be used in *D. hansenii*.	This study
pSLV37	Not1-Pst1	*SsGPD1* promoter	pSLV35	To generate alternative red peroxisomal marker construct behind *SsGPD1* promoter to be used in *D. hansenii*.	This study
pMP34	EcoR1-Hind3	100 bp upstream of *DhPMP47-HsPMP34* ORF-GAGAGA linker-yomRuby2 ORF-*SsGPD1* terminator-100 bp downstream of *DhPMP47*	pUC19	Used as a template to replace *mRuby2* with the GFP (of pSA5)	GenScript
pSLV36	Xho1-Xba1	CTG adapted GFP (with introduced stop codon) from pSA5	pMP34	Plasmid template that now has ''-GAGAGA linker-GFP (with stop codon)'' to subclone into pDh1	This study
pSLV38	BamH1-Spe1	GAGAGA linker-CTG-adapted GFP ORF-*SsGPD1* terminator (from pSLV36)	pDh1	To generate final version of C-terminal tagging construct to be used in *D. hansenii*	This study
pES1	Sac1-BamH1	*DhGPD1*	pEH116	To tag *DhGPD1* in *S. cerevisiae* with GFP at the C-terminal	Hettema Lab
pES2	Sac1-BamH1	*DhGPD2*	pEH116	To tag *DhGPD2* in *S. cerevisiae* with GFP at the C-terminal	Hettema Lab
pNA33	EcoR1-Hind3	*ScGPD1* promoter-*ScGPD1* ORF-GFP	YCplac33	To tag *ScGPD1* in *S. cerevisiae* with GFP at the C-terminal	Hettema Lab

pAS63	EcoR1-Hind3*	*HIS3* promoter-*HcRed*-SKL-PGK terminator	YCplac111	Red peroxisomal marker to be used in *S. cerevisiae* for co-localization. Asterisk means that *PGK* terminator was recombined into the vector via single digest using Hind3.	Hettema Lab
pAS131	EcoR1-Sal1	*PEX11* promoter-*PEX11* ORF	pGW023	Red peroxisomal marker to be used in *S. cerevisiae* to check co-localization	Hettema Lab
pEL30	EcoR1-Sac1	*ScCTA1* promoter	YCplac33	To create *CTA1* promoter-controlled expression plasmid to be used in *S. cerevisiae*	Elgersma *et al.*, 1993
pSC120	Sac1-Xba1	*DhPMP47* ORF	pEL30	To express untagged *DhPMP47* in *S. cerevisiae* behind *ScCTA1* promoter	This study

2.2- Bioinformatics

During the first year of this PhD study, preliminary bioinformatics research had been done by myself to identify *D. hansenii* proteins with consensus PTS1 and PTS2 patterns (that are located at the N- and C-termini respectively), using Scan Prosite Database (Sigrist *et al.*, 2002; Sigrist *et al.*, 2012). In the second year, more detailed research was conducted by using Camoes *et al.* (2015) as a point of reference. In their study, bioinformatics was used to identify all potential peroxisomal proteins of smut fungus *Ustilago maydis* based on the presence of PTS1 or PTS2 and homology to known peroxisomal proteins in other organisms. In addition, the presence of each identified peroxisomal protein in *S. cerevisiae* and *Homo sapiens* was also specified. By using blastp (Altschul *et al.*, 1990), all these *U. maydis* proteins specified were blasted against the putative *D. hansenii* proteome to detect potential *D. hansenii* homologs. Hits were then blasted back against the *U. maydis* proteome to find best hits. Where necessary, some peroxisomal proteins in *S. cerevisiae* were also blasted against *D. hansenii* by the 'BLASTP vs. fungi' feature on Saccharomyces Genome Database (SGD) (https://www.yeastgenome.org/), which is then followed by reciprocal blast. Then, each hit was analysed using Uniprot (Apweiler *et al.*, 2004) for detailed overview.

The factors to determine the best hits (that represent the potential *D. hansenii* ortholog of each protein) were lower E-value, higher percentage identity as well as higher query coverage in blastp search (Altschul *et al.*, 1990). Uniprot analysis (Apweiler *et al.*, 2004) of each hit was a second factor to determine the best hits, as it gives more detailed information about whether the corresponding blast hit shows similar protein function and similar protein domains to the query protein. It also shows whether the same protein exists in other yeasts with the same name and function. The last factor to determine the best hit was reciprocal blast (Altschul *et al.*, 1990), to see whether it gives back the query protein as a best hit.

After the potential *D. hansenii* orthologs of each protein were identified, Kyoto Encyclopedia of Genes and Genomes (KEGG) Database (Kanehisa and Goto, 2000) was used to access their DNA sequences. Clustal Omega (Sievers *et al.*, 2011) was used to align different protein sequences.

After each *U. maydis* or *S. cerevisiae* protein was blasted (Altschul *et al.*, 1990) against *D. hansenii*, the ones considered as the most likely homologs were listed. These findings were compared with the

results of the previous bioinformatics research. A list of potential peroxisomal proteins was generated (Appendix 2). Potential *D. hansenii* beta-oxidation proteins are listed in Chapter 3.

2.3- Growth media

The growth media that were used for research are described in Table 2.3. To prepare them, the media components were dissolved in the Millipore water with the help of magnetic stirrer. After the media were adjusted to the final volume, they were sterilised by autoclaving. Any amino acids or antibiotics required for some media were added after autoclaving. For amino acid dropout media, amino acid dropout mixtures were added according to the manufacturer recommendation, before autoclaving.

Yeast Nitrogen Base, Tryptone, Agar, Yeast Extract, Peptone, Casamino Acids and amino acid dropout mixtures were supplied by Formedium. Sodium Chloride, D-glucose and Glycerol were supplied by Fisher Scientific. D-Galactose and Tween 40 were supplied by Merck (formerly Sigma). Malt Extract, Ammonium Sulphate and Oleic Acid were purchased from Oxoid, BDH and MP Biomedicals respectively. The antibiotics hygromycin B (hygB), Nourseothricin Sulfate (Clonnat) and Geneticin Disulphate (G418) were purchased from Melford.

Table 2.3: The growth media that was used in this study.

Media	Components
YPD	2% w/v Bacto Peptone (Difco), 1% w/v Yeast Extract, 2% w/v D-Glucose, 2% w/v Agar for solid media
2TY	1.6% w/v Tryptone, 1% w/v Yeast Extract, 0.5% w/v NaCl, 2% w/v Agar. For 2TY-Amp, 75 µg/ml Ampicillin was added to the final concentration.
YM Deb	0.3% w/v Yeast Extract, 0.3% w/v Malt Extract, 0.5% w/v Peptone, 1% w/v Glucose, 1.5% w/v Agar for solid media. Where required; Clonnat, G418 or hygB was added to the final concentration of: -1.5 µg/ml Clonnat (if working with NCYC102 strain) or 4 µg/ml Clonnat (if working with NCYC3363 strain) -150 µg/ml G418 (if working with NCYC102 strain) or 350 µg/ml G418 (if working with NCYC3363 strain) -25 µg/ml hygB (if working with NCYC102 strain) or 50 µg/ml hygB (if working with NCYC3363 strain)
Yeast Minimal Media 1 (YM1)	0.5% w/v Ammonium Sulphate, 0.19% w/v Yeast Nitrogen Base (without ammonium sulphate and amino acids), 2% w/v D-Glucose, 2% w/v Agar for solid media. pH was adjusted to 6.5 with 10 M NaOH. For YM1 with galactose or glycerol media, same mixture was used with 2% w/v D-Galactose or 3% v/v Glycerol instead of D-Glucose.

Yeast Minimal Media 2 (YM2)	0.5% w/v Ammonium Sulphate, 0.19% w/v Yeast Nitrogen Base (without ammonium sulphate and amino acids), 1% w/v Casamino Acids, 2% w/v D-Glucose, 2% w/v Agar for solid media. pH was adjusted to 6.5 with 10 M NaOH. For YM2 with galactose or glycerol media, same mixture was used with 2% w/v D-Galactose or 3% v/v Glycerol instead of D-Glucose.
Ura^- media	YM2 was prepared and autoclaved. Then, Leucine was added to final concentration of 30 µg/ml.
Auxotrophic media (except Ura^-)	YM1 was prepared and autoclaved. Then, necessary amino acids were added from 100X working stock solutions (to the final concentration of 20 µg/ml for Uracil, Methionine, Histidine-HCl, Tryptophan and 30 µg/ml for Leucine, Lysine-HCl).
Minimal non-selective media	YM2 was prepared and autoclaved. Then, 20 µg/ml Uracil, 20 µg/ml Tryptophan and 30 µg/ml Leucine were added.
Oleate (solid media)	0.625% v/v Oleic Acid + Tween 40 mixture (they were mixed by 1:4 ratio, respectively), 0.1% w/v Yeast Extract, 0.19% w/v Yeast Nitrogen Base (without ammonium sulphate or amino acids), 0.5% w/v Ammonium Sulphate, 1% w/v Casamino Acids, 2% w/v Agar. After autoclaving, 20 ng/ml Uracil and 30 ng/ml Leucine were added.
Oleate (liquid media)	0.12% v/v Oleic Acid, 0.2% v/v Tween 40, 0.1% w/v Yeast Extract, 0.5% w/v Peptone, 10% 50 mM Potassium Phosphate Buffer with pH=6.0.

2.4- Yeast Protocols

2.4.1- Growth and maintenance

D. hansenii cells were grown at 25°C whereas *S. cerevisiae* cells were grown at 30°C, either on solid media or in liquid cultures on a shaker at 200 rpm. For the selection of antibiotic markers in *D. hansenii*, antibiotics were added to YM Deb media as required. For the selection of auxotrophic markers in *S. cerevisiae*, appropriate amino acids were added to either YM1 or YM2 media. Each newly-made strain was grown overnight in appropriate media, transferred into cryovials with an addition of glycerol to 50% v/v final volume, followed by freezing at -80 °C for the long term storage.

In order to grow a post-logarithmic culture, the cells were grown in the appropriate media for overnight until the following morning, and were analysed directly the following morning. In order to grow a logarithmic culture, the cells were grown in appropriate media for overnight. The next morning, the cells were diluted into fresh media and grown either ~4 hours (for glucose) and ~6 hours (for oleate), and were analysed afterwards.

2.4.2- *D. hansenii* transformation via electroporation

This method was used to introduce each gene deletion or tagging cassettes into *D. hansenii*. Cells were inoculated into YM Deb and grown overnight (Day=0). Next morning, the cells were diluted to OD_{600}=0.1 into fresh YM Deb and grown for 6-7 hours until OD_{600} reaches 0.6-0.9. Subsequently, the culture was inoculated to into fresh 30-50 ml YM Deb to the OD_{600} (between 0.001-0.005) which will reach the OD_{600} between 2.6-3 the next morning. The cells were grown overnight (Day=1).

The next morning (Day=3), transformation was started when OD_{600} reached around 2.6-5. Ten ml of culture (per transformation) was harvested by centrifugation at 1610 rcf for 5 minutes. The pellets were resuspended in 1 ml 50 mM sodium phosphate buffer (pH=7.5) containing 25 mM dithiothreitol (DTT) and incubated at 25°C for 15 minutes and then centrifuged at 1610 rcf for 5 minutes. The pellets were then washed with 8 ml cold sterile H_2O, centrifuged at 1610 rcf for 5 minutes and resuspended in 200 µl 1 M sorbitol. The tubes were centrifuged at 1610 rcf for 5 minutes and 160-200 µl supernatant was removed from each tube. Pellets were resuspended in remaining volume and 40 µl from each tube was transferred to 1.5 ml Eppendorf tubes. Subsequently, 500 ng of precipitated DNA in maximally 5 µl was added to each tube (for negative control without DNA, only 40 µl cell suspension was used directly). The final mixtures were transferred into pre-cooled 2 mm electroporation cuvette (Geneflow) and incubated on ice for further 5 minutes. Then, each sample was electroporated at 2.3 kV, using Biorad MicroPulser. Each electroporated sample was resuspended with 1 ml YM Deb + 0.1 M sorbitol and transferred into 2 ml tubes. Each tube was incubated at a 25°C shaker for 4 hours. Subsequently, cells were centrifuged at 664 rcf for 5 minutes and most of the supernatant was discarded. The cells were then plated out onto YM Deb plates with appropriate antibiotics and the plates were incubated at 25°C for 2-3 days.

2.4.3- High efficiency transformation for *S. cerevisiae*

This method was used to make each *S. cerevisiae* expression plasmid via homologous recombination method described in Section 2.6.10. Before starting, the solutions described in Table 2.4 were prepared.

Table 2.4: The components and preparation of each solution used for High Efficiency Transformation

Solution	Components
1X TE	1 ml 10X TE (0.1M Tris-HCl, 0.01M EDTA at pH= 7.4) + 9 ml dH_2O
1X TE/Lithium Acetate	1ml 10X TE + 1ml 1M Lithium Acetate at pH=7.5 + 8 ml dH_2O
40% PEG (Polyethylene Glycol)	3.2 ml 50% (w/v) PEG 3350 + 0.4 ml 10X TE + 0.4 ml 1M Lithium Acetate at pH=7.5

The cells were inoculated into 3 ml YPD and grown overnight. Next morning, the cells were diluted to OD_{600}=0.1 into fresh culture (the final volume was calculated based on the number of the transformations and 5 ml per transformation was required) and grown for ~ 4 hours until the OD_{600} reaches 0.3-0.8. Then, 5 ml per transformation was transferred into Falcon tube and the tubes were centrifuged at 1118 rcf for 5 minutes. Each supernatant was discarded, pellets were resuspended with 1 ml 1x TE/LiAc solution and transferred to Eppendorf tubes. The tubes were centrifuged for 2 minutes at 1844 rcf and supernatants were discarded. Each pellet was resuspended into 1 ml 1x TE/LiAc solution and centrifuged for 2 minutes at 1844 rcf again. The resultant pellet was resuspended with 50 µl 1X TE/LiAc solution. Afterwards; 5 µl digested vector (500 ng), 5 µl PCR product, 5 µl ssDNA (50 µg) (Merck with a product number of D9156) and 300 µl sterile 40% PEG 3350 were added to each tube. For the negative control, the same components were added except the 5 µl PCR product. Each tube was incubated at the room temperature for 30 minutes, at 30°C for another 30 minutes. Afterwards, the cells were heat shocked in a 42°C water bath for 15 minutes and centrifuged in a microfuge (Sigma 1-14 microfuge) at maximum speed for 1 minute. The pellets were mixed with 50 µl 1X TE and plated out onto appropriate plates, then the plates were kept at 30°C for 2-3 days. More detailed information about each solution used is described in Table 2.4.

2.4.4- One Step Transformation

One step transformation was used to introduce newly-made expression plasmids into *S. cerevisiae*. A day before, each strain was inoculated into 3 ml appropriate media and grown overnight. The next morning, 200 µl culture was centrifuged at 10625 rcf for 1 minute and the supernatant was discarded. The pellet was mixed with 3 µl plasmid (200-500 ng), 50 µl ''one step buffer'' (0.2 M LiAc pH=5, 40% PEG 3350, 100 mM DTT) and 5 µl ssDNA (50 µg) (Merck, with a product number of D9156) followed by vortex. Each tube was incubated at room temperature for a few hours, by giving them occasional vortex. Afterwards, each tube was heat-shocked at 42°C in water bath for 30 minutes. The cell suspensions were plated out onto selective plates which incubated at 30°C for 2.3 days.

2.4.5- Genomic DNA Isolation

The yeast cells were inoculated into 3 ml appropriate media and grown overnight. The day after, they were pelleted down in a 2 ml screw cap tube (by centrifuging at 10625 rcf for 1 minute). The resultant pellets were washed with 1 ml dH_2O. The pellets were resuspended in 200 µl TENTS solution (1% SDS w/v, 2% Triton X-100 v/v, 1 mM EDTA, 100 mM NaCl and 20mM Tris/HCl at pH=8), 200 µl phenol-chloroform and 200 µl 0.5 mm glass beads (BioSpec Products) were added into each tube. The tubes were placed into the bead beater (BioSpec Products) at maximum speed for 45 seconds, then centrifuged for 30 seconds at 10625 rcf. Another 200 µl TENTS solution was added into each tube followed by a brief vortex, the tubes were centrifuged at 10625 rcf for 5 minutes. The supernatants were transferred into Eppendorf tubes and another 200 µl phenol-chloroform was

added to each tube. Each tube was vortexed and centrifuged at 10625 rcf for 5 minutes. The supernatants (~300 µl) were transferred to new tubes. Each supernatant was mixed with 1/10 volume 3 M NaAc at pH=5.2 and 2.5X volume 100% EtOH, and the tubes were kept on ice for 15-30 minutes. Each tube was centrifuged at 4°C and 12000 rpm for 15 minutes, using the accuSpin Micro R centrifuge (Fisher Scientific). The pellets were washed with 300-500 µl 70% EtOH and centrifuged in Sigma 1-14 microfuge at maximum speed for 5 minutes. The pellets were resuspended with 200 µl 1X TE (at pH=7.4) + 2 µl RNAse (10 mg/ml), incubated at the room temperature for 10 minutes. Then, they were mixed with another 1/10 volume 3 M NaAc at pH=5.2 and 2.5X volume 100% EtOH, then were kept on ice for 15-30 minutes. Each tube was centrifuged at 4°C and 12000 rpm for 15 minutes, using the accuSpin Micro R centrifuge (Fisher Scientific). The pellets were washed with 300-500 µl 70% EtOH and centrifuged in Sigma 1-14 microfuge at maximum speed for 5 minutes. After the supernatants were discarded, the pellets were dried at 45°C oven until there is no remaining EtOH. Finally, each pellet was resuspended with 50 µl 1X TE at pH=7.4 and each tube was stored at -20 freezer.

2.4.6- Spot Assay

Spot assay was done to check the growth of different *D. hansenii* and *S. cerevisiae* strains on different media. The cells were inoculated into appropriate media and grown overnight. The next morning, the OD_{600} of each culture was measured and the cultures were diluted to OD_{600}=0.1 in 1 ml sterile dH_2O, using Eppendorf tubes. Two hundred µl of each diluted cell was placed in the column of the sterile 96 well plates (Greiner Bio), in between the well B2 and below (Figure 2.1). The next 3 adjacent columns were filled with 180 µl sterile dH_2O using the multichannel pipette. To do the serial dilutions, 20 µl of cell suspension from the first column starting from B2 (OD_{600}=0.1) were taken via multichannel pipette, placed into the adjacent column and mixed well, which resulted in the cells diluted to OD_{600}=0.01. It was repeated for the remaining columns (Figure 2.1). After making the 10 fold dilutions, the 96 well pin replicator was flame sterilised and cooled down. The pin replicator was dipped into the wells and swirled few times, then was placed onto the appropriate plates. The plates were incubated for 3 days and were pictured using the Gel documentation machine (from GeneSys), using the ''Manual Capture'' option of GeneSys software.

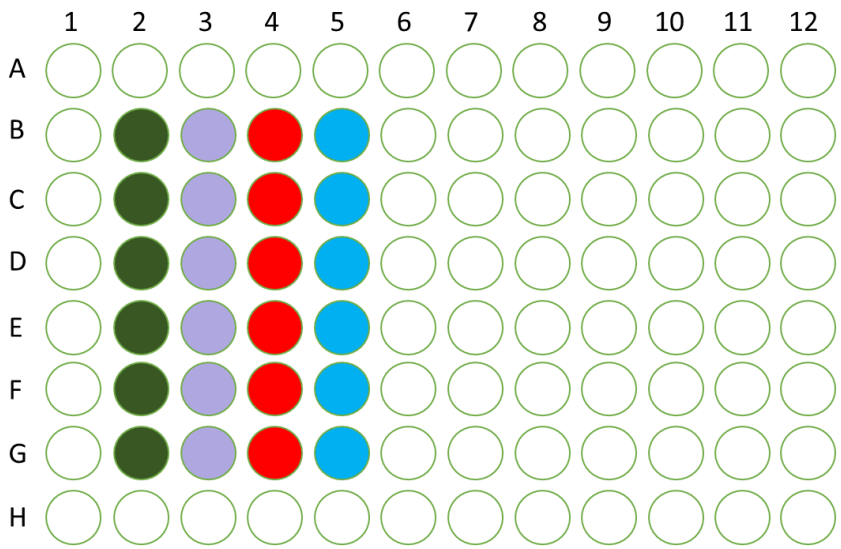

Figure 2.1: The diagram of how to load the cells into 96 well plates to do serial dilutions prior to spot assay. Firstly, 200 µl of each cell (diluted to OD_{600}=0.1) were loaded into the column, starting from the well B2 (shown in dark green). Then, the next 3 adjacent columns (shown in purple, red and blue respectively) were loaded with 180 µl sterile dH_2O. Twenty µl of the cells from the green column were taken and transferred to the purple column, followed by mixing ($0D_{600}$=0.01). Then, 20 µl of the cells from the purple column were taken and transferred to the red column, followed by mixing ($0D_{600}$=0.001). Finally, 20 µl of the cells from the red column were taken and transferred to the blue column, followed by mixing ($0D_{600}$=0.0001).

2.4.7- Growth Curve

Growth curves were done to observe the growth of *D. hansenii* cells over specific periods in liquid media. The cells were inoculated into YM2 media with 0.3% glucose and were grown overnight. The next morning, they were diluted into OD_{600}=0.05 into YM1-glucose media or OD_{600}=0.1 into oleate liquid media (t=0 hours). The cell cultures were kept on the shaker at 25°C incubator. The OD_{600} of each culture was taken at the different time points (before measuring the OD_{600} of oleate-grown cells, the cells were washed twice with sterile dH_20). The OD_{600} measurement was stopped after 3 days when the cells stopped dividing. This experiment was performed as 3 replicates which were done during different weeks with the ODs were being taken at exactly the same time points. Finally, the graph of cell density (the OD_{600}) at each time point (in hour) was plotted on GraphPad Prism software, using the three measurements for the same time point.

2.4.8- Beta-oxidation Activity Measurement

The beta-oxidation activity measurements were performed by Dr Carlo van Roermund (Laboratory Genetic Metabolic Diseases at Amsterdam UMC, The Netherlands), according to the following protocol:

The cells were harvested from 15 ml oleate culture and were centrifuged at 2310 rcf for 5 minutes. Each tube was washed with 15 ml dH_2O. They were resuspended with 9 g/L NaCl at a cell density of OD_{600} = 1. To incubate the cells, 2x 20 ml vials with a rubber septum were prepared (one tube should contain the cell suspension and incubation mixture, other should contain 500 µL of 2N NaOH). To start the measurements, 20 µl of each cell suspension was added to the reaction mixture which consists of 0.5M MES/KOH buffer at pH=6, 140 µl 9 g/L NaCl, 20 µl 100 µM [1-^{14}C]-fatty acid (200,000 dpm) as substrate. The cells were incubated at 28°C for 1 hour. The incubation was stopped by the addition of 50 µL 2.6 M perchloric acid. The chamber was left sealed for overnight at 4 °C (to allow the radiolabelled [^{14}C]-CO_2, that was released during the beta-oxidation of fatty acid, to be trapped in the tube with 500 µL 2N NaOH). The acidic mixture was then transferred to an Eppendorf tube and the tubes were centrifuged at 800 rcf for 5 minutes. Then, 250 µl of the supernatant was transferred to 5 ml glass tube. Hundred µl 2N NaOH was added to each tube, followed by the incubation at 50 °C for 30 minutes. The pH was adjusted to 4.0 by adding 75 µl 1M NaAc and 150 µl 0.5 M H_2SO_4. Then, 1.5 ml methanol/chloroform/heptane (MCH) (1.41:1.25:1.0 ratio) was added to each tube and the tubes were mixed on multivortex for 1 minute. The tubes were centrifuged at 400 rcf for 5 minutes. The under layer was removed and the new underlayer was added (H_2O:MCH=1.25:3.25) with the same volume that was previously removed. The tubes were mixed on the multivortex for 1 minute, and centrifuged at 400 rcf for 5 minutes. A 1 ml of the top layer was transferred into 20 ml plastic vial that contains the acid soluble products (ASP). Ten ml counting liquid was added to the liquid scintillation counter and the radiolabelled acid-soluble counts was measured. CO_2 and ASP were also quantified in a liquid scintillation counter and the beta-oxidation rate was determined as the sum of CO_2 and ASP production.

2.4.9- Fluorescence Microscopy Analysis

Cells were analysed using Axiovert 200M; Carl Zeiss, Inc. microscope, with Exfo Xcite 120 excitation light source, band-pass filters (Carl Zeiss, Inc. and Chroma), a Plan-Fluar 100x/1.45 NA or Plan-Apochromat 63x 1.4 NA objective lens (Carl Zeiss, Inc.) attached to the digital camera (Orca ER; Hamamatsu Phototonics). For image acquisition, Volocity Image Analysis Software Version 7.0 (Perkin Elmer) was used. The images were captured as 0.5 µm z-stacks, on the brightfield and appropriate fluorescent channels.

To edit the pictures, z-stacks of the image were exported to Openlab Software (Perkin Elmer). Multiple layers from Green and Red channels, on which the fluorescence was obvious and clear, were merged into a single image. One layer from brightfield was taken where the cells look in focus the most. The brightfield was pasted into the blue channel in in Adobe Photoshop Software. Green fluorescence merged Z-stack was pasted into the green channel of Photoshop and the Red fluorescence merged Z-stack into the Red channel of Photoshop. The merged images with green and red fluorescence were edited only by changing the levels when required. The brightfield picture was

edited using the blue channel to make only the cell walls appear on a darkened background, to attract the attention to inside the cells only. Since each microscopy picture was processed in exactly the same way in this study, the scale bar is the same for all microscopy pictures. Therefore, only 1 scale bar is shown on each Figure.

2.4.10- Peroxisome Quantification

The cells were grown in different media and imaged using fluorescence microscopy. The multiple z-stacks were captured as described in 2.4.9. Afterwards, all the different z-stacks of the same image were merged using the ''Extended Focus'' feature on Volocity Software. The number of peroxisomes (fluorescence signal seen as puncta) were counted manually. The experiment was done as 3 replicates and the values were analysed using GraphPad Prism software.

2.5- *E.coli* protocols

2.5.1- Growth and maintenance

The *E. coli* cells were grown both as a liquid culture or on solid media, using 2TY supplemented with Ampicillin where required (if selecting for plasmids). They were grown at 37°C overnight. The cells growing in liquid media were kept shaking at 200 rpm.

2.5.2- Production of chemically competent *E. coli* cells

The DH5α cells were taken out of -80°C freezer and grown on 2TY plate. They were inoculated into 5 ml 2TY and grown overnight. The next morning, the cells were diluted to OD_{600}=0.05 into 200 ml sterile 2TY (in 1 L sterile flask). The cells were kept shaking at 37°C until their OD_{600} reached 0.5. Then, the culture was placed onto the ice and cooled for 15 minutes. In a meantime, the centrifuge was cooled to 4°C. Then, 50 ml of the cell culture was aliquoted out to 4 individual Falcon tubes. The tubes were centrifuged at 4°C, at 1610 rcf for 10 minutes. The supernatants were discarded and the pellets were resuspended very gently using 1 ml ice cold RF1 solution (Table 2.5). Then, 2 Falcon tubes were pooled together and each resultant suspension was mixed with 35 ml RF1. Each tube was incubated on ice for 15 minutes. In a meantime, 80 Eppendorf tubes were labelled to indicate chemically competent cells and each tube was put onto the ice. The tubes were centrifuged at 4°C, at 1610 rcf for 10 minutes. The supernatants were discarded and the pellets were resuspended very gently using 1 ml ice cold RF2 solution (Table 2.5). The tubes were pooled together again and the final volume was brought up to 16 ml by adding ice cold RF2 solution. The final mixture was

aliquoted out to precooled Eppendorf tubes (200 µl per tube). The tubes were frozen in liquid nitrogen and were stored at -80°C freezer.

Table 2.5: The composition of RF1 and RF2 solutions with the preparation protocol to produce chemically competent *E. coli* cells.

RF1 solution	RF2 solution
100 mM Rubidium Chloride	10 mM MOPS
50 mM Manganese Chloride	10 mM Rubidium Chloride
30 mM Potassium Acetate	75 mM Calcium Chloride
10 mM Calcium Chloride	15% (w/v) Glycerol
15% (w/v) Glycerol	To prepare: All the ingredients were mixed together, the pH was adjusted to 6.8 with NaOH. Final volume was brought to 500 ml, which was sterilised by filtration.
To prepare: All the ingredients were mixed together, the pH was adjusted to 5.8 with 0.2 M Acetic Acid. Final volume was brought to 1 L, which was sterilised by filtration.	

2.5.3- Production of electrocompetent *E. coli* cells

The DH5α cells were taken out of -80°C freezer and grown on 2TY plate. Then, they were inoculated into 10 ml 2TY and grown overnight. The next morning, the cells were diluted to OD_{600}=0.05 into sterile 1 L of 2TY (in a sterile flask). The cells were kept shaking at 37°C until their OD_{600} reached 0.5. Then, the culture was placed onto the ice and cooled for 15 minutes. In a meantime, the centrifuge was cooled to 4°C. Then, 250 ml of the cell culture was aliquoted out to 4 individual pre-sterilised (rinsed with methylated spirits and dried at 37°C) 500 ml centrifuge buckets. The buckets were centrifuged at 4°C, at 1610 rcf for 15 minutes. The supernatants were discarded and the pellets were resuspended with 20 ml of ice-cold and sterile 10% glycerol. Straight after, 105 ml 10% glycerol (cold and sterile) was added into each bucket, and 2 buckets were pooled together. They were centrifuged at 4°C, at 1610 rcf for 15 minutes. The supernatants were discarded and the pellets were resuspended with 20 ml of ice-cold and sterile 10% glycerol. They were centrifuged again at 4°C, at 1610 rcf for 15 minutes. The supernatants were discarded and the pellets were resuspended with 20 ml of (sterile and ice cold) 10% glycerol. The buckets were pooled together and 10 ml of (sterile and ice cold) 10% glycerol was added into the final bucket. The bucket was centrifuged at 4°C, 1610 rcf for 15 minutes for the last time and the supernatant was discarded. The resultant pellet was resuspended with 700 µl of (sterile and ice cold) 10% glycerol and the final mixture was aliquoted out to individual Eppendorf tubes (40 µl per tube). The tubes were frozen in liquid nitrogen and were stored at -80°C freezer.

2.5.4- *E.coli* Transformation using chemically competent cells

Chemically competent cells were used for transformation of the ligated vector and insert as part of the classical cloning process, as well as the retransformation of the plasmid to obtain a fresh miniprep before working with specific plasmid from -20°C stock. The chemically competent cells were taken out of the -80°C freezer and thawed on ice. In the meantime, the plasmid or ligation mixture were cooled on ice for few minutes. Ten µl ligation mixture was mixed with 90 µl cells or 0.5-1 µl plasmid was mixed with 30-50 µl cells very gently, and they were kept on ice for 30-45 minutes. The mixtures were then heat-shocked in 42°C water bath for 2 minutes, returned to the ice immediately for 5 minutes. The cells were resuspended with 900 µl 2TY media and incubated at 37°C for 30-45 minutes. After the incubation, they were centrifuged at 4722 rcf for 1 minute and the supernatant was poured off. The cells were plated out onto 2TY-Ampicillin plates and the plates were kept in 37°C room for overnight.

2.5.5- *E.coli* transformation using electrocompetent cells

Electrocompetent cells were used to transform the yeast total DNA which contains the plasmid made in *S. cerevisiae* by homologous recombination method (described in Section 2.6.10). The electrocompetent cells were taken out of -80°C freezer and thawed on ice. The yeast DNA was diluted 10X in sterile dH_2O. Forty µl electrocompetent cells were mixed with 10 µl diluted yeast DNA. The final mixture was transferred into precooled 2 mm electroporation cuvettes (Geneflow). Each cuvette was placed into BIORAD Micropulser and electroporated using the ''EC2'' setting. Immediately after, the cells were resuspended with 600 µl 2TY and transferred into fresh Eppendorf tubes. The tubes were incubated at 37°C for 30 minutes and then were centrifuged at 1844 rcf for 5 minutes. Most of the supernatant was removed and the remainder was plated out onto 2TY-Ampicillin plates. The plates were kept at 37°C for overnight.

2.6- DNA procedures

2.6.1- PCR

The different PCR polymerases and buffers were supplied by Meridian Bioscience (formerly Bioline). The oligonucleotides were supplied by Merck (formerly Sigma-Aldrich). The PCR protocols and primers used in this research are described in Table 2.6 and Table 2.7 respectively. To set-up a PCR reaction, the components described in Table 2.6A were added into the PCR tubes on the ice rack. Then, the tubes were put into the thermocycler (purchased from Biometra, MWG-BIOTECH and SensoQuest) with the settings described in Table 2.6B.

The melting temperature and annealing temperature for each primer were calculated by the formulas below, based on the nucleotide sequences of each primer. After the annealing

temperatures are calculated, the lower value was determined as the annealing temperature of the PCR reaction (descried as ''*'' on Table 2.6b).

Melting temperature(°C) = 4(Number or C+G) + 2(Number of A+T)

Annealing temperature (°C) = Melting temperature – 5

Table 2.6: PCR protocols that were used in this research. The protocols were adapted from the manufacturer (Meridian Bioscience) and slight changes were made. A) PCR setup with the components. B) Different cycling conditions. The asterisk (*) indicates the annealing temperature of the reaction, which is determined upon the calculations above. In the extension step, ''kb'' indicates the length of the final PCR product.

A)

MyTaq	Velocity	MyFi
-5 µl 5x MyTaq reaction buffer -2.5 µl 5 µM forward primer -2.5 µl 5 µM reverse primer -0.25-1 µl MyTaq polymerase(5 Units/µl) -0.5-1 µl template DNA (if plasmid, 1 µl 1:50 diluted plasmid) -Sterile H_2O up to 25 µl	-5 µl 5x Hi-Fi reaction buffer -2.5 µl 5 µM forward primer -2.5 µl 5 µM reverse primer -2.5 µl 2.5 mM dNTP mix -0.25-1 µl Velocity polymerase (2 Units/µl) -0.5-1 µl template DNA (if plasmid, 1 µl 1:50 diluted plasmid) -Sterile H_2O up to 25 µl	-5 µl 5x MyFi reaction buffer -2.5 µl 5 µM forward primer -2.5 µl 5 µM reverse primer -0.5-1 µl MyFi polymerase (2 Units/µl) -0.5-1 µl template DNA (if plasmid, 1 µl 1:50 diluted plasmid) -Sterile H_2O up to 25 µl

B)

Cycles	Steps	MyTaq	Velocity	MyFi
1 cycle	1) Initial denaturation	95°C, 2 minutes	98°C, 2 minutes	95°C, 2 minutes
25-35 cycles	2) DNA denaturation	95°C, 30 seconds	98°C, 30 seconds	95°C, 30 seconds
	3) Primer annealing	*, 30 seconds	*, 30 seconds	*, 30 seconds
	4) Extension	72°C, 60 seconds/kb	72°, 15-30 seconds/kb	72°C, 60 seconds/kb
1 cycle	5) Final extension	72°C, 5-10 minutes		

Table 2.7: List of primers that were used in this study.

Primer Name	5'-->3' sequence	Primer Description/Application
VIP49	GTTTTCCCAGTCACGACG	In all the *E. coli* plasmids. To be used for sequencing, colony PCR and linearization of the gene deletion cassettes where necessary.
VIP50	GGAAACAGCTATGACCATG	
VIP3936	CTCGGTACCTGTATTGAAACCACGCGCCAC	To clone 1 kb upstream of *DhMDH3* into the pDh1.
VIP3937	CATGGATCCTGCTGCTCCGCAAACTGTAAC	
VIP3938	CGCTCTAGACTCTATCGACCAGGGTACTAC	To clone 1 kb downstream of *DhMDH3* into the pSLV3.

VIP3939	CTCGCATGCAATCACCTTGCCTACCCAGTC	
VIP3932	GTGAAACATCAGGGAGAGGC	~200 bp outside of 1 kb upstream of *DhMDH3* ORF.
VIP3933	TAATCGCTGACAGTGCCATAGC	~200 bp outside of 1 kb downstream of *DhMDH3* ORF.
VIP3934	TGAACTCGACCGTGCCAATTG	Within the *DhMDH3* ORF. To check the WT copy in KO genomes or the integration of tagging construct into the genome.
VIP3935	AGCATTAGGACACGCCTTAC	
VIP3940	CACTGGCAAACTGTGATGGAC	Within the *hygB*^{r} ORF. To check the integration of *hygB*^{r} marker into the genome.
VIP3941	GCCATGTAGTGTATTGACCG	
VIP3983	TAGGAACACTGCAAGCGCATC	Within the *G418*^{r} ORF. To check the integration of *G418*^{r} marker into the genome.
VIP3984	AACAGCGATCGCGTATTTCG	
VIP4112	AACACATACATAAACGAGCTCAAAATGTCACAATATAGAGCCAATC	To clone *DhGPD1* into pEH116 (For *S. cerevisiae* expression).
VIP4113	CAGGTCGACTCTAGAGGATCCTTTGAATAATGAATGGTCTCC	
VIP4114	CACATACATAAACGAGCTCAAAATGACTTCTACACCATTTAATATTG	To clone *DhGPD2* into pEH116 (For *S. cerevisiae* expression).
VIP4115	CAGGTCGACTCTAGAGGATCCATCTCTTTCTAAGATGACTGG	
VIP4089	CATGGGTACCACTATCCCCACTGGCACTTG	To clone 1 kb upstream of *DhFOX2* into the pDh1.
VIP4090	CATGACTAGTTGTTAAGTTCCTTGCCGCTC	
VIP4127	GATCGTCGACAGGCTAAGATCTAAGCTAGC	To clone 1 kb downstream of *DhFOX2* into the pSLV13.
VIP4100	CTAGAAGCTTGTGGCCACCAGAAGTCTTTC	
VIP4093	TTCTAACCTGTCCCATCAAG	~200 bp outside of 1 kb upstream of *DhMDH3* ORF.
VIP4094	CAACAATAACATCCCATGCCG	~200 bp outside of 1 kb downstream of *DhMDH3* ORF.
VIP4095	ATCAGCAACGGCAATTCCAC	Within the *DhFOX2* ORF. To check the WT copy in KO genomes.
VIP4096	ATGGTATGTCTGCTAAGGTC	
VIP81	GTTTGTATTCTTTTCTTGC	Anneals to the *TPI1* promoter in pEH116, used for sequencing.
VIP272	CCCATTAACATCACCATC	Reverse primers within GFP ORF, used for colony PCR or sequencing.
VIP466	TTGTCGGCCATGATGTATACG	
VIP4162	CATGGGTACCCATCGATGCCAATACAACCG	To clone 1 kb upstream of *GPD1* into pZA1.
VIP4163	CATGAAGCTTGGCTCTATATTGTGACATTGG	
VIP4164	CATGGCGGCCGCAGATCAGCAACGTTAAGCCG	To clone 1 kb downstream of *DhGPD1* into pSLV18 (VIP4165 was also used to check the integration of *GPD1* tag into the genome).
VIP4165	CATGGAAGCTCATCCAGATCACCGGATAGAG	
VIP4166	AACTCGCAACTGGACAAGAG	~200 bp outside of 1 kb upstream of *DhGPD1* ORF.
VIP4167	GGCCAAAGGTTACACGTAAC	~200 bp outside of 1 kb downstream of *DhGPD1* ORF.
VIP4168	CGAAATTGCTCTGGTGGTTG	Within the *DhGPD1* ORF. To check the deletion of *GPD1* (VIP4169 was also used to check the integration of *GPD1* tag into the genome).
VIP4169	GGTGACAATGCTAAATCGGC	
VIP3397	AGCACACACCCACAACAAC	Within the *SAT1* ORF. To check the integration of *SAT1* marker into the genome.
VIP3901	AGACAGCTCCTTGGCATACG	
VIP4257	AACACATACATAAACGAGCTCAAAATGGCCGAAATTGAAGAACTTGCCC	To clone *DhPMP47a* ORF into pEH117.
VIP4238	CCTTTACTCATTGCACCCGCCCCTGCTCCCTGCAGTTTAACAGCATTCTTCTTC	
VIP4237	GGCAAGATAAACGAAGGCAAAGAGCTCAAAATGGCCGAAATTGAAGAACTTGCCC	Annealing to *HIS3* promoter end and the beginning of *DhPMP47a*. Used for colony PCR to check the insert in pSLV25.
VIP4318	CACATACATAAACGAGCTCGGTACCCGGGGATCCATGTCAAGCCCTGTTACTTTAC	To introduce *DhLYS1* into pEH117.
VIP4319	CTCATTGCACCCGCCCCTGCTCCCTGCAGATCTAATCTGGCAACGTGTTTGTC	
VIP4320	GGCATGGATGAACTATACAAAGGATCCATGTCAAGCCCTGTTACTTTAC	To introduce *DhLYS1* into pEW332.
VIP4321	GATCTATCGATAAGCTTGCATGCCTGCAGTCAATCTAATCTGGCAACGTG	

VIP4380	AACACATACATAAACGAGCTCGTCGACAAAAT GAAAGGCAAATTAGCGC	Annealing to the beginning of *DhLYS1* ORF. Used for colony PCR.
VIP1712	GAGCCCTCCATGTGCACC	Annealing to mCherry. Used for colony PCR.
VIP4398	GTGTTGAAGAATTGACTAATAGGTCAGAAAAG GTAGTAACAAAGAGTAACAAACAACAAAACGG GGATCCATGCATACTAG	To generate *DhPMP47* KO construct using either *hygB*^{r} or *G418*^{r} markers of pDh1 or pDh2 respectively.
VIP4462	CGTCAACATTTTAAAATGGCTTGATAATATATT GAAGTATTTAACCAAATGCATACTTATATACTC CTGCAGGTCG ACTCTAGAG	
VIP4460	CGATAAGACTGCAAGTGTCGTGTATATAAATTG CGTCGGTATAGCTGACAAAATCAGATAATGAA GAAATCGGGGATCCATGCATACTAG	To generate *DhNPY1* KO construct using either *hygB*^{r} or *G418*^{r} markers of pDh1 or pDh2 respectively.
VIP4461	ATACACTTTATAGTCTATAGAATAAAATTTAAG TATTTTCCGATTCAATTCTAGAAATGTAACAGCC ATCCTGCAGGTCGACTCTAGAG	
VIP4425	ACGTTACAGACTCGTTCTGC	Outside of KO flanks of *DhPMP47* ORF. To check *DhPMP47* deletion (VIP4426 was also used to check the integration of *PMP47* tag into the genome).
VIP4426	CTATGCGGATGTTTATGCGG	
VIP4427	CTTGTTCGCAGGTGTGTTAC	Within the *DhPMP47* ORF. To check *DhPMP47* deletion (VIP4427 was also used to check the integration of *PMP47* tag into the genome).
VIP4428	GACAATCGCTTTGAACGTAG	
VIP4513	AACAGCTTCCAGCATGCTTC	Outside of the KO flanks of *DhNPY1* ORF. To check *DhNPY1* deletion.
VIP4514	CTCTATGTCCGCATATGAGG	
VIP4515	CTGGGTGTGGTTCTAGAGTC	Within *DhNPY1* ORF. To check *DhNPY1* deletion.
VIP4516	TTACCACTGCTCCAGTCTTC	
VIP4517	ACGGATCGAATTCGTGGAAATCTATCATTAGTA GCCAGTTATCAATCTAATAAGTCAAGACGAAGT TATGGAATGATCCAGAGG	To generate a construct to tag *DhMHD3* in *D.hansenii* genome.
VIP4519	TAATAACGACAATGGTTGCCCAATGCCTCCTGC TGCTCCGCAAACTGTAACTTTAACCATTGCGCC AGCTCCTGCACCTTTGTATAGTTCATCCATGCC	
VIP4559	CGAGGCCCATCTTCACATGTGACTCAAAGTCAT ATAACCATGATGGGGTACTAAATGTTACTTAAA CGGATCGAATTCGTGGAAATC	To extend the homology arms of *DhMHD3* tagging construct above.
VIP4560	GCAACCCCATTTGCATTAACCACATCAAATAAC GACAATTCGCTCACTTGCGGGTTTAACTTTAAT AATAACGACAATGGTTGCCC	
VIP465	CCACACAATCTGCCCTTTCG	Within GFP. To check the integration of GFP tags *D. hansenii* genome/colony PCR.
VIP467	CCATGTGTAATCCCAGCAGC	
VIP4410	CATCTGCAGCTATAATTTCGAACCAGTTACG	Anneals to the end of *DhMDH3* ORF. To check the integration of *MDH3* tag in *D. hansenii* genome.
VIP4664	TTTGGAATGGGGCCCGGCCATTAGCCCGATAA GACTGCAAGTGTCGTGTATATAAATTGCGTCGG TATAGCTGACAAAATCAGATAATGAAGAAATC GAAGTTATGGAATGATCCAGAGG	To generate a construct to tag *DhNPY1* in *D.hansenii* genome.
VIP4665	ATAATAACTATCTTGTTTCAGCTTACTGATTGAT GATTGAAATCGAATCGAAAGTCTTGGTATCTTA CTGAAAACGCCCATTGCGCCAGCTCCTGCACCT TTGTATAGTTCATCCATGCC	
VIP4704	ACGTATCCATCTCATCTTAGATAAGTTCATCTTC GTATCAGAAAGGCGTAAGTGTAGTATTATTGA AAGATTTGGAATGGGGCCCGGCCATTAG	To extend the homology arms of *DhNPY1* tagging construct above.
VIP4705	AACTATCTCTGCTCCAAAGTATGAGCTATGATC TTGTCCATGAATAGGATTTAATACGTTACCCGA CATCTTATAATAACTATCTTGTTTCAGC	
VIP4745	TTAGACAGCAAAAAATAGACGTTAAACCCTTTA TATAGGGACTTGTATACAAATTAATAATACGCC GGGGATCCATGCATACTAG	To generate *PMP47b* KO construct using *G418*^{r} marker of pDh2.

VIP4746	GATAAAACTTCTAAATAGATAACAAATTGGTAATGATGCTAATAATATTGAATAAATGCTATATGTCCTGCAGGTCGACTCTAGAG	
VIP4747	GCCGTTGTATTGCAACTTGC	Outside of KO flanks of *DhPMP47b* ORF. To check *DhPMP47b* deletion.
VIP4748	AGCTACCAGCTCAAGTGATC	
VIP4749	AATATCGTCTTGAAGGCGCC	Within *DhPMP47b* ORF. To check *DhPMP47b* deletion.
VIP4750	TTCTGTTCAGCTTTGACGGC	
VIP4751	CTGGCTCCGTCAAATTGGTCCAAATCTTCAAATTAATGTGAAAATGAAGAAGAATGCTGTTAAAGGATCCGGTGCAGGAGCTGGCGCAGTCGACCTCGAGATG	To generate a construct to tag *DhPMP47* in *D.hansenii* genome.
VIP4752	CTCTCGGCAACTGACGTCAACATTTTAAAATGGCTTGATAATATATTGAAGTATTTAACCAAATGCATACTTATATACTCTACCCAATCTATCTTCTGAGGTG	
VIP4753	AATTGATTCAATCGATCACTACAGCCGCGTTTTTATTCTACTTTAAAGAGGAATTATTAACTGGCTCCGTCAAATTGGTC	To extend the homology arms of *DhPMP47* tagging construct above.
VIP4754	CTCATTTATTGGGCAGAAAAATGAAGCATAAATCCAGCTACTGCGCATATGTTGCAGTATCACCAAATTTTTCGGGCTCTCGGCAACTGACGTCAAC	
VIP4778	CGACTCGAGATGAGTAAAGGAGAAGAACTTTC	To clone *Dh*-optimised GFP ORF into pMP34.
VIP4779	CATTCTAGACTATTTGTATAGTTCATCCATGCC	
VIP4780	CATGCGGCCGCACCCGCTCTTGACGGTTAC	To clone *MgACT1* promoter-*Dh*-optimised *mCherry* into pSA5. VIP4781 introduces PLH-SKL to the end of *mCherry* for peroxisomal marker.
VIP4781	CAGGTCGACCTAGAGTTTTGAGTGCAGTGGTTTATATAATTCATCCATACCACC	
VIP4798	CATGCGGCCGCCGAAGTTATATCTGATGTCTC	To amplify *PsGPD1* promoter and clone it into pSLV35 (for replacing with *MgACT1* promoter).
VIP4799	CAGCTGCAGGATTGATTATGACTATAATGTGTG	
VIP4016	AGGAGCGCGGTATATAGATC	Outside of 1 kb flanks of *DhARG1*. To check the integration of red marker into the *ARG1* locus.
VIP4019	CAGCGGGTATAGTTGGAATG	
VIP4793	GAAGATGGTGGTGTTGTTAC	Within mCherry. To check the integration of red marker into *DhARG1* locus.
VIP4877	TCCCATTATTTGAAGCTACTTATCAAATTATATACGGTGATGAATCTATTCAAAACTTGCCAAACTTATTAGAAGACCATTCATTATTCAAAGAATTCGAGCTCGGTACCCG	To generate a construct to tag *DhGPD1* in *D.hansenii* genome.
VIP4878	CATGCTACTGGTTGTCTAACCAAAAAAAAAAGGCGTCAAAATGAAACGCATCTAATATACATGAAACGGCTTAACGTTGCTGATCTACCTGCAGGTCGACTCTAGAG	
VIP4879	AGAAGCAGAAAAGAAATTATTGAATGGCCAATCCTCGCAAGGTATCATCACTGCAAAGGAAGTCCATGAGTTATTAAGCAATGTTGGTAAGACTGATCAATTCCCATTATTTGAAGCTAC	To extend the homology arms of *DhGPD1* tagging construct above.
VIP4880	TCGTATGTATTATAGTAATAATAAAAATCAATGATATTGTAATATTCTGTATATTTTCTATGTGATAAATAAATAACGACAAACTTAAAAATAAATTTGTCATGCTACTGGTTGTCTAAC	

2.6.2- Agarose gel electrophoresis

Agarose gel electrophoresis was done to analyse PCR and restriction digested products. One percent agarose gel for analysing PCR products or 0.7% agarose gel for analysing restriction digests was used. It was prepared by heating Agarose powder (purchased from Geneflow) in 1X TAE Buffer (0.1 M Tris-

Base, 0.1 M Acetic Acid, 10 mM EDTA,pH=8, purchased from BIORAD) until the powder melted. Then, Ethidium Bromide (from Merck) was added to a final concentration of 0.5 µg/ml.

The DNA samples were mixed with 6X purple loading dye to 1X (2.5% Ficoll®-400, 10 mM EDTA, 3.3 mM Tris-HCl, 0.08% SDS, 0.02% red/pink dye, 0.001% blue dye, pH 8. Purchased from New England Biolabs). The samples were loaded into wells along with 1 kb HyperLadder (from Bioline). They were run at 95 Volts for 35 to 60 minutes in 1X TAE (the power supply was purchased from BIORAD). After the run, the gels were analysed under ultraviolet (UV) transilluminator supplied by GeneSys, using GeneSys Software.

2.6.3- DNA precipitation

The DNA precipitation was done using the PCR products to be transformed into *D. hansenii*, prior to the transformation protocol described in Section 2.4.2. After the PCR, the PCR product was resuspended with 1/10 volume of 3 M NaAc at pH=5.2 and 2.5X volume of 100% Ethanol in 1.5 ml Eppendorf tube. The tube was kept in -20 freezer for 2 to 24 hours, centrifuged at 4°C at 12000 rpm for 15 minutes, using the accuSpin Micro R centrifuge (Fisher Scientific) . The DNA pellet was washed in 70% ethanol and centrifuged at maximum speed using Sigma 1-14 microfuge for 5 minutes. Finally, the pellet was dried and resuspended with 1X TE (10 mM Tris-HCl at pH=7.5, 0.1 mM EDTA). The precipitated DNA was quantified after being run on 1% Agarose gel, via ''Quick Quant'' feature of GeneSys software.

2.6.4- PCR purification

QIAquick PCR purification kit was used to purify the PCR products prior to classical cloning. The kit was purchased from QIAGEN and the purification was performed according to the manufacturer's protocol.

2.6.5- Restriction digest

Five hundred-1000 ng plasmid DNA, 1 µl of each restriction enzyme, 2.5 µl 10X appropriate buffer and dH_2O were brought to 25 µl final volume in Eppendorf tube and the tubes were incubated at 37°C for 4 hours or overnight. Each restriction enzyme and buffer were purchased from New England Biolabs.

2.6.6- Gel extraction

The digested samples were run on 0.7% Agarose gel before the gel extraction. Then; using the DR-45M dark reader (GRI Labcare Service), the samples were excised from the gel using a scalpel. They

were purified afterwards using QIAGEN Gel Extraction kit (from QIAGEN), according to the manufacturer recommendations.

2.6.7- Ligation

The ligase and buffer were purchased from New England Biolabs. The vector to insert ratio was calculated in size (bp) first. Then, the amount of 20-30 ng 1X copy of vector and 3X copy of insert were calculated (For example; if vector size/insert size is 5:1 and 20 ng vector is used, 5x3=15 ng insert was used). The vector, insert, 1 µl 10X T4 DNA ligase and 1 µl 10x T4 DNA ligase buffer were brought to 10 µl final volume by adding dH_2O. Then, each ligation sample was incubated at the room temperature for overnight to be transformed into *E. coli*.

2.6.8- Plasmid miniprep

The E. coli transformants that carry the plasmid were inoculated into 5 ml 2TY-Ampicillin and incubated on shaker for overnight at 37°C. The next morning, the cells were pelleted and plasmid was isolated using QIAGEN Plasmid Miniprep kit, according to manufacturer recommendations.

2.6.9- Sequencing

The DNA sequences of newly made plasmids were confirmed by Sanger Sequencing, which was carried out by Source Bioscience. The samples were prepared and shipped to Source Bioscience Labs using their recommendations. Results were received as a Snapgene file and analysed by Clustal Omega database (Sievers *et al.*, 2011), by aligning both estimated and obtained plasmid sequences.

2.6.10- Plasmid construction by homologous recombination

Plasmids for expression of *D. hansenii* genes in *S. cerevisiae*, by introducing their ORFs into yeast expression plasmids, were constructed through the homologous recombination method, also referred to as the gap repair method (Orr-Weaver and Szostak., 1983) (Figure 2.2). Firstly, the target ORF was amplified by PCR. The primers were designed to introduce 18-20 nucleotides (homology arms) to the 5' and 3' ends of the target ORF, which are identical to sites of the vector after restriction digest. The yeast-*E. coli* shuttle plasmids used are YCplac33 and YCplac111. These plasmids contain an autonomous replicating sequence and a centromere and are maintained at a level between 1 and 2 copies per cell (Gietz and Sugino, 1988). In addition, the *PGK1* terminator was inserted and various promoter to regulate expression. Moreover, the plasmids contain the ORF for either green or red fluorescent protein for either N- or C-terminal fusion with the target ORF. The required plasmid was linearized using the appropriate restriction enzymes. Both, PCR product and

linearised vector were introduced into *S. cerevisiae* by high efficiency transformation, which results in homologous recombination of the homology arms, and insertion of the target ORF into the vector. This re-circularizes the plasmids and stabilises it in *S. cerevisiae* (Figure 2.2).

After the growth of colonies were observed on selective media, total DNA of the colonies (that were imaged before to see the expression of the potential ''target ORF + fluorescent tag'' fusion) were isolated by genomic DNA isolation method. Total DNAs were transformed into electrocompetent *E. coli*. After colony PCR, the plasmid from *E. coli* colonies were miniprepped and test digested, followed by sequencing.

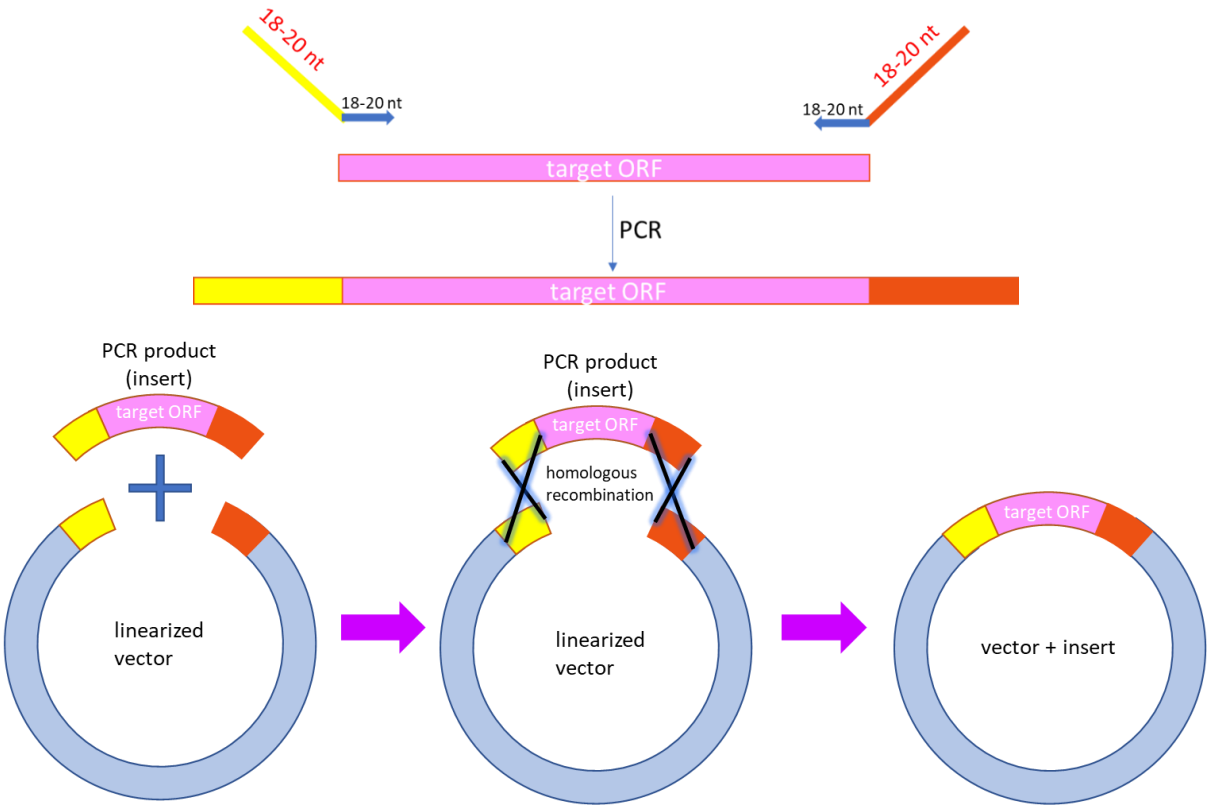

Figure 2.2: Construction of *S. cerevisiae* expression plasmids via homologous recombination method. The target ORF was amplified by PCR, using the primers that anneal to the target ORF and introduce 18-20 nucleotides of homology arms, that are identical to individual ends of double digested vector. The primers were indicated by blue arrows (18-20 nt annealing sequence) and both yellow and orange flanks (18-20 nt homology flanks), that are also present at the each ends of the linearized vector. After both insert and digested vector are introduced into *S. cerevisiae*, homologous recombination occurs in between both ends, which results in the insertion of the target ORF into the vector.

2.7- Protein procedures

2.7.1- TCA protein extraction

The yeast cultures were grown overnight until their ODs reach 1-2. That morning, 10 OD_{600} units were harvested in a 15 ml Falcon tube, centrifuged at the 4653 rcf for 5 minutes and the supernatants were removed. The pellets were resuspended with 500 µl ice cold alkaline lysis buffer (0.2M NaOH, 0.2% mercaptoethanol) and were kept on ice for 10 minutes. Then, 100 µl 30% TCA w/v (Trichloroacetic Acid) solution was added to each tube, the final mixture was resuspended and the tubes were incubated on ice for further 5 minutes. The mixtures were transferred to Eppendorf tubes and each tube was centrifuged at 4°C, in the accuSpin Micro R centrifuge (Fisher Scientific) at the maximum speed for 10 minutes. The supernatants were discarded and each pellet was resuspended in 75 µl 50% Urea. Twenty-five µl of 4x protein loading dye (250mM Tris at pH=6.8, 9.2% w/v SDS, 40% w/v Glycerol, 0.2% w/v Bromophenol brilliant blue, 100mM DTT) was added to each tube. If the mixture turned yellow (shows acidity), 1 µl of 1M Tris base was added to neutralise the mixture until the colour turned blue. Lysates were kept in -20 freezer until loading onto SDS gel.

2.7.2- SDS-PAGE Electroporesis

Before loading the lysates onto SDS-PAGE BioRad mini gels, lysates were incubated at 95-100°C for 10 minutes in dry heat block, followed by centrifugation at the maximum speed for 1 minute using the accuSpin Micro R centrifuge (Fisher Scientific).

Resolving gel (10%) and stacking gel were prepared by mixing the components on Table 2.8. After the gels polymerised, they were placed into the tank appropriately and the tank was filled with 1X protein running buffer (dilution was made from 10X stock which contains 0.25 M Tris base, 1.92 M glycine, and 1% w/v SDS. (Geneflow). After the samples were loaded, the gels were run at constant voltage (100 V) for 110-120 minutes until the dye front reached the bottom of the resolving gel.

Table 2.8: The list of reagents required to prepare resolving and stacking gels. All reagents listed were purchased from Geneflow.

Stock solutions	10% Resolving Gel (for 1 gel)	Stacking Gel (for 1 gel)
Protogel (30% w/v Acrylamide : 0.8% w/v Bis-Acrylamide)	3.3 ml	650 µl
4X Protogel Resolving Buffer (1.5 M Tris-HCl, 0.4% SDS, pH=8.8)	2.6 ml	-
Protogel Stacking Buffer (0.5 M Tris-HCl, 0.4% SDS, pH=6.8)	-	1.25 ml
10% w/v APS	100 µl	50 µl
dH_2O	4.1 ml	3.05 ml
TEMED	10 µl	5 µl

2.7.3- Western Blot Analysis

After the SDS gel was run, the blotting sandwich was assembled into the Bio-Rad gel holder cassette, with sponges, filter papers, nitrocellulose membrane and the SDS gel in the right order. The cassette was placed into the Bio-Rad electrode assembly, which was then placed into the tank. The tank was filled with transfer buffer (3.03 g Trizma Base, 14.4 g Glycine, 200 ml Methanol in 1 L final volume) and the ice pack was placed into the tank. Then, the cassette was run at constant voltage (200 V) for 2 hours, allowing the transfer of proteins from the gel onto the nitrocellulose membrane. Subsequently, the nitrocellulose membrane was placed into the tray and rinsed 3 times with TBST (10 ml of 1 M Tris-Cl at pH=7.6, 8.7 g NaCl, 1 ml Tween 20 in 1 L final volume). The membrane was stained with Ponceau S solution (0.1 % w/v in 5% acetic acid. Diluted 10X in TBST before staining) to check the transfer and loading of protein. The membrane was rinsed 3 times in TBST, then blocked with TBST+2% Marvel fat free milk for 45 minutes by rocking on an orbital shaker. Then, the membrane was rinsed 3 times with TBST, before being incubated with primary antibody solution for 2 hours, rocking on orbital shaker (anti-GFP from mouse, from Roche with a catalog number of 11814460001, was diluted 1/3000 in TBST). The membrane was rinsed 3 times with TBST, then incubated with secondary antibody for 1 hour rocking on orbital shaker (Goat-anti-Mouse, from Bio-Rad with a catalog number of 1706516, was diluted 1/1000 in TBST). The tagged protein bands were detected using EZ-ECL Chemiluminescence detection kit (Geneflow), which were captured by GBox gel doc machine (GeneSys) and GeneSys Software.

After the bands were detected using anti-GFP from mouse, the membrane was then incubated using anti-Actin (from mouse, purchased from Invitrogen) to check whether the loading has been equal. The membrane was rinsed with TBST 3 times, then was incubated in anti-Actin antibody solution (from mouse, from Invitrogen with a catalog number of MA1-744, was diluted 1/1000 diluted in 2 ml TBST) for 1 hour by rocking on the shaker. The membrane was rinsed 3 times with TBST and was incubated in secondary antibody solution (Goat-anti-Mouse antibody, from Bio-Rad with a catalog number of 1706516, was 1/10000 diluted in TBST) for 1 hour rocking on the shaker. At the end, the membrane was rinsed 3 times in TBST and the tagged protein bands were detected and captured the same way as described above.

Chapter 3- The *D. hansenii* Beta-oxidation machinery seems more elaborate than its *S. cerevisiae* counterpart

3.1-Introduction

D. hansenii is considered an oleaginous organism, as it is able to accumulate high amounts of lipids (Reviewed in Breuer and Harms, 2006). This ability to accumulate lipid is a very rare characteristic amongst yeast species (Reviewed in Ratledge, 2002). The main lipids that accumulate in *D. hansenii* are phospholipids or neutral lipids (Merdinger and Devine, 1965). This indicates that *D. hansenii* has metabolic pathways that are related to lipid metabolism, as well as proteins that are controlling these pathways (Reviewed in Breuer and Harms, 2006). Through blocking or modulating fatty acid beta-oxidation it may be possible to further increase lipid accumulation. However, fatty acid breakdown with involving proteins in *D. hansenii* has never been studied.

In *S. cerevisiae*, fatty acid beta-oxidation is restricted to peroxisomes and is well-characterized (Reviewed in van Roermund *et al.*, 2003; Knoblach and Rachubinski, 2018). A basic level of fatty acid oxidation occurs in cells but this process is highly inducible through the action of 2 transcription factors, PIP2 and OAF1, that form a heterodimer and induce expression of β-oxidation genes when the cells are grown on the long chain fatty acid oleate as sole carbon source (Karpichev and Small, 1998). The genes that are induced encode fatty acid oxidation enzymes (Karpichev *et al.*, 1997). After induction of beta-oxidation genes, fatty acids are transported across the peroxisomal membrane and oxidised via a multistep process as described in Figure 1.5. Additionally, the third step of the beta-oxidation in *S. cerevisiae* requires NAD^+ as a cofactor (Hiltunen *et al.*, 1992; reviewed in Hiltunen *et al.*, 2003). However, NAD^+ is not efficiently imported into peroxisomes and therefore requires to be regenerated inside peroxisomes (van Roermund *et al.*, 1995). This is achieved by both Malate Dehydrogenase (Mdh3) and Glycerol 3-Phosphate Dehydrogenase 1 (Gpd1) in *S. cerevisiae* (van Roermund *et al.*, 1995; Al-Saryi *et al.*, 2017a). Thus, *mdh3/gpd1Δ* cells show a remarkable growth defect on oleate and fatty acid beta-oxidation defect. Mdh3 is playing a major role whereas Gpd1 has a minor contribution. In addition, these proteins also contribute to the regeneration of NAD^+ required during the final step of lysine biosynthesis which takes places in peroxisomes in *S. cerevisiae* (Al-Saryi *et al.*, 2017a).

In this chapter, the potential beta-oxidation proteins of *D. hansenii* were identified using bioinformatics. In contrast to *in S. cerevisiae* where the core enzymes for beta-oxidation, are encoded by single genes, in *D. hansenii*, multiple genes were found that potentially encode Acyl-CoA Oxidase, and 3-Ketoacyl-CoA Thiolase. In addition to the core enzymes, some additional potential beta-oxidation proteins were identified in *D. hansenii* that are not present *S. cerevisiae*. It was also found out that some proteins such as *Dh*Gpd1, have peroxisomal targeting signals that are not accepted as consensus.

In order to study fatty acid metabolism in *D. hansenii*, new and more efficient gene deletion methods needed to be developed to generate mutants and this is described in this chapter. Using these new tools, *MDH3* and *GPD1* were successfully deleted. However, unlike in *S. cerevisiae*, neither single knock-outs nor double knock-out resulted in a growth defect on oleate.

These results indicated that beta-oxidation process seems to be more complex in *D. hansenii* compared to well-characterized *S. cerevisiae* beta-oxidation pathway, and additional proteins might be playing a role in lipid breakdown in this organism.

3.2- Identification of potential beta-oxidation related proteins in *D. hansenii* via bioinformatics

The preliminary bioinformatics research focused on detecting *D. hansenii* proteins that contain either a peroxisomal targeting signal type 1 (PTS1) or type 2 (PTS2). Using the Scan Prosite database by Expasy (Sigrist *et al.*, 2002; Sigrist *et al.*, 2012), the proteins with the possible PTS1 and PTS2 motifs were filtered amongst *D. hansenii* proteome. To identify the proteins with possible combinations of PTS1, the proteins with (S/A/C/N/P/Q/E/V)-(K/R/H/Q/N/S)-(L/M/I/F) motif near the C-terminus (Neuberger *et al.*, 2003) were analysed. To identify the proteins with possible PTS2, the proteins with (L/V/I/Q)-X-X-(L/V/I/H/Q)-(L/S/G/A/K)-X-(H/Q)-(L/A/F) motif near the N-terminus (Petriv *et al.*, 2004) were analysed. As we are aware that there will be potentially false positives and we will miss some peroxisomal matrix proteins as they might have targeting signals slightly deviating from the consensus or because they actually lack a PTS1 or PTS2, we also employed a second approach. The second approach was based on detecting the potential *D. hansenii* homologs of the peroxisomal proteins that have been identified in *S. cerevisiae* and *U. maydis* so far, using Blast searches (Altschul *et al.*, 1990) and the paper by Camoes *et al.* (2015) as a point of reference. By comparing the results of both searches, the potential proteins related to beta-oxidation in *D. hansenii* was listed which can be seen on Table 3.1. The factors to determine the potential *D. hansenii* homologs (listed in the Table 3.1) were lower E-value, higher percentage identity as well as higher query coverage in blastp search (Altschul *et al.*, 1990), Uniprot analysis (Apweiler *et al.*, 2004) to check the similarity in between the query protein and *D. hansenii* hit in terms of the protein function and protein domains, as well as reciprocal blast (Altschul *et al.*, 1990), to see whether the query protein comes up as a best hit when *D. hansenii* hit is blasted back against query organism.

Table 3.1: The list of potential peroxisomal proteins of *D. hansenii* that might be related to beta-oxidation pathway. Uniprot accession numbers of each *D. hansenii* hit are provided, as well as the information of whether their potential orthologs in *H. sapiens*, *S. cerevisiae* and *U. maydis* (indicated as *Hs*, *Sc* and *Um* on the table respectively) were identified. Query organism, E-value, percentage of identity and query coverage for each hit, that came up when each previously-identified proteins in Camoes *et al.* (2015) were blasted against *D. hansenii* proteome, are also provided on the table.

Protein	Potential hits in *D. hansenii*- Uniprot accession codes	Potential PTS1/PTS2?	in *Hs* ?	in *Sc* ?	in *Um* ?	Query organism used for blast, E-value, identity percentage (%) and query coverage (%) respectively
Acyl-CoA oxidase (Pox1)	Q6BVP3, Q6BRD5, Q6BRD8	No	Yes	Yes	Yes	*S. cerevisiae* (for all of them), Q6BRD5: 0, 44.34%, 97%. Q6BVP3: 0, 43.13%, 97%. Q6BRD8: 6e-175, 41.22%, 99%
Acyl-CoA Dehydrogenase (Acad11n)	Q6BX30	PTS1 (-SKL)	Yes	No	Yes	*U. maydis*, 6e-132, 49.28%, 87%
Acyl-CoA Dehydrogenase C (Acad11c)	Q6BQL2	PTS1 (-SKL)	Yes	No	Yes	*U. maydis*, 2e-57, 31,23%, 90%
3-hydroxyacyl-CoA dehydrogenase and enoyl-CoA hydratase (Fox2)	Q6BYL5	PTS1 (-AKI)	Yes	Yes	Yes	*U. maydis*, 0, 46.83%, 98%
3-Ketoacyl-CoA thiolase (Pot1/Fox3)	Q6BVV6, Q6BNX5, Q6BR82	Q6BVV6: PTS2 (-RLNQVLGHL), Q6BXN5: PTS2 (-RLNQLSGQL), Q6BR82: none	Yes	Yes	Yes	*S. cerevisiae* (for all of them), Q6BXN5: 2e-153, 59.17%, 94%. Q6BVV6: 5e-150, 55.27%, 99%. Q6BR82: 1e-96, 41.13%.
Sterol Carrier Protein 2 (Pox18)-like protein	Q6BYJ2	PTS1 (-AKL)	Yes	No	Yes	*U. maydis*, 6e-23, 42.98%, 97%
Malate Dehydrogenase 3 (Mdh3)	Q6BM17	PTS1 (-SKL)	No	Yes	Yes	*U. maydis*, 1e-111, 58%, 98%
Glycerol-3-phosphate Dehydrogenase (Gpd1)	Q6BM03	Non-consensus PTS2 (-RANQRLQQL)	Yes	Yes	Yes	*S. cerevisiae*, 4e-177, 63.93%, 93%
Carnitine-O-Acetyltransferase	B5RTK8	PTS1 (-AKL)	Yes	Yes	Yes	*U. maydis*, 2e-75, 28.92%, 90%
2,4-Dienoyl-CoA reductase (Sps19)	Q6BVJ4, Q6BH12	PTS1 (Q6BVJ4:-NKL, Q6BH12: -SKL)	Yes	Yes	Yes	*U. maydis* (for both), Q6BVJ4: 7e-93, 49.28%,

						90%. Q6BH12: 3e-91, 53.10%, 90%
Delta3,5-Delta2,4-dienoyl-CoA isomerase (Dci1)	Q6BML0	No	Yes	Yes	Yes	*U. maydis*, 1e-33, 31.10%, 86%
Related to Δ3,Δ2-enoyl-CoA isomerase (Eci1)	Q6BQU9, Q6BZL5	No	Yes	Yes	Yes	*U. maydis* (for both), Q6BQU9: 3e-36, 32.41%, 92%. Q6BZL5: 2e-31, 30.07%, 91%
Peroxisomal Acyl CoA Thioesterase (thioester hydrolase)	Q6BPV5, Q6BZL6, Q6BPV3, Q6BPV4	Q6BPV5: PTS1 (-AKL), Q6BZL6: PTS1 (-PKL), Q6BPV3: PTS1 (-AKL), Q6BPV4: none	Yes	Yes	Yes	*U. maydis* (for all of them), Q6BPV5: 1e-22, 24.33%, 85%. Q6BZL6: 2e-16, 25.47%, 77%. Q6BPV4: 9e-16, 25%, 80%. Q6BPV3: 1e-08, 31.91%, 47%
Related to Acyl-CoA Ligase	Q6BWM7, Q6BSB7, Q6BSB6, B5RV06, Q6BWF8, Q6BJ16	Q6BWM7: PTS1 (-SKF), Q6BSB7 & B5RV06: PTS1 (-AKF), Q6BWF8: PTS1 (-SKL). Q6BSB6 & Q6BJ16: none	Yes	Yes	Yes	*U. maydis* (for all of them), Q6BWM7: 2e-94, 29.79%, 95%. Q6BSB7: 8e-82, 27.55%, 97%. Q6BSB6: 1e-77, 26.89%, 97%. B5RV06: 3e-75, 28.68%, 90%. Q6BWF8: 1e-70, 28.15%, 90%. Q6BJ16: 1e-52, 27.3%, 80%.
Very Long Chain acyl-CoA Synthase (Fat1)	Q6BL99	PTS1 (-AKL)	Yes	Yes	Yes	*U. maydis*, 9e-119, 33.63%, 100%
Peroxisomal Half ABC Transporter (Pxa1)	Q6BUD3	No	Yes	Yes	Yes	*U. maydis*, 0, 41.64%, 78%
Peroxisomal Half ABC Transporter (Pxa2)	Q6BWT7	No	Yes	Yes	Yes	*U. maydis*, 6e-158, 38.34%, 79%
Peroxisome Membrane Protein (Pmp47/Pmp34)	Q6BI42	No	Yes	Yes	No	*U. maydis*, 5e-57, 35.35%, 89%
Adenine Nucleotide Transporter 1 (Ant1)	Q6BQ51	No	Yes	Yes	Yes	*U. maydis*, 3e-60, 34.82%, 92%
Peroxin 11 (Pex11)	Q6BYZ1	No	Yes	Yes	Yes	*S. cerevisiae*, 3e-51, 37.25%, 100%
Nudix Hydrolase (Npy1)	Q6BV93	PTS1 (-NKL)	Yes	Yes	Yes	*S. cerevisiae*, 6e-87, 39.23%, 95%

The bioinformatics study revealed that there could be multiple versions of some of the beta-oxidation enzymes. For example, there are 3 potential protein hits for Acyl-CoA Oxidase (Pox1) and 3-Ketoacyl-CoA Thiolase (Pot1), in contrast to Pox1 and Pot1 in *S. cerevisiae* that have only single version. Secondly, it showed that *D. hansenii* might have additional beta-oxidation enzymes that do not exist in *S. cerevisiae*. For example, hits for Acyl-CoA Dehydrogenase (Acad11n and Acad11c) were detected in *D. hansenii*, as well as Peroxisomal Membrane Protein 47 (Pmp47). Finally, it was found that some *D. hansenii* proteins have a potential PTS sequences that are uncommon and different from the consensus sequences. For example, Gpd1 in *S. cerevisiae* has PTS2 (Jung *et al.*, 2010), whereas the potential *D. hansenii* Gpd1 had PTS2-like sequence that did not fit the consensus PTS2 sequence. However, further experiments revealed that *Dh*Gpd1 is targeted into the peroxisomes via PTS2-dependent pathway (See Section 3.5).

3.3- Development of gene deletion strategy and different gene deletion markers for *D. hansenii*

Even though we can study some *D. hansenii* proteins by heterologous expression in *S. cerevisiae*, for which the wide range of tools are well-developed, for more detailed analysis of the beta-oxidation proteins, the ability to generate single or multiple knock-outs in *D. hansenii* was required. Therefore, gene deletion tools were developed for *D. hansenii*, using different gene deletion markers. Two new gene deletion plasmids with different antibiotics resistance markers were developed first. Then, the minimum concentration required for each antibiotic to be used was determined by Minimum Inhibitory Concentration (MIC) Assays. Finally, a homologous recombination based gene deletion strategy was developed which allowed us to successfully generate single, double or triple knock-outs in *D. hansenii*.

3.3.1- Development of new plasmids with different selectable markers for genetic manipulations in *D. hansenii*

In order to be able to perform genetic manipulations in *D. hansenii* such as gene knock-out or tagging in the genome, 2 new gene deletion plasmids were designed and synthesised. As a selectable marker, *hygB*^{r} and *KAN*^{r} were selected, that confer resistance to hygromycin B (Gritz and Davies, 1983) and kanamycin in prokaryotes and *G418* (geneticin) in eukaryotes, respectively (Davies and Jimenez, 1980; Agaphonov *et al.*, 2010). In order to allow the efficient expression of the selectable markers, heterologous promoter and terminator sequences were selected from *Schefferomyces stipitis* (*S. stipitis*), which is another CTG-clade organism that is closely related organism to *D. hansenii* with high sequence similarity (Jeffries *et al.*, 2007). The expression of *hygB*^{r} is controlled by *TEF1* promoter and terminator of *S. stipitis*, whereas *G418*^{r} expression is controlled by *ACT1* promoter and terminator from the same organism.

The DNA sequences of the antibiotic resistance ORFs were obtained from Addgene (https://www.addgene.org/). To access the promoter and terminator sequences, Tef1 and Act1 from *S. stipitis* were identified first by blast search (Altschul *et al.*, 1990), using their *S. cerevisiae* orthologs as query sequence that are available on SGD database (https://www.yeastgenome.org/). After the best hits for *Ss*Tef1 and *Ss*Act1 were analysed on Uniprot (Apweiler *et al.*, 2004), their ORF sequences with 1 kb upstream and 1 kb downstream flanking regions were accessed via KEGG database (Kanehisa and Goto, 2000). As promoter and terminator sequences, 500 bp upstream and 250 bp downstream regions of each ORF was used respectively. All the promoter, terminator and antibiotics resistance marker ORFs that were mentioned can be seen on Appendix 3.

After accessing each promoter, terminator and antibiotics resistance ORFs, they were assembled on SnapGene® software (from Insightful Science; available at snapgene.com). Both *hygB*^{r} and *G418*^{r} ORF sequences were CTG-adapted, by changing the CTG codons to another leucine codon and placed in between the appropriate promoter and terminator (Figure 3.1). The commonly used restriction sites within the expression cassette sequences were removed in a way that the corresponding amino acid sequences will not change. Both selectable marker regions were flanked by multiple cloning sites to allow cloning, as well as loxP sites going to the same direction, which will excise the marker as a circular and non-stable DNA if Cre recombinase is expressed, hence will allow us to re-use the selectable marker if necessary (Reviewed in Nagy, 2000; Kim *et al.*, 2018).

Finally, both selectable markers were synthesised artificially and cloned into pUC19 by GenScript. These plasmids were named as pDh1 and pDh2 (Figure 3.1) and checked through DNA sequence analysis.

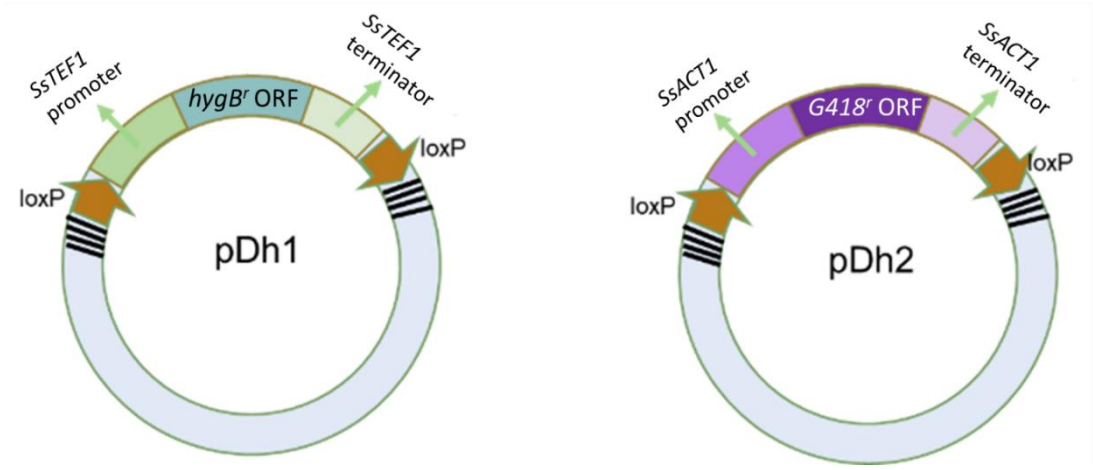

Figure 3.1: Development of pDh1 and pDh2, using *hygB*^{r} and *G418*^{r} expression cassettes respectively. The ORF sequences of *hygB*^{r} and *G418*^{r} were CTG-adapted and placed in between *TEF1* promoter and terminator and *ACT1* promoter and terminator from *S. stipitis,* respectively. Both expression cassettes are flanked by loxP sites to allow selectable marker recycling if necessary, as well as MCS (represented by black stripes) with the same orientation to allow the same gene deletion primers to fit on both plasmids where required. These cassettes were synthesised in pUC19.

3.3.2- Minimum Inhibitory Concentration (MIC) Assay

MIC Assay was performed to find out how much concentration of Nourseothricin (ClonNat), hygromycin B (hygB) and Geneticin (G418) is enough to prevent the growth of NCYC102 (YEH750) and NCYC3363 (soy WT) cells so that the gene manipulation cassettes can be used as a selectable marker in *D. hansenii*.

Dr Zeena Alwan, previously determined the minimum ClonNat concentration required to prevent growth of the *D. hansenii* isolate NCYC102 (Alwan, 2017). This concentration was then used to select for transformants that contain the ClonNat selectable marker (SAT1) cassette and allowed for selection of targeted gene deletion mutants. The same protocol was used to determine the minimum inhibitory growth concentration for ClonNat for NCYC3363 cells, as well as for hygB for both NCYC102 and NCYC3363 cells. The cells were inoculated into YM-Deb and grown overnight. The next morning, the cells were diluted to OD_{600}=1 in fresh YM Deb. In the meantime, YM Deb plates that contain various concentrations of ClonNat or hygromycin B were prepared. When the OD_{600} of the cells reach 4-5, 100 µl of the culture was plated out onto a series of YM Deb plates each containing a different concentration of ClonNat or hygromycin B. The plates were incubated at 25° for 3 days.

The minimum G418 concentration to inhibit the growth of both NCYC102 and NCYC3363 cells was determined as well. To do that, the transformation of *D. hansenii* protocol Described in 2.4.2 was performed using the cells without any insert (mock transformation). The cells were plated out onto a series of YM Deb plates each containing a different concentration of G418, and the plates were incubated at 25° for 3 days.

After 3 days of incubation, the colony number on each YM Deb plate (with different concentration of antibiotics) was analysed, with the greater focus on where the growth has remarkably decreased. The judgements about minimum antibiotics concentration to be used were based on the plates with concentrations which resulted in very little growth (only few colonies) and no growth.

The results are listed in Table 3.2. Each concentration, that was listed in Table 3.2, was used to try different gene deletions on both strains. They were confirmed by successful gene deletions. It allowed us to perform both single and multiple gene manipulations using all the markers we developed for *D. hansenii*.

Table 3.2: The MIC of ClonNat, hygB and G418 in YM-Deb medium, that were determined for both NCYC102 (YEH750) and NCYC3363 (soy WT) strains.

Antibiotics	MIC for NCYC102 strain (µg/ml) with tested concentrations	MIC for NCYC3363 strain (µg/ml) with tested concentrations
ClonNat	MIC: 1.5 (determined by Dr. Alwan).	MIC: 4 (determined in this study).
	Tested concentration range: 0.1-300 µg/ml	Tested concentration range: 1-10 µg/ml
Hygromycin B	MIC: 25 (determined in this study).	MIC: 50 (determined by Sondos Alhajouj).
	Tested concentration range: 0.5-300 µg/ml	Tested concentration range: 0.5-200 µg/ml
G418 Disulphate	MIC: 150 (determined in this study).	MIC: 350 (determined in this study).
	Tested concentration range: 0.5-300 µg/ml	Tested concentration range: 25-1000 µg/ml

3.3.3- The development of homologous recombination-based gene knock-out strategy in *D. hansenii*

At the beginning of this study, the gene deletions were performed by cloning the 1 kb upstream and 1 kb downstream of the target gene into the plasmid with selectable marker. The reason of using the long flanking regions is that in previous study, which established gene deletion system in *D. hansenii* by homologous recombination for the first time, using ~1 kb and ~500 bp flanks were reported to be efficient (Minhas, Biswas and Mondal, 2009). Based on their findings, we first generated a gene deletion cassette by introducing ~1 kb flanking regions of the target gene into selectable marker plasmid. The resulting gene disruption cassette was linearized through PCR and transformed into *D. hansenii*. This allows the homologous recombination to occur between the 1 kb flanking sequences of the cassette and the endogenous chromosome, which leads the target gene to be swapped by the selectable marker (Figure 3.2).

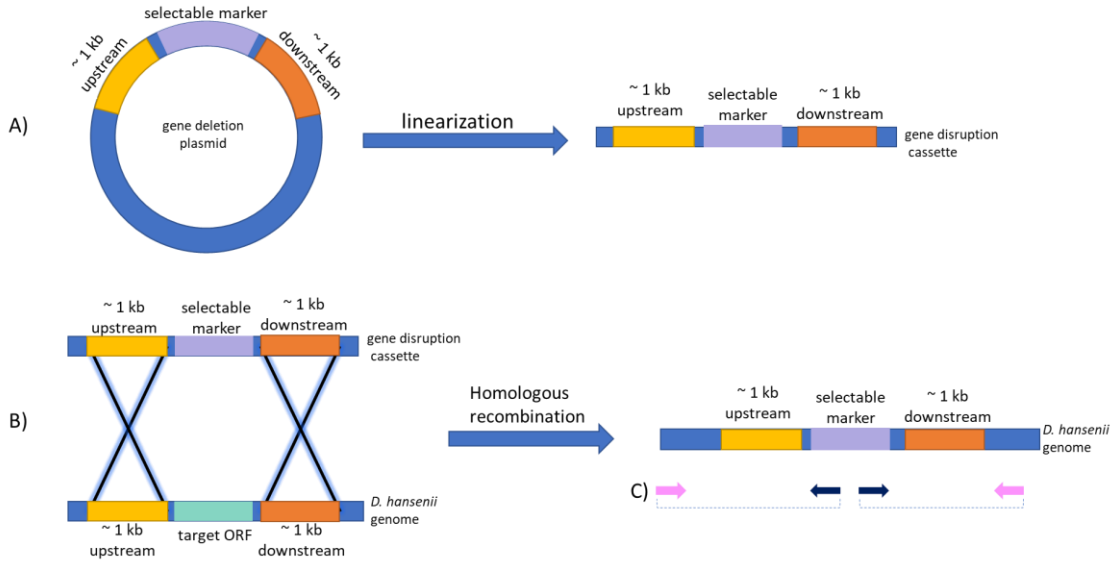

Figure 3.2: The classical gene deletion method used for *D. hansenii*, which is based on making a gene deletion plasmid first. To achieve this, ~1 kb upstream and ~1 kb downstream sequences of target gene were sequentially cloned into a plasmid containing a selectable marker. A) The resulting gene disruption cassette was released by PCR. B) The linearized cassette was transformed in *D. hansenii*, which allows homologous recombination to occur between the flanks and the chromosome, resulting in replacement of the target ORF by the selectable marker (C). The integration of the cassette into the genome was checked by PCRs, using one primer from ~200 nt outside the 1 kb flank (shown in pink) and the other primer within the selectable marker (shown in dark blue). The absence of the target gene after the deletion was also checked and confirmed, using the primer outside the 1 kb flank, and the other primer within the target gene ORF.

After it was found out in our lab that homologous recombination can also occur in between shorter flanking regions such as ~50 nucleotides in *D. hansenii*, the gene deletion method based on making gene deletion plasmid (cloning 1 kb flanks into the plasmid one after the other) was stopped as it is time consuming process. Based on previous gene disruption techniques for *S. cerevisiae* and *Schizosaccharomyces pombe* (Lorenz *et al.*, 1995; Kaur, Ingavale and Bachhawat, 1997), we designed a rapid and economical method for gene disruption in *D. hansenii*. Gene deletion cassettes started to be made directly by PCR, using the primers that introduce ~50-60 bp flanks (of target ORF) to 5' and 3' ends of the selectable marker (Figure 3.3). Transformation of this PCR product in *D. hansenii* results in the homologous recombination to occur in between the homology flanks, which results in the selectable marker being taken up by the genome and thereby replacing the target chromosomal region, normally the ORF of the target gene. This improved method accelerated the process of generation multiple gene deletions in a single strain.

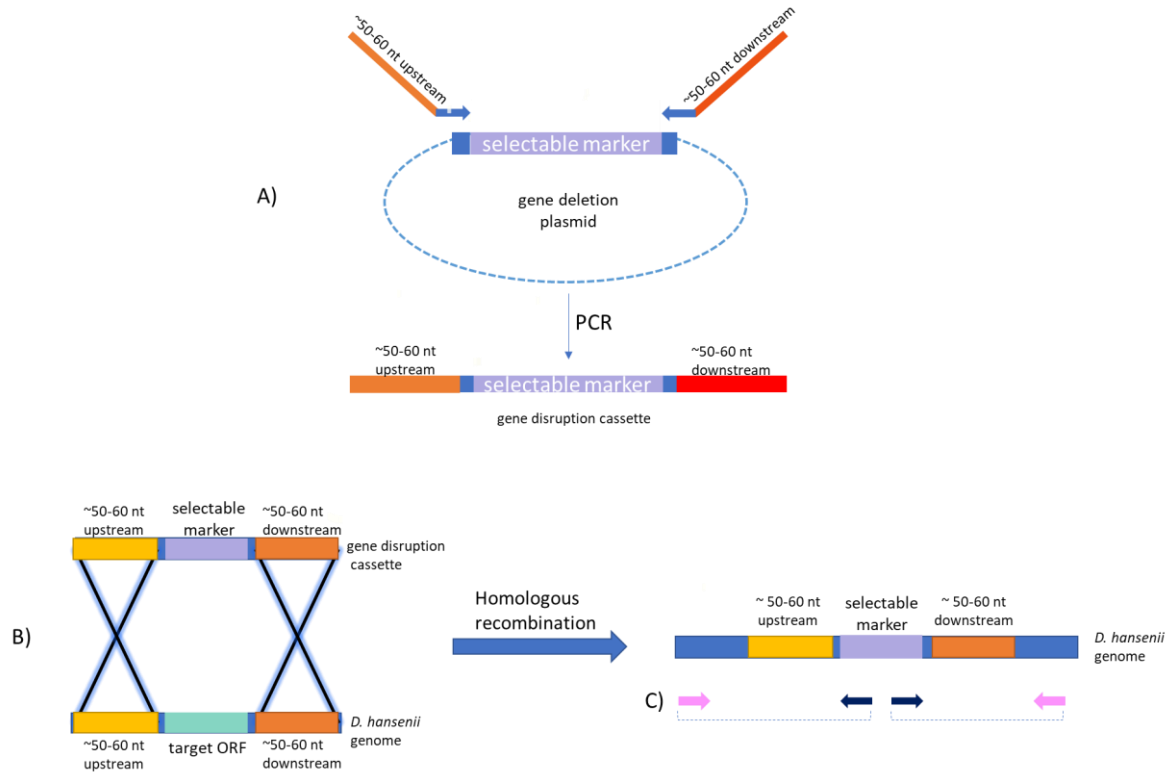

Figure 3.3: Gene deletion method in *D. hansenii* using short homology flanks. A) Using the plasmid with the selectable marker cassette as a template, the cassette is amplified by PCR using primers that introduce ~50-60 bp flanks of target ORF to 5' and 3' ends of the selectable marker region. B) The resulting product (gene disruption cassette) was transformed into *D. hansenii*, which allows homologous recombination in between the flanks and the chromosome thereby resulting in replacement of target ORF with the selectable marker C) The integration of the cassette into the genome was checked by PCRs, using one primer from outside the flank (shown in pink) and other primer within the selectable marker (shown in dark blue). The absence of the target gene after the deletion was also checked and confirmed, using the primer outside the flank, and other primer within the target gene ORF.

3.4- In *D. hansenii*, *MDH3*, *GPD1* and *GPD1/MDH3* gene knock-outs do not result in growth deficiency on oleate

After the development of the various gene manipulation cassettes mentioned in the previous section, different gene knock-outs were attempted to investigate the beta-oxidation pathway in *D. hansenii* in details so that it could be disrupted further for fatty acid accumulation. As many of the enzymes involved in fatty acid beta-oxidation in *D. hansenii* seem to be encoded by multiple genes, we first focused on Mdh3 as it seems to have only one version. In *S. cerevisiae*, Mdh3 is the major enzyme involved in regeneration of peroxisomal NAD^+, and its deletion results in a severe growth retardation on oleate medium (Al-Saryi *et al.*, 2017a). Besides, Gpd1, which only has a minor contribution to NAD^+ regeneration in *S. cerevisiae* (Al-Saryi *et al.*, 2017a) was initially not considered to be involved as it did not contain a typical peroxisomal targeting signal. Thus, Mdh3 was thought to

be the only candidate that regenerates NAD^+ for beta-oxidation in *D. hansenii*. Thus, we started our research by deleting *MDH3* (See Appendix 4 for PCR confirmation). However, when the cells were grown on oleate, no growth deficiency was detected in *mdh3Δ* cells.

After no growth defect on oleate was observed for *mdh3Δ* cells, further experiments were done to reinvestigate the presence of potential Gpd1 in *D. hansenii*. This *Dh*Gpd1 candidate was expressed in *S. cerevisiae* to see the localization and a growth complementation assay on lysine deficient medium was done to investigate its possible function, as described in Section 3.5 and 3.6 respectively. After it was observed that *Dh*Gpd1 partially localizes to peroxisomes and it restores the bradytrophy of *S. cerevisiae gpd1/mdh3Δ* cells on lysine deficient medium (will be described in Sections 3.5 and 3.6 in more details), *GPD1* was decided to be included in our gene deletion study too. Thus, we decided to generate *gpd1Δ* as well as *gpd1/mdh3Δ* cells. Using soy sauce-derived isolate (NCYC3363), *MDH3* and *GPD1* were deleted using the *hygB*^{r} and ClonNat selection markers, respectively. The gene deletions were confirmed by PCR (See Appendix 4 for further information).

Spot assay was done with all the KO strains (*mdh3Δ*, *gpd1Δ* and *gpd1/mdh3Δ*), using oleate, glucose and glycerol plates. The results showed that neither single KOs nor double KO results in growth defect on oleate (Figure 3.4) The *pex3Δ* mutant, which was generated and validated by Sondos Alhajouj, was also included as a negative control, as this mutant is unable to grow on oleate.

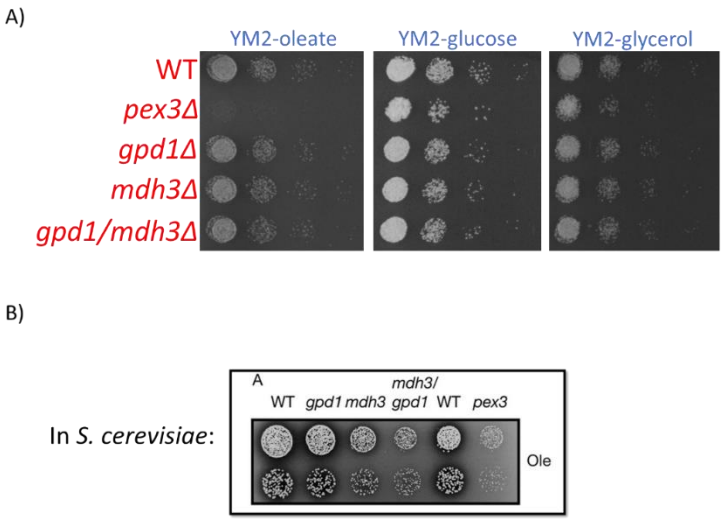

Figure 3.4: Growth analysis of *D. hansenii* WT, *mdh3Δ*, *gpd1Δ* and *gpd1/mdh3Δ* cells on different carbon sources. A) Serial dilution of cell suspension of the strains indicated were spotted onto YM2 media with oleate, glucose and glycerol as a sole carbon source and incubated for 2 days at 25°C. Prior to spotting, the cells were grown overnight in YM2 with 0.3% glucose and diluted in sterile water at OD=0.1 and 10 fold serial diluted 3 times. *pex3Δ* cells were included as a strain that cannot grow on oleate medium but grows well on the glucose and glycerol medium. B) Same growth assay in *S. cerevisiae* as previously described by Al-Saryi *et al.* (2017a).

3.5- *D. hansenii* Gpd1 is localised into peroxisomes in *S. cerevisiae* by PTS2-dependent pathway

The bioinformatics analysis identified a homologue for Gpd1 in *D. hansenii* (Figure 3.5), but this protein lacked a clear PTS. However, motivated by the lack of phenotype of a *MDH3* deletion, it was decided to inspect the potential *Dh*Gpd1 amino acid sequence more closely. A PTS2-like sequence at its N-terminus was now identified but is different at the 2nd and 5th positions from consensus PTS2 (Figure 3.5). This however, has been observed before, for instance *Sc*Gpd1 does not completely fit the consensus either (Jung *et al.*, 2010) and neither does *Dictyostelium discoideum* Farnesyl Diphosphate Synthase (Nuttall et al, 2012). Additionally, another glycerol-3-phosphate dehydrogenase was detected in *D. hansenii*, which seemed more likely to be the potential cytosolic glycerol-3-phosphate dehydrogenase (named *Dh*Gpd2). It also had PTS2-like signal, that seemed to be more unlikely to be a potential PTS2 (Figure 3.5). It was analysed in parallel to *Dh*Gpd1 hit.

PTS2 consensus sequence:
[R/K]-[L/V/I/Q]-X-X-[L/V/I/H/Q]-[L/S/G/A/K]-X-[H/Q]-[L-A-F]

```
Sc_gpd1     MS--AAARLNLTSGHLNAGRKRSSSSVSLKAAEKPFKVTVIGSGNWGTTIAKVVAENCK     58
Dh_gpd1     MSQYRANQRLQQLSNILRP---NQLSAEKSLKPETPFKVAVIGSGNWGTTIAKVLAENTA    57
Dh_gpd2     ------------------------MTSTPFNIEKPFRVAIIGSGNWGTAVAKIVSENTA    35
                                     : .    *.**:*::********::**:::**

Sc_gpd1     GYPEVFAPIVQMWVFEEEINGEKLTEIINTRHQNVKYLPGITLPDNLVANPDLIDSVKDV    118
Dh_gpd1     EKPDTFAKQVDMWVFQEKIDGTNLTEIINNKHENVKYLPGVKLPENLHAEPDIVKAAQGA    117
Dh_gpd2     EKPEVFEKQVNMWVFEEEVDGQKLTEIINTKHENVKYLPEVKLPENLVANPDVVDTVKDA    95
              *:.*   *:****:*:::* :******.:*:****** :.**:** *:**::.:.:..

Sc_gpd1     DIIVFNIPHQFLPRICSQLKGHVDSHVRAISCLKGFEVGAKGVQLLSSYITEELGIQCGA    178
Dh_gpd1     DLLVFNLPHQFLPKICKQLKGTLKPTTRAISCLKGLEVTPDGCKLLSTYITENLGIECGA    177
Dh_gpd2     DLLIFNIPHQFLPRVCKQLVGHVKPSARAISCLKGLEVGPEGCKLLSQSINDTLGVHCGV    155
            *:::**:******::*.** * :.  .********:**  .* :***  *.: **:.**.

Sc_gpd1     LSGANIATEVAQEHWSETTVAYHIPKDFRGEGKDVDHKVLKALFHRPYFHVSVIEDVAGI    238
Dh_gpd1     LSGANLAPEVARCKWSETTVAYNIPADFKGPGKDIDSAVLKEAFHRPYFHVNVIEDVAGV    237
Dh_gpd2     LSGANIANEVARERWSETTIAYNIPEDFRGKGRDIDEYVLKQLFHRTYFHVRVINDIIGA    215
            *****:* ***: :*****:**:** **:* *:*:*  ***  *** **** **:*: *

Sc_gpd1     SICGALKNVVALGCGFVEGLGWGNNASAAIQRVGLGEIIRFGQMFF------PESREETY    292
Dh_gpd1     SVAGALKNIVAIAVGFVEGLGWGDNAKSAIMRVGLIETINFSNMFF------PNSKPTTF    291
Dh_gpd2     SFAGALKNVVACAVGFVIGAGWGDNAKAAIMRIGIREIIHFASYYQKFGVKGPAPESTTF    275
            *..*****:** . *** * ***:**.:** *:*: * *.*.. :       *  .  *:

Sc_gpd1     YQESAGVADLITTCAGGRNVKVARLMATSGKDAWECEKELLNGQSAQGLITCKEVHEWLE    352
Dh_gpd1     THESAGVADLITTCSGGRNVKVGRHMSKTGESAEEAEKKLLNGQSSQGIITAKEVHELLS    351
Dh_gpd2     TEESAGVADLITTCSGGRNVKVARYMIENNVDAWEAEKIVLKGQSSQGILTAKEVHELLT    335
             .************:*******.* *  .. .* *.** :*:***:**::*.***** *

Sc_gpd1     TCGSVEDFPLFEAVYQIVYNNYPMKNLPDMIEELDLHED    391
Dh_gpd1     NVGKTDQFPLFEATYQIIYGDESIQNLPNLLEDHSLFK-    389
Dh_gpd2     NYNLSNEFPLFEATYRIIYENADVNEFPVILERD-----    369
            . .  ::******.*:*:* :  ::::* ::*
```

Figure 3.5: The protein alignment of *Sc*Gpd1, *Dh*Gpd1 and *Dh*Gpd2, which was done via Clustal Omega (Sievers *et al.*, 2011). *Dh*Gpd1 and *Dh*Gpd2 were the hits of the blast search (Altschul *et al.*, 1990), that came up when *Sc*Gpd1 was blasted against *D. hansenii.* The consensus sequence for PTS2 (Petriv *et al.*, 2004) is shown at the top of the alignment. The PTS2 sequence in *Sc*Gpd1 (Jung *et al.*, 2010) is highlighted in blue, whereas the PTS2-like sequences of putative *Dh*Gpd1 and *Dh*Gpd2 were highlighted with pink and green, respectively. The alignment revealed 65.01% identity in between the sequences of *Sc*Gpd1 and *Dh*Gpd1, whereas the sequence identity between the *Sc*Gpd1 and *Dh*Gpd2 is 61.50%.

To investigate whether *Dh*Gpd1 or *Dh*Gpd2 potentially localise to peroxisomes, they were tagged with GFP at their C-termini and expressed in *S. cerevisiae*. Dh*GPD1* and *DhGPD2* ORFs were recombined into pEH116, which is a self-replicating C-terminal tagging plasmid that contains Sc*TPI1* promoter, a multiple cloning site (MCS), followed by a ''Gly-Ala-Gly-Ala-Gly-Ala'' linker (GAGAGA linker), GFP and the *PGK1* terminator. The GAGAGA linker in between the tag and target ORF acts as a spacer to allow the proteins to be folded properly. Both Dh*GPD1* and *DhGPD2* ORFs lacking their stop codon were introduced into pEH116 between the *TPI1* promoter and in frame with the (Gly-Ala)$_3$ linker, giving rise to pES1 and pES2, respectively (Figure 3.6). The final sequence of both plasmids were confirmed by Sanger sequencing analysis. Then, each plasmid was first transformed into *S. cerevisiae* WT cells and analysed with epifluorescence microscopy. *Dh*Gpd1-GFP displayed a dual localisation in WT cells, including a clear cytosolic labelling with on top of that a faint punctate pattern, that could represent peroxisomes. *Dh*Gpd2-GFP displayed only a cytosolic pattern. In order to test whether *Dh*Gpd1-GFP could be imported into *S. cerevisiae* peroxisomes, Gpd1-GFP was expressed in the peroxisomal biogenesis deficient *pex3Δ* cells, where peroxisomes are absent. No punctate pattern was observed indicating that the punctate indeed are peroxisomes. Subsequently, *Dh*Gpd1-GFP was expressed in cells that were either blocked in PTS1 import into peroxisomes (*pex5*Δ) or PTS2 import (*pex7Δ*). As the puncta of *Dh*Gpd1-GFP were observed in *pex5Δ* cells but not *pex7Δ* cells, it can be concluded that *Dh*Gpd1-GFP associates with peroxisomes in *S. cerevisiae* through import via the PTS2 pathway (Figure 3.7). Furthermore, the puncta are peroxisomes as they co-localise with the peroxisomal red marker pAS63 that directs expression of *Hc*Red-PTS1 (Motley and Hettema, 2007) (Figure 3.7).

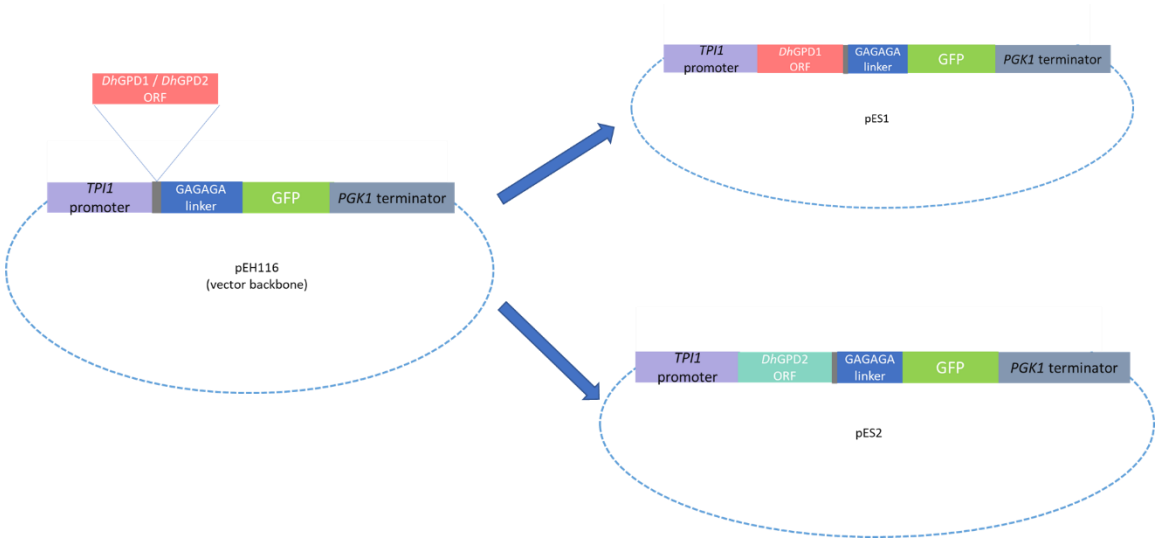

Figure 3.6: Construction of *Dh*Gpd1-GFP and *Dh*Gpd2-GFP expression plasmids for analysis in *S. cerevisiae*. The C-terminal tagging plasmid pEH116, which is a self-replicating C-terminal tagging plasmid that contains Sc*TPI1* promoter, a multiple cloning site (MCS), followed by a (Gly-Ala)$_3$-linker, GFP and the *PGK1* terminator, was used to introduce either *DhGPD1* or *DhGPD2* by homologous recombination, between the *TPI1* promoter and in frame with the (Gly-Ala)$_3$-linker. The resulting expression plasmids with the fusion of *DhGPD1*-GAGAGA-GFP or *DhGPD2*-GAGAGA-GFP were named as pES1 and pES2, respectively.

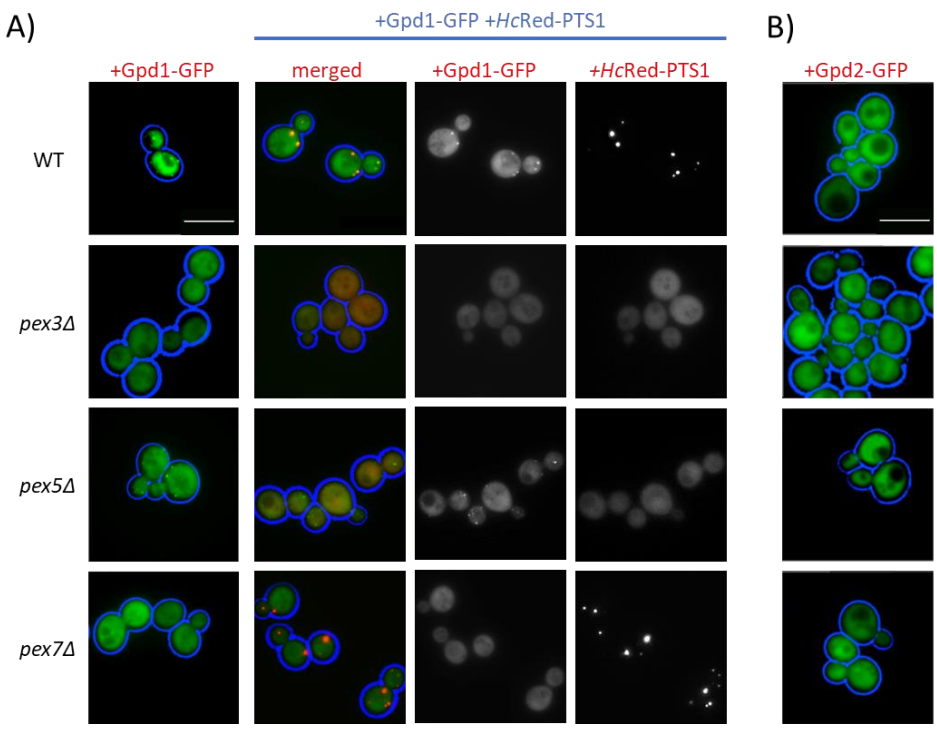

Figure 3.7: *Dh*Gpd1-GFP partially localises to *S. cerevisiae* peroxisomes dependent on the PTS2 import pathway. Epifluorescence microscopy analysis of cells expressing *Dh*Gpd1-GFP (A) or *Dh*Gpd2-GFP (B) in *S. cerevisiae* WT and the indicated peroxisome biogenesis mutants in absence or presence of HcRed-PTS1. A) *Dh*Gpd1-GFP localises to both cytosol and puncta in WT and *pex5Δ* cells whereas no puncta are observed in *pex3Δ* and *pex7Δ* cells. These puncta colocalize with *HcRed*-PTS1, implying *Dh*Gpd1 follows the PTS2-dependent import pathway. B) *Dh*Gpd2-GFP localizes to the cytosol in all strains. The cell walls were highlighted in blue. Scale bar is 5 µm.

3.6- Expression of *Dh*Gpd1 in *S. cerevisiae* rescues the growth of *gpd1/mdh3Δ* on lys$^-$ media

In *S. cerevisiae*, it was suggested that the last step of lysine biosynthesis, in which L-saccharopine is converted to L-lysine by Lys1, takes place in peroxisomes (Yofe *et al.*, 2016). This step requires NAD^+ as a co-factor. The NAD^+ needed for this step is regenerated by both Mdh3 and Gpd1. Thus, *gpd1/mdh3Δ* cells show lysine bradytrophy (slow growth) on lysine-auxotroph (lys$^-$) media (Al-Saryi *et al.*, 2017a).

In order to investigate whether *Dh*Gpd1-GFP is localized inside peroxisomes and can substitute for *S. cerevisiae* Gpd1, it was expressed in *S. cerevisiae* mutant *gpd1/mdh3Δ* and the growth on lys$^-$ medium was analysed by spot assay. The plasmids that contain *DhGPD2*-GFP (pES2) and *ScGPD1*-GFP (pNA33) were also expressed in *gpd1/mdh3Δ* cells as a negative and positive control, respectively.

The transformants were grown individually in ura$^-$ media for overnight. The next morning, they were diluted to OD_{600}=0.1 in ura$^-$ lys$^-$ media and grown for few hours. At the end of the day, they were spotted onto lys$^-$ dropout plates, as well as ura$^-$ plates as a positive control and these plates were incubated at 30°C. After every 24 hours for the next 3 days, the plates were imaged (Figure 3.8) to visualise at which rate the colonies grow. For instance, *gpd1/mdh3Δ* cells expressing *Sc*Gpd1-GFP

form larger colonies on lys⁻ medium compared to those transformed with an empty plasmid, indicating that *Sc*Gpd1-GFP complements the lysine bradytrophy in *gpd1/mdh3Δ* cells (Al-Saryi *et al.*, 2017a). Likewise, the expression of *Dh*Gpd1-GFP in *gpd1/mdh3Δ cells* restored growth on lys⁻ media in contrast to the expression of *Dh*Gpd2-GFP (Figure 3.8). It can be concluded that *Dh*Gpd1 is imported into peroxisomes from *S. cerevisiae* and can function in the regeneration of NAD^+ to support lysine biosynthesis.

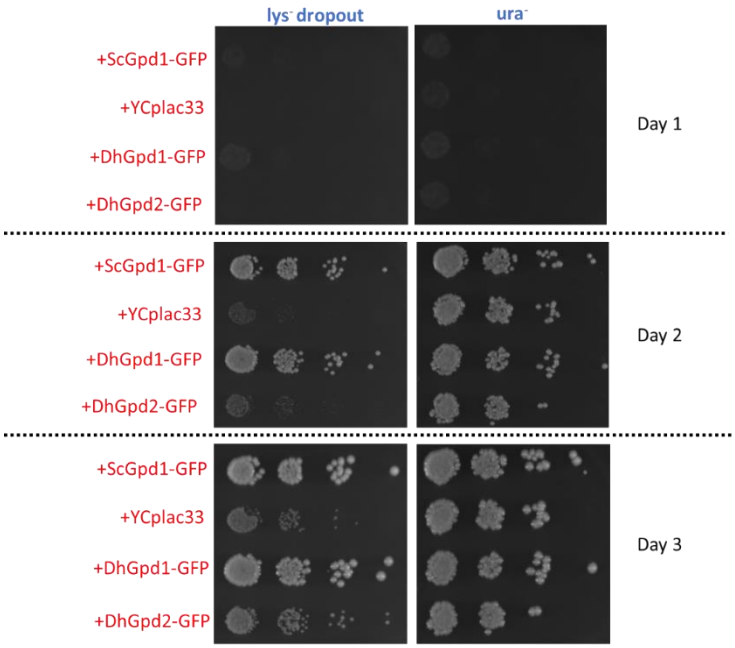

Figure 3.8: Spot assay with *S. cerevisiae mdh3/gpd1Δ* cells, that express *ScGPD1*-GFP, YCplac33 (empty plasmid), *DhGPD1*-GFP and *DhGPD2*-GFP. Serial dilution of cell suspension of the strains indicated were spotted on lys⁻ and ura⁻ plates (used as a positive control). Prior to spotting, the cells were grown overnight in YM2 ura⁻ media. Next morning, the cells were diluted to OD_{600}=0.1 in ura⁻ lys⁻ media and were grown few hours. The cells were then diluted in sterile water at OD_{600}=0.1 and 10 fold serial diluted 3 times. After spotting, the plates were incubated at 30°C and the growth was observed for the next 3 days. The pictures were taken with 24 hours of interval.

3.7- Discussion

The bioinformatics study has revealed more detailed prediction about the beta-oxidation system in *D. hansenii*. Some beta-oxidation enzymes have multiple hits in *D. hansenii*, such as 3 different potential Acyl-CoA Oxidases. In *Y. lipolytica*, which is a yeast related to *D. hansenii*, there are 5 different Acyl-CoA Oxidases identified. Each one prefers different substrates based on carbon chain lengths (Wang, *et al.*, 1999a; Wang *et al.*, 1999b). For example, one of them (Aox3) appears to be oxidizing short chain fatty acids (Wang *et al.*, 1998; Luo *et al.*, 2000), other one (Aox2) reportedly

prefers to oxidise long chain fatty acids (Wang *et al.*, 1999b; Luo *et al.*, 2002), whereas Aox5 reportedly do not have specific chain length preferences (Wang *et al.*, 1999b). Hypothetically, different Pox1s in *D. hansenii* might be similar to the ones in *Y. lipolytica* in that sense and acting on fatty acids with different chain lengths. On the other hand, our bioinformatics research has also identified 3 different potential 3-Ketoacyl-CoA Thiolases in *D. hansenii*. Similarly, recent studies reported that *Aspergillus oryzae* (*A. oryzae*) has 6 different thiolases. Three of them are localized to peroxisomes and complement the growth deficiency of *pot1Δ* on oleate. (Huang *et al.*, 2022). Similarly, the presence of more than one peroxisomal thiolases was also reported in *C. albicans* (Otzen *et al.*, 2013) and *A. thaliana* (Carrie *et al.*, 2007). Since 2 of these potential 3-Ketoacyl-CoA Thiolases we identified in *D. hansenii* have potential PTS; similarly to these organisms, there might be multiple peroxisomal thiolases in *D. hansenii*. This is different from the beta-oxidation system in *S. cerevisiae*, in which each step is catalyzed by only one protein (Revieved in Visser *et al.*, 2007).

A new form of putative PTS2 signal was identified in *Dh*Gpd1, with amino acid sequence of **R**-A-N-Q-R-**L**-Q-**Q**-**L**, which does not match at two positions (in red) with the consensus PTS2 sequence that is [R/K]-[L/V/I/Q]-X-X-[L/V/I/H/Q]-[L/S/G/A/K]-X-[H/Q]-[L-A-F] (Petriv *et al.*, 2004). However, an Alanine residue has been described previously in *Dictyostelium discoideum* (Nuttall et al, 2012), implying that the PTS2 might have organism specific differences. The localization of Gpd1 in *S. cerevisiae* peroxisomes via PTS2-dependent pathway is consistent with this finding. *Sc*Gpd1 also contains a PTS2 (Jung *et al.*, 2010), hence *Dh*Gpd1 and *Sc*Gpd1 are similar in this respect. The fact that *Dh*Gpd1 was able to rescue the growth of *mdh3/gpd1Δ* cells on lysine deficient media shows that *Dh*Gpd1 is most likely functioning the same way as *Sc*Gpd1 and that it is present inside peroxisomes. We conclude that *Dh*Gpd1 is the most likely *D. hansenii* ortholog of *Sc*Gpd1.

The newly-developed gene deletion cassettes with ClonNat, hygB and G418 markers has enabled us to generate multiple gene knock-outs in a single strain for the first time. This is a major advance in unravelling *D. hansenii* biochemistry and physiology and will allow for further development of this organism for biotechnology and metabolic engineering. We used this technology to understand the beta-oxidation system in *D. hansenii* in more details. We started with the disruption of the NAD^+ regeneration process, by generating *MDH3, GPD1* and *GPD1/MDH3* knock-outs. However; the deletion of *MDH3, GPD1* and *GPD1/MDH3* did not result in growth defect on oleate. It also is consistent with the data of the beta-oxidation activity measurements in the same strains, which were very similar to the beta-oxidation activity of WT cells (That can be seen further in Section 4.10). It suggests that there might be additional ways to supply NAD^+ for beta-oxidation and hence blocking Mdh3 and Gpd1 might not be enough to disrupt the process. This has led us to investigate the other possible ways of getting NAD^+ into the beta-oxidation in *D. hansenii*, which led to the identification of Pmp47 that will be discussed in the next chapter.

In summary, the presence of multiple versions of specific beta-oxidation enzymes, additional proteins that have not been discovered in *S. cerevisiae* and the potential other NAD^+ sources in *D. hansenii* makes the beta-oxidation more complicated compared to the beta-oxidation system in *S. cerevisiae*.

Chapter 4- Pmp47 is involved into the beta-oxidation process in *D. hansenii* by contributing to the NAD^+ flux in peroxisomes

4.1- Introduction

NAD^+ regeneration is required for the third step of fatty acid beta-oxidation which is regenerated by both Mdh3 (van Roermund *et al.*, 1995) and Gpd1 (Al-Saryi *et al.*, 2017a) in *S. cerevisiae*. However, in *D. hansenii*, the deletion of *MDH3, GPD1 or MDH3/GPD1* did not show any growth defect on oleate. It suggested that NAD^+ supply for the beta-oxidation in *D. hansenii* might also be depending on other mechanisms (Figure 4.1).

Peroxisomal Membrane Protein 47 (Pmp47) is an integral membrane protein (McCammon *et al.*, 1990) which has homology to mitochondrial solute carrier of transporters (Jank *et al.*, 1993). It was identified first in *C. boidinii* (McCammon *et al.*, 1990). Earlier study has shown that the heterologous expression of Pmp47 of *C. boidinii* resulted in peroxisomal localization when expressed in *S. cerevisiae* (McCammon *et al.*, 1990; McCammon *et al.*, 1994) and *Hansenula polymorpha* (Sulter *et al.*, 1993). An additional ortholog of Pmp47 from *Arabidopsis thaliana*, named PXN, has also been identified and its heterologous expression also led to targeting into the peroxisomes (Bernhardt *et al.*, 2012; van Roermund *et al.*, 2016). Pumpkin ortholog of Pmp47 was also reported as peroxisomal (Fukao *et al.*, 2001). Apart from the peroxisomal localization of Pmp47 and its orthologs in different organisms, there is also evidence that Pmp47 has a role in the lipid breakdown process in *C. boidinii* (Nakagawa *et al.*, 2000) as well in pumpkin (Fukao *et al.*, 2001) and *A. thaliana* (Bernhardt *et al.*, 2012). There have been various studies with different opinions about what this protein is transporting (Bernhardt *et al.*, 2012; reviewed in Linka and Esser, 2012). Earlier studies suggested that Pmp47 and its orthologs are transporting ATP (Nakagawa *et al.*, 2000; Fukao *et al.*, 2001; Visser *et al.*, 2002; van Roermund *et al.*, 2001). However, further studies done with *A. thaliana* PXN showed an evidence that this protein is a potential NAD^+ transporter (Bernhardt *et al.*, 2012; van Roermund *et al.*, 2016).

Pyrazinamidase/Nicotinamidase 1 (Pnc1) and Nudix hydrolase 1 (Npy1) are peroxisomal proteins identified in *S. cerevisiae*. Pnc1 reportedly converts nicotinamide to nicotine (Figure 4.1), as part of NAD^+ salvage pathway (Anderson *et al.*, 2003; Bedalov *et al.*, 2003). This protein does not have any identified targeting signal, but it gets imported into the peroxisomes by piggybacking on Gpd1 in *S. cerevisiae* (Effelsberg *et al.*, 2015; Kumar *et al.*, 2016; Al-Saryi *et al.*, 2017b). Whether Pnc1 contributes to NAD^+/NADH metabolism in peroxisomes (or whether NAD^+ regenerated during NAD^+ salvage pathway is used in beta-oxidation) has not been studied. On the other hand, the function of Npy1 is to convert NADH to AMP (AbdelRaheim *et al.*, 2001). The yeast peroxisomes are impermeable to NADH (van Roermund *et al.*, 1995), so once NAD^+ is reduced to NADH by the beta-oxidation, it can be converted to AMP (AbdelRaheim *et al.*, 2001), which then can leave the peroxisomes (Reviewed in Antonenkov and Hiltunen, 2012). In this way, Npy1 is helping with the NAD^+/NADH homeostasis in peroxisomes. There is evidence that in *A. thaliana*, PXN transports NAD^+ in an exchange of AMP, in which case PXN and Npy1 are in the same pathway of NAD^+/NADH transport mechanism (van Roermund *et al.*, 2016). A *S. cerevisiae* orthologue for PXN has not been described.

Bioinformatics identified homologs for Pmp47, Npy1 and Pnc1 in *D. hansenii*. In this chapter the analysis of these proteins is described. The potential role of *Dh*Pmp47 as an NAD^+ transporter was investigated. Possible scenarios regarding to co-factor exchange routes mediated by *Dh*Pmp47 (Figure 4.1) were also investigated. Our results suggest that *Dh*Pmp47 is a peroxisomal transporter involved in the supply of NAD^+ to the peroxisomal lumen but that it is most likely acting independent of Npy1. On the other hand, our results suggest that the putative Pnc1 is unlikely to be a peroxisomal enzyme and unlikely to be contributing to NAD^+ supply to the beta-oxidation.

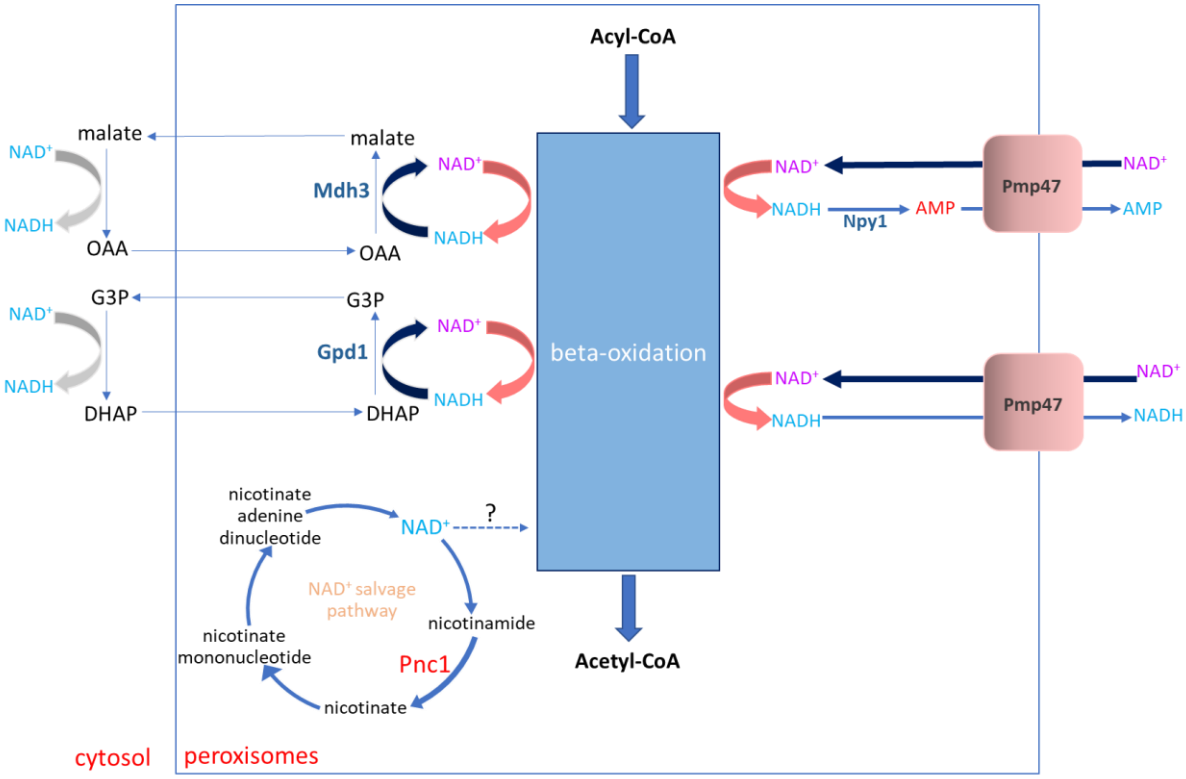

Figure 4.1: The diagram indicates the possible roles of Pmp47, Npy1 and Pnc1 in beta-oxidation in *D. hansenii*. Pmp47 might be NAD^+/AMP exchanger, similarly to PXN (van Roermund *et al.*, 2016). In this case, NAD^+ might be imported by *Dh*Pmp47. After it is reduced to NADH during the beta-oxidation, NADH then might be converted to AMP by the putative *Dh*Npy1 enzyme. AMP then might leave the peroxisomes. If this is the case, *Dh*Pmp47 might be depending on *Dh*Npy1. Alternatively, *Dh*Pmp47 might be also NAD^+/NADH exchanger, in which case NADH (that forms during the beta-oxidation) is released back to cytosol directly via *Dh*Pmp47. The NAD^+ salvation pathway, in which putative *Dh*Pnc1 might be playing a role, may be also affecting the NAD^+ availability in peroxisomes in *D. hansenii*. The diagrams were adapted from Bedalov *et al.* (2003) and van Roermund *et al.* (2016).

4.2- Identification of Pmp47, Pnc1 and Npy1 in *D. hansenii*

The potential Pmp47, Pnc1 and Npy1 in *D. hansenii* were identified by blast search (Atschul *et al.*, 1990). After the best hits were found, the protein sequences of each best hit and the query sequence were aligned using Clustal Omega database (Sievers *et al.*, 2011). The potential *Dh*Pmp47 was identified by blast search (Atschul *et al.*, 1990), by blasting the Pmp47*a* of *C. boidinii* against *D. hansenii*, whereas the potential *Dh*Pnc1 and *Dh*Npy1 were identified by blasting their *S. cerevisiae* orthologs, using ''BLASTP vs. fungi'' feature of SGD Database (https://www.yeastgenome.org/). The protein alignment of each protein versus their query sequences are shown in Figure 4.2.

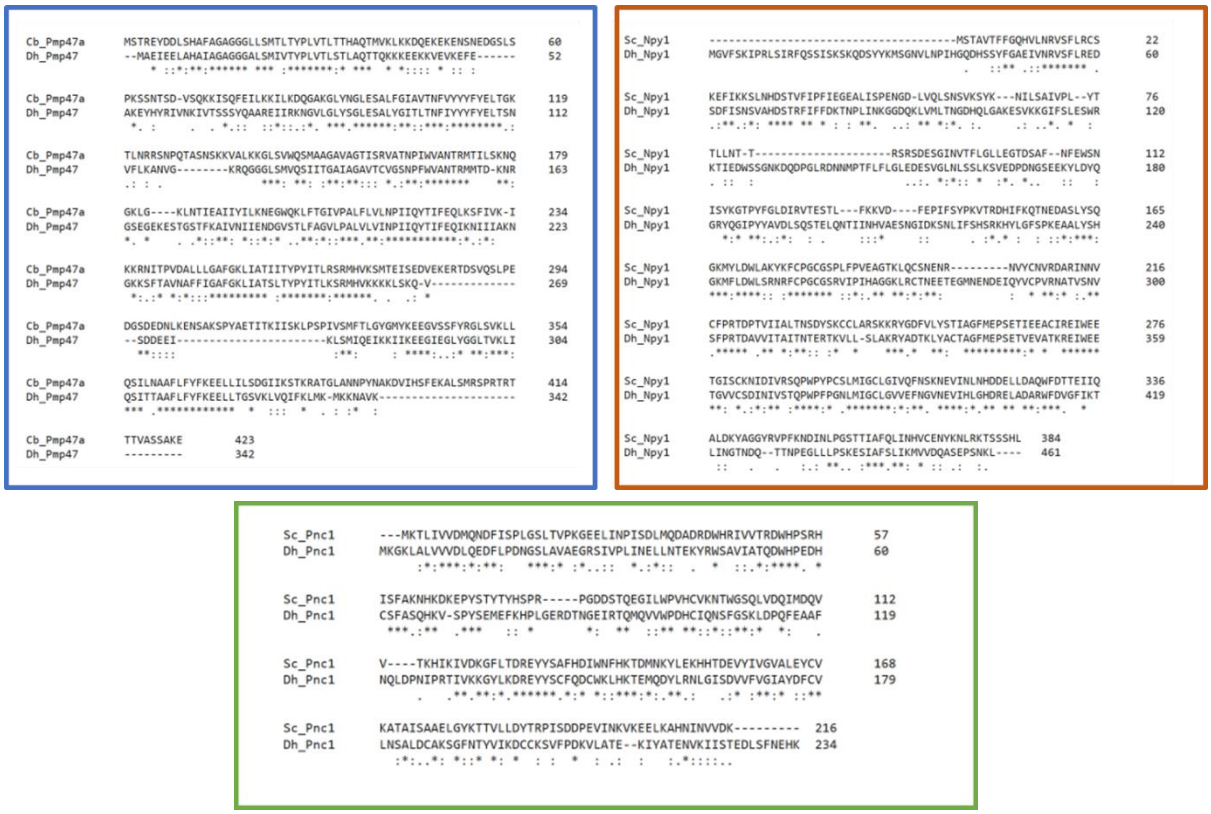

Figure 4.2: The protein alignment of *Dh*Pmp47 and *Cb*Pmp47*a* (shown in blue box), *Dh*Npy1 and *Sc*Npy1 (shown in orange box) and *Sc*Pnc1 and *Dh*Pnc1 (shown in green box). The *D. hansenii* proteins with the sequences above are the best hits that came up after the blast search. The alignments were made using Clustal Omega (Sievers *et al.*, 2011). The same database revealed 48.21% sequence identity between the protein sequences of *Cb*Pmp47*a* and *Dh*Pmp47, 40.05% sequence identity in between the protein sequences of *Sc*Npy1 and *Dh*Npy1, and 35.68% sequence identity in between the protein sequences of *Sc*Pnc1 and *Dh*Pnc1.

4.3- Pmp47 of *D. hansenii* is targeted to the peroxisomes when expressed in *S. cerevisiae*

In order to analyse the localization of *Dh*Pmp47, it was expressed in *S. cerevisiae*, by tagging with GFP at its C-terminus. The ORF of the putative *DhPMP47* lacks any CTG codons, so total DNA was used as template for PCR amplification. It was introduced into a C-terminal tagging plasmid pEH117, whose sequence is identical to pEH116 (was shown in Figure 3.6 of Section 3.5), except having a *LEU2* auxotrophic marker instead of *URA3* (see also Figure 4.4). Thus, *DhPMP47* was recombined into pEH117 in the same way as shown in Figure 3.6. Upon transformation to WT and *pex3Δ* in S. cerevisiae cells its localisation was observed using epifluorescence microscopy. The GFP puncta present in WT cells resemble those of peroxisomes. This is further supported by the lack of these puncta in the peroxisomal membrane biogenesis mutant cells (*pex3Δ* cells). In *pex3Δ* cells a weak background haze suggests localisation to cytosol. The peroxisomal localization was further confirmed by co-localization with the red peroxisomal marker (*Sc*Pex11-mRFP) (Figure 4.3).

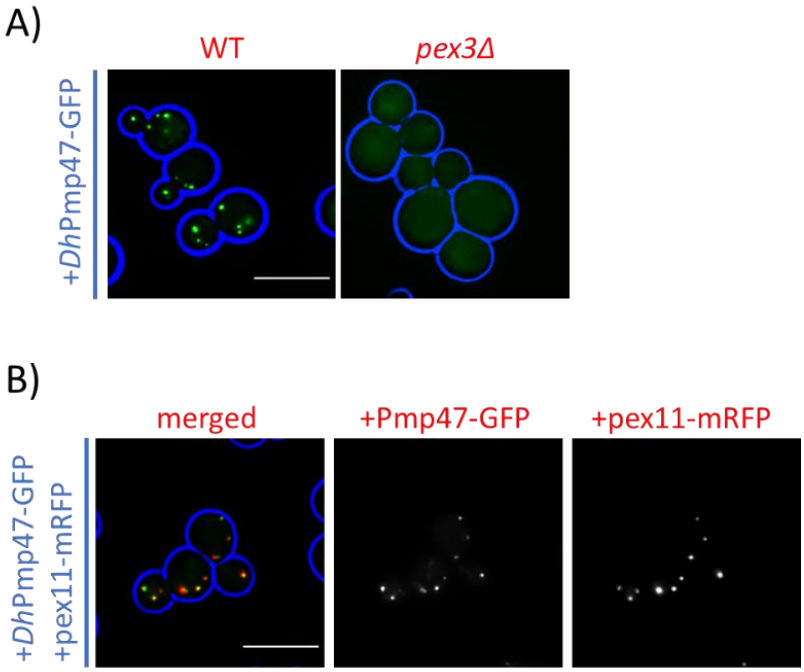

Figure 4.3: The epifluorescence microscopy analysis of *Dh*Pmp47-GFP expression in *S. cerevisiae*. A) The expression pattern of *Dh*Pmp47-GFP in WT and *pex3Δ* cells. In WT, the fluorescent signal was observed as green punctate pattern whereas in *pex3Δ*, faint cytosolic labelling was observed. B) The co-localization of *Dh*Pmp47-GFP with the red peroxisomal marker (pex11-mRFP) in *S. cerevisiae* WT cells. The cells were grown in minimal glucose media logarithmically. Each cell wall is highlighted in blue. Scale bar is 5 µm.

4.4- *Dh*Pmp47 rescues the oleate growth defect of both *mdh3Δ* and *mdh3/gpd1Δ* cells in *S. cerevisiae* when it is not tagged with GFP

In order to investigate the hypothetical function of *Dh*Pmp47 as an NAD^+ transporter, *Dh*Pmp47 was expressed in *S. cerevisiae mdh3Δ* and *mdh3/gpd1Δ* mutants, that show major growth defect on oleate due to the disruption of the NAD^+ regeneration for the beta-oxidation (van Roermund *et al.*, 1995; Al-Saryi *et al.*, 2017a). *Dh*Pmp47 was expressed either as tagged with GFP under the control of *TPI1* promoter, (*TPI1* promoter-*PMP47*-GFP-PGK1 terminator in pSLV24) or untagged under the control of oleate inducible *CTA1* promoter (*CTA1* promoter-*PMP47-CTA1* terminator in pSC120). Both design of pSLV24 and pSC120 plasmids can be seen on Figure 4.4. The plasmid sequences of both pSLV24 and pSC120 were confirmed by Sanger sequencing analysis. The growth of the mutants, that are expressing either tagged or untagged *PMP47*, were analysed by spot assay using glucose and oleate media. The results showed that the when *PMP47* is untagged with GFP, the growth defect of both mutants on oleate is restored. In contrast, when *PMP47* is tagged with GFP, the growth defect on oleate is not complemented (Figure 4.5). This suggests that Pmp47 might be functioning in a way that changes NAD^+ flux, which might have been used in beta-oxidation and led the *mdh3Δ* and *mdh3/gpd1Δ* cells to utilize the fatty acids normally. It also suggests that when *Dh*Pmp47 is tagged with GFP, the GFP tag might be disrupting the function of the protein, which might have resulted in the lack of complementation. Alternatively, the expression *PMP47* under control of the *CTA1* promoter instead of the *TPI1* promoter is more suited for complementation on oleate medium.

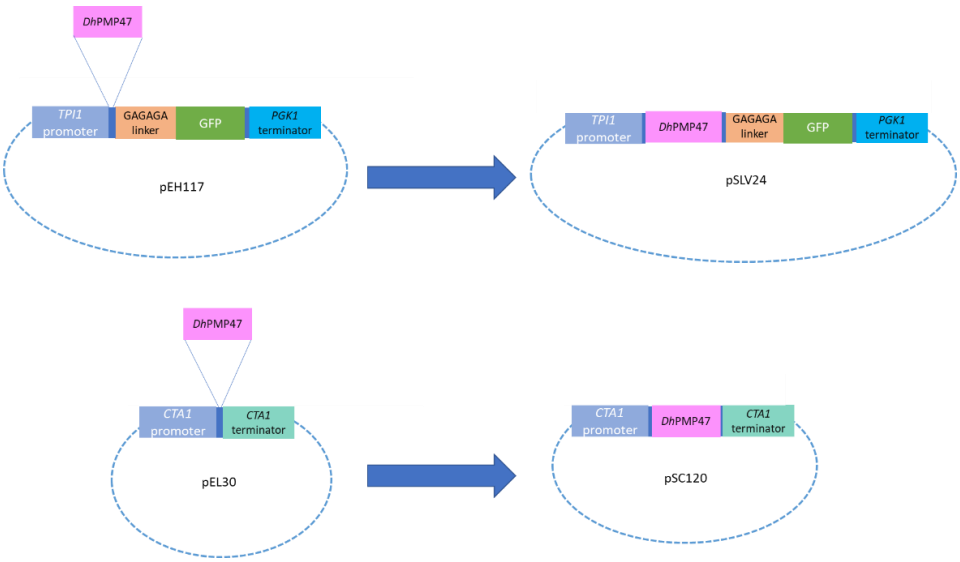

Figure 4.4: The construction of pSLV24 and pSC120 to express *Dh*Pmp47 in *S. cerevisiae*. *DhPMP47* ORF was introduced into both vector backbones (pEH117 for pSLV24 and pEL30 for pSC120) by classical cloning. In pSLV24, *DhPMP47* was tagged with GFP and the fusion protein was expressed under the control of *TPI1* promoter. In pSC120, the *PMP47* was untagged, which was expressed under the control of *CTA1* promoter.

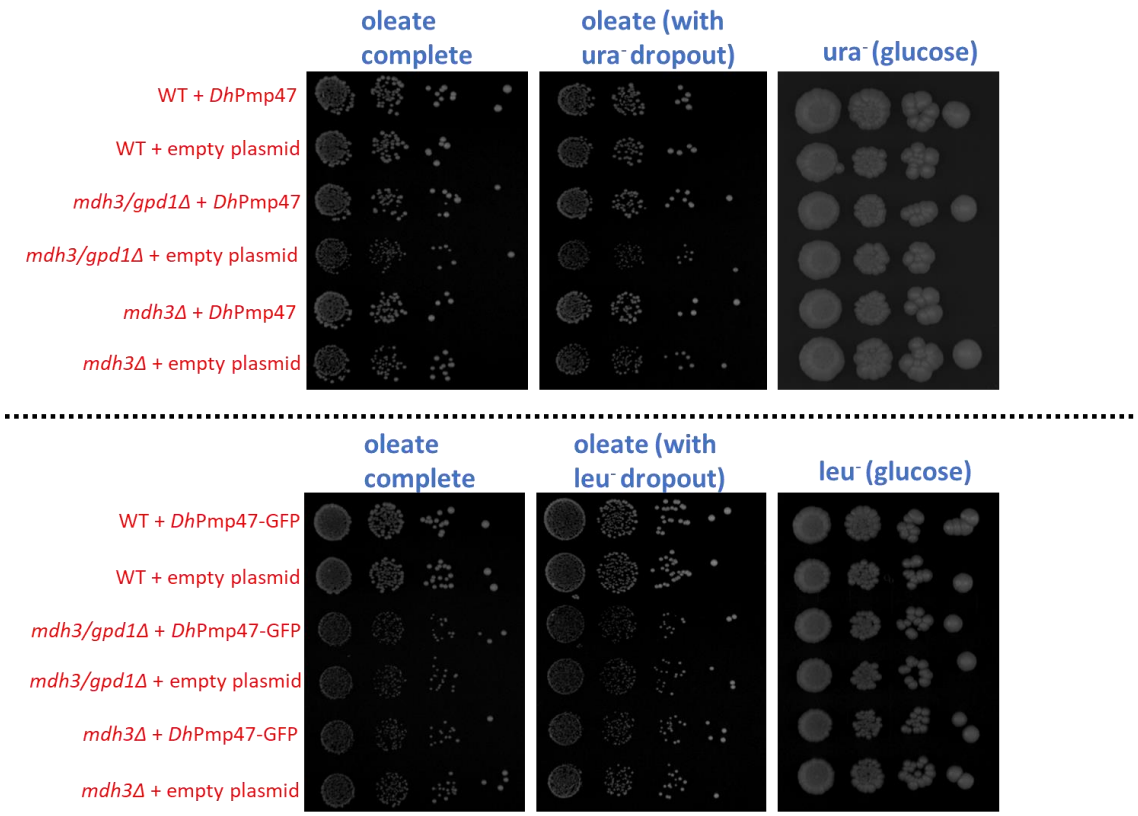

Figure 4.5: The spot growth analysis that was done using *S. cerevisiae* WT, *mdh3Δ* and *mdh3/gpd1Δ* that express either untagged *Dh*Pmp47 or *Dh*Pmp47-GFP. Serial dilution of cell suspension of the strains indicated were spotted onto minimal media with oleate and glucose (as a positive control) incubated for 4 days at 30°C. Prior to spotting, the cells were grown overnight in YM2 media with 0.3% glucose and diluted in sterile water at OD_{600}=0.1 and 10 fold serial diluted 3 times.

4.5- *Dh*Pmp47 tagged and untagged, does not restore growth of *S. cerevisiae mdh3/gpd1Δ* cells on lys⁻ media

After the expression of untagged *Dh*Pmp47 rescued the oleate growth deficiency of *S. cerevisiae mdh3/gpd1Δ* cells, the effect of ''*TPI1* promoter-*PMP47*-GFP'' or ''*CTA1* promoter-*PMP47*'' expression was tested for their ability to rescue the lysine bradytrophy observed in *mdh3/gpd1Δ* cells (Al-Saryi *et al.*, 2017a). However, neither tagged nor untagged *Dh*Pmp47 expression resulted in growth rescue on lys⁻ media (Figure 4.6) in contrast to what was observed upon the expression of *Sc*Gpd1-GFP or *Dh*Gpd1-GFP in the same mutant (Figure 3.8). It might be due to the fact that the expression of untagged Pmp47 is under the control of *CTA1* promoter, which is oleate inducible promoter. Hence, this promoter might not be active in glucose media to affect the expression of *Dh*Pmp47 in lys⁻ (which is glucose based). Secondly, as mentioned in the previous section, when *Dh*Pmp47 is tagged with GFP, the presence of GFP tag might be interfering with the function of the protein, which might have resulted in no growth rescue neither on oleate nor on lys⁻ media.

Expression of untagged *PMP47* under control of the strong *TPI1* promoter or weaker *HIS3* promoter will be required to further investigate this.

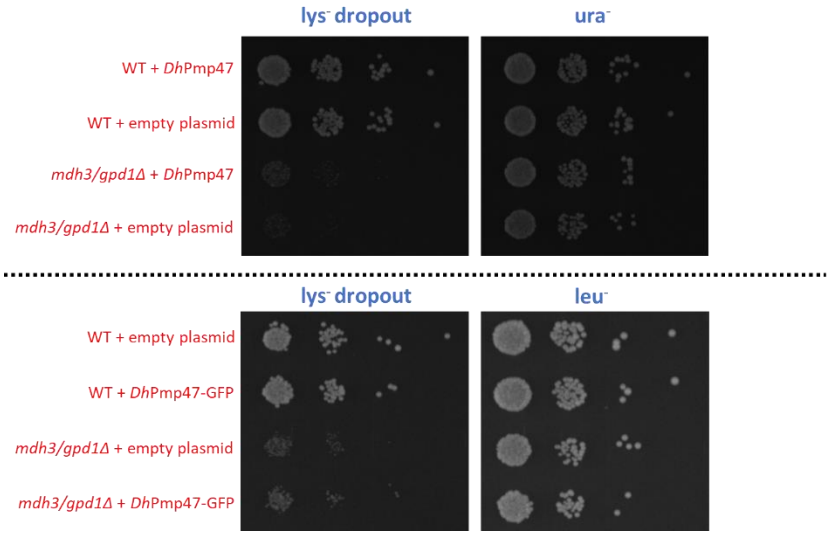

Figure 4.6: The spot assay with S. cerevisiae *mdh3/gpd1Δ* cells, that express either untagged or tagged *Dh*Pmp47, on lysine deficient medium. Serial dilution of cell suspension of the strains indicated were spotted on lys$^-$, as well as either ura$^-$ or leu$^-$ plates (as a positive control) depending on the marker. Prior to spotting, the cells were grown overnight in either ura$^-$ or leu$^-$ media with 0.3% glucose depending on the plasmid marker. Next morning, the cells were diluted to OD_{600}=0.1 in either ura$^-$lys$^-$ or leu$^-$lys$^-$ media and were grown few hours. The cells were then diluted in sterile water at OD_{600}=0.1 and 10 fold serial diluted 3 times. After spotting, the plates were incubated at 30°C and the growth was observed for the next 3 days. The pictures on the figure were taken at the 2nd day of growth.

4.6- *D. hansenii gpd1/mdh3/pmp47Δ* cells show growth retardation on oleate media

When *Dh*Pmp47 was expressed in *S. cerevisiae*, it showed peroxisomal localization and growth restoration of the *mdh3/gpd1Δ* cells on oleate when it was untagged and under the control of oleate inducible promoter. This suggested that *Dh*Pmp47 might play a role in NAD^+ maintenance in peroxisomes during beta-oxidation. To test that, *PMP47* was deleted in *D. hansenii*, as well as in *mdh3/gpd1Δ* cells, using NCYC3363 (the soy sauce isolate) as our strain of choice. After the ORF deletions were confirmed by PCR (See Appendix 4 for detailed information), the cells were spotted on oleate, glucose, galactose and glycerol plates. The results showed that *pmp47Δ* cells grow at a normal rate, whereas *gpd1/mdh3/pmp47Δ* cells show a selective slow growth phenotype on oleate. This defect can be seen more clearly in the 2nd day of the incubation at 25°C. At the third day,

gpd1/mdh3/pmp47Δ colonies are present, but they are smaller than in all the other strains except for the *pex3Δ* strain (Figure 4.7). Moreover, the phenotype on oleate turned out to be slightly more obvious if the cells were grown on the media without amino acids (Figure 4.8).

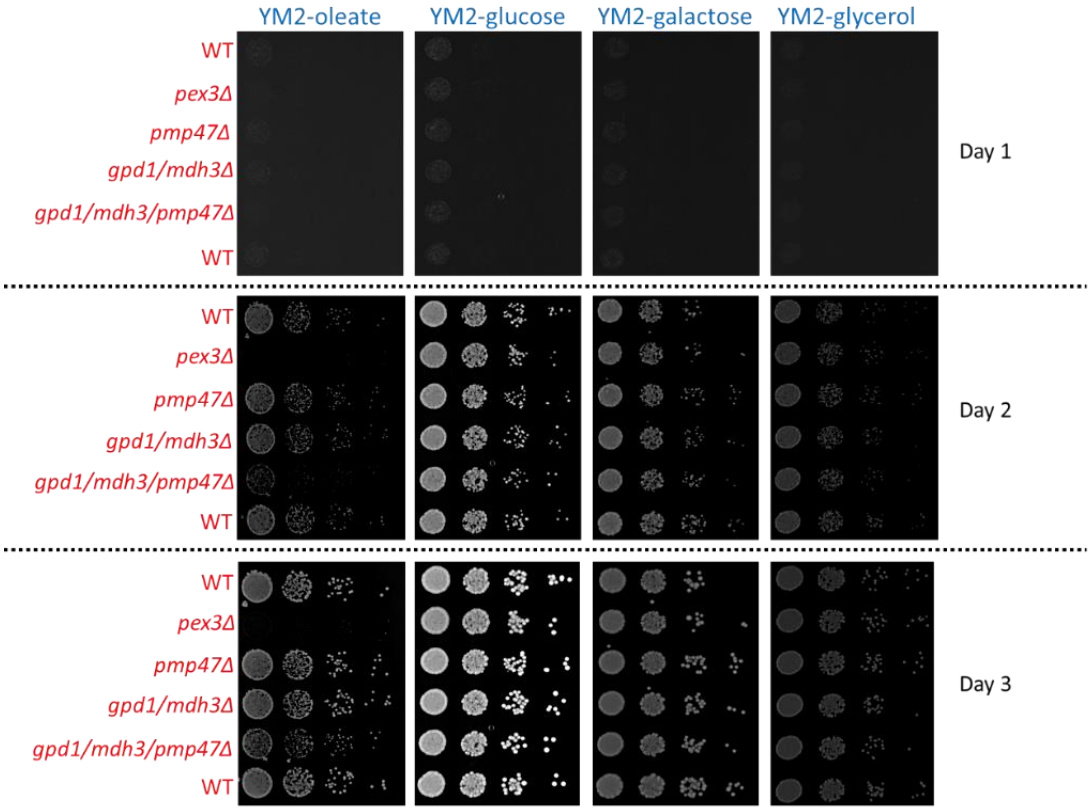

Figure 4.7: The spot assay using *D. hansenii WT, pex3Δ, pmp47Δ, gpd1/mdh3Δ* and *gpd1/mdh3/pmp47Δ* cells on different carbon sources. Cells were grown on minimal media with oleate, glucose, galactose and glycerol as a sole carbon source. Prior to spotting, the cells were grown overnight in YM2 non-selective media with 0.3% glucose. The cells were then diluted in sterile water at OD_{600}=0.1 and 10 fold serial diluted 3 times. After spotting, the plates were incubated at 25°C and the growth was observed for the next 3 days. The pictures were taken at the end of each day.

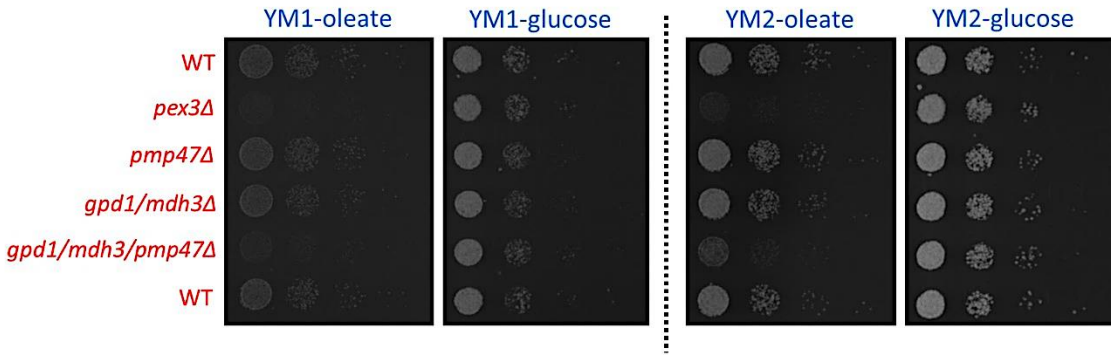

Figure 4.8: The spot assay using the *D. hansenii WT, pex3Δ, pmp47Δ, gpd1/mdh3Δ* and *gpd1/mdh3/pmp47Δ* cells on minimal oleate and glucose media, with amino acids (YM2) and without amino acids (YM1). Prior to spotting, the cells were grown overnight in YM2 non-selective media with 0.3% glucose. The cells were then diluted in sterile water at OD_{600}=0.1 and 10 fold serial diluted 3 times. After spotting, the plates were incubated at 25°C and the growth was observed for the next 3 days. The growth deficiency phenotype observed for *gpd1/mdh3/pmp47Δ* cells does not depend on the presence or absence of the amino acids in the media. The pictures were taken at the 2nd day of growth.

In order to further characterise *gpd1/mdh3/pmp47Δ* cells on oleate, cells were grown in liquid oleate medium and growth was followed over a period of 80 hours. In parallel, growth curves were determined for *WT, pex3Δ, pmp47Δ, gpd1/mdh3Δ* and *gpd1/mdh3/pmp47Δ* cells. The cell growth was analysed in oleate and glucose media. For oleate growth, 2 different oleate curves were initiated at different times of the day, to be able to observe the growth in as many different points as possible within the first 24 hours. The first oleate curve was initiated in the morning, from overnight grown cells in YM2 + 0.3% glucose media. The OD_{600} of each sample was taken at the beginning and at the end of each day for the next 3 days. The second oleate curve was initiated from the samples of the first oleate curve at t=8 hours (by the end of the day). The OD_{600} of each sample was taken at t=3, 16, 19, 22, 24 hours during the first day. As oleate medium is affecting the readings, samples were removed from the cultures and washed twice with water before the OD_{600} was measured. Glucose growth curves were included as a control using YM1-glucose media, in which the OD_{600} of the cells were taken each hour for 8-9 hours during the first day. For the next 2 days, the OD_{600} were taken at the beginning and at the end of the day.

The oleate growth curves show that *pmp47Δ* cells and *gpd1/mdh3Δ* cells grew very similarly to WT cells but the growth of *gpd1/mdh3/pmp47Δ* cells fell behind that of the other strains, showing a clear slow growth phenotype. Whereas WT and *pmp47Δ* cells reach near saturation within 24 h, *gpd1/mdh3Δ* cells and the triple mutant has not reached this OD_{600} after 80 h (Figure 4.9). It can also be seen that the growth of *gpd1/mdh3Δ* cells fell behind (the growth of WT and *pmp47Δ*) within the first 24 hours, but it almost caught up with the WT and *pmp47Δ* cells at the second day. On the other hand, analysis of growth on glucose media showed that all strains grew well on this medium (Figure 4.9).

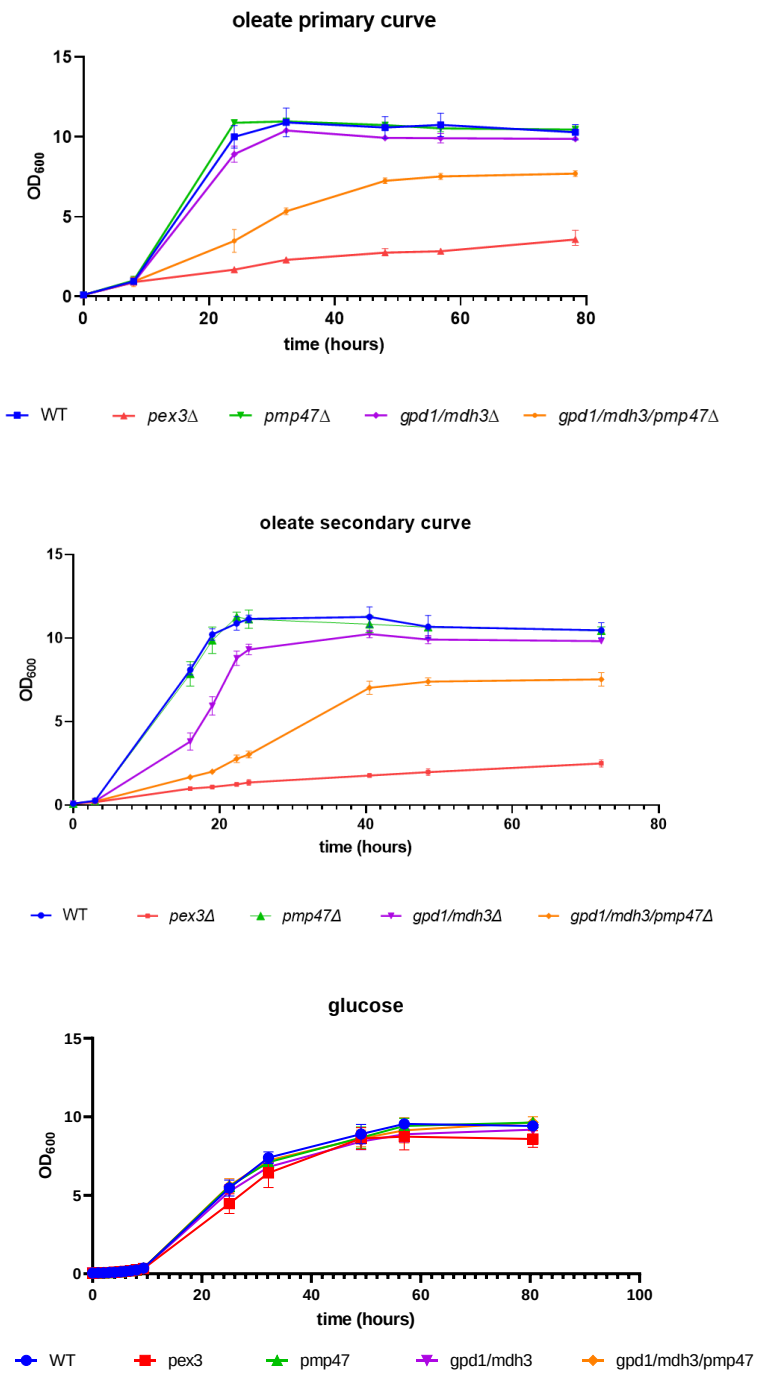

Figure 4.9: The growth curves of *D. hansenii* WT, *pex3Δ*, *pmp47Δ*, *gpd/mdh3Δ* and *gpd1/mdh3/pmp47Δ* in oleate and glucose media. *Pex3Δ* cells were included as a negative control for the oleate growth, as they cannot grow on oleate (Found by Sondos Alhajouj). Oleate primary curve was initiated in the morning, from overnight grown cells in YM2 + 0.3% glucose media. The OD_{600} of each sample was taken at the beginning and at the end of each day for the next 3 days. To initiate oleate secondary curve, OD_{600} of samples from the oleate primary curve were taken at t=8 hours (by the end of the day). Then, each sample from the primary curve was diluted to OD_{600}=0.1 in fresh oleate media, which was the start of the oleate secondary curve (t=0 hours). Then, OD_{600} of each sample was taken at t=3, 16, 19, 22, 24 hours during the first day, at t=40 and t=48 hours during the second day, at t=72 hours in the third day. Glucose curve was started after the cells were grown overnight in YM2 + 0.3% glucose media. n=3. The error bars represent standard deviation.

4.7- Identification of the putative Pmp47b in *D. hansenii*

After it was observed that the growth deficiency of *gpd1/mdh3/pmp47Δ* cells on oleate is not 100% and that beta-oxidation is not completely blocked, it was investigated whether a second peroxisomal NAD^+ transporter might take over the function. In *Candida boidinii*, 2 different Pmp47 were identified, which were named as Pmp47a and Pmp47b. They are closely related proteins, that have 95% similarity in between amino acid sequences (Moreno, *et al.*, 1994). The *C. boidinii* Pmp47b is also thought to be similar to *S. cerevisiae* Ndt1 and Ndt2, that are mitochondrial NAD^+ transporters and paralogs of each other, sharing 70% sequence identity (Todisco *et al.*, 2006)

The putative *Dh*Pmp47, that we identified and mentioned in the previous sections so far, is the best hit that came up during the blast search (Atschul *et al.*, 1990) when *C. boidinii* Pmp47a was blasted against *D. hansenii*. In the same blast search, second best hit was also detected (with Uniprot accession number of Q6BWR5). When analysed on Uniprot, it also seemed to be belonging to Solute Carrier Family 25 (Apweiler *et al.*, 2004), like other Pmp47 derivatives from different organisms. Q6BWR5 was also indicated as similar to ''YIA6'' (Ndt2) of *S. cerevisiae*. When *Sc*Ndt2 was blasted (Atschul *et al.*, 1990) against *D. hansenii*, the same hit Q6BWR5 came up. This hit was named as Pmp47b (Figure 4.10a). However, unlike Pmp47*a* and Pmp47b of *C. boidinii*, and putative Pmp47b do not seem to be closely related to *Dh*Pmp47 as their amino acid sequences are not very similar (Figure 4.10b).

To test the growth of putative Pmp47b that was identified in *D. hansenii, Dh*Pmpb47b-related KOs were generated and they were grown on oleate. Since we do not have the 4th gene deletion marker to be able to generate *gpd1/mdh3/pmp47/pmp47bΔ* in *D. hansenii* or an established Cre/LoxP marker recycling system that works in *D. hansenii*, we generated *pmp47bΔ*, *pmp47/pmp47bΔ* as well as *gpd1/mdh3/pmp47bΔ* in *D. hansenii* (see Appendix 4 for further information) followed by the spot growth analysis on oleate (and glucose as a positive control). However, none of the Pmp47b-related mutants resulted in obvious growth defect on oleate unlike the *gpd1/mdh3/pmp47Δ* cells (Figure 4.11).

A)

```
ScNdt2       MNNGD----------------NKTTLENSKNASLANGNYAIPTKL---------NRLKK      34
DhPmp47b     MVNRNPRDLEELSLTPIERDFSDRVQGEDLEFWASDEGKYQIIHKENQRNAFSPSKILSK      60
             * * :                 ::.  *: :  :  :*:* *  *          : *.*

ScNdt2       NADPRVAAISGALSGALSAMLVCPFDVAKTRLQAQGLQNM---THQSQHYKGFFGTFATI      91
DhPmp47b     FTATQLVTMSGAASGFLAGVVVCPLDVVKTRFQAHGALAQSTGSLASKKYRGFLGAFKTI      120
              :  ::.::*** ** *:.::***:**.***:**:*       :  *::*:**:*:* **

ScNdt2       FKDEGAAGLYKGLQPTVLGYIPTLMIYFSVYDFCRKYSVDIFPH-----SPFLSNASSAI      146
DhPmp47b     LREEGLRGLYRGLVPITIGYLPTWTIYFTVYERAKLFYPEFLKSHFNLETHALNHFCSAL      180
             :::**  ***:** * .:**:**  ***:**: .: :  :::       :  *.: .**:

ScNdt2       TAGAISTVATNPIWVVKTRLMLQTGIGKY----------------STHYKGTIDTFRKI      189
DhPmp47b     TAGMTSSIAVNPIWVVKTRLMIQTGSGSTIYNNNAENKSAAQPKVERTYYKGTLDAIRTM      240
             ***  *::*.***********:*** *.                    *:****:*::*.:

ScNdt2       IQQEGAKALYAGLVPALLGMLNVAIQFPLYENLKIRFGYSESTDVSTDVTSSNFQKLILA      249
DhPmp47b     YKEEGIRVFYSGLIPSLFGLLHVGIHFPVYEKLKLWLECDLK-SASADEQKSTLGRLIAA      299
              ::** :.:*:**:*:*:*:*:*.*:**:**:**: :  . . ..*:*  .*.: :** *

ScNdt2       SMLSKMVASTVTYPHEILRTRMQLKSDLPNTVQ---RHLLPLIKITYRQEGFAGFYSGFA      306
DhPmp47b     SSVSKMIASTITYPHEILRTRMQIQSSNRNKSDKQKGKLINSIIKIYQKEGLKGFYAGYG      359
             * :***:***:************::*.  *. :    :*:  *   *::**: ***:*:.

ScNdt2       TNLVRTVPAAVVTLVSFEYSKKYLTTFFQ--   335
DhPmp47b     VNLIRTVPASAVTLVSFEYFKTYLLEISGKL   390
             .**:*****:.******** *.**  :
```

B)

```
DhPmp47      -------------------------------------------------------MAE      3
DhPmp47b     MVNRNPRDLEELSLTPIERDFSDRVQGEDLEFWASDEGKYQIIHKENQRNAFSPSKILSK      60
                                                                      :::

DhPmp47      I-EELAHAIAGAGGGALSMIVTYPLVTLSTLAQTTQKKKEEKKVEVKEFEAKEYHYRIVN      62
DhPmp47b     FTATQLVTMSGAASGFLAGVVVCPLDVVKTRFQAHGALA----QSTGSLASKKY------      110
             :      :::**..* *: :*. ** .:.*  *:          .. .: :*:*

DhPmp47      KIVTSSSYQAAREIIRKNGVLGLYSGLESALYGITLTNFIYYYFYELTSNV---FLKANV      119
DhPmp47b     ----RGFLGAFKTILREEGLRGLYRGLVPITIGYLPTWTIYFTVYERAKLFYPEFLKSHF      166
                  .   * : *:*::*: *** **     *   *  **: .** :. .   ***::.

DhPmp47      GKRQGGGLSMVQSIITGAIAGAVTCVGSNPFWVANTRMMTDKNRGSEGEK----------      169
DhPmp47b     NL----ETHALNHFCSALTAGMTSSIAVNPIWVVKTRLMIQTGSGSTIYNNNAENKSAAQ      222
             .         :: : :.  ** .:.:. **:**.:**:* :.. **   :

DhPmp47      -----ESTGSTFKAIVNIIENDGVSTLFAGVLPALVLVINPIIQYTIFEQIKNIIIAKNG      224
DhPmp47b     PKVERTYYKGTLDAIRTMYKEEGIRVFYSGLIPSLFGLLHVGIHFPVYEKLKLWLECDLK      282
                     .*:.** .: :::*: .:::*::*:*. :::  *:: ::*::*  : ..

DhPmp47      KKS-----FTAVNAFFIGAFGKLIATSLTYPYITLKSRMHVKKKKLSKQVSDDEEIKLSM      279
DhPmp47b     SASADEQKSTLGRLIAASSVSKMIASTITYPHEILRTRMQIQSSNRNK----SDKQKGKL      338
             . *      *  . :  .:..*:**:::***:  *::**:::..: .*    .:: * .:

DhPmp47      IQEIKKIIKEEGIEGLYGGLTVKLIQSITTAAFL----FYFKEELLTGSVKLVQIFKLMK      335
DhPmp47b     INSIIKIYQKEGLKGFYAGYGVNLIRTVPASAVTLVSFEYFKTYLLEISGKL--------      390
             *:.* ** ::**::*:*.*  *:**::: ::*.      ***  **  * **

DhPmp47      MKKNAVK   342
DhPmp47b     -------   390
```

Figure 4.10: The sequence alignments of *Sc*Ndt2 and *Dh*Pmp47b, as well as *Dh*Pmp47 and putative *Dh*Pmp47b. The alignment was done using Clustal Omega (Sievers *et al.*, 2011). A) The sequence alignment of *Sc*Ndt2 and *Dh*Pmp47b. This alignment revealed 45.51% identity in between the aligned proteins, detected by the database. B) The sequence alignment of *Dh*Pmp47 and putative *Dh*Pmp47b. This alignment revealed 27.54% identity in between the aligned proteins, detected by the database.

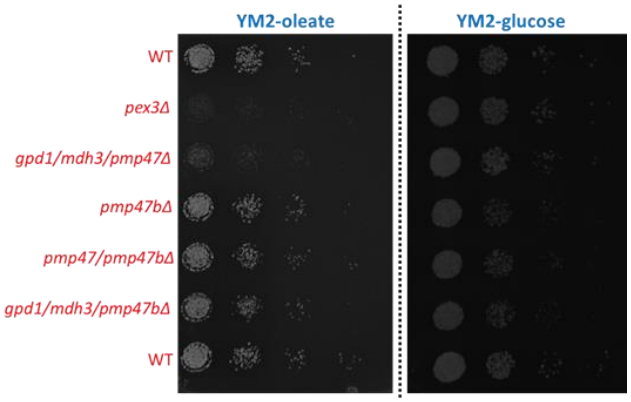

Figure 4.11: The spot assay of *D. hansenii* WT, *pex3Δ*, *gpd1/mdh3/pmp47Δ*, *pmp47bΔ*, *pmp47/pmp47bΔ* and *gpd1/mdh3/pmp47bΔ* on minimal media with oleate or glucose (used as a positive control). Prior to spotting, the cells were grown overnight in YM2 non-selective media with 0.3% glucose. The cells were then diluted in sterile water at OD_{600}=0.1 and 10 fold serial diluted 3 times. After spotting, the plates were incubated at 25°C and the growth was monitored for the next 3 days. The pictures were taken at the 2nd day of growth.

4.8- Further analysis of putative Npy1 in *D. hansenii*

The question arises whether *Dh*Pmp47 is an NAD^+/AMP exchanger as suggested for PXN (van Roermund *et al.*, 2016) or whether it is a NAD^+/NADH carrier as previously proposed (Bernhardt *et al.*, 2012). If it is acting as the former, deletion of the potential Npy1 would affect beta-oxidation in a similar way as *PMP47* deletion.

Firstly, localization of Npy1 in *D. hansenii* was studied. *Dh*Npy1 contains -NKL at its C-terminus. This is a non-consensus PTS1 but it has been shown previously to support import in certain contexts, for instance *Sc*Mdh3 (Elgersma *et al.*, 1996) and *Hs*AGT (Motley *et al.*, 1995). *Dh*Npy1 was tagged with GFP in *D. hansenii* (via our N-terminal tagging strategy that will be described in more details in Chapter 5) to test its localization.

After the colonies that show fluorescent signal were detected and the correct integration of the tagging cassette into the genome was confirmed (See Appendix 5 for further information), the cells were grown in minimal glucose media (YM2 non-selective) to check the localization. GFP-*Dh*Npy1 localized both in cytosol and punctate structures in WT cells whereas it stayed only cytosolic in *pex3Δ* cells (Figure 4.12). We conclude that *Dh*Npy1 is a peroxisomal protein.

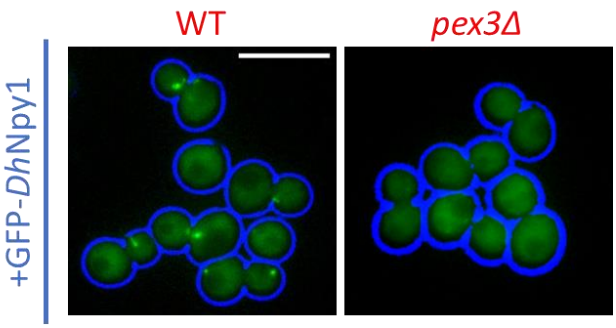

Figure 4.12: The expression of GFP-*Dh*Npy1 in *D. hansenii* WT and *pex3Δ cells*. In WT cells, both cytosolic signal and green puncta were observed. In contrast, only cytosolic GFP was observed in *pex3Δ* cells. The pictures were taken upon growing the cells logarithmically in YM2-non selective media. Each cell wall is highlighted in blue. Scale bar is 5 µm.

In order to test whether *Dh*Npy1 disruption results in the beta-oxidation defect as well as *Dh*Pmp47 (hypothetically due to the NADH being accumulated in peroxisomes which would disrupt the NAD^+/NADH balance), *NPY1* was deleted in both WT and *gpd1/mdh3Δ* cells (See Appendix 4 for further information). After the confirmation of the full gene deletion, the growth of the resulting cells on oleate and glucose as a control were analysed by spot assay. However, no obvious growth defect was observed on oleate plates in between the WT and any *NPY1*-deleted mutants (Figure 4.13).

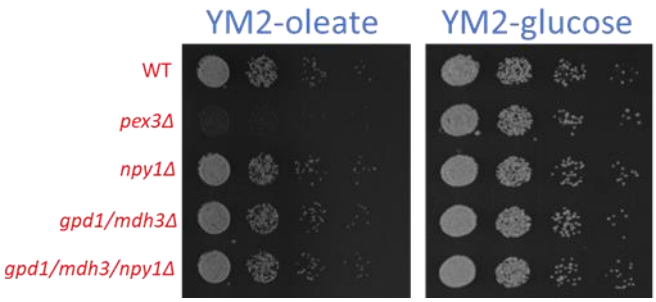

Figure 4.13: The spot assay with WT, *pex3Δ, npy1Δ, gpd1/mdh3Δ* and *gpd1/mdh3/npy1Δ* cells on minimal media with either oleate or glucose. Prior to spotting, the cells were grown overnight in YM2 non-selective media with 0.3% glucose. The cells were then diluted in sterile water at OD_{600}=0.1 and 10 fold serial diluted 3 times. After spotting, the plates were incubated at 25°C and the growth was observed for the next 3 days and the pictures were taken at the 2nd day of growth.

4.9- Expression of putative *Dh*Pnc1 in *S. cerevisiae*

After identification of potential Pnc1 in *D. hansenii*, whether it is peroxisomal and whether it is co-localizing with Gpd1-GFP (from either *D. hansenii* or *S. cerevisiae*) was investigated. To do that, a tagging plasmid pSLV29 was generated which contains ''*TPI1* promoter-*DhPNC1*-GAGAGA linker-mCherry-*PGK1* terminator''. To generate pSLV29, the CTG-adapted *DhPNC1* ORF was synthesised in pUC19 first (this plasmid was named as pNC1). To be able to tag *DhPNC1* ORF with mCherry at its C-terminus, another plasmid pGH113 that has ''-GAGAGA linker-mCherry'', was used as a backbone. *DhPNC1* ORF was replaced with the truncated *INP1 in* pGH113 by classical cloning, which gave rise to pSLV28. Finally, ''*DhPNC1* ORF-GAGAGA linker-mCherry'' region of pSLV28 replaced the ''*DhLYS1* ORF-GAGAGA linker-GFP'' of pSLV26 (the plasmid that was used to tag potential *DhLys1* at the C-terminus). It gave rise to pSLV29, which contains ''*TPI1* promoter-*DhPNC1* ORF-GAGAGA linker-mCherry-*PGK1* terminator''. The plasmid sequence of pSLV29 was confirmed by Sanger sequencing analysis. The whole process to generate pSLV29 can be seen on Figure 4.14.

First, *Dh*Pnc1-mCherry was expressed in WT *S. cerevisiae* cells. Epifluorescence microscopy showed that *Dh*Pnc1-mCherry localized to the cytosol and did not localize to puncta reminiscent of peroxisomes. As *Sc*Pnc1 requires *Sc*Gpd1 for import, the lack of peroxisome labelling of *Dh*Pnc1 could be because *Dh*Pnc1 does not contain a PTS sequence or it cannot piggy back onto *Sc*Gpd1. Therefore, we expressed *Dh*Pnc1-mCherry in *S. cerevisiae gpd1/mdh3Δ* cells co-expressing either *Sc*Gpd1-GFP or *DhGPD1*-GFP. Again, *Dh*Pnc1-mCherry only labelled the cytosol (Figure 4.15). These results indicate that *Dh*Pnc1 is not enriched in peroxisomes when expressed in *S. cerevisiae* and that it cannot piggyback onto *Dh*Gpd1. However, we cannot exclude that in *D. hansenii Dh*Pnc1 might still be imported into peroxisomes, but after it was seen that *Dh*Pnc1-GFP localized in the cytosol in *S. cerevisiae*, this protein was not characterized any further.

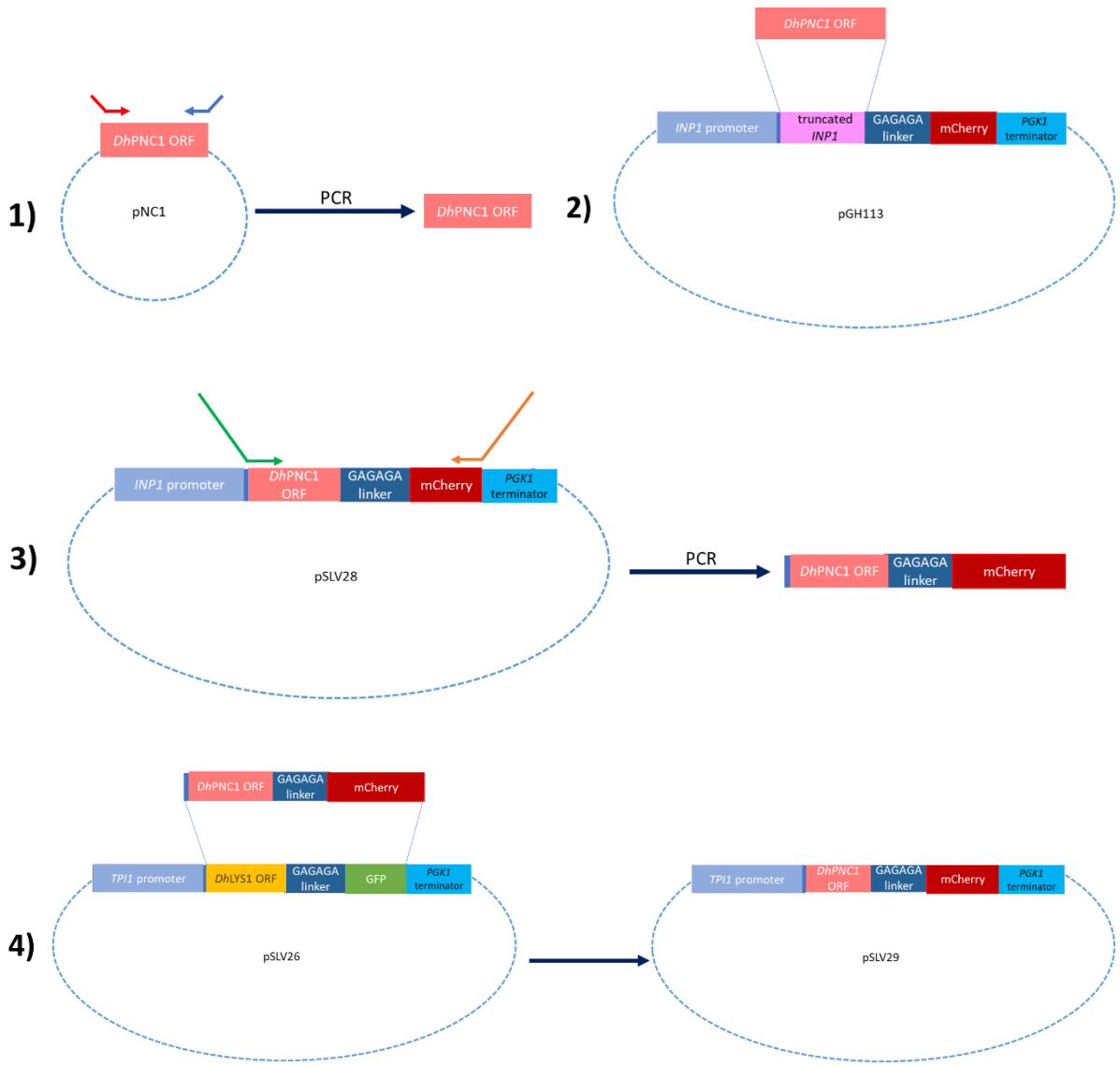

Figure 4.14: The generation of *Dh*Pnc1-mCherry expression plasmid pSLV29. 1) *DhPNC1* ORF was amplified using the pNC1, which contains *DhPNC1* ORF (without a stop codon), as a template. 2) *DhPNC1* ORF was introduced into pGH113 by classical cloning, in a way that truncated *INP1* would be swapped with *DhPNC1* ORF. It gave rise to pSLV28. 3) ''*DhPNC1* ORF-GAGAGA linker-mCherry'' region of pSLV28 was amplified by PCR. 4) The PCR product from the previous step was swapped with the ''*DhLYS1* ORF-GAGAGA linker-GFP'' region of pSLV26 by classical cloning. It gave rise to pSLV29, which contains ''*TPI1* promoter-*DhPNC1* ORF-GAGAGA linker-mCherry-*PGK1* terminator''.

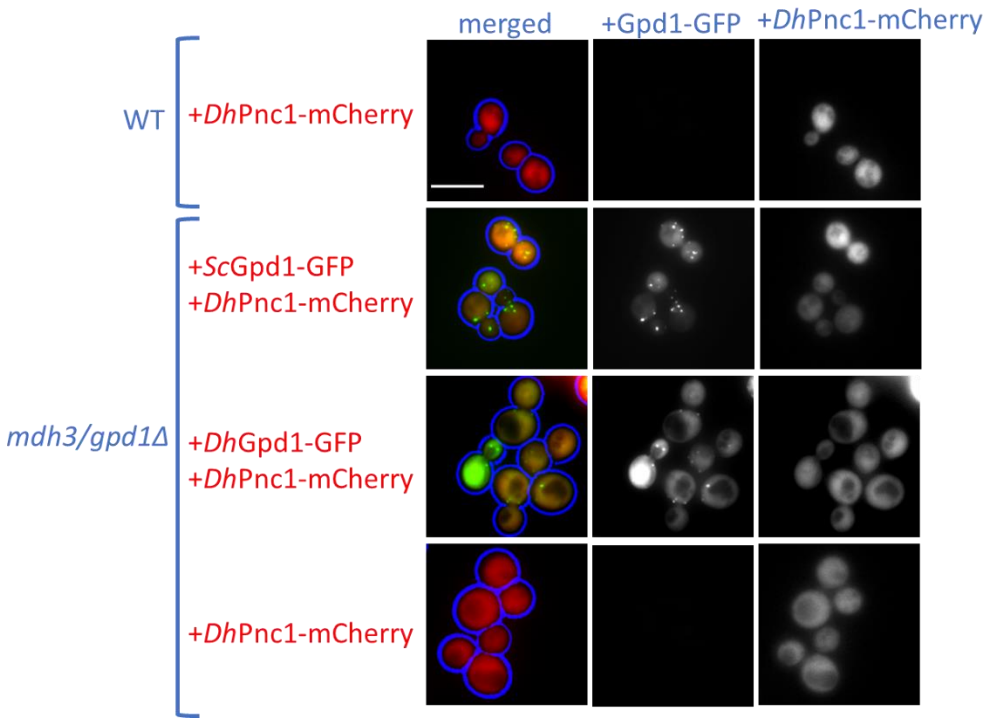

Figure 4.15: Epifluorescence microscopy analysis with *S. cerevisiae* WT and *mdh3/gpd1Δ* cells, that are expressing *Dh*Pnc1-mCherry. *Dh*Pnc1-mCherry was expressed in these cells on its own and also co-expressed with either *Sc*Gpd1-GFP or *Dh*Gpd1-GFP in *mdh3/gpd1Δ* cells. However, *Dh*Pnc1-mCherry stayed in cytosol in each cell and it also did not co-localize with the green puncta that result from the expression of either *Sc*Gpd1-GFP or *Dh*Gpd1-GFP. The cells were grown logarithmically in minimal glucose media prior to analysis. Each cell wall is highlighted in blue. Scale bar is 5 µm.

4.10- *D. hansenii gpd1/mdh3/pmp47Δ* cells are deficient in beta-oxidation activity

In order to test whether the growth defect of *gpd1/mdh3/pmp47Δ* cells on oleate is due to the disruption in the beta-oxidation pathway, the beta-oxidation activity was measured by Dr Carlo van Roermund (affiliated with Laboratory Genetic Metabolic Diseases at Amsterdam UMC, the Netherlands), in WT, *gpd1Δ, mdh3Δ, gpd1/mdh3Δ, pmp47Δ, npy1Δ, gpd1/mdh3/pmp47Δ, gpd1/mdh3/npy1Δ, pmp47bΔ, pmp47/pmp47bΔ* and *gpd1/mdh3/pmp47bΔ* cells, upon oleate induction. In order to trigger the oleate induction, the cells were grown into the medium that contains 0.1% yeast extract and 0.5% glucose for +/- 40 hours. The media was refreshed twice a day. After 40 hours, the cells were switched to oleate rich medium that is composed of 0.12% v/v oleate, 0.2% v/v Tween 80, 0.3% w/v yeast extract, 0.5% peptone, 25 mM KPi at pH=6 and the cells were grown overnight (for 16-17 hours). The next morning, the cells were harvested and the beta-oxidation activities were measured. Relative octanoate (C8:0) fatty acid oxidation rates (in %) were calculated for each mutant, by taking the beta-oxidation activity in WT as 100%.

The results showed that in *gpd1/mdh3/pmp47Δ* cells, the beta-oxidation activity was remarkably reduced compared to WT and the other mutants (the beta-oxidation was found as ~30% in this mutant). In *gpd1/mdh3/pmp47bΔ* cells, the beta-oxidation activity was ~85%. For the rest, even if

the slight reduction was observed, the beta-oxidation activity was around 90-100% (Figure 4.16). These results were consistent with the growth deficiency that was observed for *gpd1/mdh3/pmp47Δ* cells on oleate, suggesting that the oleate deficiency was caused by the disruption of the beta-oxidation activity. The fact that *gpd1/mdh3/pmp47bΔ* cells showed slightly less beta-oxidation activity than the other mutants (except for *gpd1/mdh3/pmp47Δ* cells) suggests that Pmp47b might be also playing a minor role in the beta-oxidation in *D. hansenii*. Our results showed that in *gpd1/mdh3/npy1Δ* cells beta-oxidation activity is not reduced, which is consistent with the normal growth phenotype of the same strain on oleate. This suggests that *Dh*Pmp47 acts independently from *Dh*Npy1. To test this in more details, *DhPMP47* was further expressed in variety of *S. cerevisiae* mutants followed by the measurements of the beta-oxidation activity.

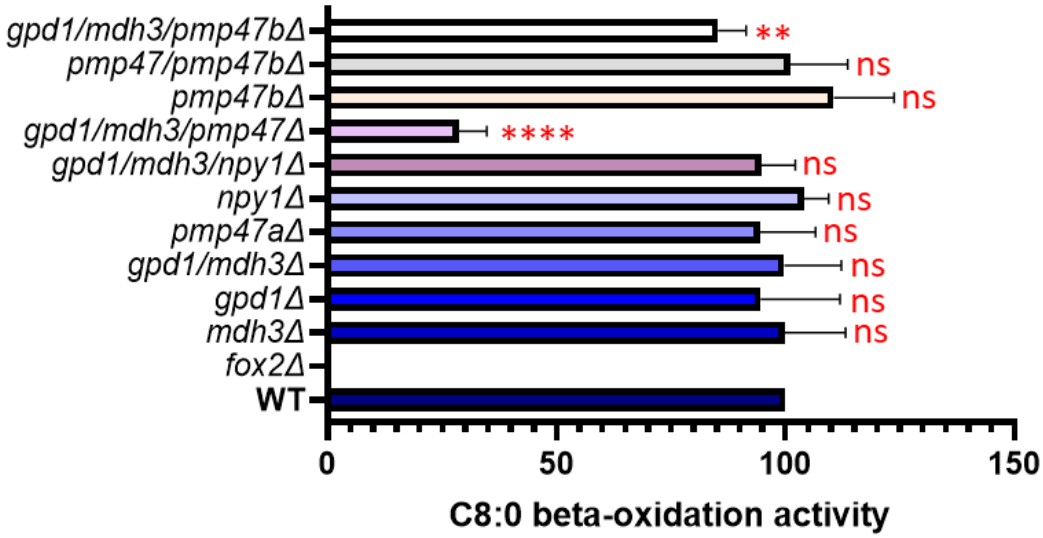

Figure 4.16: The beta-oxidation activity measurements in *D. hansenii* WT, *mdh3Δ, gpd1Δ, gpd1/mdh3Δ, pmp47Δ, npy1Δ, gpd1/mdh3/npy1Δ, gpd1/mdh3/pmp47Δ, pmp47b, pmp47/pmp47bΔ* and *gpd1/mdh3/pmp47bΔ* cells after the oleate induction. Prior to measurements, the oleate induction was triggered as described above. Then, the cells were harvested and the beta-oxidation activities were measured. Relative octanoate (C8:0) fatty acid oxidation rates (in %) were calculated for each mutant, by taking the beta-oxidation activity in WT as 100%. The *fox2Δ* cells, whose beta-oxidation activity is almost 0, were included as a negative control. The data represents the mean and the standard deviation of 3 to 9 replicates. The statistical analysis of differences in beta-oxidation activity of each mutant compared to WT are included, which was calculated using the unpaired t-test with two-tailed P-value. ns: non-significant (P>0.05), ****: significantly different (P<0.0001), **: significantly different (P=0.0023).

4.11- Expression of *DhPMP47* in *S. cerevisiae* mutants

The *D. hansenii* mutant *gpd1/mdh3/pmp47*Δ shows a ~70% loss of beta-oxidation activity, whereas *gpd1/mdh3/npy1Δ* cells did not show a loss in beta-oxidation. This strongly suggests that *Dh*Pmp47 might not be depending on *Dh*Npy1 for its activity. In order to validate the contribution of *Dh*Pmp47 as a NAD^+ provider and in order to test whether *Dh*Pmp47 acts independently from *Dh*Npy1, *DhPMP47* was expressed in several *S. cerevisiae* mutants with decreased beta-oxidation activity, that are *gpd1Δ*, *mdh3Δ*, *mdh3/gpd1Δ*, *mdh3/npy1Δ*, *ant1Δ* and *mdh3/ant1Δ*. This was performed by both Serhii Chornyi and Dr Carlo van Roermund (affiliated with Laboratory Genetic Metabolic Diseases at Amsterdam UMC, The Netherlands). It is followed by the beta-oxidation activity measurements, which were done by Dr Carlo van Roermund (affiliated with Laboratory Genetic Metabolic Diseases at Amsterdam UMC, the Netherlands).

Untagged *Dh*Pmp47 was expressed under the control of the strong oleate inducible *CTA1* promoter. The cells were grown under the same conditions as described in Section 4.10 for oleate induction. Relative octanoate (C8:0) fatty acid oxidation rates (in %) were calculated for each mutant, by taking the beta-oxidation activity in WT as 100%.

The results showed that the expression of *Dh*Pmp47 increased the beta-oxidation activity of each mutant to a different extent, except for the *ant1Δ* + *PMP47* cells. Full reversion upon *Dh*Pmp47 expression was observed in *mdh3Δ* cells and *mdh3/npy1Δ* cells. This indicates that *Dh*Pmp47 is not dependent on the conversion of NADH to AMP to supply the peroxisome lumen with NAD^+ (Figure 4.17).

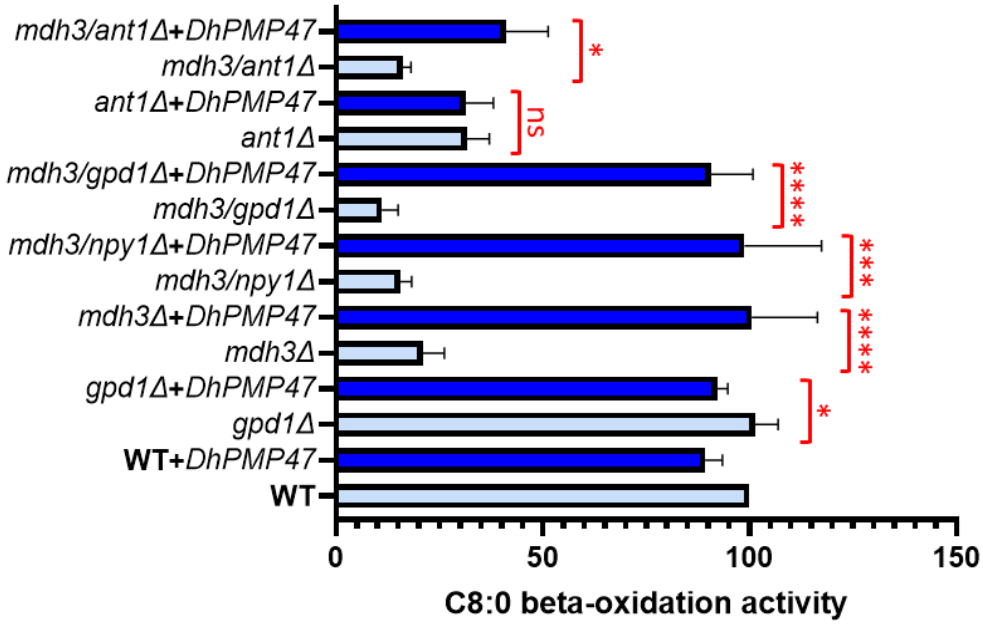

Figure 4.17: The beta-oxidation activity measurements of *S. cerevisiae mdh3Δ, gpd1Δ, mdh3/gpd1Δ, mdh3/npy1Δ, ant1Δ* and *mdh3/ant1Δ* cells, upon the expression of *DhPMP47*. Prior to measurements, the oleate induction was triggered as described above. Then, the cells were harvested and the beta-oxidation activities were measured. Relative octanoate (C8:0) fatty acid oxidation rates (in %) were calculated for each mutant, by taking the beta-oxidation activity in WT as 100%. The *fox2Δ* cells were included as a negative control. The data represents the mean and the standard deviation of 3 to 4 replicates. Unpaired t-test with two-tailed P-value was used to calculate the statistical significance in beta-oxidation activity differences of each mutant with *DhPMP47* compared to the same corresponding mutant without *DhPMP47*. ns: non-significant (P>0.05), *: Significantly different (P is in between 0.01 and 0.05), ***: significantly different (P=0.0001) ****: significantly different (P<0.0001).

4.12- Lysine biosynthesis is not associated with peroxisomes in *D. hansenii*

4.12.1 - In *D. hansenii*, *mdh3Δ*, *gpd1Δ* and *gpd1/mdh3Δ* cells are not lysine bradytrophs

After *Dh*Gpd1 rescued the growth of *S. cerevisiae gpd1/mdh3Δ* cells on lys$^-$, it was investigated whether *D. hansenii* peroxisomes could also be associated with lysine metabolism in the same way as in *S. cerevisiae*. *D. hansenii mdh3Δ*, *gpd1Δ* and *gpd1/mdh3Δ* strains were spotted on lys$^-$ plates (as well as ura$^-$ plates as a positive control) in the same way described in Section 3.6. However, unlike in *S. cerevisiae*, there was no obvious growth defect observed for any mutants and they all grew very similarly to the WT cells (Figure 4.18). Additionally, when potential *D. hansenii Lys1*, that has no PTS1 or PTS2 (or any PTS1/PTS2-like sequence) was tagged in *S. cerevisiae* via either N-terminal or C-terminal tagging, both fusion proteins localised to the cytosol, suggesting *DhLys1* is not a peroxisomal protein (Figure 4.19).

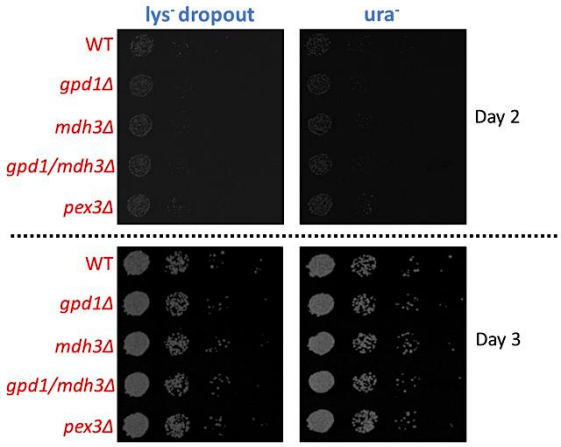

Figure 4.18: Spot assay with *D. hansenii mdh3Δ*, *gpd1Δ* and *gpd1/mdh3Δ* cells. Serial dilution of cell suspension of the strains indicated were spotted on lys⁻ and ura⁻ plates (used as a positive control). Prior to spotting, the cells were grown overnight in YM2 ura⁻ media. Next morning, the cells were diluted to OD_{600}=0.1 in ura⁻lys⁻ media and were grown few hours. The cells were then diluted in sterile water at OD_{600}=0.1 and 10 fold serial diluted 3 times. After spotting, the plates were incubated at 25°C and the growth was observed for the next 3 days. The pictures were taken at the second and third days of growth with 24 hours of interval.

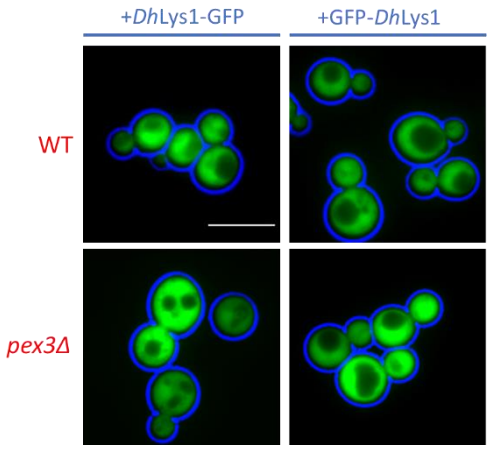

Figure 4.19: The expression of putative *DhLys1* in *S. cerevisiae* WT and *pex3Δ* cells. The expression of both N-terminal (+GFP-*Dh*Lys1) and C-terminal (+*Dh*Lys1-GFP) tagging plasmids resulted in cytosolic labelling. The pictures were taken after the cells were grown logarithmically in minimal glucose media. The cell walls were highlighted in blue. Scale bar is 5 µm.

4.12.2- Growth on lysine deficient medium does not seem to be affected by the disruption of *GPD1/MDH3/PMP47* or *GPD1/MDH3/NPY1* in *D. hansenii*

In order to see whether *Dh*Pmp47 or *Dh*Npy1 might have a role in lysine metabolism in *D. hansenii*, both *gpd1/mdh3/pmp47Δ* and *gpd1/mdh3/npy1Δ* cells were also grown on lys$^-$ media via spot assay. However, both strains did not show an obvious slow growth (Figure 4.20), suggesting that they might not be playing role in the lysine biosynthesis in *D. hansenii*.

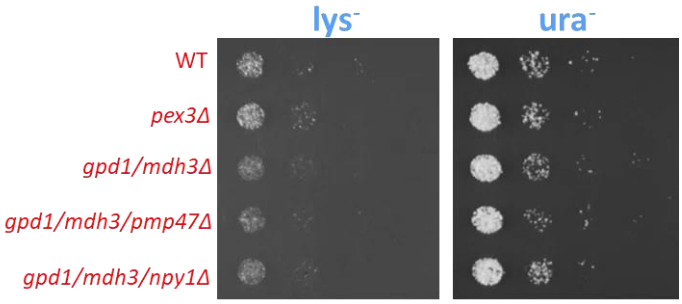

Figure 4.20: Spot growth assay with *gpd1/mdh3/pmp47Δ* and *gpd1/mdh3/npy1Δ* on lys$^-$ and ura$^-$ (was used as a positive control) media. Prior to spotting, the cells were grown overnight in YM2 ura$^-$ media. Next morning, the cells were diluted to OD_{600}=0.1 in ura$^-$lys$^-$ media and were grown few hours. The cells were then diluted in sterile water at OD_{600}=0.1 and 10 fold serial diluted 3 times. After spotting, the plates were incubated at 25°C and the growth was observed for the next 3 days and the plate pictures were taken after 2 days of incubation.

4.13- Discussion

The availability of NAD^+ in peroxisomes is important for various metabolic reactions, especially for the beta-oxidation (Reviewed in Visser *et al.*, 2007). In *S. cerevisiae*, NAD^+ to be used in beta-oxidation relies on regeneration by both Mdh3 and Gpd1 (Al-Saryi *et al.*, 2017a), with a major contribution of Mdh3 (van Roermund *et al.*, 1995; Al-Saryi *et al.*, 2017a) within the peroxisomes. Thus, *mdh3/gpd1Δ* cells result in a severe growth defect on oleate due to the disruption in the NAD^+ supply to the beta-oxidation pathway (Al-Saryi *et al.*, 2017a). However, some beta-oxidation is still taking place in this mutant, suggesting alternative routes of NAD^+ availability in *S. cerevisiae* (van Roermund *et al.*, 2016). As was shown in this chapter, the disruption of *MDH3* and *GPD1* in *D. hansenii* did not affect the growth on oleate which suggests that an alternative NAD^+ supply mechanisms is highly active in this organism.

Previously, *PMP47* orthologues in various organisms were suggested to be potential NAD^+ transporters. This was mainly based on the transport assays after reconstitution of purified plant homologue PXN into liposomes (Agrimi *et al.*, 2012a; Bernhardt *et al.*, 2012). The identification of

potential *D. hansenii* Pmp47 during our bioinformatics search have brought up the idea that *D. hansenii* might be also transporting NAD^+ from cytosol across the peroxisomal membrane via Pmp47. In this case, the presence of alternative NAD^+ transport mechanism to peroxisomes might be causing the *gpd1/mdh3Δ* to still grow normally on oleate with no remarkably reduced beta-oxidation activity.

The expression of *Dh*Pmp47-GFP in *S. cerevisiae* WT and *pex3Δ* cells, followed by co-localization with a red marker showed that it is localized in peroxisomes in this organism and our tagging strategy has been successful (C-terminal tagging based on the previous studies and the presence of the transmembrane domains at the very N-terminal end of the *Dh*Pmp47). It is consistent with the previous studies which show that the various Pmp47 orthologs in different organisms also localized to peroxisomes (McCammon *et al.*, 1990; Sulter *et al.*, 1993; McCammon *et al.*, 1994; Fukao *et al.*, 2001; Bernhardt *et al.*, 2012; van Roermund *et al.*, 2016).The further tagging experiment in *D. hansenii* genome also resulted in peroxisomal membrane labelling pattern (will be discussed in more details in the next chapter).

The growth rescue of *S. cerevisiae mdh3Δ* and *mdh3/gpd1Δ* cells on oleate, upon the expression of untagged *DhPMP47* under the control of oleate inducible *CTA1 promoter* strongly supports our hypothesis that *Dh*Pmp47 is contributing to the peroxisomal NAD^+ supply for beta-oxidation. In contrast, when *PMP47* was tagged with GFP and the expression was controlled by the *TPI1* promoter, no rescue was observed. The reason for this might be that when *PMP47* is tagged with GFP, the tag might be disrupting the function of the protein or expression was not at the right level.

Even though the expression of *PMP47* in *S. cerevisiae mdh3Δ* and *mdh3/gpd1Δ* cells restored growth on oleate, we could not test whether the expression restores the lysine bradytrophy of *mdh3/gpd1Δ* cells. It might be explained by 2 reasons. Firstly, when *PMP47* was expressed under control of the *TPI1* promoter when it was tagged with GFP, the tag might be disrupting the function of the protein. It is consistent with the fact that the same expression did not rescue the oleate growth of the same cells (as well as *mdh3Δ* cells). Secondly, the expression of untagged *Dh*Pmp47 was controlled by oleate inducible promoter, which is repressed during growth on glucose. Since lysine deficient medium is glucose-based media, the promoter for untagged *PMP47* might not be active to induce the expression. Further experiment will be needed in which the *PMP47* is expressed under the control of *TPI1* promoter without the GFP tag.

The further characterization of *Dh*Pmp47 in *D. hansenii* cells (the generation of *gpd1/mdh3/pmp47Δ* mutant cells followed by the growth assay in both solid and liquid oleate media, as well as the beta-oxidation activity measurements) supported the hypothesis of potential involvement of Pmp47 in beta-oxidation. The fact that expression of *Dh*Pmp47 increased the beta-oxidation activities of *S. cerevisiae* mutants, in which the beta-oxidation was impaired due to the disruption of NAD^+ regeneration, suggests that *Dh*Pmp47 contributes to the NAD^+ supply. It is consistent with the previous studies that identified different orthologs of Pmp47 from plants as an NAD^+ transporter (Agrimi *et al.*, 2012a; Bernhrdt *et al.*, 2012; van Roermund *et al.*, 2016). As a result, *Dh*Pmp47, that was identified in this study, is more likely to be a protein that helps with the NAD^+ supply for the beta-oxidation, potentially by transporting NAD^+.

On the other hand, even though the growth curves of *D. hansenii gpd1/mdh3Δ* in oleate revealed that this mutant showed slightly slow growth within the first 24 hours as shown in Figure 4.9 (after 24 hours, they almost caught up with the WT and *pmp47Δ*), it still cannot be certainly concluded that both Gpd1 and Mdh3 are involved in the NAD^+ regeneration for the beta-oxidation in *D. hansenii*. If both of them are involved, our experiments cannot make it clear how much each one

contributes to the NAD^+ regeneration (whether one is more dominant whereas other has a minor contribution). More detailed experiments are required to gain more insight about the contribution of each protein in this process. One possible experiment could be making *mdh3/pmp47Δ* and *gpd1/pmp47Δ* cells in *D. hansenii*, followed by growth assay using oleate media.

The expression of the potential *Dh*Pnc1 in *S. cerevisiae*, that did not localize into the peroxisomes, suggests that *Dh*Pnc1 might not be peroxisomal enzyme and therefore it might not be contributing to NAD^+/NADH redox balance in peroxisomes. Therefore, it was hypothesised that since it is most likely not to be peroxisomal, it is hypothetically not associated with any aspect of NAD^+/NADH redox balance in *D. hansenii* peroxisomes (therefore the beta-oxidation) or with *Dh*Pmp47 during the transport of NAD^+. Hence, it was not characterized any further. However, we cannot exclude that it might localize to peroxisomes when expressed in *D. hansenii*. Further experiments are required to express it in *D. hansenii* to see its localization and whether it co-localizes with *Dh*Gpd1 in *gpd1Δ* cells.

The tagging of potential Npy1 in *D. hansenii* showed that it partially localizes in peroxisomes. However, unlike in *A. thaliana* in which the NAD^+ transport activity of PXN depends on Npy1 (van Roermund *et al.*, 2016), our findings suggest that *Dh*Pmp47 and *Dh*Npy1 might not be acting collaboratively in NAD^+ transport pathway. Van Roermund and his colleagues expressed *A. thaliana* PXN in *S. cerevisiae mdh3Δ* as well as *mdh3/npy1Δ* and measured the beta-oxidation activity. They found that PXN reverted the beta-oxidation defect in *mdh3Δ*, but not of *mdh3/npy1Δ* cells (van Roermund *et al.*, 2016). Their findings suggested that the activity of PXN depends on the availability of peroxisomal AMP produced by Npy1 (van Roermund *et al.*, 2016). The reason is that in *mdh3/npy1Δ* cells, the absence of Npy1, whose function is converting NADH to AMP (AbdelRaheim *et al.*, 2001), results in accumulation of NADH and drastic decrease of AMP. When there is plenty of NADH, PXN did not act on the beta-oxidation activity towards increasing it. However, in *mdh3Δ* mutant, in which NADH is still converted to AMP, PXN could still act on the beta oxidation and rescued it (van Roermund *et al.*, 2016). They concluded that the availability of AMP in *mdh3Δ* triggered the activity of PXN and hence, PXN is most likely transporting NAD^+ in exchange of AMP (van Roermund *et al.*, 2016). However, when the beta-oxidation activity was measured in the same *S. cerevisiae* mutants after the expression of *Dh*Pmp47, the beta-oxidation activity was reverted remarkably in *mdh/npy1Δ* mutant compared to what was observed after PXN expression. Additionally, *D. hansenii gpd1/mdh3/npy1Δ* cells did not show any growth defect on oleate and remarkable loss of beta-oxidation activity. These results suggest that *Dh*Npy1 is unlikely to be associated with the NAD^+ transport mediated by *Dh*Pmp47, hence *Dh*Pmp47 might not be NAD^+/AMP antiporter. Formally, it cannot be excluded that *Dh*Npy1 that we characterized might not be the ortholog of *Sc*Npy1, because it has not been tested in *S. cerevisiae*. Further experiments are required to express it in *S. cerevisiae*, to test whether it localises properly to peroxisomes and whether it complements the beta-oxidation defect observed in *S. cerevisiae mdh3/npy1Δ* cells expressing PXN.

Even though there is a remarkable loss in beta-oxidation in *gpd1/mdh3/pmp47Δ* cells, there is still a residual activity (which is consistent with the growth on oleate). It might be explained by the presence of additional proteins that help with NAD^+ supply. We recently identified the potential Pmp47b in *D. hansenii* and in *gpd1/mdh3/pmp47bΔ* cells, the beta-oxidation activity was slightly more decreased compared to other mutants we tested (except for *gpd1/mdh3/pmp47Δ*). According to this data, Pmp47b might be also involved in providing NAD^+ for the beta-oxidation. However, we have not tagged this protein with fluorescent protein to see where it localizes. Further experiments are needed to tag this protein in *S. cerevisiae* and in *D. hansenii* to see the localization. Additionally, its overexpression in *S. cerevisiae mdh3Δ* and *mdh3/gpd1Δ* mutants, followed by growth

complementation assays on oleate and beta-oxidation activity measurements would clarify its involvement as an NAD^+ supplier. Furthermore, additional deletion marker development is needed to be able to generate *gpd1/mdh3/pmp47/pmp47bΔ* KO in *D. hansenii* to see whether there is further decrease in oleate growth and beta-oxidation activity.

Although our results indicate that *Dh*Pmp47 is unlikely to be associated with *Dh*Npy1, *Dh*Npy1 might still be important for another transport pathway that has a contribution to the beta-oxidation in *D. hansenii*. For instance, it might be involved in *Dh*Pmp47b-dependent transport of NAD^+ (if *Dh*Pmp47b is also found to be peroxisomal NAD^+ transporter). Similarly, in *S. cerevisiae*, the presence of similar peroxisomal NAD^+ transport mechanism is under consideration (van Roermund *et al.*, 2016). Putative *Dh*Pmp47b seems similar to the mitochondrial membrane protein *Sc*Ndt2 (Todisco *et al.*, 2006) that is thought to be also potential peroxisomal NAD^+ transporter in *S. cerevisiae*. The further reduction in the beta-oxidation activity of *S. cerevisiae mdh3/npy1Δ* cells (van Roermund *et al.*, 2016) suggests that Npy1 plays a role in the beta-oxidation. It is possible that *Sc*Npy1 might be also helping with the NAD^+ transport mechanism mediated by this potential transporter. However, the mechanisms of NAD^+ provision might have evolved in different ways for separate organisms, and it is possible that *S. cerevisiae* has lost the NAD^+ transport pathway mediated by Pmp47 ortholog. This might be the reason that *S. cerevisiae* relies mostly on regenerating NAD^+ (van Roermund *et al.*, 1995; Al-Saryi *et al.*, 2017a). However, potential NAD^+ transport pathway that may be mediated by Ndt2, depending on Npy1, might have a minor contribution to the peroxisomal NAD^+ availability in *S. cerevisiae*, similarly to potential *Dh*Pmp47b-related transport in *D. hansenii*. Our results suggest that *D. hansenii*, NAD^+ transport might be more important as deletion of *PMP47*, only along with *GPD1* and *MDH3*, resulted in remarkable growth reduction as well as beta-oxidation deficiency.

Finally, based on the fact that none of the *mdh3Δ, gpd1Δ, gpd1/mdh3Δ, gpd1/mdh3/pmp47Δ* and *gpd1/mdh3/npy1Δ* mutants showed a remarkable growth defect on lys^- media, it was concluded that lysine biosynthesis is unlikely to be associated with peroxisomes in *D. hansenii*. The cytosolic localization of putative *DhLys1* in *S. cerevisiae* is consistent with this finding.

Chapter 5- Characterization of the GFP-tagged Mdh3, Gpd1 and Pmp47 in *D. hansenii* under different media conditions

5.1- Introduction

In the previous chapter, various *D. hansenii* proteins of interests, including Gpd1 and Pmp47 and Pnc1 were tagged with GFP in *S. cerevisiae* expression plasmids and transformed into *S. cerevisiae.* The use of colocalization studies and peroxisome biogenesis and import mutants revealed that Pmp47-GFP and Gpd1-GFP localised to peroxisomes in *S. cerevisiae.* Apart from their heterologous expression in *S. cerevisiae*, it is also important to validate where these proteins localize in the native host. As reported in Chapter 4, Npy1 was tagged with GFP in *D. hansenii* and found to localise to puncta that were absent in *pex3Δ* cells, suggesting it localises to peroxisomes.

In this chapter, the expression and localisation of our protein of interests, Mdh3, Gpd1 and Pmp47, in *D. hansenii* is described. Since expression plasmids that were attempted to be developed for *D. hansenii* in our lab do not inherit efficiently, expression in a cell population varied enormously ranging from no expression to extremely high overexpression. Therefore, a strategy was adapted to tag these proteins in the genome using homologous recombination. In order to achieve this, both N-terminal and C-terminal tagging cassettes were developed that allowed for tagging with GFP. In addition, a red peroxisomal marker (mCherry-PTS1) was also developed for double labelling. This study shows that Pmp47, Mdh3 and Gpd1 are localised to peroxisomes in *D. hansenii*.

5.2- Development of peroxisomal marker ''mCherry-SKL'' and its expression in *D. hansenii*

In order to label peroxisomes in WT cells, a red universal peroxisomal marker construct was generated based on the initial design of a fluorescent protein marker for peroxisomes in *Pichia pastoris* (Kalish *et al.*, 1996). A peroxisomal form of GFP was generated through extension of the GFP ORF with the six amino acids sequence "P-L-H-S-K-L'', which contains the common Peroxisomal Targeting Signal 1 (PTS1) -SKL (Kalish *et al.*, 1996). The PTS1 (-SKL) directs proteins into peroxisomes in a wide range of eukaryotes (Gould *et al.*, 1989). GFP-PTS1 has been used in animals (Motley *et al.*, 2000), plants (Hayashi *et al.*, 2005), fungi (Kalish *et al.*, 1996), slime mould (Rai *et al.*, 2011) and kinetoplastida (Gualdron-Lopez, 2013).

By analogy, we , added -P-L-H-S-K-L to the 3' end of the CTG codon-adapted mCherry, which created mCherry-P-L-H-S-K-L as a marker (which will be referred as ''mCherry-SKL''). The expression of mCherry-SKL was controlled by either *Meyerozyma guilliermondii ACT1* promoter (*MgACT1* promoter) or *Schefferomyces stipitis GPD1* promoter (*SsGPD1* promoter) in 2 different marker plasmids, that gave rise to pSLV35 and pSLV37, respectively (Figure 5.1).

5.2.1- Development of the red marker plasmids pSLV35 and pSLV37

To create the peroxisomal marker plasmids with mCherry-SKL under the control of either *MgACT1* promoter or *PsGPD1* promoter, ''*MgACT1* promoter-mCherry-SKL'' PCR product was cloned into pSA4 plasmid which contains *G418*^{r} marker in between the 1 kb upstream and 1 kb downstream flanks of *D. hansenii ARG1*. The *MgACT1* promoter and CTG-adapted mCherry sequences were gift in a plasmid pAYCU257 from Defosse *et al.* (2018), based on their work on development of genetic toolkit for CTG-clade organisms (Defosse *et al.*, 2018). The ''*MgACT1* promoter-mCherry-SKL'' construct was introduced into pSA4 in between ~1 kb *DhARG1* flanks, into a region behind the *G418*^{r} marker via classical cloning, so that the red marker could be targeted into the *DhARG1* locus. The resulting plasmid was named as pSLV35. An additional marker plasmid was developed with the same layout except the *MgACT1* promoter swapped with *SsGPD1* promoter, which gave rise to pSLV37. *SsGPD1* promoter region was synthesised in pUC19 by GenScript. To obtain *SsGPD1* promoter region, Gpd1 from *S. stipitis* was identified first by blast search (Altschul *et al.*, 1990), using its *S. cerevisiae* ortholog as a query sequence which is available on SGD database (https://www.yeastgenome.org/). After the best hit for *Ss*Gpd1 was analysed on Uniprot (Apweiler *et al.*, 2004), its ORF sequence with 1 kb upstream and 1 kb downstream flanking regions was accessed via KEGG database (Kanehisa and Goto, 2000). As promoter and terminator sequences, 500 bp upstream and 250 bp downstream regions of *SsGPD1* ORF was used. All the promoter, terminator and fluorescence marker ORF sequences, that were mentioned in this section, can be seen on Appendix 3.

The final plasmids pSLV35 and pSLV37 are described in details on Figure 5.1. The sequence of both plasmids were confirmed by Sanger sequencing analysis.

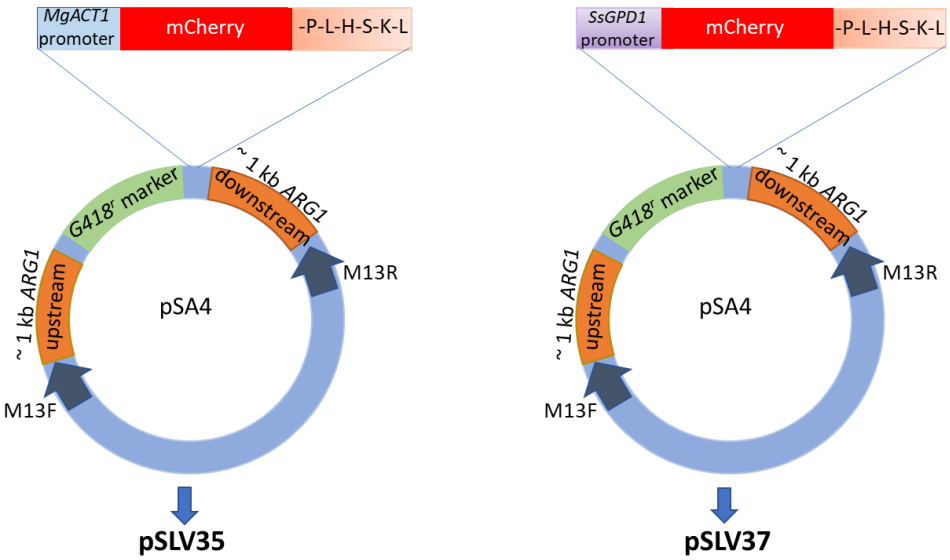

Figure 5.1: The peroxisomal marker plasmids pSLV35 and pSLV37. The plasmid pSA4 was used as a backbone, which contains *G418*^{r} marker that is surrounded by the 1 kb upstream and 1 kb downstream flanks of *D. hansenii ARG1.* Two different red marker vectors pSLV35 and pSLV37 were developed with ''mCherry-SKL'', under the control of *MgACT1* and *SsGPD1* promoters respectively. The red markers were cloned behind the *G418*^{r} marker of pSA4. In this case, *G418*^{r} and red marker are flanked by 1 kb upstream and downstream of *ARG1*. The 1 kb upstream and 1 kb downstream of *DhARG1* are surrounded by M13 Forward (indicated as M13F) and M13 Reverse (indicated as M13R) primers to allow linearization of the whole construct by PCR.

5.2.2- Strategy to express red peroxisomal marker constructs in *D. hansenii*

The expression of the red peroxisomal markers was developed in such way that they will integrate into the genome, into *D. hansenii ARG1* locus. We used *ARG1* locus as a safe landing site for our red marker because the strain NCYC102, that was used for the protein localisation experiments, turned out to have two copies of *ARG1* (which was discovered by our colleague Sondos Alhajouj). In this case, after the integration of the red marker construct at this locus; the second copy of *ARG1* in the genome could prevent the cells from becoming arginine auxotroph.

After the plasmids pSLV35 and pSLV37 were made, the whole marker cassette (*ARG1* upstream-*G418*^{r} marker-*MgACT1/SsGPD1* promoter-mCherry-SKL- *ARG1* downstream) was amplified by PCR, using M13 Forward and M13 Reverse primers. Transformation of the linear cassettes into *D. hansenii* allowed the homologous recombination in between *ARG1* flanks to occur, which resulted in the integration of the red marker into the *ARG1* locus (Figure 5.2).

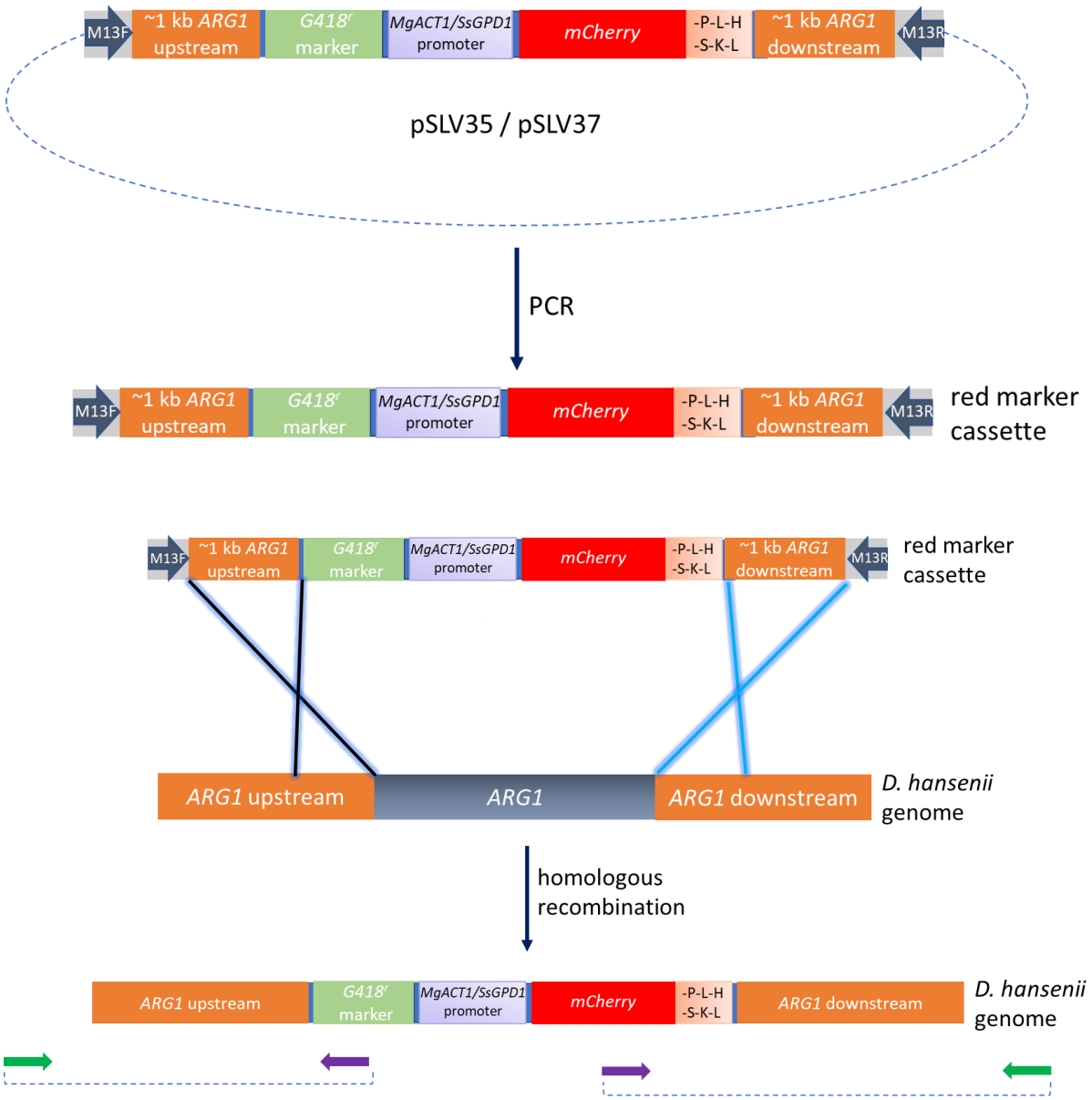

Figure 5.2: The strategy of red peroxisomal marker expression in *D. hansenii*. Using red marker plasmid (pSLV35 or pSLV37) as a backbone, the red marker cassette (*G418*^{r} marker-*MgACT1/SsGPD1* promoter-mCherry-SKL, that is surrounded by *DhARG1* homology flanks) was amplified with M13 Forward (indicated as M13F) and M13 Reverse (indicated as M13R) primers. After the linearization of the red marker cassette by PCR, it was transformed into *D. hansenii*, which allowed the homologous recombination to occur between homology flanks. As a result, ''*G418*^{r} marker-*MgACT1/SsGPD1* promoter-mCherry-SKL'' integrated into the *ARG1* locus on *D. hansenii* genome. The integration was checked by PCR, using one primer outside the *ARG1* flank (indicated as green arrow at the bottom) and other primer annealing to either *G418*^{r} marker or mCherry ORF (indicated as purple arrow at the bottom).

5.2.3- The red peroxisomal marker is successfully expressed in *D. hansenii*

To test whether the newly-developed peroxisomal marker is functional, the marker construct with ''*SsGPD1* promoter-mCherry-SKL'' was amplified by PCR. The PCR product was transformed into NCYC102 and the isogenic *pex3Δ* cells. The transformants were analysed for mCherry expression by epifluorescence microscopy. The results showed that in WT cells, a red punctate pattern was observed. This punctate pattern was absent in *pex3Δ* cells and was replaced by a cytosolic diffuse labelling (Figure 5.3). The punctate pattern that was observed in WT cells was similar to what was observed in other yeasts (especially in *S. cerevisiae*) after the expression of peroxisomal proteins or peroxisomal markers. Besides, the fact that the fluorescent signal depended on Pex3 showed that the punctate pattern in WT cells are peroxisomes. We conclude that our newly-developed peroxisomal marker is functional and our strategy for its expression has been successful.

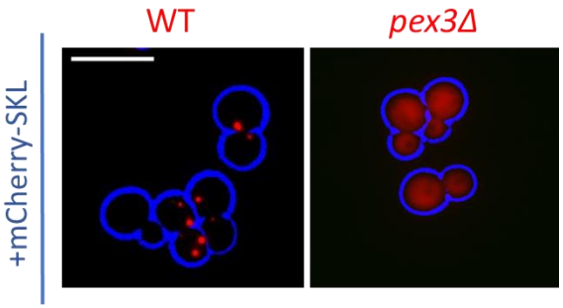

Figure 5.3: The expression of the red peroxisomal marker ''*SsGPD1* promoter-mCherry-SKL'' in *D. hansenii* WT and *pex3Δ* cells. In WT cells, red peroxisomal puncta was observed which were not present in *pex3Δ*. Whereas in *pex3Δ* cells, the red marker localized in cytosol. The pictures were taken after the cells were grown in YM2 non-selective media logarithmically. Each cell wall is highlighted in blue. Scale bar is 5 µm.

5.3- GFP-Mdh3 localises to peroxisomes in *D. hansenii*

5.3.1- Development of N-terminal tagging strategy for *D. hansenii*

Most of the peroxisomal matrix proteins have a PTS1 signal at the C-terminus of their protein sequences (Kalish *et al.*, 1996). The PTS1 needs to be at the extreme C-terminus of the protein to be recognised by its receptor (Gould *et al.*, 1988). Hence, when PTS1 proteins are tagged with a fluorescent marker, the tag should be placed at the N-terminus of the target protein in order to prevent its PTS1 signal from being disrupted. The selectable marker (with promoter, selectable marker ORF and terminator) is placed in front of the fusion protein (fluorescent tag-target ORF with

PTS1). In this case, the fusion protein needs an additional promoter to allow its expression. If this promoter is a strong promoter, the overexpression of the fusion protein might disrupt the physiology of the peroxisomes. In contrast, for proteins with an N-terminal or internal targeting signal, the tag is placed at the C-terminus of the target protein, the selectable marker is placed after the fusion protein. In that case, the fusion protein does not require an extra promoter as its expression is controlled directly by the endogenous promoter of the target protein.

The first tagging strategy was developed for N-terminal tagging of Mdh3 and Npy1, because both of them contain a putative PTS1, -SKL and -NKL, respectively. To obtain the N-terminal tagging construct, the vector pSA5, that contains ''*hygB*^{r} marker- *MgACT1* promoter-CTG codon adapted GFP-P-L-H-S-K-L-'' flanked by 1 kb upstream and 1 kb downstream of *DhARG1* (Figure 5.4), was used as a template. The CTG codon adapted GFP ORF in this plasmid was a gift from Defosse *et al.* (2018) in a plasmid pAYCU273, based on their work on development of genetic toolkit for CTG-clade organisms (Defosse *et al.*, 2018). The region of ''*hygB*^{r} marker-*MgACT1* promoter-GFP (without the stop codon)'' was amplified by PCR, using the forward primer which introduces the last 50-60 nt of the upstream region of the target gene, and the reverse primer which introduces GAGAGA linker and the first 50-60 nt of the target gene. The primers, which anneal to the N-terminal tagging cassette on the plasmid, were designed in a way that no frameshift will occur on the resulting fusion of ''GFP-GAGAGA linker-target ORF''. The resulting PCR product was subsequently amplified by PCR to extend the homology arms of the tagging construct, as we noticed that the longer flanks provide a higher efficiency of targeted integration. The final PCR product was then transformed into *D. hansenii*, which allows the homologous recombination to occur between the homology arms and the target locus in the genome. It results in the insertion of the ''*hygB*^{r} marker-*MgACT1* promoter-GFP-GAGAGA linker'' right in front of the target gene, in which case the GFP is fused with the target ORF. This strategy is shown in details on Figure 5.4.

After the construct was transformed into *D. hansenii* and the colonies were checked for the correct integration of the cassette into the genome (See Appendix 5 for further information), the colonies were screened under the microscope to detect the fluorescent signal.

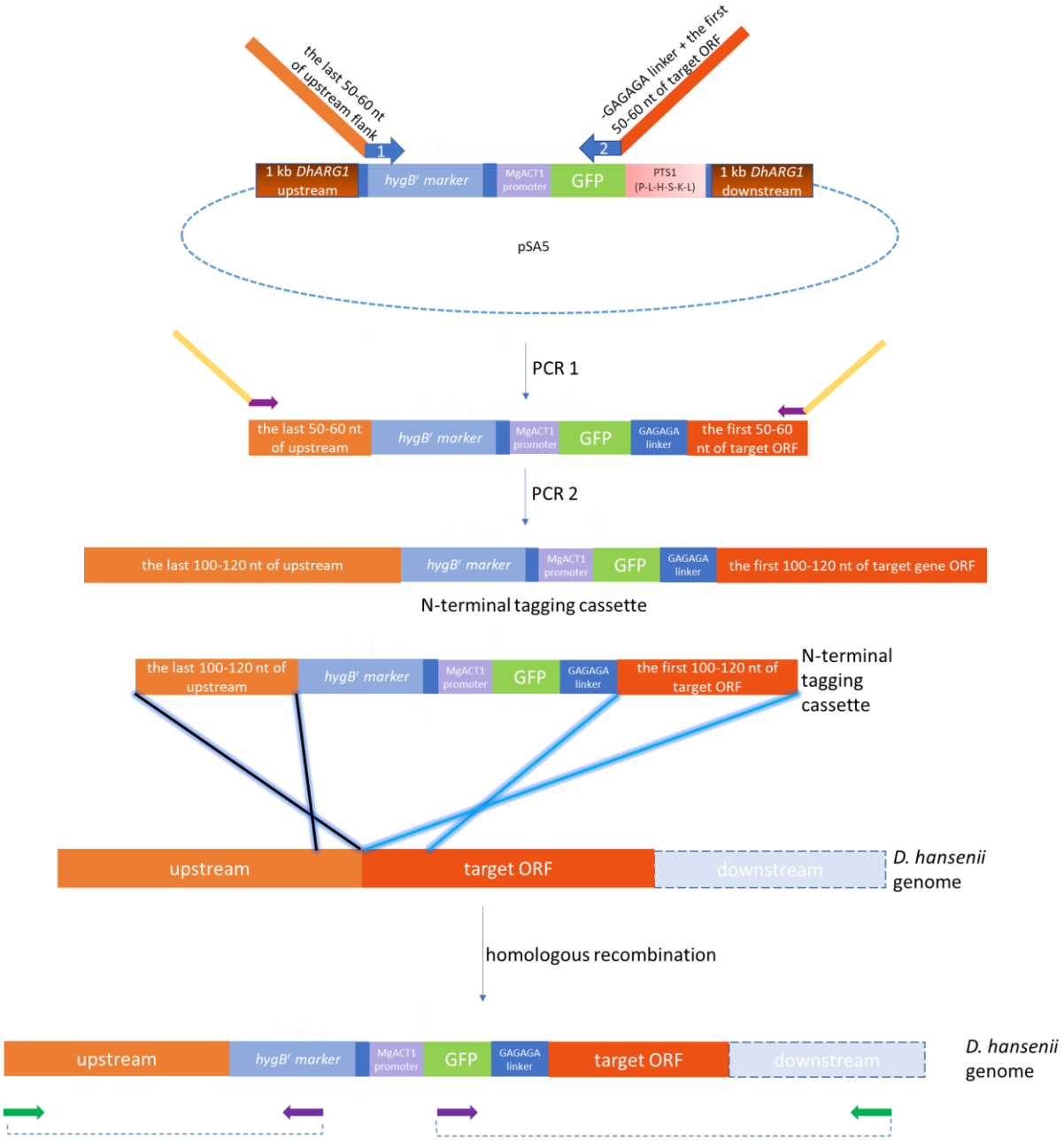

Figure 5.4: Strategy for N-terminal tagging in the genome for *D. hansenii*. The ''*hygB*^{r} marker-*MgACT1* promoter-GFP'' region (excluding -PTS1) of pSA5 was amplified by PCR, using the forward primer that is flanked by the last 50-60 nt upstream of target gene, and the reverse primer that is flanked by the first 50-60 nt of the target gene ORF. The annealing sequences of these primers (labelled as ''1'' and ''2'') can be seen on Appendix 6. The resulting product was amplified by a second PCR, with the primers that anneal right at the 5' and 3' ends of the first product, that adds the adjacent 50-60 nt of upstream and target ORF. The final product with longer homology arms is transformed into *D. hansenii*. The homologous recombination in between the identical sequences allows the ''*hygB*^{r} marker-*MgACT1* promoter-GFP-GAGAGA linker'' to be inserted right in front of the target ORF, where the fusion occurs in between GFP and the target ORF. The correct integration was checked via PCR using one primer annealing to the outside of the homology flank (indicated as green arrows) and the other primer annealing to either *hygB*^{r} marker ORF or GFP ORF (indicated as purple arrows).

5.3.2- Expression of newly-developed N-terminal tagging construct to tag Mdh3 in *D. hansenii*

In order to tag Mdh3 using the newly-developed N-terminal tagging strategy shown in Figure 5.4, the ''*hygB*^{r} marker-*MgACT1* promoter-GFP'' region was amplified using pSA5 as a template, to introduce the homology flanks (the last 60 nt of *MDH3* upstream to the 5' end and GAGAGA linker-the first 60 nt of *MDH3* ORF to the 3' end). Using 65 nucleotides as homology flanks, ~30 colonies were observed and 5 colonies were fluorescent. However, the fluorescence we observed was faint and diffuse unlike the punctate pattern we expected. When the genomic DNAs of these colonies were screened by PCR, none of them had the integration of the N-terminal tagging cassette into the right place at the genome. Subsequently, the homology arms were increased to 125 nucleotides by a second PCR. The final PCR product was transformed into both NCYC102 (WT) and isogenic *pex3Δ* cells and transformants were selected. After transformation and selection, 62 colonies of ''WT+GFP-Mdh3'' transformation were observed of which 15 showed fluorescence and 12 colonies showed a clear punctate pattern. PCR analysis showed that the transformants containing the punctate GFP pattern integrated the tagging construct at the correct genomic site, whereas the diffuse ones were not. Out of 30 colonies screened for ''*pex3Δ*+GFP-Mdh3'' transformation, 7 colonies showed fluorescence as cytosolic diffuse. PCR analysis showed that 6 transformants containing the cytosolic GFP integrated the tagging construct at the correct genomic site.

Epifluorescence microscopy analysis, that was done after the cells were grown logarithmically in YM2 non-selective media, showed that in WT cells, a green punctate pattern was observed whereas a green diffuse, cytosolic signal was observed in *pex3Δ* cells (Figure 5.5). The puncta pattern resembles that of peroxisomes in other yeasts and its dependence on Pex3 supports our hypothesis that *Dh*Mdh3 is a peroxisomal protein.

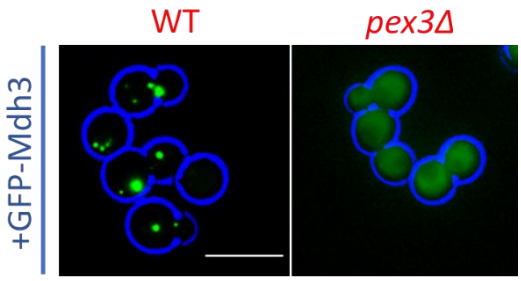

Figure 5.5: GFP-*Dh*Mdh3 localises to structures dependent upon Pex3. Epifluorescence microscopy analysis that shows the expression of N-terminal GFP-tagged Mdh3 in *D. hansenii* WT and *pex3Δ* cells. The cells were grown using YM2 non-selective media (glucose) logarithmically prior to microscopy analysis. The fluorescence was captured using the green channel. Each cell wall of was highlighted in blue. Scale bar is 5 µm.

5.3.3- Both red marker constructs are well expressed in *D. hansenii* WT/*pex3Δ*+GFP-Mdh3 cells, the green punctate pattern in +GFP-Mdh3 cells co-localize with both red markers

After the successful N-terminal tagging of Mdh3 in both WT and *pex3Δ* cells, the red marker was co-expressed in the same cells expressing GFP-Mdh3 to test whether GFP-Mdh3 colocalises with the peroxisomal marker mCherry-SKL. We decided to express both ''*MgACT1* promoter-mCherry-SKL'' and ''*SsGPD1* promoter-mCherry-SKL'' this time to check whether both constructs are functional. Only ''*SsGPD1* promoter-mCherry-SKL'' had been tested in WT and *pex3Δ* cells previously as described in Section 5.2.3.

Both cassettes in plasmid pSLV35 and pSLV37 were amplified by M13F and M13R primers, which resulted in 2 PCR products that are ''*MgACT1* promoter-mCherry-SKL'' and ''*SsGPD1* promoter-mCherry-SKL'', each flanked by 1 kb *DhARG1* homology arms to direct integration into the *ARG1* locus. These PCR products were transformed into GFP-Mdh3 expressing NCYC102 and isogenic *pex3Δ* cells. Transformants were analysed for mCherry expression. Out of 60-70 transformants that were observed on each plate with the insert, 30 transformants were checked under the microscope and ~20 of them were fluorescent. The transformants were also checked for the correct integration.

The colonies with the correct integration (See Appendix 5 for further information) were analysed by epifluorescence microscopy, after the cells were grown in YM2 non-selective media (glucose) logarithmically. The results showed that both *MgACT1* and *SsGPD1*-controlled mCherry-SKL constructs are well-expressed in *D. hansenii*. In WT cells, a red punctate pattern was observed which was co-localizing with the green punctate due to the expression of GFP-Mdh3. In contrast, in *pex3Δ* cells, the cytosolic red fluorescent signal was observed which was also overlapping with the cytosolic green cytosolic signal due to GFP-Mdh3 expression (Figure 5.6). These results show that the puncta to which GFP-Mdh3 localises are peroxisomes as it colocalises with a well-established marker for peroxisomes and is dependent on Pex3. After it was discovered that both red marker cassettes are well-expressed, the random choice was made to proceed with the ''*SsGPD1*-mCherry-SKL'' construct for the rest of the co-localization experiments.

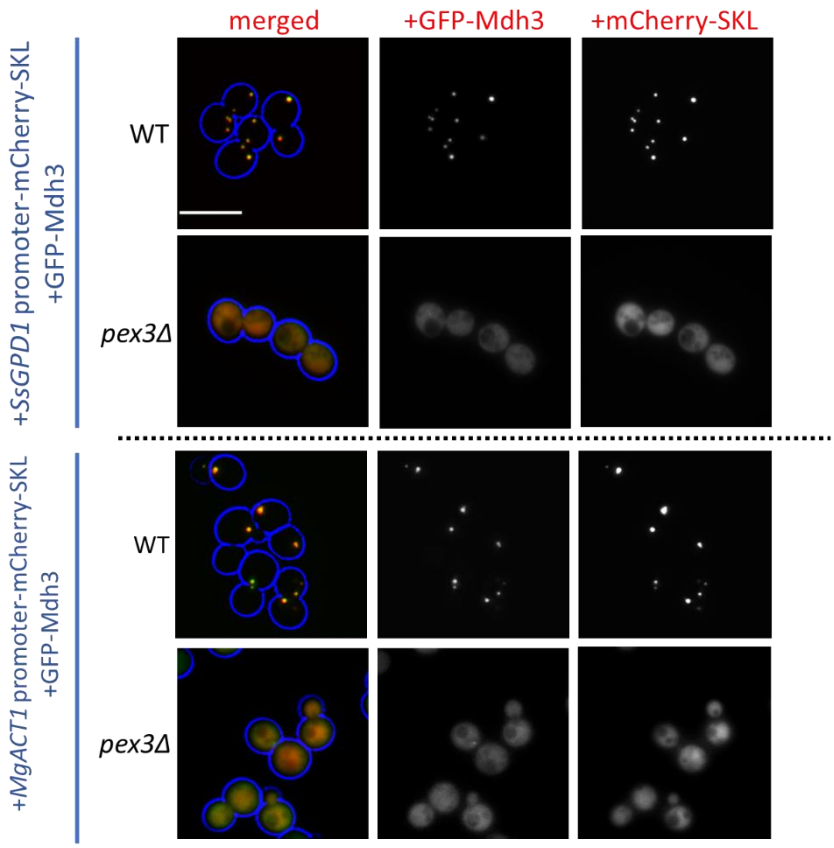

Figure 5.6: *Dh*Mdh3 is a peroxisomal enzyme. Epifluorescence microscopy analysis of GFP-Mdh3 expressed *D. hansenii* WT and *pex3Δ* cells, that were transformed with ''*MgACT1 promoter*/*SsGPD1* promoter-mCherry-SKL'' constructs. Both peroxisomal marker constructs co-localized with the green punctate pattern, showing that both red marker constructs are functional. The cells were imaged after being grown in YM2 non-selective media (glucose) logarithmically. Each cell wall was highlighted in blue. Scale bar is 5 µm.

5.4- Gpd1-GFP localizes to peroxisomes in *D. hansenii*

5.4.1- The development of C-terminal tagging strategy for *D. hansenii*

In order to tag both Gpd1 and Pmp47 in *D. hansenii*, a C-terminal tagging strategy was developed (Figure 5.7) and was first used for tagging of Gpd1. The development of C-terminal tagging was required because *Dh*Gpd1 contains a non-canonical PTS2 signal at its N-terminus and *Dh*Pmp47 contains several transmembrane domains at its N-terminus (the first transmembrane domain is located in between the 12th and 34th amino acids). Thus, the tagging constructs needed to be placed at their C-termini in order not to disrupt targetting. As it was mentioned in Section 5.3.1, the selectable marker (*hygB*^{r} marker was used for this experiment) is placed behind the fusion protein.

Besides, since there are no other tagging cassette components in front of the fusion protein (target ORF+GFP tag), its expression is controlled by the endogenous promoter of the target gene.

The development of C-terminal tagging strategy was started by construction of a C-terminal tagging plasmid, that contains ''-GAGAGA linker-CTG codon-adapted GFP (with a stop codon)-*SsGPD1* terminator-*hygB*^{r} marker'' which is named as pSLV38. The ''CTG codon-adapted GFP'' was a gift in a plasmid pAYCU273 from Defosse *et al.* (2018), based on their work on development of toolkit for CTG-clade organisms (Defosse *et al.*, 2018). *SsGPD1* terminator region was synthesised in pUC19 by GenScript. To obtain it, Gpd1 from *S. stipitis* was identified first by blast search (Altschul *et al.*, 1990), using its *S. cerevisiae* ortholog as a query sequence which is available on SGD database (https://www.yeastgenome.org/). After the best hit for *Ss*Gpd1 was analysed on Uniprot (Apweiler *et al.*, 2004), its ORF sequence with 1 kb flanking regions was accessed via KEGG database (Kanehisa and Goto, 2000). We used 250 bp downstream of *SsGPD1* ORF as a terminator region. The sequence of *SsGPD1* terminator region can be seen on Appendix 3.

This C-terminal tagging cassette in pSLV38 can then be used as template in a PCR to generate a product with the last 60-90 bp of target ORF without stop codon, and the first 60-90 bp of downstream of target ORF. The sequences of each primer, which anneal to the C-terminal tagging cassette, were chosen in a way that no frameshift will occur on the resulting fusion of ''target ORF-GAGAGA linker-GFP''. The resulting PCR product can subsequently be amplified again to extend the homology arms further. The final product is then ready to be transformed into *D. hansenii*, which allows the insertion of the tagging construct between the end of the target ORF and the downstream sequence as a result of homologous recombination. In this way, the target ORF is fused with the GFP at its C-terminus and the tagged protein is expressed behind its own promoter. The whole process is shown in details on Figure 5.7.

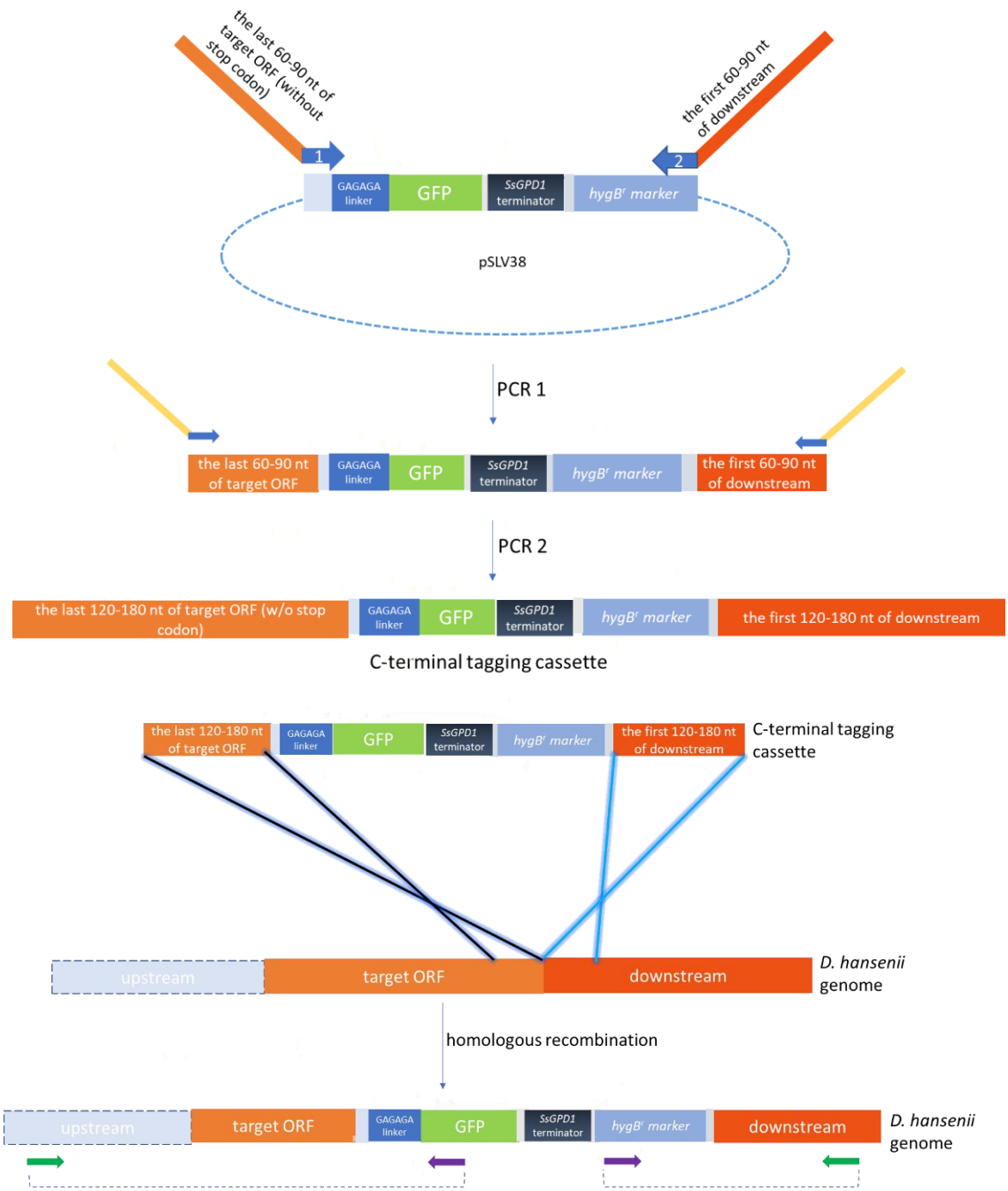

Figure 5.7: The C-terminal tagging in the genome strategy. The''-GAGAGA linker-GFP (with a stop codon)-*SsGPD1* terminator-*hygB*^{r} marker'' region of pSLV38 was amplified by PCR, using the forward primer that introduces the last 60-80 nt of the target ORF (without the stop codon), and the reverse primer that introduces the first 60-80 nt of downstream of target ORF. The annealing sequences of these primers (labelled as ''1'' and ''2'') can be seen on Appendix 6. The resulting product was amplified by a second PCR with the primers that add the adjacent 60-80 nt of target ORF and the adjacent 60-80 nt downstream (of the target ORF) to the 5' and 3' ends respectively. The final product with longer homology arms was transformed into *D. hansenii*. The homologous recombination in between the identical sequences allowed the tagging construct to be inserted right behind the target ORF, where the fusion occurs in between the target gene and GFP tag. The correct integration was checked via PCR using one primer annealing to the outside of the homology flank (indicated as green arrows) and the other primer annealing to either GFP ORF or *hygB*^{r} marker ORF (indicated as purple arrows).

5.4.2- Co-expression of Gpd1-GFP and mCherry-SKL in *D. hansenii*

Using the newly-developed C-terminal tagging plasmid as a template, the region of ''GAGAGA linker-GFP-*SsGPD1* terminator-*hygB*^{r} marker'' was amplified by PCR to introduce the homology flanks (the last 90 nt of *GPD1* ORF without stop codon to the 5' end and the first 85 nt of *GPD1* downstream to the 3' end). Then, the homology arms were increased to 180 nucleotides by a second PCR. This resulted in the final product ''the last 180 bp of *GPD1* ORF-GAGAGA linker-GFP-*SsGPD1* terminator-*hygB*^{r} marker-the last 185 bp of *GPD1* downstream''.

The final PCR product was transformed into both NCYC102 (WT) and isogenic *pex3Δ* cells, followed by epifluorescence microscopy analysis. The correct integration of the C-terminal construct into the genomes of transformants with fluorescence was confirmed by PCR (See Appendix 5 for further information). The results showed that in WT cells, a green punctate pattern was observed. This is different of what was observed when *Dh*Gpd1-GFP was expressed in *S. cerevisiae*, where it displayed a dual distribution between peroxisomes and cytosol. A green cytosolic diffuse signal was observed in all *pex3Δ* cells. In some cells there was an additional single green punctum. Then, ''*SsGPD1* promoter-mCherry-SKL'' construct was co-expressed in both Gpd1-GFP expressed WT and *pex3Δ* cells. The transformants were analysed under the microscope to select the fluorescent colonies. The integration of the red marker into the genome was confirmed by PCR. In WT cells, all the green punctate pattern co-localized with the red puncta. In contrast, the occasional green puncta in *pex3Δ* cells did not colocalise with mCherry-SKL. In fact, the mCherry-SKL expressed *pex3Δ* cells resulted in only cytosolic red signal (Figure 5.8). Thus, it was concluded that our C-terminal tagging set-up was functional and *Dh*Gpd1 localizes to the peroxisomes, when it is tagged in *D. hansenii*. The origin of the occasional green punctum in *pex3Δ* cells could be an artefact of mislocalisation and could represent localisation to another organelle or more likely protein aggregates.

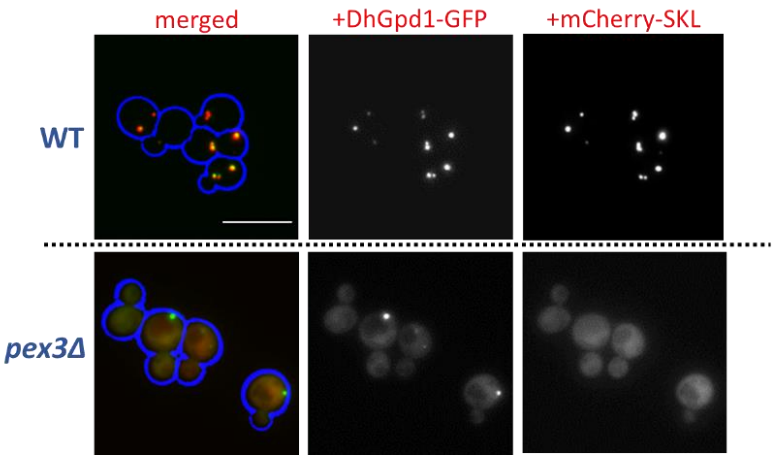

Figure 5.8: *Dh*Gpd1 is a peroxisomal enzyme. The epifluorescence microscopy analysis to show the co-expression of C-terminal ''Gpd1-GFP'' tag and red peroxisomal marker (*SsGPD1* promoter-mCherry-SKL) in both NCYC102 (WT) and *pex3Δ* cells. The cells were imaged after being grown in YM2 non-selective media (glucose) logarithmically. Each cell wall is highlighted in blue. Scale bar is 5 µm.

5.5- *Dh*Pmp47 is localized to the peroxisomal membrane

After the sucessful expression of our C-terminal tagging construct that was used to tag *Dh*Gpd1, the same C-terminal tagging strategy in Section 5.4.1 was used in WT cells to tag *Dh*Pmp47. It was followed by co-transformation of our red peroxisomal marker mCherry-SKL. After the transformation of both constructs, the colonies were examined by the epifluorescence microscopy analysis to check the transformants for the fluorescence and PCR to check the integration (See Appendix 5 for further information).

The microscopy analysis was done after growing the cells in oleate media. The green fluorescence due to Pmp47-GFP expression could not be detected clearly after the growth in YM2 non-selective (glucose) media which will be discussed in more details in Section 5.7. The green fluorescence signal was detectable after the cells were grown in oleate and it was observed as a bright green halo pattern, which was surrounding the red peroxisomal puncta (resulted from the expression of mCherry-SKL marker). It was concluded that this green signal pattern is the most likely to be due to the peroxisomal membrane localization (Figure 5.9).

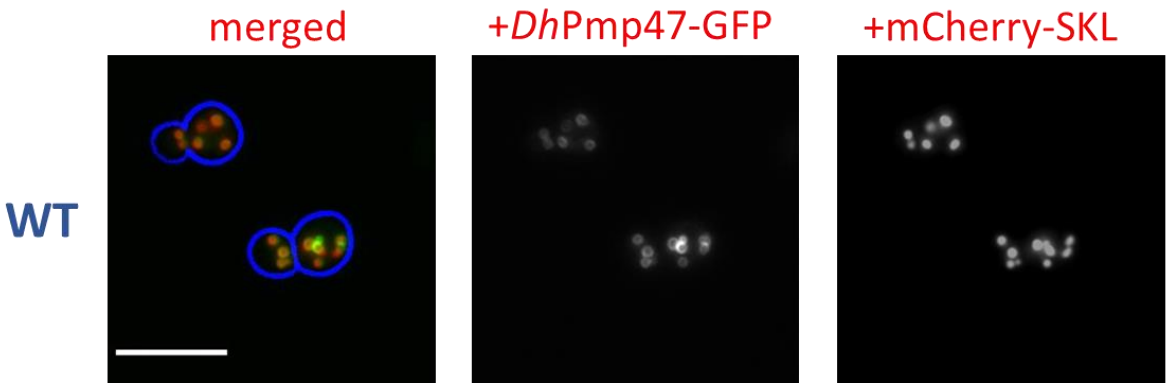

Figure 5.9: *Dh*Pmp47-GFP localizes in peroxisomal membrane. The epifluorescence microscopy analysis that shows the localization of both *Dh*Pmp47-GFP and *SsGPD1* promoter-mCherry-SKL in WT cells, using the oleate media. The cells were imaged after being grown in oleate media post-logarithmically. Each cell wall is highlighted in blue. Scale bar is 5 µm.

5.6- Morphology of the peroxisome compartment depends on growth conditions

After showing the peroxisomal localization of Mdh3, Gpd1 and Pmp47 that were validated by the successful expression of red peroxisomal marker *SsGPD1* promoter-mCherry-SKL, the cells that are expressing GFP-Mdh3 and Gpd1-GFP (as well as the red marker) were grown in different carbon sources under the different growth conditions. The cells that express only the red marker were used as a control to make sure that what is observed in the green channel is not a bleed-through affect caused by the red channel (when the pictures of different z-stacks are taken via Velocity Software, the z-stacks in the red channel are taken before the z-stacks in green channel). The growth media that were tested were glucose (YM2 non-selective) and oleate, whereas the growth conditions were post-logaritmic growth versus logarithmic growth.

According to the epifluorescence microscopy analysis, when the cells were grown on oleate medium, both in logarithmically and post-logarithmically, the amount of peroxisomes seemed always more increased than the amount of peroxisomes in the cells grown in glucose (Figure 5.10). Subsequent quantitation of peroxisome number per cell in WT cells expressing only the red marker, after being grown in glucose and oleate logaritmically, has resulted in consistent data with this argument (Figure 5.11A). When the cells were grown in glucose media, the cells had only few peroxisomes and there were cells that do not have any peroxisomes (Figure 5.10 and 5.11B). In contrast, when the cells were grown in oleate, the peroxisome number was more increased and every cell had peroxisomes. Moreover, most peroxisomes in the cells grown in oleate were found to be usually smaller in contrast to the peroxisomes in glucose-grown cells (Figure 5.10). On the other hand, no remarkable difference was found in how the peroxisomes look in both logarithmic and post-logarithmic cultures. Hence, we decided to do the further analyses using the logarithmic culture.

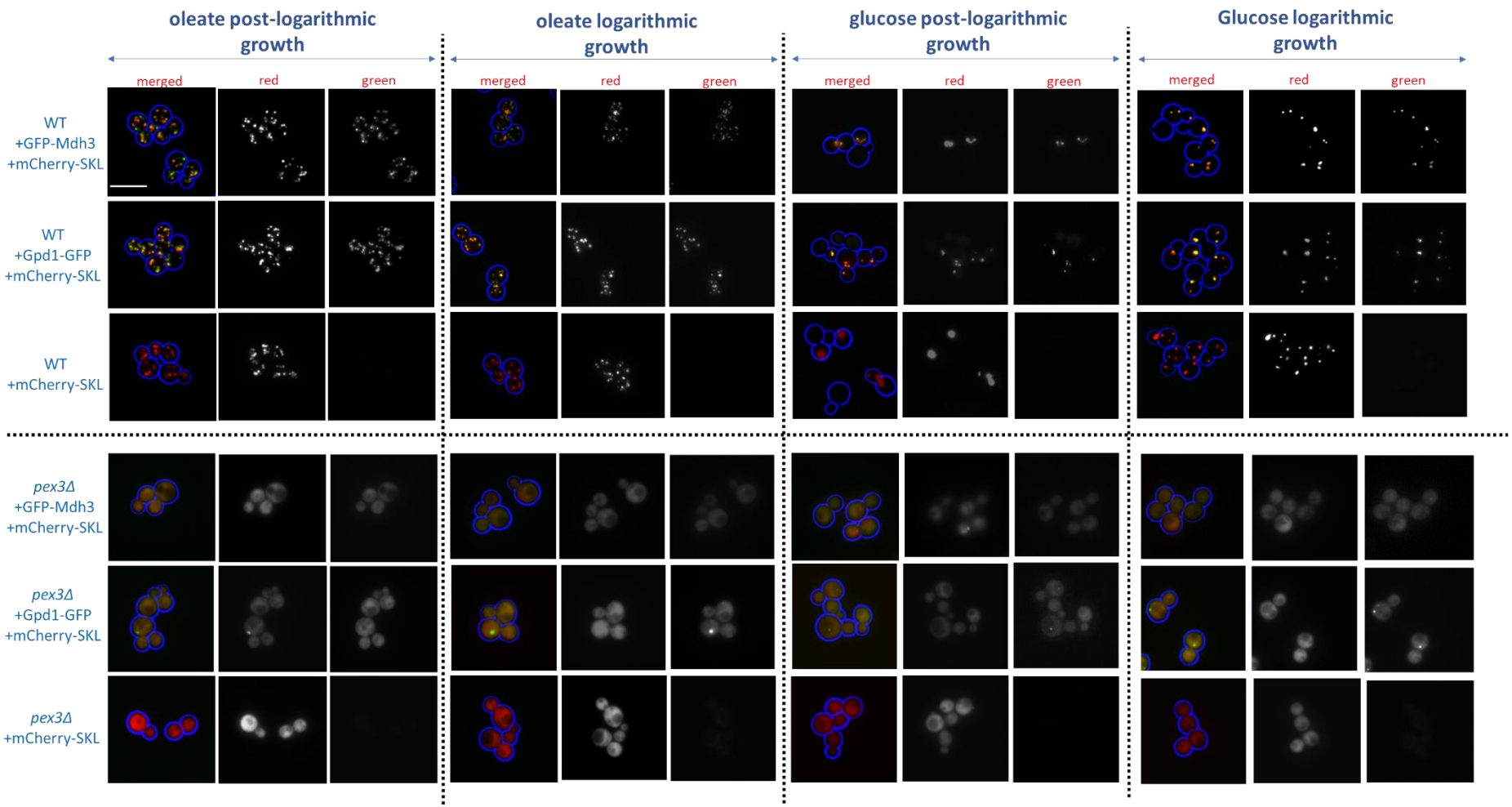

Figure 5.10: The epifluorescence microscopy analysis of *Dh*GFP-Mdh3 and Gpd1-GFP expressed WT and isogenic *pex3Δ* cells, that also express peroxisomal red marker (*SsGPD1* promoter-*mCherry*-SKL). The WT and *pex3Δ* cells, that express only the red marker, were also used as a control to show that what was observed on green channel (for GFP-tagged cells) is not a bleed-through effect caused by the red channel. The cells were grown both glucose and oleate media, both logarithmically and post logarithmically. Each cell wall was highlighted in blue. Scale bar is 5 µm.

A)

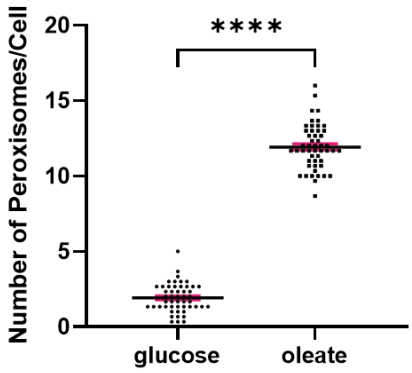

B)

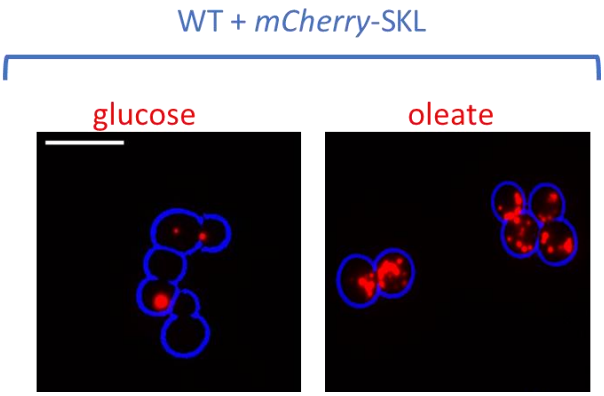

Figure 5.11: The effect of glucose and oleate media on *D. hansenii* peroxisomes. The cells were analysed after being grown in YM2 non-selective (glucose) and oleate media logarithmically. A) Peroxisome quantification of WT cells that are expressing mCherry-SKL, after the cells were grown in glucose or oleate. The graph represents the peroxisome number per each cell. Fifty cells were counted per replicate. n=3. The error bars are shown in red. Unpaired t-test with two-tailored P-value was used to calculate the significant difference. The asterisks represent the significant difference between peroxisome number in glucose and in oleate media. P value<0.0001. B) Same amount of random cells from the same quantification experiment, from each media to indicate the difference in peroxisome numbers. Each cell wall are highlighted with blue. Scale bar is 5 µm.

5.7- *Dh*Pmp47 expression is induced on oleate

WT cells co-expressing Pmp47-GFP and mCherry-SKL were grown logarithmically in glucose, glycerol and oleate media and analysed by fluorescence microscopy. The results showed that in both glucose and glycerol media, the green fluorescent signal was not detectable whereas in oleate media, the signal became detectable as a bright green halo pattern that surrounds the red peroxisomes (Figure 5.9 and 5.12). Even if an increase in the exposure time of the GFP channel revealed a very dim green fluorescent signal for Pmp47-GFP on glucose and glycerol, the signal was still barely detectable in these media (Figure 5.12). These findings suggest that Pmp47 might be induced upon growth in oleate.

In order to address whether Pmp47 is oleate inducible, the protein expression pattern was observed via Western Blot analysis upon growth in oleate and glucose media. As a control, Gpd1-GFP expressing WT cells were also included. The reason of choosing these cells for Western Blot analysis and excluding the ones with GFP-Mdh3 expression is that both Pmp47 and Gpd1 were tagged via C-terminal tagging, whereas Mdh3 was tagged via N-terminal tagging. Both Pmp47-GFP and Gpd1-GFP are controlled by their own promoter, whereas the expression of Mdh3 is driven by exogenous promoter due to the set-up of N-terminal tagging. Hence, the expression patterns of the proteins that were controlled by their endogenous promoters would give us more accurate insight of how their expression is controlled in different media and culturing conditions. Moreover, it is frequently observed that the peroxisomal fatty acid beta-oxidation proteins are induced on oleate (Veenhuis *et al.*, 1987).

Cells were harvested right after overnight growth in either glucose or oleate media and lysed. The proteins were then seperated by SDS-PAGE, followed by the transfer onto the nitrocellulose membrane. The fusion proteins were detected by anti-GFP antibody. The results showed that after glucose growth, expression of Pmp47-GFP was not detected. In contrast, it is well-expressed during oleate growth (Figure 5.13a).

On the other hand, the results also showed that Gpd1-GFP is expressed after both glucose and oleate growth. Moreover, the expression of Gpd1-GFP increased when the cells are grown in oleate. This is validated by another Western Blot analysis, in which the Gpd1-GFP expressed WT cells were harvested after being grown overnight in glucose, grown in oleate for 6 hours (switched from glucose to oleate) as well as after being grown overnight in oleate. The intensity of the Gpd1-GFP band increased with the order of glucose overnight, oleate 6 hours and oleate overnight (Figure 5.13b).

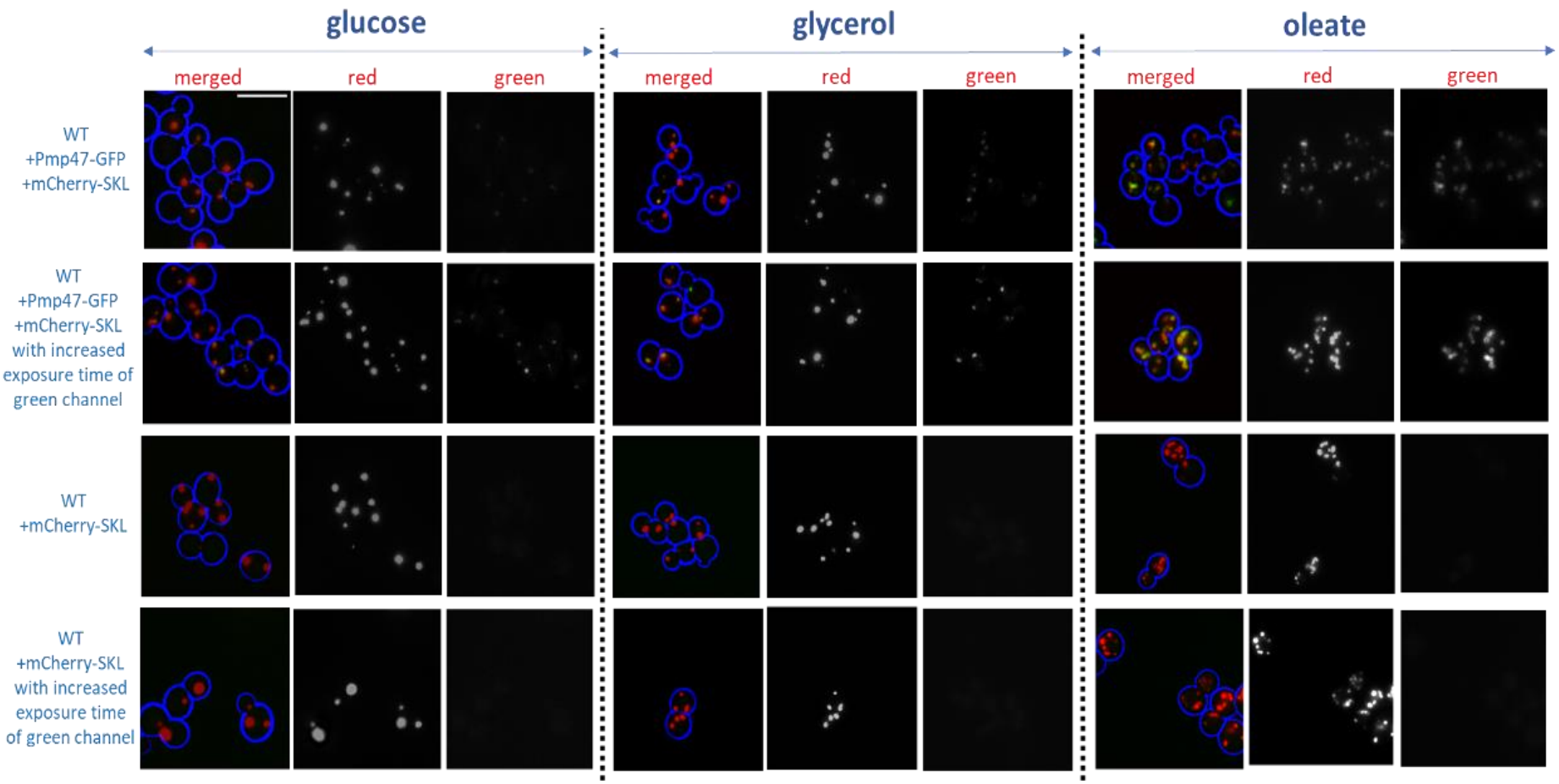

Figure 5.12: The epifluorescence microscopy analysis with WT cells, that express *Dh*Pmp47-GFP and *SsGPD1* promoter-mCherry-SKL. The cells were imaged after being grown logarithmically in glucose, glycerol and oleate. The cells that are expressing only mCherry-SKL were used as a negative control to show that what was observed on the green channel (for WT+Pmp47-GFP cells) is not a bleed-through effect caused by the red channel. The z-stacks of the green channel were captured first by using the exposure time of 170 ms. To take images with an increased exposure time of the green channel, the exposure time was increased from 170 ms to 300 ms (whereas the exposure time of the red channel was not changed). Each cell wall is highlighted in blue. Scale bar is 5 µm.

A)

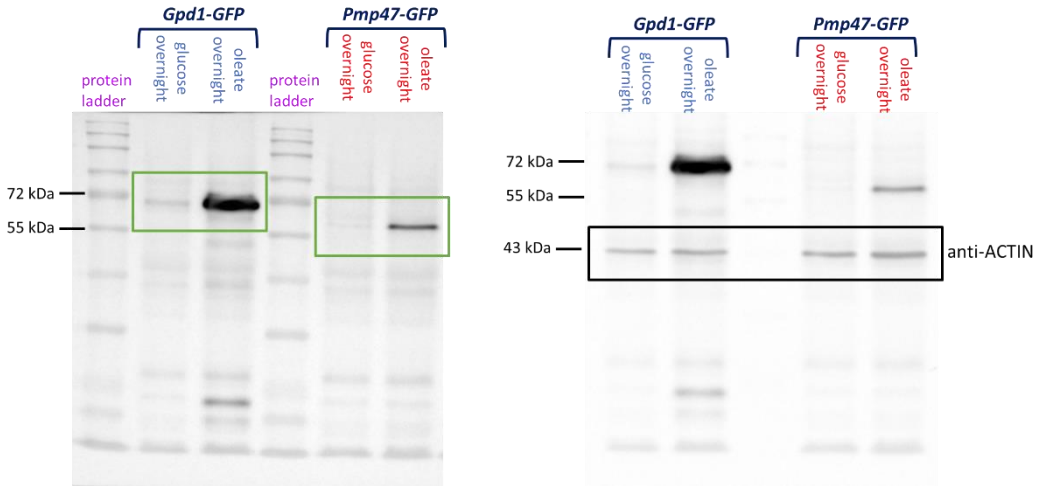

B)

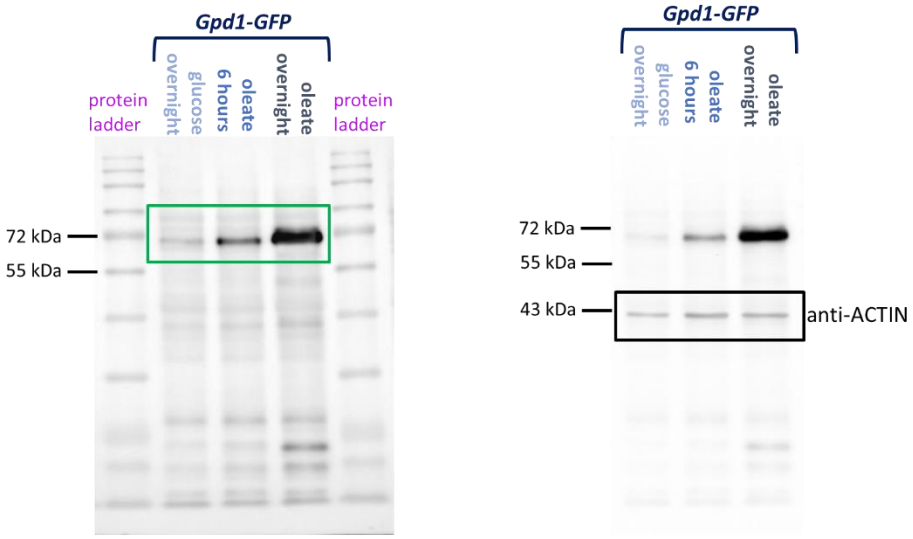

Figure 5.13: Expression of *Dh*Gpd1 and *Dh*Pmp47 are induced on oleate medium. Western Blot analysis using the WT cells expressing Gpd1-GFP and Pmp47-GFP. The protein bands of Gpd1-GFP and Pmp47-GFP that were detected by anti-GFP antibody are indicated in green box. The bands of anti-ACTIN (42 kDa), that were detected afterwards as a loading control, are indicated in black box. A) The Western Blot analysis of WT cells with the expression of Gpd1-GFP and Pmp47-GFP, after being grown overnight in either glucose or oleate. The sizes of Gpd1-GFP bands are 69.4 kDa whereas the sizes of Pmp47-GFP bands are 64.7 kDa. B) The Western Blot analysis with WT cells expressing Gpd1-GFP, after the cells were grown overnight in glucose, in oleate for 6 hours (inoculated from overnight glucose culture) and grown overnight in oleate. The sizes of Gpd1-GFP bands are 69.4 kDa.

5.8- Discussion

Apart from expressing the target proteins in *S. cerevisiae* to investigate the localization, which offers wide range of tools for tagging experiments (Reviewed in Baseda-Lombana, McTaggart and Da Silva, 2018), it is also important to validate the localization of the same protein in the native host. In this study, the tools to tag the ORF of interests with GFP, at both N- or C- terminus, were successfully developed. In addition, the co-localization marker cassette with mCherry-SKL was also successfully developed. Both CTG-optimised GFP and mCherry were well-expressed in *D. hansenii*. The successful development of tagging and co-localization marker enabled us to validate the peroxisomal localization of *Dh*Mdh3, *Dh*Gpd1 and *Dh*Pmp47 in the native host after the expression of two of them (*Dh*Gpd1 and *Dh*Pmp47) in *S. cerevisiae*. Our analyses after tagging *DhGPD1* with GFP in *D. hansenii* also revealed that Gpd1 is localized only peroxisomes in *D.* hansenii, compared to what was observed when the same protein was tagged in *S. cerevisiae* which localized both in cytosol and in peroxisomes (Jung *et al.*, 2010). The peroxisomal localization of Gpd1 is most likely due to the putative PTS2 sequence we identified at its N-terminus, that is not matching the consensus PTS2 motif. Our results regarding tagging *DhGPD1* both in *D. hansenii* and *S. cerevisiae* suggest that the putative non-consensus PTS2 in *Dh*Gpd1 seems very efficient in *D. hansenii*, whereas it did not seem to act strongly effective in *S. cerevisiae*.

Apart from showing the peroxisomal localization of our proteins of interest, the development of these tagging cassettes gave more insight about about how peroxisomes of *D. hansenii* behaved under changing conditions, which has never been studied before. For example, tagging *MDH3* and *GPD1* and growing them in glucose and oleate revealed that the peroxisomes look bigger and fewer (as well as not present in every cell) in glucose, whereas in oleate they looked smaller but there has been a remarkable increase in peroxisome number. The microscopy pictures were also consistent with the peroxisome quantification of our peroxisomal marker, which showed a significant difference in peroxisome number in glucose versus in oleate. It suggests that peroxisomes in *D. hansenii* proliferate in oleate, which is the case for other yeasts including *S. cerevisiae* (Veenhuis *et al.*, 1987).

On the other hand, tagging *PMP47,* together with the Western Blot analysis using Pmp47-GFP, showed that the *Dh*Pmp47 is inducible on oleate. The fact that there was no obvious GFP signal in Pmp47-GFP expressed cells during the microscopy analysis after the growth in glucose or glycerol media compared to the microscopy analysis after oleate growth, as well as the difference in the Pmp47-GFP protein bands in the Western Blot analysis observed after the growth in glucose versus oleate, supported this hypothesis. On the other hand, the Western Blot using the Gpd1-GFP expressed WT cells showed that the expression of Gpd1 also increases in oleate media, compared to when the same cells were grown in glucose. However, more detailed Western Blot analysis is needed in order to show the expression of both Gpd1-GFP and Pmp47-GFP under different conditions or when they are switched from one media to another in more detailed way. In the future, another Western Blot analysis need to be designed using both Pmp47-GFP and Gpd1-GFP cells that are harvested after being grown in glucose, glycerol and oleate media individually, after the glucose and glycerol-grown cells are shifted to oleate, as well as after the oleate-grown cells are shifted to glucose and glycerol.

CHAPTER 6- DISCUSSION

6.1- Bioinformatics study to identify potential proteins in *D. hansenii*

Our bioinformatics study was an important starting point to identify potential peroxisomal proteins in *D. hansenii*, with and without potential targeting signals. It revealed that the beta-oxidation machinery might be more elaborate in *D. hansenii* compared to the one in *S. cerevisiae*, in terms of multiple putative beta-oxidation related genes that might be encoding the same enzyme and additional NAD^+ transport mechanism. The bioinformatics research also revealed different forms of targeting signals used in *D. hansenii*, that do not fit into the consensus sequences for PTS1 and PTS2 that were commonly used by other organisms, including *S. cerevisiae*.

The bioinformatics study also revealed that there are some potential beta-oxidation related proteins in *D. hansenii* that have not been identified in *S. cerevisiae*, but also exist in humans. In this aspect, *D. hansenii* shows high similarity to the smut fungus *U. maydis*, that was suggested as a good model organism for studying the proteins that are shared with humans (Munsterkotter and Steinberg, 2007; Steinberg and Perez-Martin, 2008). An advantage of *D. hansenii* over that of *U. maydis* with respect to studying peroxisomal beta-oxidation processes is that beta-oxidation is restricted to peroxisomes and no redundant mitochondrial beta-oxidation system is present as has been reported for *U. maydis* (Camoes *et al.*, 2015). Consequently, phenotypes of *D. hansenii* mutants should be easily identified through growth on oleate. In this case, *D. hansenii* could serve as a better model organism to investigate some human metabolic events that cannot be studied in *S. cerevisiae*.

6.2- Development of a genetic toolbox to be used in *D. hansenii*

The development of multiple selectable markers to be used in *D. hansenii* was an important starting point, which enabled us to perform further genetics and molecular biology techniques. At the beginning of this study, there was only one selectable marker available (ClonNat, that was developed by Dr. Zeena Alwan) which was limiting factor on investigating multiple steps of the same metabolic pathway. When investigating the possible function of the specific protein and identifying other proteins that might be playing a role in the same specific pathway, generating multiple gene deletions is important as deleting only one gene might not give the expected phenotype if other proteins are involved. The development of alternative selectable markers enabled us to perform multiple gene deletions in the same *D. hansenii* strain for the first time, which enabled us to study more than one potential beta-oxidation proteins at the same time. It gave us more insight about how beta-oxidation might be operating in *D. hansenii,* how different it is from *S. cerevisiae* and how the proteins we characterized might be involved into the process.

Apart from the ability to study more than one protein by gene deletion, our selectable markers were also used in our tagging constructs. We were lacking effectively replicating expression plasmids as well as the auxotrophic markers. Hence, integrating our N-terminal tagging, C-terminal tagging and

as co-localization cassettes into the genome with the selection of our newly-developed antibiotics markers seemed a good strategy, that worked efficiently.

The optimization of fluorescent markers GFP and mCherry, for tagging in *D. hansenii* was also an important advance that enabled us to visualise *D. hansenii* peroxisomes in living cells. This allowed us to study changes in peroxisome number and shape under different growth conditions, for the first time in the literature. Besides, both tagging cassettes and peroxisomal marker development enabled us to confirm that our proteins Mdh3, Gpd1, Pmp47 and potential Npy1 were peroxisomal proteins in *D. hansenii*. Usually, heterologous expression of target proteins in other organisms, especially in *S. cerevisiae*, is a convenient solution because *S. cerevisiae* offers a wide range of genetic tools to tag heterologous proteins easily (Reviewed in Baseda-Lombana, McTaggart and Da Silva, 2018). However, this is sometimes challenged by the fact that *D. hansenii* is a CTG-clade organism (Miranda *et al.*, 2006). It means that if the target gene to be expressed in *S. cerevisiae* has CTG codon(s) within its ORF, these then need changing in order not to disrupt the corresponding amino acid sequence that would normally be used in *D. hansenii*. In this case, expressing the target proteins in *S. cerevisiae* might become less inconvenient and more time consuming. Moreover, the same protein might localize differently in native host and other organisms (such as *Dh*Gpd1, which localized both to cytosol and peroxisomes in *S. cerevisiae*, whereas it localized only in peroxisomes in *D. hansenii*). Hence, the fluorescent marker expression strategy we developed for *D. hansenii* has been a robust way to show protein localization in the native host. On the other hand, the availability of anti-GFP antibody and the presence of GFP in our tagging cassette offer a good way to study how the expression of C-terminal tagged proteins (under the control of their native promoter) are affected in different media and culturing conditions by Western Blot. In the future, the protein expression could be analysed by tagging the target ORF with GFP, followed by Western Blot analysis using anti-GFP antibody.

Even if our newly developed antibiotics selectable markers have been a good starting point towards developing *D. hansenii* as a good model organism, the presence of more selectable markers or a way to recycle our existing plasmids is necessary for the future. It would allow us to perform more than 3 genome modifications in a single strain and this will be important for further development of *D. hansenii* as a good model organism in the future.

6.3- Identification of alternative NAD^+ transport mechanism in *D. hansenii* by Pmp47

Our C-terminal tagging system revealed that *Dh*Pmp47 is localized in peroxisomal membrane in *D. hansenii*. Our gene deletion strategies followed by oleate growth assays, as well as our beta-oxidation activity measurements in both *D. hansenii* mutants and *S. cerevisiae* mutants, confirmed that *Dh*Pmp47 plays role in the beta-oxidation by providing NAD^+. Our results taken together, confirm that *Dh*Pmp47 is a membrane protein that transports NAD^+ across the peroxisomal matrix.

Earlier research that focused on *A. thaliana* PXN discovered that PXN transports NAD^+ in exchange of AMP (van Roermund *et al.*, 2016). However, our experiments on *Dh*Pmp47 suggest that *Dh*Pmp47 is different from PXN in this context. The full beta-oxidation activity complementation, that was observed in *S. cerevisiae mdh3/npy1Δ* cells after the expression of *Dh*Pmp47 brought up the question of whether *Dh*Pmp47 might be NAD^+/NADH exchanger instead. In *mdh3/npy1Δ* cells, there

is high amount of NADH accumulation (AbdelRaheim *et al.*, 2001). It is likely that high amount of NADH in these cells could be driving *Dh*Pmp47 to act on the beta-oxidation to complement it. Further experiments are required to test this argument in details.

6.4- Potential beta-oxidation pathway in *D. hansenii*

Firstly, based on the fact that in *pex3Δ* mutant, which are supposed to be lacking functional peroxisomes (Hettema *et al.*, 2000), *D. hansenii* cells cannot utilize oleate (Found by Sondos Alhajouj) and also based on the fact that orthologs of *U. maydis* mitochondrial beta-oxidation related genes mentioned in Camoes *et al.* (2015) could not be detected in our bioinformatics search, it is hypothesised that beta-oxidation is limited to peroxisomes in *D. hansenii*.

Our bioinformatics research has identified 6 hits that could be potential Fatty Acid CoA Ligases (synthetises) with and without targeting signal, Pxa1 and Pxa2 half transporters without targeting signals, as well as potential ortholog of *Sc*Fat1 with PTS1. Out of 6 potential Fatty Acid-CoA ligases detected, 4 of them have potential PTS1 targeting signal. When these proteins were further analysed via bioinformatics, it was discovered that the ones with PTS1 signal are more similar to the peroxisomal acyl-CoA synthase *Sc*Faa2 (activating middle chain FAs), and one of the remaining hits without targeting signal was more similar to the cytosolic acyl-CoA synthase *Sc*Faa1 (activating long chain FAs). Although these proteins were not studied in more details, but based on our preliminary bioinformatics data, it is predicted that fatty acids could be activated to ''Fatty Acid-CoA'' outside the peroxisomes by our putative activator without targeting signal and transported into the peroxisomes via putative Pxa1/Pxa2 complex. Alternatively, medium chain fatty acids might be also moving into the peroxisomes and activated to Fatty Acid-CoA by the putative Fatty Acid CoA Ligase hits with potential PTS1 inside the peroxisomal matrix. The potential orthologs of Faa2 with targeting signal could be also re-ligating the FAs with CoA inside the peroxisomes, if CoA is cleaved and released into the peroxisomes during the transport of FAs via Pxa1/Pxa2 complex as suggested by van Roermund *et al.* (2021). Even though our study provides an evidence for transport of NAD^+ inside peroxisomes, it does not clarify how other metabolites such as ATP and CoA, are provided to *D. hansenii* peroxisomes. However, our bioinformatics study also identified a potential Ant1 which is highly similar to *Sc*Ant1, which suggests that ATP that is required for FA activation might be transported across the peroxisomes. The uptake of CoA might be mediated by the potential Pxa1/Pxa2 complex or the potential CoA transporter, similarly to human Pmp34 (Agrimi *et al.*, 2012) or its zebrafish orthologs (Kim *et al.*, 2020). Even if such peroxisomal CoA transporter has not been described in *S. cerevisiae* (van Roermund *et al.*, 2021), future studies might reveal it for *D. hansenii* similarly to the discovery of NAD^+ transport pathway.

According to our bioinformatics study, *D. hansenii* has all the potential enzymes for the beta-oxidation pathway. Interestingly, as it was mentioned in Chapter 3, for the first and the last step of the beta-oxidation, there are multiple hits for one protein (3 different hits for potential Acyl-CoA Oxidase and 3 different hits for potential 3-Ketoacyl-CoA Thiolases). Even if the candidate Acyl-CoAs did not have targeting signals similarly to *S. cerevisiae* Pox1 (Klein *et al.*, 2002), the fact that the same situation was observed in related fungus *Y. lipolytica* (Wang *et al.*, 1999a; Wang *et al.*, 1999b) suggests that all of these *D. hansenii* hits might be also peroxisomal and functioning depending of the FA chain length. On the other hand, out of 3 potential thiolases, 2 of them are predicted to be

real orthologs of peroxisomal 3-Ketoacyl-CoA Thiolase as they have a potential PTS2, similarly to its orthologs in other organisms including *S. cerevisiae* (Erdmann, 1994). On the other hand, it is predicted that there is only one gene encoding the potential multifunctional enzyme. The reason is that *fox2Δ* cells, that was also used as a negative control for the beta-oxidation activity measurements in *D. hansenii* (because it shows almost no beta-oxidation activity), results in severe growth defect on oleate (Shown in Appendix 7).

Another interesting hits that our bioinformatics search detected were potential Acyl-CoA Dehydrogenase-related proteins in *D. hansenii* (Acad11n and Acad11c). Acad11 is an enzyme that reportedly plays a role in both peroxisomal and mitochondrial beta-oxidation in mammals (Reviewed in Shen and Burger, 2009). It was also identified in *U. maydis* (Camoes *et al.*, 2015), but it has not been identified in *S. cerevisiae*. It was reported that in mammals, this protein consists of 2 different domains, that are ACAD domain and Aminoglycoside Phosphotransferase (APH) domain (Shen *et al.*, 2009; Camoes *et al.*, 2015). Interestingly, in fungi, these 2 domains are separated to 2 different proteins which are named as Acad11n and Acad11c. They were also identified in *U. maydis* and both proteins localize in peroxisomes in this organism (Camoes *et al.*, 2015). Both putative Acad11n and Acad11c in *D. hansenii* has PTS1 and the tagging Acad11n with GFP in S. cerevisiae resulted in peroxisomal localization (Shown on Appendix 8). The fact that Acad11n has Acyl-CoA Oxidase domain, raised the question of whether Acad11n, in collaboration with Acad11c or separately, might be involved in beta-oxidation in *D. hansenii*. This might be further tested by expression in *S. cerevisiae*. On the other hand, the detection of these hits in *D. hansenii* and their absence in *S. cerevisiae*, is another supporting argument to why *D. hansenii* could be a good candidate model organism in the future to study human metabolic pathways that are not conserved in *S. cerevisiae*. In this aspect, *D. hansenii* shows high similarity to the smut fungus *U. maydis*, that was also suggested as a good model organism for studying the proteins that are shared with humans (Camoes *et al.*, 2015). An advantage of *D. hansenii* over that of *U. maydis* with respect to studying peroxisomal beta-oxidation processes is that beta-oxidation is restricted to peroxisomes and no redundant mitochondrial beta-oxidation system is present as has been reported for *U. maydis* (Camoes *et al.*, 2015). Consequently, phenotypes of *D. hansenii* mutants should be easily identified through growth on oleate.

Our study strongly suggests that the NAD^+/NADH redox balance in *D. hansenii* peroxisomes might be depending on both regeneration and transport, unlike the one in *S. cerevisiae* which seems to mostly rely on malate-oxaloacetate and G3P-DHAP redox shuttles (van Roermund *et al.*, 1995; Al-Saryi *et al.*, 2017a). Our observations regarding *Dh*Gpd1 revealed that it is localized solely in peroxisomes in *D. hansenii*, contrary to *Sc*Gpd1 which is normally both a cytosolic and a peroxisomal protein (Jung *et al.*, 2010; Al-Saryi *et al.*, 2017a). According to our Western Blot results, *Dh*Gpd1 seems to be strongly induced on oleate which is consistent with the fact that the beta-oxidation proteins are induced in fatty acid media such as oleate (Veenhuis *et al.*, 1987). *Dh*Gpd1 also complemented the growth deficiency of the *S. cerevisiae* Gpd1. Based on these observations, it is predicted that *Dh*Gpd1 is most likely to be involved in the beta-oxidation by regenerating NAD^+. Based on our tagging results, it is hypothesised that the peroxisomal part of G3P shuttle might be catalyzed by only *Dh*Gpd1 whereas cytosolic part of G3P shuttle might be catalyzed only by *Dh*Gpd2 in *D. hansenii*, in contrast to G3P shuttle in *S. cerevisiae* in which Gpd1 is both on peroxisomal and cytosolic side of the shuttle (Al-Saryi *et al.*, 2017a). Apart from *Dh*Gpd1, even though it is also anticipated that *Dh*Mdh3 also regenerates NAD^+ for the beta-oxidation, it is not clear whether one contributes more than the other in *D. hansenii*, similarly to what was observed in *S. cerevisiae* (Al-Saryi *et al.*, 2017a). However, it is hypothesised that since *Dh*Gpd1-GFP localized solely in peroxisomes (unlike *Sc*Gpd1-GFP whose peroxisomal localization is not abundant) and strongly induced in oleate, *Dh*Gpd1 might be having

more contribution to the beta-oxidation than *Sc*Gpd1 or even *Dh*Mdh3. Further experiments, that involve the generation of *mdh3/pmp47Δ* and *gpd1/pmp47Δ* cells in *D. hansenii* followed by oleate growth and fatty acid beta-oxidation assays, are required to test this hypothesis.

Even though more detailed analyses are still required, based on our beta-oxidation activity measurement results related to *Dh*Pmp47b, it is also hypothesised that potential *Dh*Pmp47b also has a minor contribution to the beta-oxidation in *D. hansenii* by potentially transporting NAD^+. It is possible that *Dh*Pmp47b might be an NAD/AMP exchanger and *Dh*Npy1 might be collaborating with *Dh*Pmp47b instead of *Dh*Pmp47.

Finally, our bioinformatics research identified a putative Carnitine Acetyltransferase (Cat2) with potential PTS1 and potential hits for glyoxylate cycle enzymes, including Malate Synthase 1 (Mls1), Citrate Synthase 2 (Cit2), Aconitase, Isocitrate Lyase 1 (Icl1) and Malate Dehydrogenase 2 (Mdh2). In *S. cerevisiae*, both Cit2 and Mls1 have peroxisomal targeting signal. However, only potential hit for *Dh*Mls2 seems to have predicted weak PTS1 (-EKL) whereas potential *Dh*Cit2 has no PTS2 and -IKA at its C-terminus, which is not considered as a form of PTS1. Even though these predicted proteins have not been characterized yet, it is predicted that Acetyl-CoA, the end product of beta-oxidation, is further processed by both Acetyl Carnitine Shuttle and glyoxylate cycle in *D. hansenii*, similarly to *S. cerevisiae*. Based on the putative beta-oxidation related proteins that our bioinformatics research identified, as well as our results, Figure 6.1 represents the potential model for how beta-oxidation might be operating in *D. hansenii*.

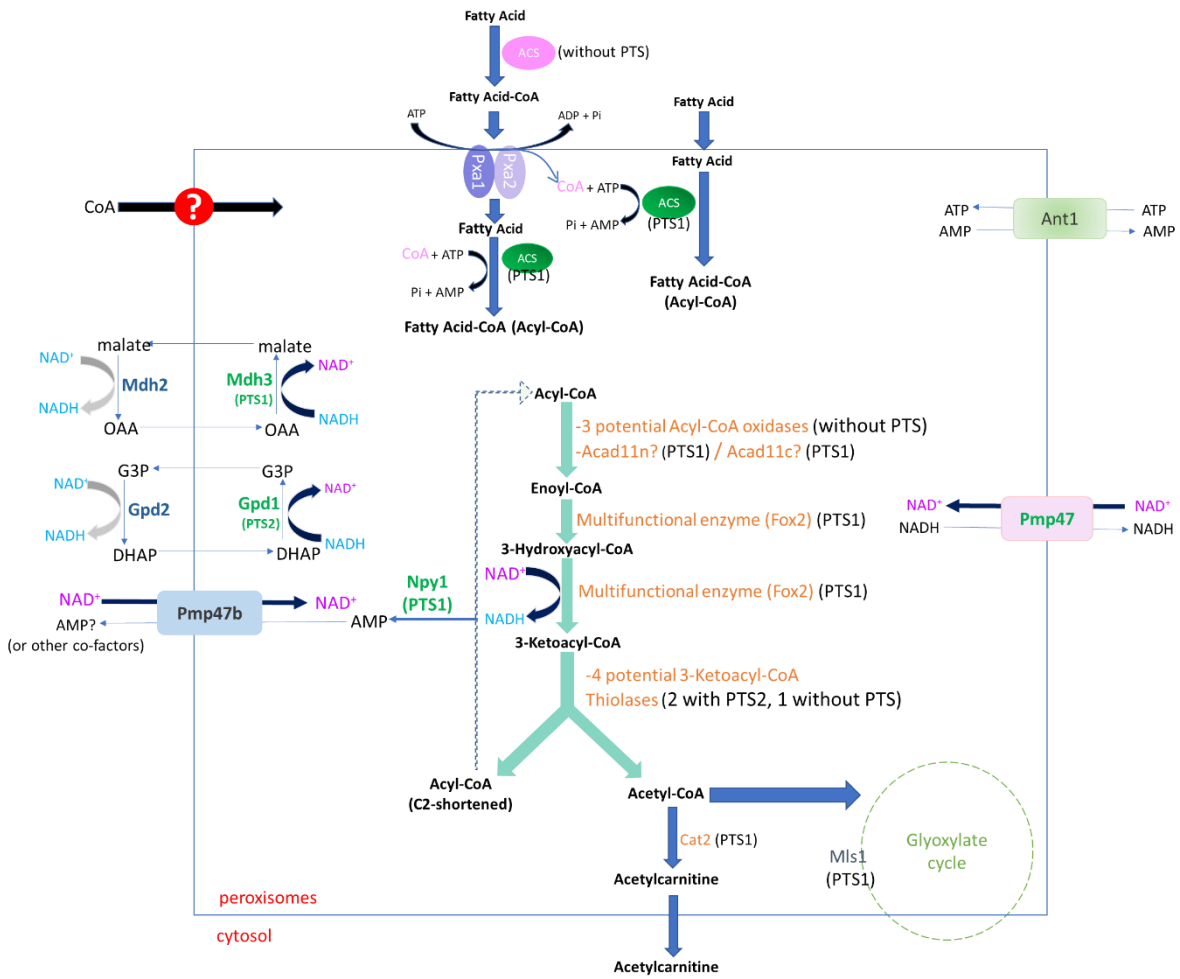

Figure 6.1: The putative model for how beta-oxidation might be operating in *D. hansenii* peroxisomes. This model was predicted based on our bioinformatics research, our experimental data related to *Dh*Gpd1, *Dh*Mdh3, *Dh*Pmp47 and *Dh*Pmp47b and what has been discovered so far in other organisms (especially *S. cerevisiae*). The predicted proteins based on bioinformatics analysis with the presence of potential PTS were indicated in black. The proteins which were found to be peroxisomal in this study were indicated in green (Gpd1, Mdh3, Npy1 and Pmp47). It is hypothesised that fatty acids can either be activated first outside of peroxisomes by putative potential Acyl-CoA Syntyhetase(s) (ACS, that is shown in pink), transported to peroxisomes by putative Pxa1/Pxa2 complex, and re-activated to Acyl-CoA again in peroxisomes by putative peroxisomal ACS(s) (shown in green). Alternatively, medium chain fatty acids might be moving to peroxisomes directly and activated to Acyl-CoA by potential peroxisomal ACS(s) (shown in green). Then, Acyl-CoA might be processed further by the beta-oxidation (that was shown in light green arrows), by the putative enzymes that were identified by our bioinformatics research (shown in orange). During the third step, which requires NAD^+ as a co-factor, it is predicted that the required NAD^+ is both generated via *Dh*Gpd1 and *Dh*Mdh3 mediated shuttles and also transported by Pmp47 in an exchange of NADH. Pmp47b in *D. hansenii* peroxisomes is hypothesised to have a minor contribution to peroxisomal NAD^+ supply by also transporting NAD^+, potentially in collaboration with Npy1. OAA: Oxaloacetate, G3P: Glycerol-3-Phosphate, DHAP: Dihydroxyacetone Phosphate.

6.5- Conclusion

D. hansenii is considered as a very promising organism to be used as a production host for fatty acids with the aspect of being highly oleaginous, compared to many known yeasts (Reviewed in Breuer and Harms, 2006), and it has been known as ''Cinderella'' as there has been very little known about this organism (Reviewed in Prista *et al.*, 2016). This study has been useful initiative to unravel *D. hansenii* and change this common view. Our newly-developed genetic toolbox, has been a good starting point towards making *D. hansenii* a suitable host for further genetic engineering studies. *D. hansenii* accumulates high amount of lipids, hence it has a high potential to be used for bio-sustainable production of fatty acids if the lipid metabolism is well-studied (Reviewed in Breuer and Harms *et al.*, 2006; reviewed in Prista *et al.*, 2016). Even though more detailed analyses are required to find out how the complete lipid metabolism operates in *D. hansenii*, our studies have been good initiative to gain more detailed overview about how they are degraded via peroxisomal beta-oxidation, which is an important step to block the break-down to achieve lipid accumulation. On the other hand, we discovered a NAD^+ transport pathway with the protein which does not seem to exist in *S. cerevisiae*.

The previous reviews have focused more on the aspect of *D. hansenii* to serve as a good lipid production host. However, our study also shows that *D. hansenii* could also serve as a good model organism. Our bioinformatics study shows that there are potential proteins in D. hansenii, that are also conserved amongst humans but not present in commonly-used model organisms. *S. cerevisiae* is a well-established yeast that is widely used to study human diseases and metabolic pathways. However, this organism can be sometimes limiting for studying the human proteins (and associated potential metabolic events) whose orthologs are not present in *S. cerevisiae*. Thus, working with a yeast that contains these proteins would be a better solution to advance in human research. *D. hansenii* could be further exploited on this purpose, and our study was a good initiative to establish it more widely-used organism in future.

REFERENCES

AbdelRaheim, S. R. *et al.* (2001) 'The NADH Diphosphatase Encoded by the Saccharomyces cerevisiae NPY1 Nudix Hydrolase Gene is Located in Peroxisomes', *Archives of Biochemistry and Biophysics*, 388(1), pp. 18-24. doi: https://doi.org/10.1006/abbi.2000.2268

Adler, L. and Gustafsson, L. (1980) 'Polyhydric Alcohol Production and Intracellular Amino Acid Pool in Relation to Halotolerance of the Yeast Debaryomyces hansenii', *Archives of Microbiology*, 124(2-3), pp. 123-130. Available at: https://link.springer.com/article/10.1007/BF00427716 (Accessed: 11 September 2022).

Agaphonov, M. *et al.* (2010) 'A Novel Kanamycin/G418 Resistance Marker for Direct Selection of Transformants in Escherichia coli and Different Yeast Species', *Yeast*, 27(4), pp. 189-195. doi: https://doi.org/10.1002/yea.1741

Aggarwal, M., Bansal, P. K. and Mondal, A. K. (2005) 'Molecular Cloning and Biochemical Characterization of a 3'(2'),5'-Bisphosphate Nucleotidase from Debaryomyces hansenii', *Yeast*, 22(6), pp. 457-470. doi: https://doi.org/10.1002/yea.1223

Aggarwal, M. and Mondal, A. K. (2006) 'Role of N-terminal Hydrophobic Region in Modulating the Subcellular Localization and Enzyme Activity of the Bisphosphate Nucleotidase from Debaryomyces hansenii', *Eukaryotic Cell*, 5(2), pp. 262-271. doi: https://doi.org/10.1128/EC.5.2.262-271.2006

Agrimi, G. *et al.* (2012a) 'The Peroxisomal NAD+ Carrier of Arabidopsis thaliana Transports Coenzyme A and Its Derivatives', *Journal of Bioenergetics and Biomembranes*, 44(3), pp. 333-340. doi: https://doi.org/10.1007/s10863-012-9445-0

Agrimi, G. *et al.* (2012b) 'The Human Gene SLC25A17 Encodes a Peroxisomal Transporter of Coenzyme A, FAD and NAD+', *Biochemical Journal*, *443*(1), pp. 241-247. doi: https://doi.org/10.1042/BJ20111420

Al-Saryi, N. A. *et al.* (2017a) 'Two NAD-Linked Redox Shuttles Maintain the Peroxisomal Redox Balance in Saccharomyces cerevisiae. *Scientific Reports*, 7(1), 11868. doi: https://doi.org/10.1038/s41598-017-11942-2

Al-Saryi, N. A. *et al.* (2017b) 'Pnc1 Piggy-Back Import Into Peroxisomes Relies on Gpd1 homodimerisation', *Scientific Reports*, 7, 42579. doi: https://doi.org/10.1038/srep42579

Altmann, K., Durr, M. and Westermann, B. (2007) 'Saccharomyces cerevisiae as a Model Organism to Study Mitochondrial Biology: General Considerations and Basic Procedures', *Methods in Molecular Biology,* 372, pp. 81-90. doi: https://doi.org/10.1007/978-1-59745-365-3_6

Altschul, S. F. *et al.* (1990) 'Basic Local Alignment Search *Tool*', *Journal of Molecular Biology,* 215(3), pp. 403-410. doi: https://doi.org/10.1016/S0022-2836(05)80360-2

Alwan, Z. C. O. (2017) *Neutral Lipid Production by the Yeast Debaryomyces hansenii NCYC102 Under Different Stress Conditions*. PhD thesis. University of Sheffield.

Anderson, R. M. *et al.* (2003) 'Nicotinamide and PNC1 Govern Lifespan Extension by Calorie Restriction in Saccharomyces cerevisiae', Nature, 423(6936), pp. 181-185. doi: https://doi.org/10.1038/nature01578

Antonenkov, V. D. and Hiltunen, J. K. (2012) 'Transfer of Metabolites Across the Peroxisomal Membrane', *Biochimica et Biophysica Acta (BBA)*, 1822(9), pp. 1374-1386. doi: https://doi.org/10.1016/j.bbadis.2011.12.011

Apweiler, R. *et al.* (2004) 'UniProt: the Universal Protein Knowledgebase', *Nucleic Acids Research,* 32, pp. D115-119. doi: https://doi.org/10.1093/nar/gkh131

Bamber, L. *et al.* (2007) 'The Yeast Mitochondrial ADP/ATP Carrier Functions as a Monomer in Mitochondrial Membranes', *Proceedings of the National Academy of Sciences of the United States of America*,104(26), pp. 10830-10834. doi: https://doi.org/10.1073/pnas.0703969104

Bartoszewska, M. *et al.* (2011) 'The Significance of Peroxisomes in Secondary Metabolite Biosynthesis in Filamentous Fungi', *Biotechnology Letters*, 33(10), pp. 1921-1931. doi: https://doi.org/10.1007/s10529-011-0664-y

Baudhuin, P., Beaufay, H. and De Duve, C. (1965) 'Combined Biochemical and Morphological Study of Particulate Fractions from Rat Liver. Analysis of Preparations Enriched in Lysosomes or in Particles Containing Urate Oxidase, D-amino Acid Oxidase, and Catalase', *Journal of Cell Biology,* 26(1), pp. 219-243. doi: https://doi.org/10.1083/jcb.26.1.219

Baumgart, E. *et al.* (1996) 'L-Lactate Dehydrogenase A_4- and A_3B Isoforms Are Bona Fide Peroxisomal Enzymes in Rat Liver', *Cell Biology and Metabolism*, 271(7), pp. 3846-3855. doi: https://doi.org/10.1074/jbc.271.7.3846

Bedalov, A. *et al.* (2003) 'NAD+-Dependent Deacetylase Hst1p Controls Biosynthesis and Cellular NAD+ Levels in Saccharomyces cerevisiae', *Molecular and Cellular Biology*, 23(19), pp. 7044-7054. doi: https://doi.org/10.1128/MCB.23.19.7044-7054.2003

Bernhardt, K. *et al.* (2012) 'A Peroxisomal Carrier Delivers NAD(+) and Contributes to Optimal Fatty Acid Degradation During Storage Oil Mobilization', *The Plant Journal*, 69(1), pp. 1-13. doi: https://doi.org/10.1111/j.1365-313X.2011.04775.x

Besada-Lombana, P. B., McTaggart, T. L. and Da Silva, N. A. (2018) 'Molecular Tools for Pathway Engineering in Saccharomyces cerevisiae', *Current Opinion in Biotechnology*, 53, pp. 39-49. doi: https://doi.org/10.1016/j.copbio.2017.12.002

Bonaiti, C. *et al.* (2004) 'Deacidification by Debaryomyces hansenii of Smear Soft Cheeses Ripened Under Controlled Conditions: Relative Humidity and Temperature Unfluences', *Journal of Dairy Science*, 87(11), pp. 3976–3988. doi: https://doi.org/10.3168/jds.S0022-0302(04)73538-9

Breitenbach, M., Crameri, R. and Lehrer, S. B. (2002) 'Fungal allergy and pathogenicity', *Chemical Immunology*, 81, pp. 296-301. doi: https://doi.org/10.1159/000058869

Breitling, R. *et al.* (2002) 'Loss of Compartmentalization Causes Misregulation of Lysine Biosynthesis in Peroxisome-Deficient Yeast Cells', *Eukaryotic Cell*, 1(6), pp. 978-986. doi: https://doi.org/10.1128/EC.1.6.978-986.2002

Breuer, U. and Harms, H. (2006) 'Debaryomyces hansenii--An Extremophilic Yeast With Biotechnological Potential', *Yeast*, 23(6), pp. 415-437. doi: https://doi.org/10.1002/yea.1374

Camoes, F. *et al.* (2015) 'New Insights Into the Peroxisomal Protein Inventory: Acyl-CoA Oxidases and -Dehydrogenases are an Ancient Feature of Peroxisomes', *Biochimica et Biophysica Acta (BBA),* 1853(1), pp. 111-125. doi: https://doi.org/10.1016/j.bbamcr.2014.10.005

Cano-García, L., Belloch, C. and Flores, M. (2014) 'Impact of Debaryomyces hansenii Strains Inoculation on the Quality of Slow Dry-Cured Fermented Sausages', *Meat Science*, 96(4), pp. 1469-1477. doi: https://doi.org/10.1016/j.meatsci.2013.12.011

Carrie, C. *et al.* (2007) 'Nine 3-ketoacyl-CoA Thiolases (KATs) and Acetoacetyl-CoA Thiolases (ACATs) Encoded by Five Genes in Arabidopsis thaliana are Targeted Either to Peroxisomes or Cytosol but not to Mitochondria'*, Plant Molecular Biology*, 63(1), pp. 97-108. doi: https://doi.org/10.1007/s11103-006-9075-1

Chen, L., Zhang, J. and Chen, W. N. (2014) 'Engineering the Saccharomyces cerevisiae β-Oxidation Pathway to Increase Medium Chain Fatty Acid Production as Potential Biofuel', *PLoS ONE*, 9(1), e84853. doi: https://doi.org/10.1371/journal.pone.0084853

Chornyi, S. *et al.* (2021) 'Peroxisomal Metabolite and Cofactor Transport in Humans', *Frontiers in Cell and Developmental Biology*, *8*, pp. 613892. doi: https://doi.org/10.3389/fcell.2020.613892

Cohen, G. Rapatz, W. and Ruis, H. (1988) 'Sequence of the Saccharomyces cerevisiae CTA1 Gene and Amino Acid Sequence of Catalase A Derived from It', *European Journal of Biochemistry*, 176(1), pp. 159-163. doi: https://doi.org/10.1111/j.1432-1033.1988.tb14263.x

Dalton, H. K., Board, R. G. and Davenport, R. R. (1984) 'The Yeasts of British Fresh Sausage and Minced Beef', *Antonie van Leeuwenhoek*, 50(3), pp. 227-248. doi: https://doi.org/10.1007/BF02342134

Davies, J. and Jimenez, A. (1980) 'A New Selective Agent for Eukaryotic Cloning Vectors, *The American Journal of Tropical Medicine and Hygiene*, 29(5 Suppl), pp. 1089-1092. doi: https://doi.org/10.4269/ajtmh.1980.29.1089

De Duve, C. (1983) 'Microbodies in the Living Cell', *Scientific American*, 248(5), pp. 74-87. Available at: https://www.jstor.org/stable/24968898 (Accessed: 12 September 2022).

De Duve, C. and Baudhuin, P. (1966) 'Peroxisomes (Microbodies and Related Particles)', *Physiological Reviews,* 46(2), pp. 323-357. doi: https://doi.org/10.1152/physrev.1966.46.2.323

De Marcos Lousa, C. *et al.* (2013) 'Intrinsic acyl-CoA Thioesterase Activity of a Peroxisomal ATP Binding Cassette Transporter is Required for Transport and Metabolism of Fatty Acids', *Proceedings of the National Academy of Sciences of the United States of America*, *110*(4), pp. 1279-1284. doi: https://doi.org/10.1073/pnas.1218034110

Defosse, T. A. *et al.* (2018) 'A Standardized Toolkit for Genetic Engineering of CTG Clade Yeasts', *Journal of Microbiological Methods*, 144, pp. 152-156. doi: https://doi.org/10.1016/j.mimet.2017.11.015

Desnos-Ollivier, M. *et al.* (2008) 'Debaryomyces hansenii (Candida famata), a Rare Human Fungal Pathogen Often Misidentified as Pichia guilliermondii (Candida guilliermondii)', *Journal of Clinical Microbiology*, 46(10), pp. 3237-3242. doi: https://doi.org/10.1128/JCM.01451-08

Dmochowska, A. *et al.* (1990) 'Structure and Transcriptional Control of the Saccharomyces cerevisiae POX1 Gene Encoding Acyl-coenzyme A Oxidase', *Gene*, 88(2), pp. 247-252. doi: https://doi.org/10.1016/0378-1119(90)90038-s

Dodt, G., *et al.* (2001) 'Domain Mapping of Human PEX5 Reveals Functional and Structural Similarities to Saccharomyces cerevisiae Pex18p and Pex21p', *Journal of Biological Chemistry,* 276(45), pp. 41769-41781. doi: https://doi.org/10.1074/jbc.M106932200

Dommes, V., Baumgart, C. and Kunau, W. H. (1981) 'Degradation of Unsaturated Fatty Acids in Peroxisomes. Existence of a 2,4-Dienoyl-CoA Reductase Pathway', *Journal of Biological Chemistry*, 256(16), pp. 8259-8262. Available at: https://pubmed.ncbi.nlm.nih.gov/7263650/ (Accessed: 20 August, 2022).

Douglass, S. A., Criddle, R. S. and Breidenbach, R. W. (1973) 'Characterization of Deoxyribonucleic Acid Species from Castor Bean Endosperm: Inability to Detect a Unique Deoxyribonucleic Acid Species Associated with Glyoxysomes', *Plant Physiology*, 51(5), pp. 902-906. doi: https://doi.org/10.1104/pp.51.5.902

Durá, M.A., Flores, M. and Toldrá, F. (2004) 'Effect of Growth Phase and Dry-Cured Sausage Processing Conditions on Debaryomyces spp. Generation of Volatile Compounds From Branched-Chain Amino Acids', *Food Chemistry*, 86(3), pp. 391-399. doi: https://doi.org/10.1016/j.foodchem.2003.09.014

Duntze, W. *et al.* (1969) 'Studies on the Regulation and Localization of the Glyoxylate Cycle Enzymes in Saccharomyces cerevisiae', *European Journal of Biochemistry*, 10(1), pp. 83-89. doi: https://doi.org/10.1111/j.1432-1033.1969.tb00658.x

Dyer, J. M., McNew, J. A. and Goodman, J. M. (1996) 'The Sorting Sequence of the Peroxisomal Integral Membrane Protein PMP47 is Contained within a Short Hydrophilic Loop', *Journal of Cell Biology,* 133(2), pp. 269-280. doi: https://doi.org/10.1083/jcb.133.2.269

Effelsberg, D. *et al.* (2015) 'Role of Pex21p for Piggyback Import of Gpd1p and Pnc1p into Peroxisomes of Saccharomyces cerevisiae', *Journal of Biological Chemistry*, 290(42), pp. 25333-25342. doi: https://doi.org/10.1074/jbc.M115.653451

Einwachter, H. *et al.* (2001) 'Yarrowia lipolytica Pex20p, Saccharomyces Cerevisiae Pex18p/Pex21p and Mammalian Pex5pL Fulfil a Common Function in the Early Steps of the Peroxisomal PTS2 Import Pathway', *EMBO Reports*, 2(11), pp. 1035-1039. doi: https://doi.org/10.1093/embo-reports/kve228

Elgersma, Y. and Tabak, H. F. (1996) 'Proteins Involved in Peroxisome Biogenesis and Functioning', *Biochimica et Biophysica Acta (BBA)*, 1286(3), pp. 269-283. doi: https://doi.org/10.1016/S0304-4157(96)00012-3

Elgersma, Y. *et al.* (1993) 'An Efficient Positive Selection Procedure for the Isolation of Peroxisomal Import and Peroxisome Assembly Mutants of Saccharomyces cerevisiae'. *Genetics,* 135(3), pp. 731-40. doi: https://doi.org/10.1093/genetics/135.3.731

Elgersma, Y. *et al.* (1995) 'Peroxisomal and Mitochondrial Carnitine Acetyltransferases of Saccharomyces cerevisiae are Encoded by a Single Gene', *The EMBO Journal,* 14(14), pp. 3472-3479. doi: https://doi.org/10.1002/j.1460-2075.1995.tb07353.x

Elgersma, Y. *et al.* (1996) 'Analysis of the Carboxyl-Terminal Peroxisomal Targeting Signal 1 in a Homologous Context in Saccharomyces cerevisiae', *Journal of Biological Chemistry,* 271(42) pp. 26375-26382. doi: https://doi.org/10.1074/jbc.271.42.26375

Elgersma, Y. *et al.* (1998) 'A Mobile PTS2 Receptor for Peroxisomal Protein Import in Pichia pastoris', *Journal of Cell Biology*, 140(4), pp. 807-820. doi: https://doi.org/10.1083/jcb.140.4.807

Erdmann, R. (1994) 'The Peroxisomal Targeting Signal of 3-Oxoacyl-CoA Thiolase from Saccharomyces cerevisiae', *Yeast*, 10, pp. 935-44. doi: https://doi.org/10.1002/yea.320100708

Fang, Y. *et al.* (2004) 'PEX3 Functions as a PEX19 Docking Factor in the Import of Class I Peroxisomal Membrane Proteins', *Journal of Cell Biology*, 164(6), pp. 863-875. doi: https://doi.org/10.1083/jcb.200311131

Fernandez, E., Moreno, F. and Rodicio, R. (1992) 'The ICL1 Gene from Saccharomyces cerevisiae', *European Journal of Biochemistry*, 204(3), pp. 983-990. doi: https://doi.org/10.1111/j.1432-1033.1992.tb16720.x

Ferreira, A. D. and Viljoen, B. C. (2003) 'Yeasts as Adjunct Starters in Matured Cheddar Cheese', *Interntional Journal of Food Microbiology*, 86(1-2), pp. 131-140. doi: https://doi.org/10.1016/s0168-1605(03)00252-6

Footitt, S. *et al.* (2002) 'Control of Germination and Lipid Mobilization by COMATOSE, the Arabidopsis Homologue of Human ALDP', *The EMBO Journal*, 21(12), pp. 2912-2922. doi: https://doi.org/10.1093/emboj/cdf300

Forrest, S. I., Robinow, C. F. and Lachance, M. A. (1987) 'Nuclear Behaviour Accompanying Ascus Formation in Debaryomyces polymorphus', *Canadian Journal of Microbiology*, 33(11), pp. 967-970. doi: https://doi.org/10.1139/m87-170

Fujiki, Y. (1997) 'Molecular Defects in Genetic Diseases of Peroxisomes', *Biochimica et Biophysica Acta (BBA)*, 1361(3), pp. 235-250. doi: https://doi.org/10.1016/s0925-4439(97)00051-3

Fujioka, M. and Nakatani, Y. (1970) 'A Kinetic Study of Saccharopine Dehydrogenase Reaction', *European Journal of Biochemistry*, 16(1), pp. 180-186. doi: https://doi.org/10.1111/j.1432-1033.1970.tb01070.x

Fukao, Y. *et al.* (2001) 'Developmental Analysis of a Putative ATP/ADP Carrier Protein Localized on Glyoxysomal Membranes During the Peroxisome Transition in Pumpkin Cotyledons', *Plant and Cell Physiology*, *42*(8), pp. 835-841. doi: https://doi.org/10.1093/pcp/pce108

Gabriel, F. *et al.* (2014) 'A Fox2-Dependent Fatty Acid ss-oxidation Pathway Coexists Both in Peroxisomes and Mitochondria of the Ascomycete Yeast Candida lusitaniae', *PLoS One*, 9(12), pp. e114531. doi: https://doi.org/10.1371/journal.pone.0114531

Gee, R., *et al.* (1974) 'Glycerol Phosphate Dehydrogenase in Mammalian Peroxisomes', *Archives of Biochemistry and Biophysics*, 161(1) pp. 187-193. doi: https://doi.org/10.1016/0003-9861(74)90250-1

Genin, E. C. *et al.* (2011) 'Substrate Specificity Overlap and Interaction Between Adrenoleukodystrophy Protein (ALDP/ABCD1) and Adrenoleukodystrophy-Related Protein (ALDRP/ABCD2)', *Journal of Biological Chemistry*, 286(10), pp. 8075-8084. doi: https://doi.org/10.1074/jbc.M110.211912

Gietz, R. D. and Sugino, A. (1988) 'New Yeast-Escherichia coli Shuttle Vectors Constructed with in vitro Mutagenized Yeast Genes Lacking Six-Base Pair Restriction Sites', *Gene*, 74(2), pp. 527-534. doi: https://doi.org/10.1016/0378-1119(88)90185-0

Gírio, F. *et al.* (2000) 'Polyols Production During Single and Mixed Substrate Fermentations in Debaryomyces hansenii', *Bioresource Technology*, 71(3), pp. 245-251. doi: https://doi.org/10.1016/S0960-8524(99)00078-4

Gladden, L. B. (2004) 'Lactate Metabolism: A New Paradigm for the Third Millennium', The Journal of Physiology, 558(Pt 1), pp. 5-30. doi: https://doi.org/10.1113/jphysiol.2003.058701

Gotte, K. *et al.* (1998) 'Pex19p, a Farnesylated Protein Essential for Peroxisome Biogenesis, *Molecular and Cellular Biology*, 18(1), pp. 616-628. doi: https://doi.org/10.1128/MCB.18.1.616

Gould, S. J., Keller, G. A. and Subramani, S. (1987) 'Identification of a Peroxisomal Targeting Signal at the Carboxy Terminus of Firefly Luciferase', *Journal of Cell Biology,* 105(6 Pt 2), pp. 2923-2931. doi: https://doi.org/10.1083/jcb.105.6.2923

Gould, S. J., Keller, G. A. and Subramani, S. (1988) 'Identification of Peroxisomal Targeting Signals Located at the Carboxy Terminus of Four Peroxisomal Proteins', *Journal of Cell Biology,* 107(3), pp. 897-905. doi: https://doi.org/10.1083/jcb.107.3.897

Gould, S. J. *et al.* (1989) 'A Conserved Tripeptide Sorts Proteins to Peroxisomes', *Journal of Cell Biology,* 108(5), pp. 1657-1664. doi: https://doi.org/10.1083/jcb.108.5.1657

Gritz, L. and Davies, J. (1983) 'Plasmid-Encoded Hygromycin B Resistance: The Sequence of Hygromycin B Phosphotransferase Gene and its Expression in Escherichia coli and Saccharomyces cerevisiae', *Gene*, 25(2-3), pp. 179-188. doi: https://doi.org/10.1016/0378-1119(83)90223-8

Gronemeyer, T. *et al.* (2013) 'The Proteome of Human Liver Peroxisomes: Identification of Five New Peroxisomal Constituents by a Label-Free Quantitative Proteomics Survey', *PLoS One*, 8(2), e57395. doi: https://doi.org/10.1371/journal.pone.0057395

Grunau, S. *et al.* (2009) 'Peroxisomal Targeting of PTS2 Pre-Import Complexes in the Yeast Saccharomyces cerevisiae' *Traffic*, 10(4), pp. 451-460. doi: https://doi.org/10.1111/j.1600-0854.2008.00876.x

Gualdron-Lopez, M. *et al.* (2013) 'Ubiquitination of the Glycosomal Matrix Protein Receptor PEX5 in Trypanosoma brucei by PEX4 Displays Novel Features', *Biochimica et Biophysica Acta (BBA),* 1833(12), pp. 3076-3092. doi: https://doi.org/10.1016/j.bbamcr.2013.08.008

Haferkamp, I. and Schmitz-Esser, S. (2012) 'The Plant Mitochondrial Carrier Family: Functional and Evolutionary Aspects', *Frontiers in Plant Science*, 3. doi: https://doi.org/10.3389/fpls.2012.00002

Hajra, A. K., Burke, C. L. and Jones, C. L. (1979) 'Subcellular Localization of Acyl Coenzyme A: Dihydroxyacetone Phosphate Acyltransferase in Rat Liver Peroxisomes (Microbodies)', *Journal of Biological Chemistry*, 254(21), pp. 10896-10900. Available at: https://pubmed.ncbi.nlm.nih.gov/500614/ (Accessed: 20 August, 2022).

Hannaert, V. and Michels, P. A. (1994) 'Structure, Function, and Biogenesis of Glycosomes in Kinetoplastida', *Journal of Bioenergetics and Biomembranes*, 26(2), pp. 205-212. doi: https://doi.org/10.1007/BF00763069

Hartig, A. *et al.* (1992) 'Differentially Regulated Malate Synthase Genes Participate in Carbon and Nitrogen Metabolism of S. cerevisiae', *Nucleic Acids Research*, 20(21), pp. 5677-5686. doi: https://doi.org/10.1093/nar/20.21.5677

Hettema, E. H. and Tabak, H. F. (2000) 'Transport of Fatty Acids and Metabolites Across the Peroxisomal Membrane', *Biochimica et Biophysica Acta (BBA)*, 1486(1), pp. 18-27. doi: https://doi.org/10.1016/S1388-1981(00)00045-7

Hettema, E. H. *et al.* (1996) 'The ABC Transporter Proteins Pat1 and Pat2 are Required for Import of Long-Chain Fatty Acids into Peroxisomes of Saccharomyces cerevisiae', *The EMBO Journal,* 15(15), pp. 3813-3822. Available at: https://www.ncbi.nlm.nih.gov/pmc/articles/PMC452064/ (Accessed: 20 August, 2022).

Hettema, E. H. *et al.* (2000) 'Saccharomyces cerevisiae Pex3p and Pex19p are Required for Proper Localization and Stability of Peroxisomal Membrane Proteins', *The EMBO Journal,* 19(2), pp. 223-233. doi: https://doi.org/10.1093/emboj/19.2.223

Hettema, E. H. *et al.* (2014) 'Evolving Models for Peroxisome Biogenesis', *Current Opinion in Cell Biology,* 29, pp. 25-30. doi: https://doi.org/10.1016/j.ceb.2014.02.002

Hillebrand, M. *et al.* (2007) 'Live cell FRET Microscopy: Homo- and Heterodimerization of Two Human Peroxisomal ABC transporters, the Adrenoleukodystrophy Protein (ALDP, ABCD1) and PMP70 (ABCD3)', *The Journal of Biological Chemistry*, 282(37), pp. 26997-27005. doi: https://doi.org/10.1074/jbc.M702122200

Hiltunen, J. K. *et al.* (1992) 'Peroxisomal Multifunctional Beta-Oxidation Protein of Saccharomyces cerevisiae. Molecular Analysis of the Fox2 Gene and Gene Product', *Journal of Biological Chemistry,* 267(10) pp. 6646-6653. Available at: https://pubmed.ncbi.nlm.nih.gov/1551874/ (Accessed: 20 August 2022).

Hiltunen, J. K. *et al.* (2003) 'The Biochemistry of Peroxisomal Beta-Oxidation in the Yeast Saccharomyces cerevisiae', *FEMS Microbiology Reviews,* 27(1), pp. 35-64. doi: https://doi.org/10.1016/S0168-6445(03)00017-2

Hoepfner, D. *et al.* (2005) 'Contribution of the Endoplasmic Reticulum to Peroxisome Formation', *Cell*,122(1), pp. 85-95. doi: https://doi.org/10.1016/j.cell.2005.04.025

Hofhuis, J. *et al.* (2016) 'The Functional Readthrough Extension of Malate Dehydrogenase Reveals a Modification of the Genetic Code', *Open Biology*, 6(11), 160246. doi: https://doi.org/10.1098/rsob.160246

Hohfeld, J., Veenhuis, M. and Kunau, W. H. (1991) 'PAS3, a Saccharomyces cerevisiae Gene Encoding a Peroxisomal Integral Membrane Protein Essential for Peroxisome Biogenesis', *The Journal of Cell Biology*, 114(6), pp. 1167–1178. doi: https://doi.org/10.1083/jcb.114.6.1167

Holzinger, A., Kammerer, S. and Roscher, A. A. (1997) 'Primary Structure of Human PMP69, a Putative Peroxisomal ABC-Transporter', *Biochemical and Biophysical Research Communications*, 237(1), pp. 152-157. doi: https://doi.org/10.1006/bbrc.1997.7102

Honsho, M. *et al.* (1998) 'Mutation in PEX16 is Causal in the Peroxisome-Deficient Zellweger Syndrome of Complementation Group D', American Journal of Human Genetics, 63(6), pp. 1622-1630. doi: https://doi.org/10.1086/302161

Honsho, M., Hiroshige, T. and Fujiki, Y. (2002) 'The Membrane Biogenesis Peroxin Pex16p. Topogenesis and Functional Roles in Peroxisomal Membrane Assembly', The *Journal of Biological Chemistry,* 277, pp. 44513-24. doi: https://doi.org/10.1074/jbc.M206139200

Huang, H. *et al.* (2022) 'Identification of Six Thiolases and Their Effects on Fatty Acid and Ergosterol Biosynthesis in Aspergillus oryzae', *Applied and Environmental Microbiology*, 88(6), e0237221. doi: https://doi.org/10.1128/aem.02372-21

Igual, J. C. *et al.* (1991) 'A New Glucose-Repressible Gene Identified from the Analysis of Chromatin Structure in Deletion Mutants of Yeast SUC2 Locus', *Yeast*, 7(4), pp. 379-389. doi: https://doi.org/10.1002/yea.320070408

Islinger, M. *et al.* (2009) 'Hitchhiking of Cu/Zn Superoxide Dismutase to Peroxisomes--Evidence for a Natural Piggyback Import Mechanism in Mammals, *Traffic,* 10(11), pp. 1711-1721. doi: https://doi.org/10.1111/j.1600-0854.2009.00966.x

Islinger, M. and Schrader, M. (2011) 'Peroxisomes', *Current Biology*, 21(19), pp. R800-801. doi: https://doi.org/10.1016/j.cub.2011.07.024

Jacques, N., Mallet, S. and Casaregola, S. (2009) 'Delimitation of the Species of the Debaryomyces hansenii Complex by Intron Sequence Analysis', *International Journal of Systemic and Evolutionary Microbiology*, 59(Pt 5), pp. 1242-51. doi: https://doi.org/10.1099/ijs.0.004325-0

Jain, U. *et al.* (2021) 'Debaryomyces is Enriched in Crohn's Disease Intestinal Tissue and Impairs Healing in Mice', *Science*, 371(6534), pp. 1154-1159. doi: https://doi.org/10.1126/science.abd0919

Jamieson, D. J. (1998) 'Oxidative Stress Responses of the Yeast Saccharomyces cerevisiae', *Yeast*, 14(16), pp. 1511-1527. doi: https://doi.org/10.1002/(SICI)1097-0061(199812)14:16<1511::AID-YEA356>3.0.CO;2-S

Jank, B. *et al.* (1993) 'PMP47, a Peroxisomal Homologue of Mitochondrial Solute Carrier Proteins', *Trends in Biochemical Sciences*, 18(11), pp. 427-428. Available at: https://pubmed.ncbi.nlm.nih.gov/8291088/ (Accessed: 11 September 2022).

Jedd, G. (2011) 'Fungal Evo-Devo: Organelles and Multicellular Complexity', *Trends in Cell Biology, 21*(1), pp. 12-19. doi: https://doi.org/10.1016/j.tcb.2010.09.001

Jedd, G. and Chua, N. H. (2000). 'A New Self-Assembled Peroxisomal Vesicle Required for Efficient Resealing of the Plasma Membrane', *Nature Cell Biology*, 2(4), pp. 226-231. doi: https://doi.org/10.1038/35008652

Jeffries, T. W. *et al.* (2007) 'Genome Sequence of the Lignocellulose-Bioconverting and Xylose-Fermenting Yeast Pichia stipitis', *Nature Biotechnology, 25*(3), pp. 319-326. doi: https://doi.org/10.1038/nbt1290

Johnson, D. R. *et al.* (1994) 'Saccharomyces cerevisiae Contains Four Fatty Acid Activation (FAA) Genes: An Assessment of Their Role in Regulating Protein N-Mristoylation and Cellular Lipid Metabolism', *Journal of Cell Biology*, 127(3), pp. 751-762. doi: https://doi.org/10.1083/jcb.127.3.751

Jones, J. M., Morrell, J. C. and Gould, S. J. (2001) 'Multiple Distinct Targeting Signals in Integral Peroxisomal Membrane Proteins', *Journal of Cell Biology*, 153(6), pp. 1141-1150. doi: https://doi.org/10.1083/jcb.153.6.1141

Jones, J. M., Morrell, J. C. and Gould, S. J. (2004) 'PEX19 is a Predominantly Cytosolic Chaperone and Import Receptor for Class 1 Peroxisomal Membrane Proteins', *The Journal of Cell Biology*, 164(1), pp. 57-67. doi: https://doi.org/ 10.1083/jcb.200311131

Jung, S. *et al.* (2010) 'Dynamic Changes in the Subcellular Distribution of Gpd1p in Response to Cell Stress', *Journal of Biological Chemistry*, 285(9), pp. 6739-6749. doi: https://doi.org/10.1074/jbc.M109.058552

Kalish, J. E. *et al.* (1996) 'Characterization of a Novel Component of the Peroxisomal Protein Import Apparatus Using Fluorescent Peroxisomal Proteins', *The EMBO Journal*, 15(13), pp. 3275-3285. Available at: https://pubmed.ncbi.nlm.nih.gov/8670828/ (Accessed: 9 September 2022).

Kamijo, K. *et al.* (1990) 'The 70-kDa Peroxisomal Membrane Protein is a Member of the Mdr (P-glycoprotein)-Related ATP-Binding Protein Superfamily', *The Journal of Biological Chemistry*, 265(8), pp. 4534-4540. Available at: https://pubmed.ncbi.nlm.nih.gov/1968461/ (Accessed: 12 September 2022)

Kamiryo, T. and Okazaki, K. (1984) 'High-Level Expression and Molecular Cloning of Genes Encoding Candida tropicalis Peroxisomal Proteins', *Molecular and Cellular Biology*, 4(10), pp. 2136-2141. doi: https://doi.org/10.1128/mcb.4.10.2136-2141.1984

Kamiryo, T. *et al.* (1982) 'Absence of DNA in Peroxisomes of Candida tropicalis', *Journal of Bacteriology*, 152(1), pp. 269-274. doi: https://doi.org/10.1128/jb.152.1.269-274.1982

Kanehisa, M. and Goto, S. (2000) 'KEGG: Kyoto Encyclopedia of Genes and Genomes', *Nucleic Acids Research,* 28(1), pp. 27-30. doi: https://doi.org/10.1093/nar/28.1.27

Karpichev, I. V. *et al.* (1997) 'A Complex Containing Two Transcription Factors Regulates Peroxisome Proliferation and the Coordinate Induction of Beta-Oxidation Enzymes in Saccharomyces cerevisiae', *Molecular and Cellular Biology*, 17(1), pp. 69-80. doi: https://doi.org/10.1128/MCB.17.1.69

Karpichev, I. V. and Small, G. M. (1998) 'Global Regulatory Functions of Oaf1p and Pip2p (Oaf2p), Transcription Factors That Regulate Genes Encoding Peroxisomal Proteins in Saccharomyces cerevisiae', *Molecular and Cellular Biology*, 18(11), pp. 6560-6570. doi: https://doi.org/10.1128/mcb.18.11.6560

Kashiwayama, Y. *et al.* (2009) '70-kDa Peroxisomal Membrane Protein Related Protein (P70R/ABCD4) Localizes to Endoplasmic Reticulum not Peroxisomes, and NH2-Terminal Hydrophobic Property

Determines the Subcellular Localization of ABC Subfamily D proteins', *Experimental Cell Research*, 315(2), pp. 190-205. doi: https://doi.org/10.1016/j.yexcr.2008.10.031

Kaur, R., Ingavale, S. S. and Bachhawat, A. K. (1997) 'PCR-Mediated Direct Gene Disruption in Schizosaccharomyces pombe', *Nucleic Acids Research*, 25(5), pp. 1080-1081. doi: https://doi.org/ 10.1093/nar/25.5.1080

Kiel, J. A., Veenhuis, M. and Klei, I. J. (2006) 'PEX Genes in Fungal Genomes: Common, Rare or Redundant', *Traffic*, 7(10), pp. 1291-1303. doi: https://doi.org/10.1111/j.1600-0854.2006.00479.x

Kim, P. K. and Hettema, E. H. (2015). 'Multiple Pathways for Protein Transport to Peroxisomes', *Journal of Molecular Biology,* 427(6 Pt A), pp. 1176-1190. doi: https://doi.org/10.1016/j.jmb.2015.02.005

Kim, H. *et al.* (2018) 'Mouse Cre-LoxP System: General Principles to Determine Tissue-Specific Roles of Target Genes', *Laboratory Animal Research*, 34(4), pp. 147-159. doi: https://doi.org/10.5625/lar.2018.34.4.147

Kim, Y. I. *et al.* (2020) 'Slc25a17 Acts as a Peroxisomal Coenzyme A Transporter and Regulates Multiorgan Development in Zebrafish', *Journal of Cellular Physiology*, 235(1), pp. 151-165. doi: https://doi.org/10.1002/jcp.28954

Klein, A. T. *et al.* (2002) 'Saccharomyces cerevisiae Acyl-CoA Oxidase Follows a Novel, non-PTS1, Import Pathway into Peroxisomes That is Dependent on Pex5p', *Journal of Biological Chemistry*, 277(28), pp. 25011-25019. doi: https://doi.org/10.1074/jbc.M203254200

Klingenberg, M. (2008) 'The ADP and ATP Transport in Mitochondria and its Carrier', *Biochimica et Biophysica Acta (BBA)*, 1778(10), pp. 1978-2021. doi: https://doi.org/10.1016/j.bbamem.2008.04.011

Knoblach, B. and Rachubinski, R. A. (2018) 'Reconstitution of Human Peroxisomal Beta-Oxidation in Yeast', *FEMS Yeast Research*, 18(8). doi: https://doi.org/10.1093/femsyr/foy092

Kolarov, J., Kolarova, N. and Nelson, N. (1990) 'A Third ADP/ATP Translocator Gene in Yeast', The *Journal of Biological Chemistry*, 265(21), pp. 12711-12716. Available at: https://pubmed.ncbi.nlm.nih.gov/2165073/ (Accessed: 12 September 2022)

Kong, F. *et al.* (2018) 'Lipid Catabolism in Microalgae', *New Phytologist,* 218(4), pp. 1340-1348. doi: https://doi.org/10.1111/nph.15047
Kreger van Rij, N. J. and Veenhuis, M. (1975) 'Electron Microscopy of Ascus Formation in the Yeast Debaryomyces hansenii', *Journal of General Microbiology*, 89(2), pp. 256-264. doi: https://doi.org/10.1099/00221287-89-2-256

Kumar, S. *et al.* (2016) 'Stress Exposure Results in Increased Peroxisomal Levels of Yeast Pnc1 and Gpd1, Which are Imported via a Piggy-Backing Mechanism', *Biochimica et Biophysica Acta (BBA)*, 1863(1), pp. 148-156. doi: https://doi.org/10.1016/j.bbamcr.2015.10.017

Kunau, W. H. (2005) 'Peroxisome Biogenesis: End of the Debate', *Current Biology*, 15(18), pp. R774-776. doi: https://doi.org/10.1016/j.cub.2005.08.056

Kunau, W. H., Dommes, V. and Schulz, H. (1995) 'Beta-Oxidation of Fatty Acids in Mitochondria, Peroxisomes, and Bacteria: a Century of Continued Progress', *Progress in Lipid Research*, 34(4), pp. 267-342. doi: https://doi.org/10.1016/0163-7827(95)00011-9

Kunji, E. R. S. *et al.* (2020) 'The SLC25 Carrier Family: Important Transport Proteins in Mitochondrial Physiology and Pathology', *Physiology (Bethesda)*, 35(5), pp. 302-327. doi: https://doi.org/10.1152/physiol.00009.2020

Kunze, M. *et al.* (2002) 'Targeting of Malate Synthase 1 to the Peroxisomes of Saccharomyces cerevisiae Cells Depends on Growth on Oleic Acid Medium', *European Journal of Biochemistry*, 269(3), pp. 915-922. doi: https://doi.org/10.1046/j.0014-2956.2001.02727.x

Lazarow, P. B. and Fujiki, Y. (1985) 'Biogenesis of Peroxisomes', *Annual Review of Cell Biology*, 1, pp. 489-530. doi: https://doi.org/10.1146/annurev.cb.01.110185.002421

Leighton, F. *et al.* (1968) 'The Large-Scale Separation of Peroxisomes, Mitochondria, and Lysosomes From the Livers of Rats Injected with Triton WR-1339. Improved Isolation Procedures, Automated Analysis, Biochemical and Morphological Properties of Fractions', *Journal of Cell Biology*, 37(2), pp. 482-513. doi: https://doi.org/10.1083/jcb.37.2.482

Leon, S., Goodman, J. M. and Subramani, S. (2006) 'Uniqueness of the Mechanism of Protein Import into the Peroxisome Matrix: Transport of Folded, Co-Factor-Bound and Oligomeric Proteins by Shuttling Receptors', *Biochimica et Biophysica Acta (BBA)*, 1763(12), pp. 1552-1564. doi: https://doi.org/10.1016/j.bbamcr.2006.08.037

Lewin, A. S., Hines, V. and Small, G. M. (1990) 'Citrate Synthase Encoded by the CIT2 Gene of Saccharomyces cerevisiae is Peroxisomal', *Molecular and Cellular Biology*, 10(4), pp. 1399-1405. doi: https://doi.org/10.1128/mcb.10.4.1399-1405.1990

Li, Y., Chen, J. and Lun, S.Y. (2001) 'Biotechnological Production of Pyruvic Acid', *Applied Microbiology and Biotechnology*, 57(4), pp. 451-459. doi: https://doi.org/10.1007/s002530100804

Linka, N. *et al.* (2008) 'Peroxisomal ATP Import is Essential for Seedling Development in Arabidopsis thaliana', *Plant Cell*, 20(12), pp. 3241-3257. doi: https://doi.org/10.1105/tpc.108.062042

Linka, N. and Esser, C. (2012) 'Transport Proteins Regulate the Flux of Metabolites and Cofactors Across the Membrane of Plant Peroxisomes', *Frontiers in Plant Science*, 3. doi: https://doi.org/ 10.3389/fpls.2012.00003

Lombard-Platet, G. *et al.* (1996) 'A Close Relative of the Adrenoleukodystrophy (ALD) Gene Codes for a Peroxisomal Protein with a Specific Expression Pattern', *Proceedings of the National Academy of Sciences of the United States of America*, 93(3), pp. 1265-1269. doi: https://doi.org/10.1073/pnas.93.3.1265

Lorenz, M. C. *et al.* (1995) 'Gene Disruption with PCR Products in Saccharomyces cerevisiae', *Gene*, 158(1), pp. 113-117. doi: https://doi.org/10.1016/0378-1119(95)00144-u

Luo, Y. S. *et al.* (2000) 'Purification and Characterization of the Recombinant Form of Acyl CoA Oxidase 3 From the Yeast Yarrowia lipolytica', *Archives of Biochemisty and Biophysics*, 384(1), pp. 1-8. doi: https://doi.org/10.1006/abbi.2000.2079

Luo, Y. S. *et al.* (2002) 'The Acyl-CoA Oxidases From the Yeast Yarrowia lipolytica: Characterization of Aox2p', *Archives of Biochemisty and Biophysics*, 407(1), pp. 32-38. doi: https://doi.org/10.1016/s0003-9861(02)00466-6

Mannaerts, G. P. *et al.* (1982) 'Evidence That Peroxisomal Acyl-CoA Synthetase is Located at the Cytoplasmic Side of the Peroxisomal Membrane', *The Biochemical Journal*, 204(1), pp. 17-23. doi: https://doi.org/10.1042/bj2040017

Marquina, D. *et al.* (2001) 'Production and Characteristics of Debaryomyces hansenii Killer Toxin', *Microbiological Research*, 156(4), pp. 387-391. doi: https://doi.org/10.1078/0944-5013-00117

Marzioch, M. *et al.* (1994) 'PAS7 Encodes a Novel Yeast Member of the WD-40 Protein Family Essential for Import of 3-Oxoacyl-CoA Thiolase, a PTS2-Containing Protein, into Peroxisomes', *The EMBO Journal*, 13(20), pp. 4908-4918. doi: https://doi.org/10.1002/j.1460-2075.1994.tb06818.x

Matsuzono, Y. *et al.* (1999) 'Human PEX19: cDNA Cloning by Functional Complementation, Mutation Analysis in a Patient with Zellweger Syndrome, and Potential Role in Peroxisomal Membrane Assembly', *Proceedings of the National Academy of Sciences of the United States of America*, 96(5), pp. 2116-2121. doi: https://doi.org/10.1073/pnas.96.5.2116

McCammon, M. T. *et al.* (1990) 'Sorting of Peroxisomal Membrane Protein PMP47 From Candida boidinii into Peroxisomal Membranes of Saccharomyces cerevisiae', *Journal of Biological Chemistry*, 265(33), pp. 20098-20105. Available at: https://pubmed.ncbi.nlm.nih.gov/2243083/ (Accessed: 11 September 2022).

McCammon, M. T. *et al.* (1994) 'An Internal Region of the Peroxisomal Membrane Protein PMP47 is Essential for Sorting to Peroxisomes', *Journal of Cell Biology,* 124(6), pp. 915-925. doi: https://doi.org/10.1083/jcb.124.6.915

McClelland, G. B. *et al.* (2003) 'Peroxisomal Membrane Monocarboxylate Transporters: Evidence for a Redox Shuttle System?', *Biochemical and Biophysical Research Communications*, 304(1), pp. 130-135. doi: https://doi.org/10.1016/s0006-291x(03)00550-3

McGroarty, E. and Tolbert, N. E. (1973) 'Enzymes in Peroxisomes', *Journal of Histochemistry and Cytochemistry*, 21(11), pp. 949-954. doi: https://doi.org/10.1177/21.11.949

Merdinger, E. and Devine, E. M. (1965) 'Lipids of Debaryomyces hansenii', *Journal of Bacteriology*, 89, pp. 1488-93. doi: https://doi.org/10.1128/jb.89.6.1488-1493.1965

Mettler, I. J. and Beevers, H. (1980) 'Oxidation of NADH in Glyoxysomes by a Malate-Aspartate Shuttle', *Plant Physiology*, 66(4), pp. 555-560. doi: https://doi.org/10.1104/pp.66.4.555

Michels, P. A., Hannaert, V. and Bringaud, F (2000) 'Metabolic Aspects of Glycosomes in Trypanosomatidae - New Data and Views', *Parasitology Today*, 16(11), pp. 482-489. doi: https://doi.org/10.1016/s0169-4758(00)01810-x

Minard, K. I. and McAlister-Henn, L. (1991) 'Isolation, Nucleotide Sequence Analysis, and Disruption of the MDH2 Gene from Saccharomyces cerevisiae: Evidence for Three Isozymes of Yeast Malate Dehydrogenase', *Molecular and Cellular Biology*, 11(1), pp. 370-380. doi: https://doi.org/10.1128/mcb.11.1.370-380.1991

Minhas, A., Biswas, D. and Mondal, A. K. (2009) 'Development of Host and Vector for High-Efficiency Transformation and Gene Disruption in Debaryomyces hansenii', *FEMS Yeast Research*, 9(1), pp. 95-102. doi: https://doi.org/10.1111/j.1567-1364.2008.00457.x

Miranda, I., Silva, R. and Santos, M. A. (2006) 'Evolution of the Genetic Code in Yeasts', *Yeast*, 23(3), pp. 203-213. doi: https://doi.org/10.1002/yea.1350

Moreno, M. *et al.* (1994) 'The Peroxisomal Membrane Proteins of Candida boidinii: Gene Isolation and Expression', *Yeast*, 10(11), pp. 1447-1457. doi: https://doi.org/10.1002/yea.320101108

Mortilla-Martinez, M. *et al.* (2015) 'Distinct Pores for Peroxisomal Import of PTS1 and PTS2 Proteins', *Cell Reports*, 13(10), pp. 2126-2134. doi: https://doi.org/10.1016/j.celrep.2015.11.016

Mosser, J. *et al.* (1993) 'Putative X-Linked Adrenoleukodystrophy Gene Shares Unexpected Homology with ABC Transporters', *Nature*, 361(6414), pp. 726-730. doi: https://doi.org/10.1038/361726a0

Motley, A. *et al.* (1995) 'Mammalian Alanine/Glyoxylate Aminotransferase 1 is Imported into Peroxisomes via the PTS1 Translocation Pathway. Increased Degeneracy and Context Specificity of the Mammalian PTS1 Motif and Implications for the Peroxisome-to-Mitochondrion Mistargeting of AGT in Primary Hyperoxaluria Type 1', *Journal of Cell Biology*, 131(1), pp. 95-109. doi: https://doi.org/10.1083/jcb.131.1.95

Motley, A. *et al.* (2000) 'Caenorhabditis elegans Has a Single Pathway to Target Matrix Proteins to Peroxisomes', *EMBO Reports*, 1(1), pp. 40-46. doi: https://doi.org/10.1093/embo-reports/kvd010

Munsterkotter, M. and G. Steinberg (2007) 'The Fungus Ustilago maydis and Humans Share Disease-Related Proteins That are Not Found in Saccharomyces cerevisiae', *BMC Genomics*, 8, pp. 473. doi: https://doi.org/10.1186/1471-2164-8-473

Muntau, A. C. *et al.* (2003) 'The Interaction Between Human PEX3 and PEX19 Characterized by Fluorescence Resonance Energy Transfer (FRET) Analysis', *European Journal of Cell Biology*, 82(7), pp. 333-342. doi: https://doi.org/10.1078/0171-9335-00325

Nagy, A. (2000) 'Cre Recombinase: The Universal Reagent for Genome Tailoring', *Genesis*, 26(2), pp. 99-109. doi: https://doi.org/10.1002/(SICI)1526-968X(200002)26:2<99::AID-GENE1>3.0.CO;2-B

Nakagawa, T. *et al.* (2000) 'Peroxisomal Membrane Protein Pmp47 is Essential in the Metabolism of Middle-Chain Fatty Acid in Yeast Peroxisomes and is Associated with Peroxisome Proliferation', *Journal of Biological Chemistry*, 275(5), pp. 3455-3461. doi: https://doi.org/10.1074/jbc.275.5.3455

Neuberger, G. *et al.* (2003) 'Motif Refinement of the Peroxisomal Targeting Signal 1 and Evaluation of Taxon-Specific Differences', *Journal of Molecular Biology*, 328(3), pp. 567-579. doi: https://doi.org/10.1016/s0022-2836(03)00318-8

Norkrans, B. (1966) 'Studies on Marine Occurring Yeasts: Growth Related to pH, NaCl Concentration and Temperature', A*rchiv für Mikrobiologie*, 54, pp. 374-392. Available at: https://link.springer.com/article/10.1007/BF00406719 (Accessed: 11 September 2022).

Norkrans, B. (1968) 'Studies on Marine Occurring Yeasts: Respiration, Fermentation and Salt Tolerance', *Archiv für Mikrobiologie,* 62(4), pp. 358-372. Available at: https://link.springer.com/article/10.1007/BF00425641 (Accessed: 11 September 2022).

Nuttall, J. M., Hettema, E. H. and Watts, D. J. (2012) 'Farnesyl Diphosphate Synthase, the Target for Nitrogen-Containing Bisphosphonate Drugs, is a Peroxisomal Enzyme in the Model System Dictyostelium discoideum', *The Biochemical Journal*, 447(3), pp. 353-361. doi: https://doi.org/10.1042/BJ20120750

Nuttall, J. M., Motley, A. and Hettema, E. H. (2011) 'Peroxisome Biogenesis: Recent Advances', *Current Opinion in Cell Biology*, 23(4), pp. 421-426. doi: https://doi.org/10.1016/j.ceb.2011.05.005

Opperdoes, F. R. (1987) 'Compartmentation of Carbohydrate Metabolism in Trypanosomes', *Annual Review of Microbiology*, 41, pp. 127-151. doi: https://doi.org/10.1146/annurev.mi.41.100187.001015

Orr-Weaver, T. L., Szostak, J. W. and Rothstein, R. J. (1983) 'Genetic Applications of Yeast Transformation with Linear and Gapped Plasmids', *Methods of Enzymology*, 101, pp. 228-245. doi: https://doi.org/10.1016/0076-6879(83)01017-4

Otera, H. *et al.* (2000) 'The Mammalian Peroxin Pex5pL, the Longer Isoform of the Mobile Peroxisome Targeting Signal (PTS) Type 1 Transporter, Translocates the Pex7p. PTS2 Protein Complex into Peroxisomes via its Initial Docking Site, Pex14p', *Journal of Biological Chemistry,* 275(28), pp. 21703-21714. doi: https://doi.org/10.1074/jbc.M000720200

Otzen, C. *et al.* (2013) 'Phylogenetic and Phenotypic Characterisation of the 3-Ketoacyl-CoA Thiolase Gene Family From the Opportunistic Human Pathogenic Fungus Candida albicans', *FEMS Yeast Research*, 13(6), pp. 553-564. doi: https://doi.org/ 10.1111/1567-1364.12057

Otzen, M. *et al.* (2005) 'Hansenula polymorpha Pex20p is an Oligomer That Binds the Peroxisomal Targeting Signal 2 (PTS2)', *Journal of Cell Science,* 118(Pt 15), pp. 3409-3418. doi: https://doi.org/10.1242/jcs.02463

Palmieri, L. *et al.* (2001) 'Identification and Functional Reconstitution of the Yeast Peroxisomal Adenine Nucleotide Transporter', *The EMBO Journal,* 20(18), pp. 5049-5059. doi: https://doi.org/10.1093/emboj/20.18.5049

Parajó, J. C., Domínguez, H. and Domínguez, J. M. (1995) 'Production of Xylitol From Raw Wood Hydrolysates by Debaryomyces hansenii NRRL Y-7426', *Bioprocess engineering*, 13(3), pp. 125-131. Available at: https://link.springer.com/article/10.1007/BF00369695 (Accessed: 11 September 2022).

Petriv, O. I. *et al.* (2004) 'A New Definition for the Consensus Sequence of the Peroxisome Targeting Signal Type 2', *Journal of Molecular Biology*, 341(1), pp. 119–134. doi: https://doi.org/10.1016/j.jmb.2004.05.064

Pracharoenwattana, I., Cornah, J. E. and Smith, S. M. (2007) 'Arabidopsis Peroxisomal Malate Dehydrogenase Functions in Beta-Oxidation but not in the Glyoxylate Cycle', *The Plant Journal,* 50(3), pp. 381-390. doi: https://doi.org/10.1111/j.1365-313X.2007.03055.x

Prista, C. *et al.* (2016) 'The Halotolerant Debaryomyces hansenii, the Cinderella of Non-Conventional Yeasts', *Yeast*, 33(10), pp. 523-533. doi: https://doi.org/10.1002/yea.3177

Prohl, C. *et al.* (2001) 'The Yeast Mitochondrial Carrier Leu5p and its Human Homologue Graves' Disease Protein are Required for Accumulation of Coenzyme A in the Matrix', *Molecular and Cellular Biology*, 21(4), pp. 1089-1097. doi: https://doi.org/10.1128/MCB.21.4.1089-1097.2001

Purdue, P. E., Yang, X. and Lazarow, P. B. (1998) 'Pex18p and Pex21p, a Novel Pair of Related Peroxins Essential for Peroxisomal Targeting by the PTS2 Pathway', *Journal of Cell Biology*, 143(7), pp. 1859-1869. doi: https://doi.org/10.1083/jcb.143.7.1859

Rai, A. *et al.* (2011) 'Dictyostelium Dynamin B Modulates Cytoskeletal Structures and Membranous Organelles', *Cellular and Molecular Life Sciences*, 68(16), pp. 2751-2767. doi: https://doi.org/10.1007/s00018-010-0590-5

Ramírez-Orozco, M., Hernández-Saavedra, N. Y. and Ochoa, J. L. (2001) 'Debaryomyces hansenii Growth in Nonsterile Seawater ClO2-Peptone-Containing Medium', *Canadian Journal of Microbiology*, 47, pp. 676-679. doi: https://doi.org/10.1139/w01-056

Rapoport, T. A. (2007) 'Protein Translocation Across the Eukaryotic Endoplasmic Reticulum and Bacterial Plasma Membranes', *Nature*, 450(7170), pp. 663-669. doi: https://doi.org/10.1038/nature06384

Ratledge, C. (2002) 'Regulation of Lipid Accumulation in Oleaginous Micro-Organisms', *Biochemical Society Transactions*, 30(6), pp. 1047-1050. doi: https://doi.org/10.1042/bst0301047

Rehling, P. *et al.* (1996) 'The Import Receptor for the Peroxisomal Targeting Signal 2 (PTS2) in Saccharomyces cerevisiae is Encoded by the PAS7 Gene', *The EMBO Journal*, 15(12), pp. 2901-2913. doi: https://doi.org/10.1002/j.1460-2075.1996.tb00653.x

Rhodin, J. (1954) *Correlation of ultrastructural organization and function in normal and experimentally changed proximal convoluted tubule cells of the mouse kidney*. PhD Thesis. Karolinska Institutet.

Rottensteiner, H. and Theodoulou, F. L. (2006) 'The Ins and Outs of Peroxisomes: Co-ordination of Membrane Transport and Peroxisomal Metabolism', *Biochimica et Biophysica Acta (BBA)*, 1763(12), pp. 1527-1540. doi: https://doi.org/10.1016/j.bbamcr.2006.08.012

Rottensteiner, H. *et al.* (1996) 'Pip2p: a Transcriptional Regulator of Peroxisome Proliferation in the Yeast Saccharomyces cerevisiae', *The EMBO Journal*, 15(12), pp. 2924-2934. Available at: https://www.ncbi.nlm.nih.gov/pmc/articles/PMC450233/ (Accessed: 20 August, 2022).

Sacksteder, K. A. *et al.* (2000) 'PEX19 Binds Multiple Peroxisomal Membrane Proteins, is Predominantly Cytoplasmic, and is Required for Peroxisome Membrane Synthesis', *Journal of Cell Biology*, 148(5), pp. 931-944. doi: https://doi.org/10.1083/jcb.148.5.931

Saha, B. C. and Bothast, R. J. (1996) 'Glucose Tolerant and Thermophilic ß-glucosidases From Yeasts', *Biotechnology Letters*, 18(2), pp. 155-158. Available at: https://link.springer.com/article/10.1007/BF00128671 (Accessed: 11 September 2022).

Saldanha-da-Gama, A., Malfeito-Ferreira, M. and Loureiro, V. (1997) 'Characterization of Yeasts Associated with Portuguese Pork-Based Products', *International Journal of Food Microbiology*, 37(2-3), pp. 201-207. doi: https://doi.org/10.1016/s0168-1605(97)00078-0

Saunders, P. P. and Broquist, H. P. (1966) 'Saccharopine, an Intermediate of the Aminoadipic Acid Pathway of Lysine Biosynthesis. IV. Saccharopine dehydrogenase', *Journal of Biological Chemistry*, 241(14), pp. 3435-3440. Available at: https://pubmed.ncbi.nlm.nih.gov/4287986/ (Accessed: 11 September 2022).

Schrader, M. and Fahimi, H. D. (2008) 'The Peroxisome: Still a Mysterious Organelle', *Histochemistry and Cell Biology*, 129(4), pp. 421-440. doi: https://doi.org/10.1007/s00418-008-0396-9

Schueren, F. *et al*. (2014) 'Peroxisomal Lactate Dehydrogenase is Generated by Translational Readthrough in Mammals', *eLife*, 3, e03640. doi: https://doi.org/10.7554/eLife.03640

Schuldiner, M. *et al.* (2008) 'The GET Complex Mediates Insertion of Tail-Anchored Proteins into the ER Membrane', *Cell*, 134(4), pp. 634-645. doi: https://doi.org/10.1016/j.cell.2008.06.025

Schulz, H. (1996) 'Oxidation of fatty acids', in Vance, D. E. and Vance, J. E. (eds.) *Biochemistry of Lipids, Lipoproteins and Membranes*. New York: Elsevier, pp. 75-99.

Seiler, H. and Busse, M. (1990) 'The Yeasts of Cheese Brines', *International Journal of Food Microbiology*, 11(3-4) pp. 289-303. doi: https://doi.org/10.1016/0168-1605(90)90022-W

Shani, N. and Valle, D. (1996) 'A Saccharomyces cerevisiae Homolog of the Human Adrenoleukodystrophy Transporter is a Heterodimer of Two Half ATP-Binding Cassette Transporters', *Proceedings of the National Academy of Sciences of the United States of America*, 93(21), pp. 11901-11906. doi: https://doi.org/10.1073/pnas.93.21.11901

Shani, N., Watkins, P. A. and Valle, D. (1995) 'PXA1, a Possible Saccharomyces cerevisiae Ortholog of the Human Adrenoleukodystrophy Gene', *Proceedings of the National Academy of Sciences of the United States of America*, 92(13), pp. 6012-6016. doi: https://doi.org/10.1073/pnas.92.13.6012.

Shen, Y. Q. and Burger, G. (2009) 'Plasticity of a Key Metabolic Pathway in Fungi', *Functional and Integrative Genomics*, 9(2), pp. 145-151. doi: https://doi.org/10.1007/s10142-008-0095-6

Shen, Y. Q., *et al.* (2009). 'Diversity and Dispersal of a Ubiquitous Protein Family: Acyl-CoA Dehydrogenases', *Nucleic Acids Research*, 37(17), pp. 5619-5631. doi: https://doi.org/10.1093/nar/gkp566

Sherman, F. (1991) 'Getting Started with Yeast', *Methods in Enzymology*, *194*, pp. 3-21. doi: https://doi.org/10.1016/0076-6879(91)94004-v

Sibirny, A. A. (2016) 'Yeast Peroxisomes: Structure, Functions and Biotechnological Opportunities', *FEMS Yeast Research*, 16(4). doi: https://doi.org/10.1093/femsyr/fow038

Sievers, F. *et al.* (2011) 'Fast, Scalable Generation of High-Quality Protein Multiple Sequence Alignments Using Clustal Omega', *Molecular System Biology*, 7(1), 539. doi: https://doi.org/10.1038/msb.2011.75

Sigrist, C. J. A. *et al.* (2002) 'PROSITE: A Documented Database Using Patterns and Profiles as Motif Descriptors', *Briefings in Bioinformatics*, 3(3), pp. 265-274. doi: https://doi.org/10.1093/bib/3.3.265

Sigrist, C. J. A. *et al.* (2012) 'New and Continuing Developments at PROSITE', *Nucleic Acids Research*, 41(D1), pp. D344–D347. doi: https://doi.org/10.1093/nar/gks1067

South, S. T. and Gould, S. J. (1999) 'Peroxisome Synthesis in the Absence of Preexisting Peroxisomes', *The Journal of Cell Biology*, 144(2), pp. 255-266. doi: https://doi.org/10.1083/jcb.144.2.255

Spasskaya, D. S. *et al.* (2021) 'CRISPR/Cas9-Mediated Genome Engineering Reveals the Contribution of the 26S Proteasome to the Extremophilic Nature of the Yeast Debaryomyces hansenii', *ACS Synthetic Biology*, 10(2), pp. 297-308. doi: https://doi.org/10.1021/acssynbio.0c00426

Stabenau, H., Winkler, U. and Saftel, W. (1984) 'Enzymes of Beta-Oxidation in Different Types of Algal Microbodies', *Plant Physiology,* 75(3), pp. 531-533. doi: https://doi.org/10.1104/pp.75.3.531

Stanley, W. A. *et al.* (2006) 'Recognition of a Functional Peroxisome Type 1 Target by the Dynamic Import Receptor Pex5p', *Molecular Cell,* 24(5), pp. 653-663. doi: https://doi.org/10.1016/j.molcel.2006.10.024.

Steinberg, G. and Perez-Martin, J. (2008) 'Ustilago maydis, a New Fungal Model System for Cell Biology', *Trends in Cell Biology*, 18(2), pp. 61-67. doi: https://doi.org/10.1016/j.tcb.2007.11.008

Strucko, T. *et al.* (2021) 'A CRISPR/Cas9 Method Facilitates Efficient Oligo-Mediated Gene Editing in Debaryomyces hansenii', *Synthetic Biology (Oxford, England)*, 6(1). doi: https://doi.org/10.1093/synbio/ysab031

Sulter, G. J. *et al.* (1993) 'Expression and Targeting of a 47 kDa Integral Peroxisomal Membrane Protein of Candida boidinii in Wild Type and a Peroxisome-Deficient Mutant of Hansenula polymorpha', *FEBS Letters*, 315(3), pp. 211-216. doi: https://doi.org/10.1016/0014-5793(93)81166-W

Swinkels, B. W. *et al.* (1991) 'A novel, Cleavable Peroxisomal Targeting Signal at the Amino-Terminus of the Rat 3-Ketoacyl-CoA Thiolase', *The EMBO Journal*, 10(11), pp. 3255-3262. doi: https://doi.org/10.1002/j.1460-2075.1991.tb04889.x

Tanabe, Y. *et al.* (2011) 'Peroxisomes are Involved in Biotin Biosynthesis in Aspergillus and Arabidopsis', *Journal of Biological Chemistry*, 286(35), pp. 30455-30461. doi: https://doi.org/10.1074/jbc.M111.247338

Theodoulou, F. L., Holdsworth, M. and Baker, A. (2006) 'Peroxisomal ABC transporters', *FEBS Letters*, 580(4), pp. 1139-1155. doi: https://doi.org/10.1016/j.febslet.2005.12.095

Thoms, S. *et al.* (2012) 'Peroxisome Formation Requires the Endoplasmic Reticulum Channel Protein Sec61', *Traffic,* 13(4), pp. 599-609. doi: https://doi.org/10.1111/j.1600-0854.2011.01324.x

Thoms, S., Gronborg, S. and Gartner, J. (2009) 'Organelle Interplay in Peroxisomal Disorders', *Trends in Molecular Medicine,* 15(7), pp. 293-302. doi: https://doi.org/10.1016/j.molmed.2009.05.002

Titorenko, V. I. *et al.* (2002) 'Acyl-CoA Oxidase is Imported as a Heteropentameric, Cofactor-Containing Complex into Peroxisomes of Yarrowia lipolytica', *Journal of Cell Biology*, 156(3), pp. 481-494. doi: https://doi.org/10.1083/jcb.200111075

Todisco, S. *et al.* (2006). 'Identification of the Mitochondrial NAD+ Transporter in Saccharomyces cerevisiae', *The Journal of Biological Chemistry*, 281(3), pp. 1524-1531. doi: https://doi.org/10.1074/jbc.M510425200

Valadi, A. *et al.* (2004) 'Distinct Intracellular Localization of Gpd1p and Gpd2p, the Two Yeast Isoforms of NAD+-Dependent Glycerol-3-Phosphate Dehydrogenase, Explains Their Different Contributions to Redox-Driven Glycerol Production', *Journal of Biological Chemistry*, 279(38), pp. 39677-39685. doi: https://doi.org/10.1074/jbc.M403310200

van den Bosch, H. *et al.* (1992) 'Biochemistry of Peroxisomes'. *Annual Reviews of Biochemistry,* 61(1), pp. 157-197. Available at: https://www.annualreviews.org/doi/10.1146/annurev.bi.61.070192.001105 (Accessed: 20 August, 2022).

van der Walt, J. P., Taylor, M. B. and Liebenberg, N. V. (1977) 'Ploidy, Ascus Formation and Recombination in Torulaspora (Debaryomyces) hansenii', *Antonie Van Leeuwenhoek*, 43(2), pp. 205-18. doi: https://doi.org/10.1007/BF00395675

van der Zand, A., Braakman, I. and Tabak, H. F. (2010) 'Peroxisomal Membrane Proteins Insert into the Endoplasmic Reticulum', *Molecular Biology of the Cell*, 21(12), pp. 2057– 2065. doi: https://doi.org/10.1091/mbc.E10-02-0082

van Roermund, C. W. T. *et al.* (1995) 'The Membrane of Peroxisomes in Saccharomyces cerevisiae is Impermeable to NAD(H) and Acetyl-CoA Under in vivo Conditions' *The EMBO Journal,* 14(14), pp. 3480-3486. doi: https://doi.org/10.1002/j.1460-2075.1995.tb07354.x

van Roermund, C. W. T. *et al.* (1999) 'Molecular Characterization of Carnitine-Dependent Transport of Acetyl-CoA From Peroxisomes to Mitochondria in Saccharomyces cerevisiae and Identification of a Plasma Membrane Carnitine Transporter, Agp2p', *The EMBO Journal,* 18(21), pp. 5843-5852. doi: https://doi.org/10.1093/emboj/18.21.5843

van Roermund, C. W. T. *et al.* (2001) 'Identification of a Peroxisomal ATP Carrier Required for Medium-Chain Fatty Acid Beta-Oxidation and Normal Peroxisome Proliferation in Saccharomyces cerevisiae', *Molecular and Cellular Biology*, 21(13), pp. 4321-4329. doi: https://doi.org/10.1128/MCB.21.13.4321-4329.2001

van Roermund, C. W. T. *et al.* (2003) 'Fatty Acid Metabolism in Saccharomyces cerevisiae', *Cellular and Molecular Life Sciences (CLMS*), 60(9), pp. 1838-1851. doi: https://doi.org/10.1007/s00018-003-3076-x

van Roermund, C. W. T. *et al.* (2008) 'The Human Peroxisomal ABC Half Transporter ALDP Functions as a Homodimer and Accepts Acyl-CoA Esters', *The FASEB Journal*, 22(12), pp. 4201-4208. doi: https://doi.org/10.1096/fj.08-110866

van Roermund, C. W. T. *et al.* (2011) 'Differential Substrate Specificities of Human ABCD1 and ABCD2 in Peroxisomal Fatty Acid β-oxidation', *Biochimica et Biophysica Acta (BBA)*, 1811(3), pp. 148-152. doi: https://doi.org/10.1016/j.bbalip.2010.11.010

van Roermund, C. W. T. *et al.* (2016) 'The Peroxisomal NAD Carrier from Arabidopsis Imports NAD in Exchange with AMP', *Plant Physiology*, 171(3). pp. 2127-2139. doi: https://doi.org/10.1104/pp.16.00540

van Roermund, C. W. T. *et al.* (2021) 'The Saccharomyces cerevisiae ABC Subfamily D Transporter Pxa1/Pxa2p Co-Imports CoASH into the Peroxisome', *FEBS Letters*, 595(6), pp. 763-772. doi: https://doi.org/10.1002/1873-3468.13974

van Roermund, C. W. T. *et al.* (2022) 'Peroxisomal ATP Uptake Is Provided by Two Adenine Nucleotide Transporters and the ABCD Transporters', *Frontiers in Cell and Developmental Biology*, 9. doi: https://doi.org/10.3389/fcell.2021.788921

van Veldhoven, P. P., Just, W. W. and Mannaerts, G. P. (1987) 'Permeability of the Peroxisomal Membrane to Cofactors of Beta-Oxidation. Evidence for the Presence of a Pore-Forming Protein', *Journal of Biological Chemistry*, 262(9), pp. 4310-4318. Available at: https://pubmed.ncbi.nlm.nih.gov/3031070/ (Accessed: 11 September 2022).

Veenhuis, M. *et al.* (1987) 'Proliferation of Microbodies in Saccharomyces cerevisiae', *Yeast*, 3(2), pp. 77-84. doi: https://doi.org/10.1002/yea.320030204

Verleur, N. *et al.* (1997) 'Cytosolic Aspartate Aminotransferase Encoded by the AAT2 Gene is Targeted to the Peroxisomes in Oleate-Grown Saccharomyces cerevisiae', *European Journal of Biochemistry*, 247(3), pp. 972-980. doi: https://doi.org/10.1111/j.1432-1033.1997.00972.x

Visser, W. F. *et al.* (2002) 'Identification of Human PMP34 as a Peroxisomal ATP Transporter', *Biochemical and Biophysical Research Communications*, 299(3), pp. 494-497. doi: https://doi.org/10.1016/s0006-291x(02)02663-3

Visser, W. F. *et al.* (2007) 'Metabolite Transport Across the Peroxisomal Membrane', *Biochemical Journal*, 401(2), pp. 365-375. doi: https://doi.org/10.1042/BJ20061352

Wagner, D. *et al.* (2005) 'Breakthrough Invasive Infection Due to Debaryomyces hansenii (Teleomorph Candida famata) and Scopulariopsis brevicaulis in a Stem Cell Transplant Patient Receiving Liposomal Amphotericin B and Caspofungin for Suspected Aspergillosis', *Infection*, 33(5-6), pp. 397-400. doi: https://doi.org/10.1007/s15010-005-5082-4

Wanders, R. J. and Waterham, H. R. (2006) 'Biochemistry of Mammalian Peroxisomes Revisited', *Annual Review of Biochemistry*, *75*, pp. 295-332. doi: https://doi.org/10.1146/annurev.biochem.74.082803.133329

Wanders, R. J. *et al.* (2010) 'The Enzymology of Mitochondrial Fatty Acid Beta-Oxidation and Its Application to Follow-up Analysis of Positive Neonatal Screening Results', *Journal of Inherited Metabolic Disease*, 33(5), pp. 479-494. doi: https://doi.org/10.1007/s10545-010-9104-8

Wang, H. J. *et al.* (1998) 'Cloning and Characterization of the Peroxisomal Acyl CoA Oxidase ACO3 Gene From the Alkane-Utilizing Yeast Yarrowia lipolytica', *Yeast*, 14(15), pp. 1373-1386. doi: https://doi.org/10.1002/(SICI)1097-0061(199811)14:15<1373::AID-YEA332>3.0.CO;2-1

Wang, H. J. *et al.* (1999a) 'Cloning, Sequencing, and Characterization of Five Genes Coding for Acyl-CoA Oxidase Isozymes in the Yeast Yarrowia lipolytica', *Cell Biochemistry and Biophysics*, 31(2), pp. 165-174. Available at: https://link.springer.com/article/10.1007/BF02738170 (Accessed: 10 September 2022)

Wang, H. J. *et al.* (1999b) 'Evaluation of Acyl coenzyme A Oxidase (Aox) Isozyme Function in the N-Alkane-Assimilating Yeast Yarrowia lipolytica', *Journal of Bacteriology,* 181(17), pp. 5140-5148. doi: https://doi.org/10.1128/JB.181.17.5140-5148.1999

Wiese, S. *et al.* (2007) 'Proteomics Characterization of Mouse Kidney Peroxisomes by Tandem Mass Spectrometry and Protein Correlation Profiling', *Molecular and Cellular Proteomics*, 6(12), pp. 2045-57. doi: https://doi.org/10.1074/mcp.M700169-MCP200

Wroblewska, J. P. *et al.* (2017) 'Saccharomyces cerevisiae Cells Lacking Pex3 Contain Membrane Vesicles That Harbor a Subset of Peroxisomal Membrane Proteins', *Biochimica et Biophysica Acta Molecular Cell Research*, 1864(10), pp. 1656-1667. doi: https://doi.org/10.1016/j.bbamcr.2017.05.021

Wylin, T. *et al.* (1998) 'Identification and Characterization of Human PMP34, a Protein Closely Related to the Peroxisomal Integral Membrane Protein PMP47 of Candida boidinii', *European Journal of Biochemistry*, 258(2), pp. 332-338. doi: https://doi.org/10.1046/j.1432-1327.1998.2580332.x

Xu, H. *et al.* (2006) 'The Alpha-Aminoadipate Pathway for Lysine Biosynthesis in Fungi', *Cell Biochemistry and Biophysics*, 46(1), pp. 43-64. doi: https://doi.org/10.1385/CBB:46:1:43

Yofe, I. *et al.* (2016) 'One Library to Make Them All: Streamlining the Creation of Yeast Libraries via a SWAp-Tag Strategy', *Nature Methods*, 13(4), pp. 371-378. doi: https://doi.org/10.1038/nmeth.3795

Zabriskie, T. M. and Jackson, M. D. (2000) 'Lysine Biosynthesis and Metabolism in Fungi', *Natural Product Reports*, 17(1), pp. 85-97. doi: https://doi.org/10.1039/A801345D

Zallot, R. *et al.* (2013) 'Identification of Mitochondrial Coenzyme A Transporters From Maize and Arabidopsis', *Plant Physiology*, 162(2), pp. 581-588. doi: https://doi.org/10.1104/pp.113.218081

APPENDICES

Appendix 1- Plasmid maps for each toolbox plasmid developed for *D. hansenii*, that were used for gene deletions as well as tagging in the genome. Each map was constructed via SnapGene® software (from Insightful Science; available at snapgene.com). Plasmids pDh1, pDh2 and pZA1 were used to generate gene deletion cassettes. Plasmids pSA5 and pSLV38 were used as a backbone to generate N-terminal and C-terminal tagging cassettes respectively, whereas pSLV35 and pSLV37 were used for co-localization. Upon publication, the plasmids will be deposited at Addgene including DNA sequence files.

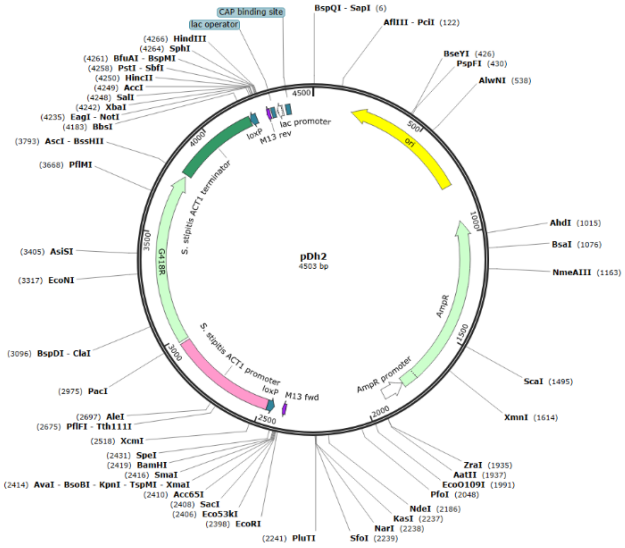

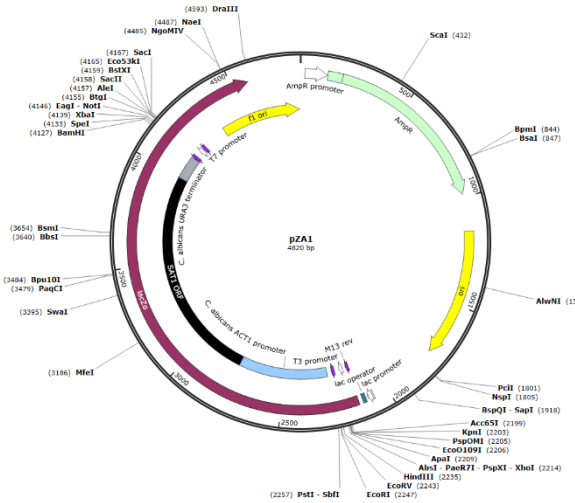

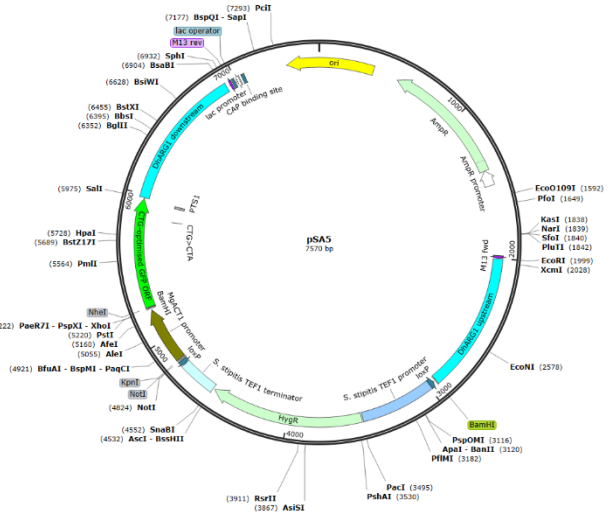

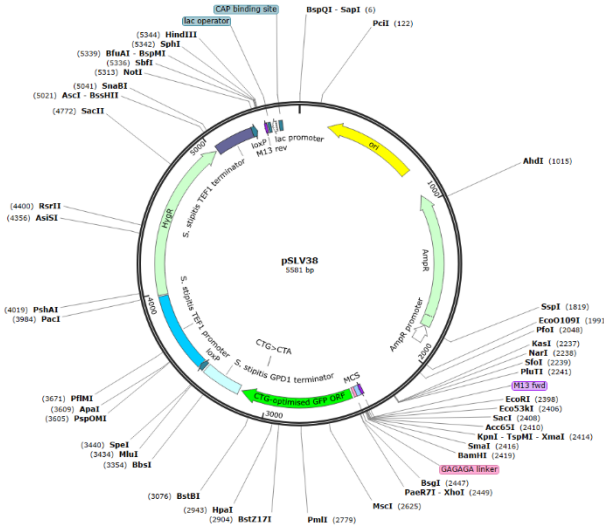
pSLV38
5581 bp
CAP binding site
lac operator
BspQI - SapI (6)
PciI (122)
(5344) HindIII
(5342) SphI
(5339) BfuAI - BspMI
(5336) SbfI
(5313) NotI
(5041) SnaBI
(5021) AscI - BssHII
(4772) SacII
AhdI (1015)
(4400) RsrII
(4356) AsiSI
(4019) PshAI
(3984) PacI
(3671) PflMI
(3609) ApaI
(3605) PspOMI
(3440) SpeI
(3434) MluI
(3354) BbsI
(3076) BstBI
(2943) HpaI
(2904) BstZ17I
PmlI (2779)
MscI (2625)
PaeR7I - XhoI (2449)
BsqI (2447)
GAGAGA linker
BamHI (2419)
SmaI (2416)
KpnI - TspMI - XmaI (2414)
Eco53kI (2406)
SacI (2408)
Acc65I (2410)
EcoRI (2398)
M13 fwd
PmeI (2241)
NarI (2238)
KasI (2237)
SfoI (2239)
SspI (1819)
EcoO109I (1991)
PfoI (2048)
AmpR
AmpR promoter
S. stipitis GPD1 terminator
CTG-optimised GFP ORF
CTG>CTA
MCS
S. stipitis TEF1 promoter
S. stipitis TEF1 terminator
HygR
lac promoter
M13 rev
loxP
ori

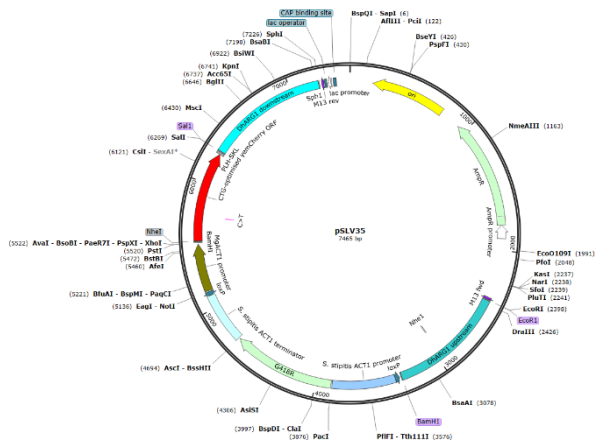
pSLV35
7465 bp
CAP binding site
lac operator
BspQI - SapI (6)
AflIII - PciI (122)
BseYI (426)
PspFI (430)
NmeAIII (1163)
(7226) SphI
(7198) BsaBI
(6922) BsiWI
(6741) KpnI
(6737) Acc65I
(6646) BglII
(6430) MscI
(6209) SalI
(6121) CsiI - SexAI*
(5522) AvaI - BsoBI - PaeR7I - PspXI - XhoI
(5520) PstI
(5472) BstBI
(5466) AfeI
(5221) BfuAI - BspMI - PaqCI
(5136) EagI - NotI
(4694) AscI - BssHII
(4306) AsiSI
(3997) BspDI - ClaI
(3876) PacI
PflFI - Tth111I (3576)
BamHI
BsaAI (3078)
EcoRI
EcoR1
PmeI
NarI (2238)
SfoI (2239)
PluTI (2241)
EcoO109I (1991)
PfoI (2048)
KasI (2237)
AmpR
AmpR promoter
M13 rev
DsaBCI promoter
S. stipitis ACT1 promoter
S. stipitis ACT1 terminator
G418R
RLM-SAT1
CTG-optimised mCherry ORF
MgtA1 promoter
SAT1
NheI
C>T
ori
lac promoter
M13 rev
SphI

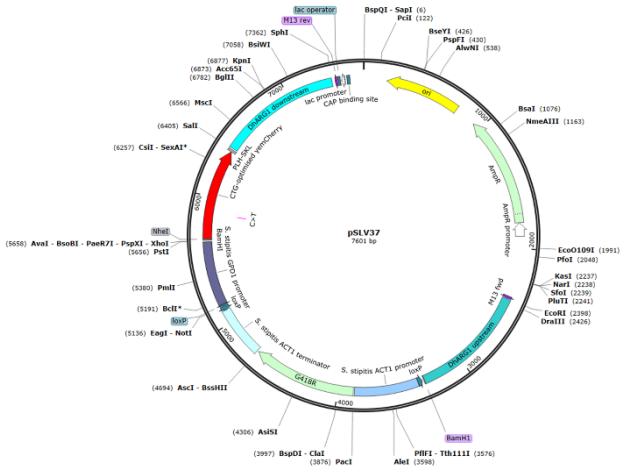
pSLV37
7601 bp
lac operator
M13 rev
BspQI - SapI (6)
PciI (122)
BseYI (426)
PspFI (430)
AlwNI (538)
BsaI (1076)
NmeAIII (1163)
(7362) SphI
(7058) BsiWI
(6877) KpnI
(6873) Acc65I
(6782) BglII
(6566) MscI
(6405) SalI
(6257) CsiI - SexAI*
(5658) AvaI - BsoBI - PaeR7I - PspXI - XhoI
(5656) PstI
(5380) PmlI
(5191) BclI*
(5136) EagI - NotI
(4694) AscI - BssHII
(4306) AsiSI
(3997) BspDI - ClaI
(3876) PacI
AleI (3598)
PflFI - Tth111I (3576)
BamHI
EcoO109I (1991)
PfoI (2048)
KasI (2237)
NarI (2238)
SfoI (2239)
PluTI (2241)
EcoRI (2398)
DraIII (2426)
AmpR
AmpR promoter
M13 fwd
DsaBCI promoter
S. stipitis ACT1 promoter
S. stipitis ACT1 terminator
G418R
S. stipitis GPD1 promoter
S. stipitis GPD1 terminator
RLM-SAT1
CTG-optimised mCherry
NheI
C>T
ori
lac promoter
CAP binding site

Appendix 2- List of potential peroxisomal proteins in *D. hansenii*, as well as the proteins with potential PTS1 and PTS2 tags, identified by bioinformatics research.

	protein name	present in D. hansenii?	good hit?	present in pattern search?	PTS1/PTS2?	present in S. cerevisiae?	present in humans?
Perox. inheritance / motility	Inp1	yes (Q6BSB0)	no	no	No PTS	yes (INP1_YEAST)	no
	Inp2	no				yes (INP2_YEAST)	no
	Myo2	yes (Q6BSW2)	yes	yes	PTS2 in the middle	yes (MYO2_YEAST)	MY0Va-c
Glycolate / glyoxylate metabolism	related to hydroxyacid oxidase	yes: B5RTR4 & Q6BR05(?)	yes	yes (B5RTR4)	PTS1 (SKL)	yes	yes
	related to hydroxyacid oxidase	yes (Q6BVL8)	yes	yes	PTS1 (AKL)	yes	yes
	IDH1	yes (Q6BUG8)	yes	no	No PTS	yes	yes
	Isocitrate dehydrogenase, IDP1/2	yes (Q6BPU8) & (Q6BND1)	yes	no	No PTS	yes	
	IDH2	yes (Q6BJ24)	yes	no	No PTS	yes	yes
	Citrate synthase	yes (B5RUK1)	yes	no	No PTS	yes (CIT2 is peroxisomal)	yes
	Malate synthase (MLS)	yes (B5RU08)	yes	yes	weak PTS1 (EKL)	yes (MLS1 is perox.)	no
	Malate dehydrogenase (MDH)	yes (Q6BM17 seems to be the peroxisomal one)	yes	yes (Q6BM17)	PTS1 (SKL) (Q6BM17)	yes (MDH3 is peroxisomal)	no
Mannosylerythritol lipid synthesis	MAC1	no				no	no
	MAC2	no				no	no
Lysine metabolism	LYS4	yes (Q6BM98)	yes	no	No PTS	yes	no
	LYS1 (Saccharopine dehydrogenase)	yes (Q6BUY2)	yes	no	No PTS	yes	yes
	PIPOX (sarcosine oxidase)	yes: Q6BN42, Q6BZA7, Q6BZB0, Q6BN43	yes	yes	only 2 of them: Q6BZB0:SHL, Q6BN43:PHL	no	yes (Q9P0Z9)
Purines and pyrimidines	Uricase	yes (Q6BYT1)	yes	yes	PTS1 (SKL)	no	no
	Xanthine dehydrogenase (XDH)	no				no	yes (P47989)
FA beta-oxidation	Acyl-CoA oxidase (ACOX, POX…etc)	yes: DEHA2C01078, DEHA2D17248, DEHA2D17204	yes	no	No PTS	yes	yes
	ACAD	yes (Q6BX30)	yes	yes	PTS1 (SKL)	no	yes
	ACAD11C	yes (Q6BQL2)	yes	yes	PTS1 (SKL)	no	yes
	AidB-like ACAD	no				no	no
	Related to ACAD with CytB5 domain	no				no	no
	CytB5 domain bearing ACAD	no				no	no
	Rel. to Enoyl CoA hydratase	no					
	Related to Enoyl-CoA Hydratase protein 3	no					
	MFE-2 like enoyl-CoA hydratase	no				no	
	3-Hydroxyacyl-CoA dehydrogenase type 2	no				no	yes
	Peroxisomal multifunctional enzyme MFE2	yes (Q6BYL5)	yes	yes	PTS1 (AKI)	yes (FOX2)	yes
	putative POT1- Acetyl CoA C Acetyltransferase (3-Ketoacyl-CoA thiolases)	yes: Q6BVV6, Q6BNX5, Q6BR82, Q6BM30(?)	yes	yes (except Q6BR82)	Q6BVV6 & Q6BNX5--> PTS2, Q6BM30-->SKL	yes (POT1)	yes (THIK)
	Sterol carrying protein x (SCPx)	no				no	yes
	SCP2-like protein A	yes (Q6BYJ2)	yes	yes	PTS1 (AKL)	no	no
	SCP2-like protein B	no				no	no
alpha oxidation	Alpha-methylacyl-CoA racemase (AMACR)	not sure		no	No PTS	no	yes
	Phytanoyl-CoA 2-hydroxylase peroxisomal (PHYH)	no ?				no	yes (O14832)
	2-hydroxyphytanoyl-CoA lyase / 2-Hydroxyacyl-CoA lyase 1 (HPCL2)	yes (B5RTJ8, Q6BXD8, Q6BHI3, Q6BSB5)	yes	no	No PTS	yes	yes (Q9UJ83): HACL1
	Fatty Aldehyde Dehydrogenase (ALDH3A2)	yes (Q6BIL7)	yes	no	No PTS	yes	yes
Saturation PUFAS	2,4-Dienoyl-CoA reductase (DECR2)	yes (Q6BVJ4) & (Q6BH12)	yes	yes	PTS1 (Q6BVJ4:NKL, Q6BH12: SKL)	yes (SPS19)	yes
	Delta3,5-Delta2,4-dienoyl-CoA isomerase	yes (Q6BML0: Delta3,5-Delta2,4-dienoyl-CoA isomerase)	yes	no	it has IKL which is not part of our PTS list.	yes (DCI1)	yes
	Rel. to Δ3,Δ2-enoyl-CoA isomerase ECI1	yes (Q6BQU9) & (Q6BZL5)	yes	no	Q6BQU9 has -HKM & Q6BZL5 has -NKM which are not part of our list	yes (ECI1)	yes
	3,2-Trans-enoyl-CoA isomerases / Rel. to Δ3,Δ2-enoyl-CoA isomerase ECI2	no				no	yes

FA-CoA deactivation / export	Peroxisomal Acyl CoA thioesterase (thioester hydrolase)	yes Q6BPV5 & (Q6BZL6, Q6BPV3, Q6BPV4 ?)	yes	yes	PTS1: Q6BPV5-->AKL , Q6BZL6--> PKL, Q6BPV3-->AKL, Q6BPV4-->YKL which is not part of the list	no	yes
	Hypothetical thioester hydrolase	no					
	Hypothetical thioester hydrolase	no					
	Hypothetical thioester hydrolase	no					
	Rel. to Short chain acyl-CoA synthetase 3	no					
	Rel. to Ectomycorrhiza-regulated esterase	no				yes	no
	Rel. to Ectomycorrhiza-regulated esterase	not sure				yes	
	Carnitine-O-acetyltransferase (CRAT)	yes (B5RTK8)	yes	yes	PTS1 (AKL)	yes (cat2)	yes
	Perox. carnitine O-octanoyltransferase (CROT)	no				no	yes (Q9UKG9)
omega-oxidation	Long chain fatty alcohol oxidase (FAO1)	yes (Q6BQL4)	yes	yes	PTS1 (ARL)	no	no
FA-CoA transport	Peroxisomal half ABC transporter PXA2	yes (Q6BWT7)	yes	no	No PTS	yes	yes
	Peroxisomal half ABC transporter PXA1	yes (Q6BUD3)	yes	no	No PTS	yes	yes
Fatty acid activation	Rel. to Long-chain-fatty-acid-CoA ligase 6	yes. 1) Q6BWM7, 2) Q6BSB7 3)Q6BSB6 4) B5RV06 5) Q6BWF8 come up as "Long Chain FA-CoA ligase" proteins. Not sure about Q6BJ16	yes	yes (except 3)	1) SKF, 2) PKL, 3) IRL which does not exist in our PTS list, 4) PKL, 5) SKL	yes	yes
	VLCFACS (FAT1)	yes (Q6BL99)	yes	yes	PTS1(AKL)	yes (FAT1_YEAST)	yes
	FACL2-like/long-chain fatty acid coA ligase	no				no	no
	PCS60 - AMP-binding protein, peroxisomal (PCS60: Oxalyl-CoA synthase)	no				yes	no
	Rel. to Acyl-CoA synthetase	yes. 2 "Acetate-CoA ligases" come up: Q6BQF2(ACS1) & Q6BS00(ACS2)	yes	no	No PTS	non-peroxisomal ACS1/ACS2?	yes
	Oleate induced Po lipid transfer protein (SCP2-domain containing protein)	no ?					
Other acyl activating enzymes	Related to 4-coumarate-CoA ligase 1	no				no	no
	Related to 4-coumarate-CoA ligase 1	no				no	no
	Related to 4-coumarate-CoA ligase 1	no				no	no
Etherlipid synthesis	Dihydroxyacetone phosphate acyltransferase/Glyceronephosphate O-acyltransferase (GNPAT/DHAPAT)	yes (Q6BWH4) - protein with GPAT/DHAPAT domains	yes	yes	PTS1 (AKL)	no	yes (O15228)
	Alkyldihydroxyacetonephosphate synthase (AGPS)	no				no	yes (O00116)
	acyl/alkyl DHAP reductase	yes Q6BKY3 & Q6BLR1(?)	yes	no	No PTS	yes (AYR1)	yes
	Fatty acyl-CoA reductase (FAR1/2)	no				no	yes
	Glycerol-3-phosphate Dehydrogenase (GPD1)	yes (Q6BM03)	yes	no	Weak PTS2 !	yes	yes
Oxygen metabolism / Oxidation redox equivalents	Related to Epoxide hydrolase 2	no				no	yes
	Related to Epoxide hydrolase 1	no				no	yes
	Similar to Epoxide hydrolase	no				no	
	Related to Glutathione S-transferase κ	no				no	yes
	Related to Glutathione S-transferase	no				no	
	Omega-class glutathione transferase (GTO1)	Q6BTR1 and Q6BTR2 (but not sure)	no	no	no PTS	yes	yes
	Catalase (CAT)	yes (Q6BLU7)	yes	no	No PTS	yes (CTA1)	yes
	Peroxiredoxin 1 (PRDX1)	no ?				no (but what about PRX1, mitochondrial?)	yes
	Peroxiredoxin 5 (PRDX5)	yes (Q6BP01, Q6BZD0, Q6BWX3, Q6BHK5)	yes	Q6BP01 & Q6BHK5	PTS1: Q6BP01-->AKL, Q6BHK5--> ERL. Q6BZD0 has SQI which are not part of our PTS list	yes	yes
	Superoxide Dismutase 1 (SOD1)	yes. O42724-->similar to SOD1 (there's also another SOD in Dh: Q6BQZ1-->sim. to ScSOD2 with PTS1!)	yes	no	No PTS	yes	yes
	Nitric oxide synthase 2 (NOS2)	no				no	yes (P35228)
	Copper chaperone of SOD1 (CCS)	yes (Q6BK66)	yes	no	No PTS	yes (CCS1)	yes (O14618)
	Cytochrome c peroxidase	yes Q6BKY9 & Q6BIB1 (but still not sure)	yes	no	No PTS	yes (CCP1)	no

Related to aminoacid metabolism	Cystathionine beta lyase (STR3)	yes (Q6BYU9)	yes	yes	PTS1 (PKL)	yes	no
	3-hydroxy-3-methylglutaryl CoA lyase (HMGCL)	no				no	yes
	Rel. to D-amino-acid oxidase (DAO)	yes (Q6BX17, Q6BPK9, Q6BH52)	yes	yes	Q6BX17-->SKL, Q6BPK9-->VKL, Q6BH52--> SKL	no	yes
	Alanine-glyoxylate aminotransferase (AGXT)	yes (Q6BQW6)	yes	no	No PTS	yes (AGX1)	yes
	D-aspartate oxidase (DDO)	no				no	yes
	Cytosolic aspartate aminotransferase (AAT2)	yes: Q6BQN8 with PTS1, Q6BV55(might be mitochondrial), Q6BXH3(sim. to mitochondrial AAT2 in humans), unnamed protein and Q6BXK3(sim. to cytosolic AAT2 in humans)	yes	only Q6BQN8	PTS1(SKL)	yes	yes
	Acetolactate synthase	yes (Q6BJI8)	yes	no	No PTS	yes	no
	Methylcrotonyl-CoA carboxylase beta chain	no				no	yes
	Rel. to fumarylacetoacetate hydrolase	yes (Q6BVP7, Q6BTI3, Q6BT05)	yes	no	No PTS	no	no
Cleavage of cofactors	Related to CoA diphosphatase (NUDT7)	yes (B5RTX4)	yes	no	No PTS	yes	yes
	Rel. to NADH pyrophosphatase NUDT12	yes (Q6BV93)	yes	yes	PTS1 (NKL)	yes	yes
	Rel. to Nudix motif 19 (NUDT19)	no				no	yes
Retinoid metabolism	Rel. to Short chain alcohol dehydrogenase-Dehydrogenase/reductase SDR 4	yes? (Q6BWS7, Q6BWI9)		yes	PTS1 Q6BWS7: AKF , Q6BWI9: AHL	no	yes
Proteases	Insulin degrading enzyme (IDE)	yes (Q6BZ22:insulysin)	yes	yes	PTS1(AHL)	yes	yes (P14735)
	Serine hydrolase-like protein 2 (SERHL)	no				no	yes (Q9H4I8)
	Peroxisomal LON protease-like (LONP)	yes (Q6BJJ8)	yes	no	It has YHL which is not part of our PTS list.	yes	yes
Phosphatases	2C protein phosphatase (PP2C family)	yes (Q6BY99)	good	yes	PTS1 (PKL)	yes (PTC5 with PRL?)	yes
	Histidine phosphatase domain containing protein	yes (Q6BZ00)	yes	no	No PTS	yes (TFC7)	no
L-Ascorbate synthesis	L-gulonolactone oxidase	Q6BZA0(?)	good ish	no	No PTS	no	no
Biotin synthesis	8-amino-7-oxononanoate synthase	no				no	no
Amine metabolism	polyamine oxidase, Cu containing	yes Q6BJ27, Q6BQS6(?)	yes	no	No PTS	no	yes
	Rel. to polyamine oxidase	A9E360 (Diacetylspermine oxidase) & Q6BZB9 (amine oxidase)	yes	no	No PTS	yes (FMS1)	
Carboxylesterases	Sim. to para-nitrobenzyl esterase	no ?				no	yes
Carbohydrate metabolism	Rel. to glucose 6 phosphate dehydrogenase	yes (Q6BUJ0)	yes	no	Dh version has GKM which is not part of our PTS list, but Um one has also GKM which they considered as PTS1!	yes	yes
	Probable fructose biphosphate aldolase	yes (Q6BRB0)	yes	no	Dh version has GQL which might be very rare PTS1, but Um one has also GKM which they considered as PTS1!	yes	no
	Glyceraldehyde-3-phosphate Dehydrogenase (Gapd)	yes (Q6BMK0)	yes	no	It has ASN which is not part of our PTS list	yes	yes
Misc. peroxisomal membrane proteins	ANT1	yes (Q6BQ51)	yes	no	No PTS	yes	no
	PXMP2	no				no	yes
	PXMP4	yes (Q6BNB7)	yes	no	No PTS	no	yes
	MPV17-like protein 2	Q6BMY0:SYM1 & Q6BMY1 are appearing as "PXMP/MPV family" proteins	yes	no		yes (SYM1 is appearing which is homolog of human mitochondrial MPV17)	yes (Q567V2)
	PMP47/PMP34	Q6BI42 (solute carrier family 25, peroxisomal adenine nucleotide transporter), member 17)	yes	no	No PTS	no	yes (O43808)
	PMP52 (TMEM135)	no				no	yes (Q86UB9)
	acbd5	2 potential ACB proteins were detected (Q6BKE4 & Q6BRC0)	no	no	No PTS	no	yes (Q5T8D3)
	MOSC2 (mARC)	no				no	yes (Q969Z3)
Perox. division	Fis1	yes (Q6BLG8)	no	no	No PTS	yes	yes
	Dnm1	yes (Q6BUC4)	yes	no	No PTS	yes	yes
	Caf4	no ?	no	no	No PTS	yes	no
	Vps1	yes (Q6BPN2)	yes	no	No PTS	yes	yes
Perox. Organisation	Djp1	yes Q6BQR2, Q6BW22(?)	no	no	No PTS	yes	yes
	Probable RHO1 GTP-binding protein	yes (Q6BWG4)	yes	no	No PTS	yes	yes

Alkyl nitronates oxidation	Related to 2-Nitropropane dioxygenase/ nitronate monooxygenase	yes (Q6BYZ6)	good ish	no	No PTS	yes	no
	Putative 2-Nitropropane dioxygenase/ nitronate monooxygenase	no					
Other proteins with PTS1 in Um or Hs	Acetoacetyl-CoA synthetase	no				no	yes
	gmc type oxireductase	no				no	yes
	betaine aldehyde dehydrogenase (ALD4)	not sure				yes (ALD4)	yes
	Soluble quinone reductase	yes Q6BK84(?)	yes	no	No PTS	yes	yes
	Uncharacterized short chain reductase (SDR)	yes (Q6BIV0) & Q6BTX3	yes	yes (Q6BIV0)	PTS1 (PKL)	no	no
	Related to 2-Dehydropantoate-2 reductase	yes Q6BQB8, Q6BQB9 & Q6BWX6(?)	yes	no	No PTS	yes	no
	Histidine triad protein	yes Q6BHX9(?)	yes	yes	weak PTS1 (EKL)	yes	yes
	Probable cytochrome b5	no?				yes	yes
	Phenol 2-monooxygenase	yes (Q6BTZ3)	yes	no	No PTS	no	no
	Zinc binding Alcohol Dehydrogenase (ZADH2: Prostaglandin reductase 3)	no ?				no	yes (Q8N4Q0-SKL)
	beta lactamase like protein 2	no				no	yes
	Ribonuclease UK114	B5RTI1 appears as UK114 protein family	yes	yes	PTS1 (PKL)	yes	yes
	Probable translation elongation factor eEF1β	yes (Q6BUE7)	yes	yes	PTS1 (QKL)	yes	yes
	Hydroxysteroid dehydrogenase-like 2	no ?				no	yes

Ones with putative PTS1- Uniprot code	Last 3 amino acids	predicted function based on Uniprot
sp|Q6BQZ1|SODM_DEBHA	SHL	SOD
tr|Q6BWH4|Q6BWH4_DEBHA	AKL	DHAPAT
tr|Q6BL99|Q6BL99_DEBHA	AKL	VLCFACS
tr|Q6BM16|Q6BM16_DEBHA	SKL	Rel. to beta-lactamase
tr|Q6BV81|Q6BV81_DEBHA	AKL	Acyl_CoA_N-acyltransferase
tr|Q6BT50|Q6BT50_DEBHA	AHF	tRNA ligase
tr|Q6BS18|Q6BS18_DEBHA	AHL	NAPDH dehydrogenase (old yellow enzyme) (EPB1)
tr|B5RSX8|B5RSX8_DEBHA	CKF	MFS domain containing protein
tr|Q6BX17|Q6BX17_DEBHA	SKL	DAO
tr|Q6BK75|Q6BK75_DEBHA	PRF	BUD23
tr|Q6BWM7|Q6BWM7_DEBHA	SKF	FAA - appears to be one of the homologs of ''long chain FA-CoA ligase'' of Um
tr|Q6BQL4|Q6BQL4_DEBHA	ARL	Long chain alcohol oxidase
tr|Q6BKY6|Q6BKY6_DEBHA	AKL	FAD_binding_3 domain-containing protein (appearing as ''salicylate hydroxylase'' in few other yeasts)
tr|Q6BSM6|Q6BSM6_DEBHA	PKL	Tyrosine Phosphatase 2 dom. containing protein
tr|Q6BVQ0|Q6BVQ0_DEBHA	SKL	PKS_ER domain-containing protein (appearing as ''alcohol dehydrogenase'' when blasted w/o organism)
tr|Q6BK61|Q6BK61_DEBHA	AKL	Glucosamine-6-Phosphate Isomerase
tr|Q6BZL6|Q6BZL6_DEBHA	PKL	Acyl_CoA_hydrolase - appears to be one of the homologs of ''Acyl CoA thioesterase'' of Um
tr|Q6BZ22|Q6BZ22_DEBHA	AHL	Metal ion binding, metalloendopeptidase activity - appears to be ''insulin degrading enzyme'' in Um

tr|Q6BQ10|Q6BQ10_DEBHA	SKL	AB (alpha beta) hydrolase
tr|Q6BHQ1|Q6BHQ1_DEBHA	AKL	ureidoglycolate hydrolase&lyase
tr|B5RTI1|B5RTI1_DEBHA	PKL	MMF1 - appears to be hom. of Um ''Ribonuclease UK114''
tr|Q6BTG8|Q6BTG8_DEBHA	SKL	Zinc containing alcohol dehydrogenase
tr|Q6BZE0|Q6BZE0_DEBHA	CKL	PALP domain cont. prot. (L-serine/L-threonine ammonia-lyase)
tr|Q6BY22|Q6BY22_DEBHA	CRL	uncharacterised protein
tr|Q6BH52|Q6BH52_DEBHA	SKL	D-aa-oxidase (DAO) & FAD binding
tr|Q6BUG6|Q6BUG6_DEBHA	CKL	Transmembrane
tr|B5RV06|B5RV06_DEBHA	PKL	Long chain fatty acid CoA ligase
tr|Q6BRH7|Q6BRH7_DEBHA	SKL	Glutathione S transferase
tr|Q6BN43|Q6BN43_DEBHA	PHL	DAO domain cont. prot. (appears to be PIPOX in humans)
tr|Q6BWF8|Q6BWF8_DEBHA	SKL	Long chain fatty acid CoA ligase
tr|Q6BX30|Q6BX30_DEBHA	SKL	ACAD11
tr|Q6BH12|Q6BH12_DEBHA	SKL	Peroxisomal 2,4-dienoyl-CoA reductase (SPS19)
tr|Q6BLK4|Q6BLK4_DEBHA	PKL	uncharacterised protein with ''Serine-type endopeptidase activity''
tr|Q6BYT1|Q6BYT1_DEBHA	SKL	urate oxidase activity (uricase)
tr|Q6BM29|Q6BM29_DEBHA	PRL	uncharacterised protein with unknown ''FL(I)LHE(L)TA'' domain
tr|Q6BPV5|Q6BPV5_DEBHA	AKL	acyl CoA hydrolase (it appears to be homolog of peroxisomal acyl coa thioesterase in Um)
tr|Q6BZN6|Q6BZN6_DEBHA	CHL	uncharacterized protein
tr|Q6BSB7|Q6BSB7_DEBHA	PKL	AMP-dependant synthetase/ligase (appears to be long chain coA ligase homolog of Um)
tr|Q6BWJ8|Q6BWJ8_DEBHA	AKL	Rel. to Carboxymuconolactone decarboxylase
tr|Q6BM30|Q6BM30_DEBHA	SKL	Acetyl CoA C-acetyltransferase
tr|Q6BIV0|Q6BIV0_DEBHA	PKL	Short chain dehydrogenase/reductase SDR (alcohol dehydrogenase)
sp|Q6BWQ9|CFD1_DEBHA	ARF	Cytosolic Fe-S cluster assembly factor CFD1
tr|Q6BL79|Q6BL79_DEBHA	PKF	membrane fusion protein Fig1 domain (for mating)
tr|Q6BWI9|Q6BWI9_DEBHA	AHL	Short chain dehydrogenase/reductase SDR (alcohol dehydrogenase)

tr|Q6BP18|Q6BP18_DEBHA	SKL	Cruciform cutting endonuclease 1 with Ydc2 catalyt domain
tr|Q6BP01|Q6BP01_DEBHA	AKL	Peroxiredoxin with PRX5-like dom (was entered as ''alkyl hydroperoxide reductase 1'' to KEGG)
tr|Q6BPV3|Q6BPV3_DEBHA	AKL	acyl CoA thioesterase
tr|Q6BQN8|Q6BQN8_DEBHA	SKL	Aspartate aminotransferase
tr|Q6BM17|Q6BM17_DEBHA	SKL	Malate dehydrogenase
tr|Q6BMV0|Q6BMV0_DEBHA	SKL	NADH & NAD+ kinase activity (involved in ox. Stress)
tr|Q6BPJ2|Q6BPJ2_DEBHA	PKL	uncharacterised protein
tr|Q6BWS7|Q6BWS7_DEBHA	AKF	Short chain dehydrogenase/reductase SDR
sp|Q6BMB8|TPIS_DEBHA	SRL	triosephosphate isomerase (TPI1)
tr|Q6BQL2|Q6BQL2_DEBHA	SKL	protein kinase - appears to be homolog of ACADc in Um
tr|Q6BVL8|Q6BVL8_DEBHA	AKL	FMN hydroxy acid dehydrogenase domain-containing protein - appearing as ''rel. to hydroxyacid oxidase'' homolog of Um
tr|Q6BK85|Q6BK85_DEBHA	PRL	uncharacterised protein with ''CBS (Cystathionine beta-synthase) domain''
tr|Q6BYU9|Q6BYU9_DEBHA	PKL	cystathione beta lyase /cysteine-S-conjugate beta-lyase
tr|Q6BZB0|Q6BZB0_DEBHA	SHL	DAO dom. cont. protein (seems to be eq. of PIPOX in humans)
tr|B5RTR4|B5RTR4_DEBHA	SKL	FMN dependent dehydrogenase, appearing as ''cyt b2'' on similar proteins) -appearing as ''related to hydroxyacid oxidase'' homolog of Um
tr|B5RTK8|B5RTK8_DEBHA	AKL	carnitine O-acetyltransferase (CAT2)
tr|Q6BUP2|Q6BUP2_DEBHA	PKL	Hotdog acyl-CoA thioesterase
tr|Q6BL21|Q6BL21_DEBHA	SKF	FMN binding & NAD(P)H dehydrogenase activity
tr|Q6BYJ2|Q6BYJ2_DEBHA	AKL	oleate ind. POX18/ SCP2 sterol binding protein
tr|Q6BX51|Q6BX51_DEBHA	SKF	snRNA assoc. LSM4
tr|Q3V7I3|Q3V7I3_DEBHA	SRL	Pyridoxal-phosphate dependent enzyme
tr|Q6BY99|Q6BY99_DEBHA	PKL	protein phosphatase type 2C- appears to be ''PP2C'' in Um
tr|Q6BQ11|Q6BQ11_DEBHA	PKL	AB (alpha beta) hydrolase
tr|Q6BTC7|Q6BTC7_DEBHA	SKL	uncharacterised protein

tr|B5RUK5|B5RUK5_DEBHA	SKF	protein kinase with DUF3698 domain (domain of unknown function)
TPC1_DEBHA	KKL	Mitochondrial thiamine pyrophosphate carrier 1 (TPC1)
B5RTD1_DEBHA	NRL	MFS dom. Containing protein
Q6BH85_DEBHA	NRL	uncharacterized prot.
Q6BIE8_DEBHA	NKL	Single-strand telomeric DNA-binding protein
Q6BKG4_DEBHA	KKL	NUC173 dom. cont. protein
Q6BL12_DEBHA	VKL	Ubiquitin activating enzyme 1 (Uba1)
Q6BME8_DEBHA	NRL	membrane protein with Sur7 domain
Q6BP06_DEBHA	KKL	TPT dom. cont. protein
Q6BPK9_DEBHA	VKL	D-aminoacid oxidase (DAO)
Q6BQ53_DEBHA	NKL	DBR1 dom. cont. protein
Q6BR74_DEBHA	KKL	lysosome-related (with ''BLOC1 domain'')
Q6BS76_DEBHA	VKL	2-methoxy-6-polyprenyl-1,4-benzoquinol methylase (COQ5)
Q6BS82_DEBHA	QKL	Acyl carrier protein
Q6BUE7_DEBHA	QKL	Glutathione S-transferase, C-terminal domain (seems to be homolog of Um trans. elong. factor 1 beta)
Q6BV93_DEBHA	NKL	NADH pyrophosphatase - appears to be homolog of ''NUDX hydrolase NUDT12'' in Um
Q6BVI9_DEBHA	VKL	NAD(P)H-hydrate epimerase
Q6BVJ4_DEBHA	NKL	NAD(P)-binding domain (2,4-dienoyl CoA reductase SPS19 in other yeasts)
Q6BWE0_DEBHA	QKL	Doa1 protein
Q6BWV3_DEBHA	KKL	Rho GTPase-activating protein domain cont. prot.
W0TYT8_DEBHA	KKL	RING type dom. cont. prot.
Q6BRI8_DEBHA	SSL	MFS dom. Containing protein
Q6BZD7_DEBHA	SSL	Nuclear pore protein
Q6BI65	PRI	Methionine aminopeptidase
Q6BKY4	AKI	lipase?
Q6BWC8	SKI	TCA cycle enzyme?
Q6BYL5	AKI	fox2 (peroxisomal)
B5RU08	EKL	mls1
Q6BHK5	ERL	peroxiredoxin-like

Q6BHX9	EKL	Adenosine 5'-monophosphoramidase - appears to be homolog of "histidine triad protein" in Um
Q6BZF7	EKL	cyanamide hydratase
Q6BI20	SQL	enolase
Q6BIM4	AVL	Glutaredoxin domain-containing protein
Q6BK62	AAL	N-acetylglucosamine-6-phosphate deacetylase
Q6BMH3	SNL	FSH1(fam. of serine hydrolase) - domain-containing protein
Q6BWU1	ANL	CoA_binding domain-containing protein
Q6BLB9	EKL	26S protease subunit RPT4

the ones with PTS2 motif-Uniprot code	PTS2 sequence	PTS2 position	Predicted function based on uniprot
ATG23_DEBHA	RIQEVAEQL	811-819	ATG23
OCA5_DEBHA	RLVLVLLHA	325-333	Oxidant-induced cell-cycle arrest protein 5
XRN2_DEBHA	RQMRISDQL	258-266	5'-3' exoribonuclease 2 (RAT1)
B5RTU5_DEBHA	RQDVLALQL	1658-1665	1-phosphatidylinositol 4-kinase
ALG11_DEBHA	RLTNIASQL	653-661	Ubiquitin protein ligase binding
B5RUS9_DEBHA	RIPTLAIHL	158-166	metalloaminopeptidase & zinc Binding
B5RUT6_DEBHA	RLLSLLNHL	418-426	BEACH (Beige and Chediak-Higashi) domains, implicated in membrane trafficking
B5RV40_DEBHA	RLGEI APHL	636-644	NADH-ubiquinone oxidoreductase
Q6BHC4_DEBHA	RIVKIANQL	255-263	succinate/fumarate antiporter
Q6BJE5_DEBHA	RLFNHSYHL	440-448	not specified anywhere
Q6BJK1_DEBHA	RVLGVSTHL	168-176	Ribosome biogenesis BMS1 & ATP and GTP binding
INO80_DEBHA	RLMQQSTQA	349-357	Chromatin remodelling ATPase INO80
MAD1_DEBHA	KLNSISEQL	176-184	Spindle assembly checkpoint component MAD1
MED14_DEBHA	KLYLIARQL	363-371	Mediator of RNA polymerase II transcription subunit 1
NU4LM_DEBHA	KIIYLGGQF	35-43	NADH-ubiquinone oxidoreductase chain 4L
PBN1_DEBHA	KLRIQLNQF	52-60	PBN1
Q6BKI0_DEBHA	RVTKLLRHL	9 and 17	Dihydrofolate synthetase
Q6BLU5_DEBHA	RLTFLAIHL	7 and 15	transmembrane
Q6BNW5_DEBHA	RLALILNQL	1122-1130	zinc ion binding
Q6BNX5_DEBHA	RLNQLSGQL	3 and 11	3-ketoacyl-CoA thiolase (POT1) (peroxisomal)
Q6BP56_DEBHA	RLAQLLRQL	709-798	26S proteasome regulatory subunit RPN1
Q6BPF4_DEBHA	RLVVVLSQA	37-45	rRNA small subunit methyltransferase NEP1, EMG1
Q6BRE3_DEBHA	RQSFISSQL	11 and 19	Sod_Fe_C domain-containing protein
Q6BSI8_DEBHA	RVKVHLDQA	21 and 29	60S ribosomal protein L13
Q6BSW2_DEBHA	RQSHISLQA	808-816	Actin binding protein (Myo2)
Q6BUA4_DEBHA	RLMRLLPHA	577-585	Prot. Kinase (has Ser/Tyr kinase domain)
Q6BUI6_DEBHA	RVVPVGVHL	220-228	Prot. Kinase (Tyr kinase)
Q6BUI7_DEBHA	RVVPVGVHL	220-228	Prot. Kinase (Tyr kinase)
Q6BVV6_DEBHA	RLNQVLGHL	3 and 11	3-ketoacyl-CoA thiolase (POT1) (peroxisomal)
Q6BX65_DEBHA	RLQLHLRQA	706-714	Protein phosphatase binding
Q6BZA3_DEBHA	RIGYIAQHA	820-828	ATPase &nucleus binding, ABC transporter
ALG11_DEBHA	RVLWQAVQA	130-138	Alpha-1,2-mannosyltransferase ALG11
CCR4_DEBHA	RQKTQGRQL	304-312	Glucose-repressible alcohol dehydrogenase transcriptional effector
DDI1_DEBHA	KVNGVLVQA	214-222	DNA Damage Inducible protein (DDI1)
GRPE_DEBHA	KVDPIGEQF	186-194	GrpE mitochondrial

INO80_DEBHA	RLMQQSTQA	349-357	Chromatin remodelling ATPase INO80
MAD1_DEBHA	KLNSISEQL	176-184	Spindle assembly checkpoint component MAD1
MED14_DEBHA	KLYLIARQL	363-371	Mediator of RNA polymerase II transcription subunit 14
NU4LM_DEBHA	KIIYLGGQF	35-43	NADH-ubiquinone oxidoreductase chain 4L
PBN1_DEBHA	KLRIQLNQF	52-60	PBN1
PEX3_DEBHA	KLANLLAQL	363-371	Pex3
RL44_DEBHA	KQKGQALQF	98-106	60S Ribosomal protein L44
ROK1_DEBHA	KIGILSKQL	217-225	ATP-dependent RNA helicase ROK1
SWR1_DEBHA	KVLDILEQF	1359-1367	Helicase SWR1
B5RSZ6_DEBHA	KQMVIGPHL	52-60	Related to N-lysine methyltransferase EFM1
B5RTD1_DEBHA	KILPHKYHA	442-450	transmembrane
B5RTD3_DEBHA	KQHLLKGHF	683-691	Sfi1 (spindle body duplication related)
B5RTE2_DEBHA	KLAVVGAHL	484-492	biotin carboxilase / urea carboxilase
B5RTF4_DEBHA	RIVILAEQF	184-192	L-aminoadipate-semialdehyde dehydrogenase /LYS2
B5RTH2_DEBHA	KIIKILNQL	445-453	RNA binding prot. (has K homology domain)
B5RTK7_DEBHA	RQLSQSSQL	76-84	RFX-type winged-helix domain-containing protein (DNA binding)
B5RTS2_DEBHA	RLMEQLKQL	791-799	Uncharacterised protein
B5RTU0_DEBHA	RQEHLKRHF	767-775	nucleic acid binding (has C2H2 type domain)
B5RU12_DEBHA	KIKLLKFQL	169-177	it has Vacuolar prot. Sorting-assoc. domain Vta1
B5RU38_DEBHA	KVNGLLIQL	133-141	Formate_THF_ligase
B5RU84_DEBHA	RIFRQGVHF	274-282	it has Nucleotide-diphospho-sugar transferases dom.
B5RUA9_DEBHA	KLYLQLNQL	348-356	it has TPR domain
B5RUB6_DEBHA	RIDQQKQQA	341-349	ribosome LS & tRNA binding
B5RUJ5_DEBHA	KLKSILPHA	224-232	it has SH3 domain
B5RUM4_DEBHA	RISRQLPQL	2094 - 2102	Serine/threonine-protein kinase TOR
B5RUX9_DEBHA	RLLNLKDQL	53-61	holo-[acyl-carrier-protein] synthase & 4-PPantetheinyl_Trfase_dom. containing protein
B5RV00_DEBHA	KLEELKVQA	632-640	Sda1
B5RV52_DEBHA	RQHPVSVHF	664-672	Ecm16 (n. acid binding &helicase activity)
Q6BGP8_DEBHA	RLFK LANQF	417 - 425	beta-galactosidase complex
Q6BHB5_DEBHA	KIDELKP QF	14 - 22	Cys-Gly metallodipeptidase DUG1
Q6BHC2_DEBHA	Kqarhkgql	297 - 305	Ubiquitin carboxyl-terminal hydrolase
Q6BIN4_DEBHA	RLGDIKIQL	282 - 290	protein which has Arrestin C domain
Q6BJ64_DEBHA	KLATILPQF	378 - 386	it has TPR domain
Q6BJH6_DEBHA	RIPTLAPHF	206 - 214	metalloaminopeptidase activity w/ M18 domain
Q6BJL1_DEBHA	RLDALKTQA	671 - 679	Structural maintenance of chromosomes protein (SMC)
Q6BJV0_DEBHA	KISDLADHL	575 - 583	it has DNA binding and transcription factor domain
Q6BK45_DEBHA	KLEEHKNQL	65 - 73	BSD domain-containing protein
Q6BK50_DEBHA	KLYGVANHF	851-859	thiol-dependent ubiquitinyl hydrolase
Q6BK70_DEBHA	RIAYIKQHA	738-746	nucleotide binding (it has ABC transporter & elongation factor 3 domain)
Q6BKU6_DEBHA	KIPKLAEHF	215-223	prot. w/ aminopeptidase/ metallopeptidase domain
Q6BL63_DEBHA	KIGFLSLQF	674-682	protein with Symplekin/Pta1 domain
Q6BLN3_DEBHA	KIRNVKSHL	98-106	formamidopyrimidine-DNA glycosylase (FPG_CAT domain-containing protein)
Q6BLR9_DEBHA	RLFEQALHA	631-639	structural constituent of nuclear pore (Nup188)
Q6BM88_DEBHA	KVDSILPHL	242-250	phosphatidylinositol binding
Q6BMB5_DEBHA	RVYEIGRQF	321-329	Lysine--tRNA ligase (Lysyl-tRNA synthetase)
Q6BME1_DEBHA	KQPDLLHQL	429-437	DNA binding prot. w/ JmjC domain (which is involved in histone demetylation)
Q6BMH2_DEBHA	KLNELKIQF	369-377	protein w/ TATA element modulatory factor 1 (TMF1) domain
Q6BMN6_DEBHA	RIAILKDHA	457-465	Acyl-CoA desaturase
Q6BNU5_DEBHA	KIIEISSQL	329-337	Protein arginine methyltransferase NDUFAF7
Q6BNV2_DEBHA	RLLDQLQQL and KLNALKAQF	1465-1473 and 1697- 1705	protein import into nucleus via TPR/MLP1 domain
Q6BP04_DEBHA	KLILVALQL	112-120	YCF-like potein w/ ABC transporter domain
Q6BPD4_DEBHA	KVQRQAIQL	46-54	Ribosomal_L14e domain-containing protein
Q6BPE2_DEBHA	KIANQLSQF	73-81	Uncharacterised protein
Q6BQN1_DEBHA	KLEAQLAHA	237-245	Chorismate synthase
Q6BQS9_DEBHA	KISTIKSHY	7 and 15	Pyr_redox_2 domain-containing protein
Q6BR66_DEBHA	KLENLAKQF	274-282	Phytanoyl-CoA dioxygenase family protein
Q6BSG7_DEBHA	KQPEIGVQAI	206-214	Elongation factor Tu
Q6BSQ9_DEBHA	KLMKIKKQL	112-120	Uncharacterised protein
Q6BTR0_DEBHA	RLDVLKRHL	299-307	N. acid binding prot. w/ ZnF_C2H2 domain

Q6BUA4_DEBHA	KIQDILAQL and RLMRLLPHA	496-504 and 577-585	protein kinase with Ser/Thr kinase dom.
Q6BUG0_DEBHA	RQLELKKQL	173-181	Translation Initiation Factor activity
Q6BUG9_DEBHA	KLQYQKFQA	36-44	mitochondrial proton-transporting ATP synthase complex assembly
Q6BUR1_DEBHA	KVVLLKSQA	561-569	Elongator complex protein 1
Q6BV02_DEBHA	KLPLLSHHA	112-120	transmembrane
Q6BV20_DEBHA	KINELKQQL	424-432	Protein with Rab-GTPase_TBC_sf domain
Q6BV48_DEBHA	KLDKLKTQL	268-276	soluble NSF attachment protein
Q6BV66_DEBHA	KLERIKDHL	57-65	26S protease regulatory subunit 4
Q6BVL9_DEBHA	RLAHLSAQF	371-379	oxireductase (has Aldehyde dehydrogenase domain)
Q6BVM6_DEBHA	RIKLILKHF	248-256	chromatin binding & remodelling
Q6BVN6_DEBHA	KIDKLLSQL	1226-1234	structural constituent of nuclear pore
Q6BWT2_DEBHA	KVTEQKLQA	218-226	ER to Golgi vesicle-mediated transport
Q6BXB7_DEBHA	KIDYLKFQF	61-69	54S ribosomal protein L31, mitochondrial
Q6BYB7_DEBHA	RLQAQGTHA	471-479	transmembrane transport
Q6BYD4_DEBHA	KVSAISAHF	1600-1608	prot. w/ Glutamine amidotransferase type-1 and ATP-grasp domain
Q6BYL0_DEBHA	RLTYILSHF	157-165	delta24(24-1) sterol reductase
Q6BYL5_DEBHA	KVNAVAPHA	491-499	3-hydroxyacyl-CoA dehydrogenase & enoyl CoA hydratase (peroxisomal hydratase-dehydrogenase-epimerase)
Q6BYS5_DEBHA	KLALLSLHA	131-139	1,3-beta-D-glucan synthase
Q6BZ81_DEBHA	RLIYHGEQF	52-60	Coatomer subunit gamma (SEC21)
Q6BZA3_DEBHA	RIGYIAQHA	820-828	nucleotide binding (it has ABC transporter & chromo domain)
Q6BZG4_DEBHA	KVVAQASQF	253-261	

Appendix 3- The promoter, terminator, selectable marker and fluorescent marker sequences that were used in this study and mentioned in Chapter 5.

Insert name	DNA sequence	Present in	Source
S. stipitis TEF1 promoter	GGAATGATCCAGAGGCGCGACATTTATGCAGACAATTTGTGTTTTGTCGCAAAC GATGTTATAGCGAAATTTTTCACTCTGTCAGATAAATGGATTTTGTCAAAAGGGG GAAGTAGAAGGAGAATGGGCCCGAGATGTTCTGCCAAATTCTCAGTAGCATAAT GTGAAAGAAGCCCTTACATTGTCCAGCCTCTGGCATCATTAAAAACCGTAGCGG AAACCAATTGTCTCTGTTCTTCCCTGGCACACCCTGGTAGCCCCATCCAGTTGTAG TACATCTCACACGCTGGCAACTTGGGACAATCAGCAACTTTTTTTCTTTTAATTTT TTCAGCGCGACATTTTGCCTCTTCTGCGAGAACAGACTTTTTCACCTCCATCTCAC CCCCCTTTGCACTTATATAAATTGGACCAGTTCCTCCCATTGTAGAAAAAATTTTG CTGGACCTTTTTCTCTTTTTTTTGTCCTTTAGTTTCATACAATCTAAGTCTATCTACA	pDh1, pSLV38, pSA5	This study
S. Stipitis TEF1 terminator	GCTGATTAATTTACGTATATTCAGTTTAATATCAATACGTTAGCTACATTTCCAAT GAACGATACTAGATATTGTTTAGGATTATTGAACTGGTATAGATAATTTTAGTGT ATATTCATGTACTTGATAAATGTAATAATATGTGAAAATGTAGTTGTACATTAACT GATAGACAACATGCTGGAGTATATGGCATTAAGGTTGCTACAAAGTAGAAGCAA CCTAGACACACCTCAGAAGATAGATTGGG	pDh1, pSLV38, pSA5	This study
S. Stipitis ACT1 promoter	AAGTTCCGAGCTTCAGCAAACGCTTGTGTGGAAAGCTCCACCAGTGCTAAGGTG GAGTCGGGTTGGGGAAATGTCGCGAACGACACAATTTTTCAGCTCAGACGGCAC CCCACCAAAAGAATGATAGCAGATAGCCTGGAGAGAGCCCAGATCAGCCAAAG AATAGCACTAATATACAAATAATACGAAACCCCAAAATACGACATTGTCCTCCCT TATACACACAGATGTGGGCTATTTGTGGATGCCAAAATATACCCAATCATGTCGC TATCTAGTGTCTTTTGACTTATCTTCCACATTGTTCCCTCTGTGTAGCATGAGCACT CAGCAATGTCGCGTGTCGTGCAAATTTTTCCTTGTGTGCGACTTTCCCACCCACCG ATATTTATAACCAACGCAGTTTTTCTTTTCGTGAGCACAATCCCCTTTTCTTCTTTT TTCAGTAGGTTTCTGTaatattagtacaatcccttatattataatcatatagatcaaac	pDh2, pSA4, pSLV35, pSLV37	This study

S. Stipitis ACT1 terminator	Aaccacttgcaaaatcctttgtattcttgttctgcaaacattttgtccaatctcttatctttctacgatgttgaa gaacatacatttttgttagtccagcttgttatccttttttttattaaataaaaaattttattgttaaagttgttttt cttctttgtctgtcctgttttaactcatatatattctatatattacagaaagaaagtagatcatctaaaataaa catttatttgatgAGACAAAGTAGGTTTTTTAGAATACAATGTAGCATCCTCTAATATA CAATAGAGTTGTTTTATAAAAGCGATACATTTAATATTATGACAGGACTGGTGAA GTGTATAGAATTGTGCTAATCTGGCAAACGAACCCAAGAAGACGTTAAAGCAAA TAGTGCA	pDh2, pSA4, pSLV35, pSLV37	This study
S. Stipitis GPD1 promoter	ATCTGATGTCTCAAATAAGGTATCAAGACAACGAATCAATGATCAACCAAGAAA GATTATTAGAGAAATTGGATGGATCAGCTGTGCTTGTGGAAACACTGATACGAC ATGCCAGTAAACGAAGTAGAAAAAACTAACTGTATATTCGCTAACAAAAAAATT GTATTATTTTTAGACATCGTAAATGGGGCTGTAGCCCTAATTATTTTTCATTTCTC GTGATCTGCACGTGTACTGTTGATTTTTTTGTGCGATTGAAATTATATTGTGCTGT TATCTTAATAAAATCAGTCATACCTTTTTTTTTTTGGGTTTTTGTTGTTTAATTTGT GATAAACATCCCATGAGGAACAGCGAGAAAGTTTTTTGCTGTTCACTTTCTCGTT CAACTTTTGCAAAGTAAAGTAAAGAAAAAAAAATTTTCCCTCGTCATCTTGATTTT TACTTCTTCTTCTTCTTCTTCTTTTTCCTTTCTTCACACATTATAGTCATAATCAATC	pSLV37	This study
S. Stipitis GPD1 terminator	TTCTCCATTTTTATAAATCCTACGGTTGCATATATATAGGGAAATAGCTTAATAGC CGGGTATAGTACATAATCTTATTTATAATTAGACTTTTTGAGGGATTCACATTTTT CTGGGTGCCAAACTCCAAAACCATTATATTATAGTGATGTGCATGACTTTTGAAG ACTGCTCTCCCCACAATGAGGTGTTACTCGGCAATCCAACCAATCACACAACCTG TGCTCATTTATATTCATTGACACTTGTA	pSLV5, pSLV35, pSLV37, pSLV38	This study
CTG-adapted hygB^r	ATGGGTAAAAAGCCTGAACTCACCGCGACGTCTGTCGAGAAGTTTCTAATCGAA AAGTTCGACAGCGTCTCCGACCTAATGCAGCTCTCGGAGGGCGAAGAATCTCGT GCTTTCAGCTTCGATGTAGGAGGGCGTGGATATGTCCTACGGGTAAATAGCTGC GCCGATGGTTTCTACAAAGATCGTTATGTTTATCGGCACTTTGCATCGGCCGCGC TCCCGATTCCGGAAGTGCTTGACATTGGGGAATTTAGCGAGAGCCTAACCTATT GCATCTCCCGCCGTGCACAGGGTGTCACGTTGCAAGACCTACCTGAAACCGAAC TACCCGCTGTTCTACAGCCGGTCGCGGAGGCCATGGATGCGATCGCTGCGGCCG ATCTTAGCCAGACGAGCGGGTTCGGCCCATTCGGACCGCAAGGAATCGGTCAAT ACACTACATGGCGTGATTTCATATGCGCGATTGCTGATCCCCATGTGTATCACTG GCAAACTGTGATGGACGACACCGTCAGTGCGTCCGTCGCGCAGGCTCTCGATGA GCTAATGCTTTGGGCCGAGGACTGCCCCGAAGTCCGGCACCTCGTGCACGCGGA TTTCGGCTCCAACAATGTCCTAACGGACAATGGCCGCATAACAGCGGTCATTGAC TGGAGCGAGGCGATGTTCGGGGATTCCCAATACGAGGTCGCCAACATCTTCTTC TGGAGGCCGTGGTTGGCTTGTATGGAGCAGCAGACGCGCTACTTCGAGCGGAG GCATCCGGAGCTTGCAGGATCGCCGCGGCTCCGGGCGTATATGCTCCGCATTGG TCTTGACCAACTCTATCAGAGCTTGGTTGACGGCAATTTCGATGATGCAGCTTGG GCGCAGGGTCGATGCGACGCAATCGTCCGATCCGGAGCCGGGACTGTCGGGCG TACACAAATCGCCCGCAGAAGCGCGGCCGTCTGGACCGATGGCTGTGTAGAAGT ACTCGCCGATAGTGGAAACCGACGCCCCAGCACTCGTCCGAGGGCAAAGGAAT AA	pDh1, pSLV38, pSA5	This study
CTG-adapted G418^r	atgggtaaggaaaagactcacgtttcgaggccgcgattaaattccaacatggatgctgatttatatgggta taaatgggctcgcgataatgtcgggcaatcaggtgcgacaatctatcgattgtatgggaagcccgatgcg ccagagttgtttctaaaacatggcaaaggtagcgttgccaatgatgttacagatgagatggtcagactaaa ctggctaacggaatttatgcctcttccgaccatcaagcattttatccgtactcctgatgatgcatggttactc accactgcgatccccggcaaaacagcattccaggtattagaagaatatcctgattcaggtgaaaatattgt tgatgcgcttgcagtgttcctacgccggttgcattcgattcctgtttgtaattgtccttttaacagcgatcgcg tatttcgtctcgctcaggcgcaatcacgaatgaataacggtttggttgatgcgagtgattttgatgacgagc gtaatggctggcctgttgaacaagtctggaaagaaatgcataagctattgccattctcaccggattcagtc gtcactcatggtgatttctcacttgataaccttatttttgacgaggggaaattaataggttgtattgatgttgg acgagtcggaatcgcagaccgataccaggatcttgccatcctatggaactgcctcggtgagttttctccttc attacagaaacggctttttcaaaaatatggtattgataatcctgatatgaataaattgcagtttcatttgatg ctcgatgagtttttctaa	pDh2, pSA4, pSLV35, pSLV37	This study
CTG-adapted GFP	ATGAGTAAAGGAGAAGAACTTTTCACTGGAGTTGTCCCAATTCTTGTTGAATTAG ATGGTGATGTTAATGGGCACAAATTTTCTGTCAGTGGAGAGGGTGAAGGTGATG CAACATACGGAAAACTTACCCTTAAATTTATTTGCACTACTGGAAAACTACCTGTT CCATGGCCAACACTTGTCACTACTTTCACTTATGGTGTTCAATGCTTTTCAAGATA CCCAGATCATATGAAACGGCATGACTTTTTCAAGAGTGCCATGCCCGAAGGTTAT GTACAGGAAAGAACTATATTTTTCAAAGATGACGGGAACTACAAGACACGTGCT GAAGTCAAGTTTGAAGGTGATACCCTTGTTAATAGAATCGAGTTAAAAGGTATT GATTTTAAAGAAGATGGAAACATTCTTGGACACAAATTGGAATACAACTATAACT CACACAATGTATACATCATGGCAGACAAACAAAAGAATGGAATCAAAGTTAACT TCAAAATTAGACACAACATTGAAGATGGAAGCGTTCAACTAGCAGACCATTATC	pSA5, pSLV38	Defosse *et al.* (2018)

	AACAAAATACTCCAATTGGCGATGGCCCTGTCCTTTTACCAGACAACCATTACCT ATCCACACAATCTGCCCTTTCGAAAGATCCCAACGAAAAGAGAGACCACATGGT CCTTCTTGAGTTTGTAACAGCTGCTGGGATTACACATGGCATGGATGAACTATAC AAA		
CTG-adapted mCherry	ATGGTTTCAAAAGGTGAAGAAGATAATATGGCTATTATTAAAGAATTTATGAGA TTTAAAGTTCATATGGAAGGTTCAGTTAATGGTCATGAATTTGAAATTGAAGGTG AAGGTGAAGGTAGACCATATGAAGGTACTCAAACTGCTAAATTGAAAGTTACTA AAGGTGGTCCATTACCATTTGCTTGGGATATTCTGTCACCACAATTTATGTATGGT TCAAAAGCTTATGTTAAACATCCAGCTGATATTCCAGATTATTTAAAATTGTCATT TCCAGAAGGTTTTAAATGGGAAAGAGTTATGAATTTTGAAGATGGTGGTGTTGT TACTGTTACTCAAGATTCATCATTACAAGATGGTGAATTTATTTATAAAGTTAAAT TGAGAGGTACTAATTTTCCATCAGATGGTCCAGTTATGCAAAAAAAAACTATGG GTTGGGAAGCTTCATCAGAAAGAATGTATCCAGAAGATGGTGCTTTAAAAGGTG AAATTAAACAAAGATTGAAATTAAAAGATGGTGGTCATTATGATGCTGAAGTTA AAACTACTTATAAAGCTAAAAAACCAGTTCAATTACCAGGTGCTTATAATGTTAA TATTAAATTGGATATTACTTCACATAATGAAGATTATACTATTGTTGAACAATATG AAAGAGCTGAAGGTAGACATTCAACTGGTGGTATGGATGAATTATATAAA	pSLV35, pSLV37	
MgACT1 promoter	ACCCGCTCTTGACGGTTACCCAATGCGGTTATAAGCCAACAGTCTGTTGTGCGAC TAGGCTCGCTTGGCACCTGCACAGATGCTGCGACAGCTCTCACGCACAGAAATG GTCACCTAGAGTCGATTTCCGCGCCTCGTTGCCGCCGGTCTCCGCGCGGTGAATC CTGTACATAGTCATCTCCGATTCACTTTCACTAGACGAATCCGGCACATGAGTGA TCCGGCGTGCACACAATAGCAATCTCCCTGCACACACCGGGACGCGATTGCCGG GTAATCCCTGGTTGGGTCGTTTCTGCCTCGTTGTTTGATACCAGCGCTCACCCCTT TCGAAAAATTTACTTTTGACTAGGTATTAATATAGTATAGCAAA	pSA5, pSLV35	

Appendix 4- The PCR verifications of gene deletions in *D. hansenii*. The PCR validations of *GPD1* and *MDH3* deletions in the *gpd1/mdh3/pmp47Δ*, *gpd1/mdh3/npy1Δ* and *gpd1/mdh3/pmp47bΔ* cells (not shown), as well as the validation of *GPD1* deletion in *gpd1/mdh3Δ* cells (not shown) were done with the same principle as the appropriate PCRs that were shown below (shown for *gpd1Δ* and *mdh3Δ* cells only). Similarly, *PMP47* and *PMP47b* deletions (using hygB^r and G418^r respectively) in *pmp47/pmp47bΔ* cells (not shown) were done with the same principles as the appropriate PCRs described above, that were shown for *pmp47Δ* and *pmp47bΔ* cells only.

PCR check	Schematic representation	Gel Picture
GPD1::*SAT1* (in newly-generated *gpd1Δ* cells), replacement of *GPD1* ORF with *SAT1*	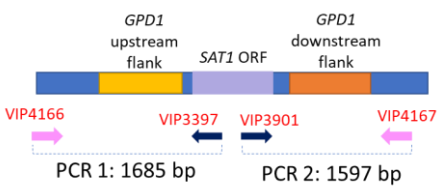	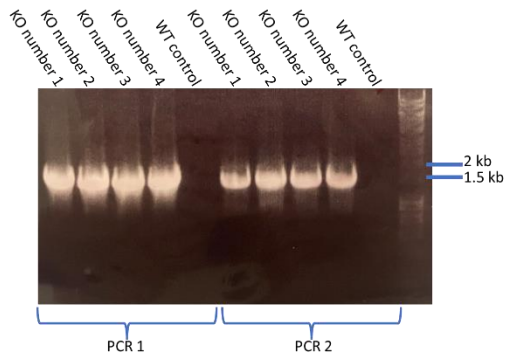

GPD1::*SAT1* (in newly-generated *gpd1Δ* cells), absence of *GPD1* ORF	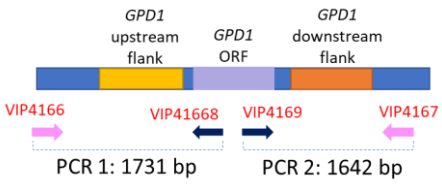	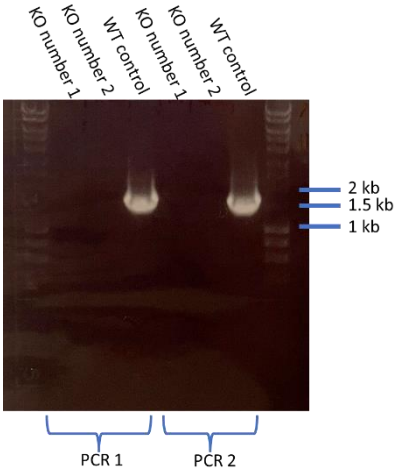
MDH3::*hygB*^{r} (in newly-generated *mdh3Δ* cells), replacement of *MDH3* ORF *hygB*^{r}	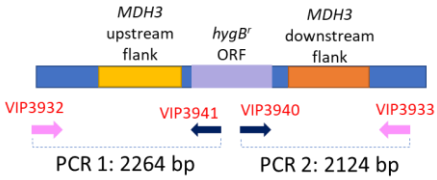	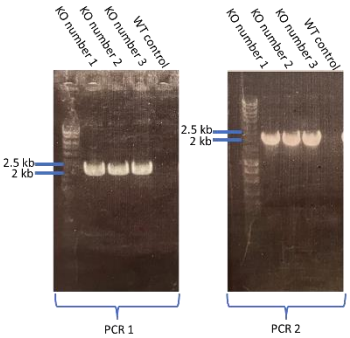
MDH3::*hygB*^{r} (in newly-generated *mdh3Δ* cells), absence of *MDH3* ORF	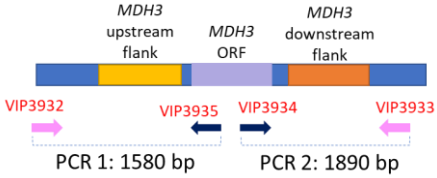	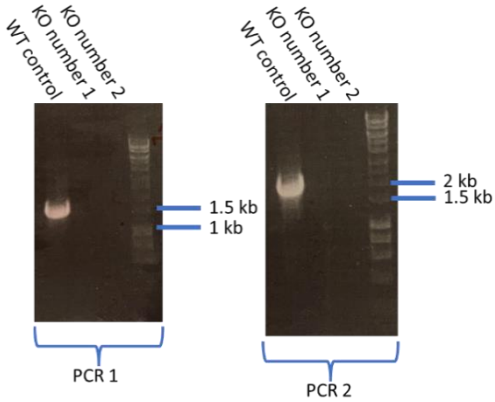

PMP47::*hygB*^{r} (in newly-generated *pmp47Δ* cells), replacement of *PMP47* ORF with *hygB*^{r}	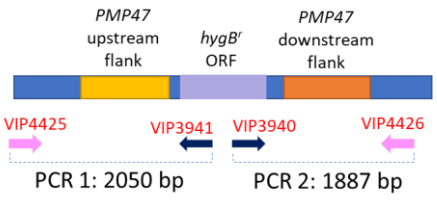	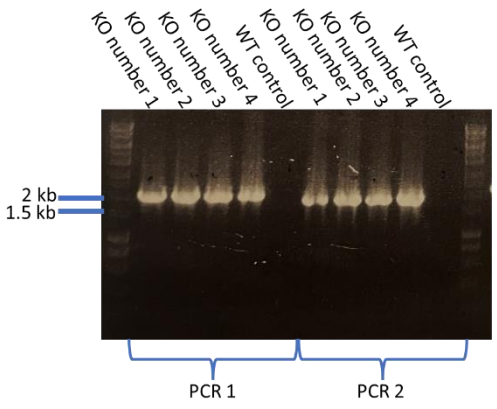
PMP47::*hygB*^{r} (in newly-generated *pmp47Δ* cells), absence of *PMP47* ORF	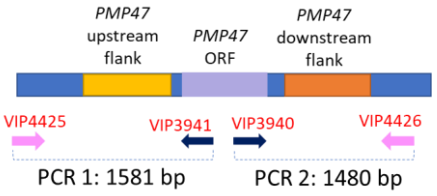	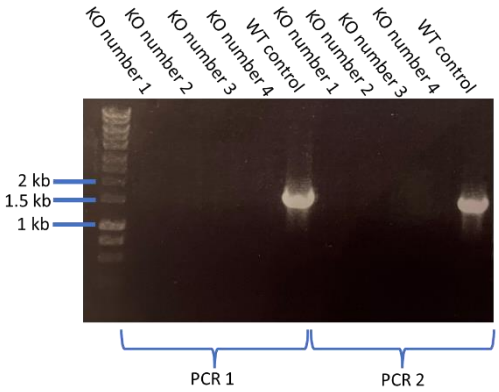
NPY1::*hygB*^{r} (in newly-generated *npy1Δ* cells), replacement of *NPY1* ORF with *hygB*^{r}	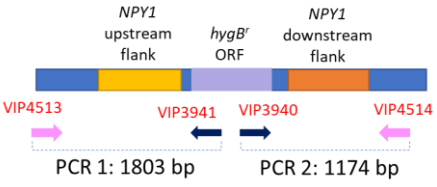	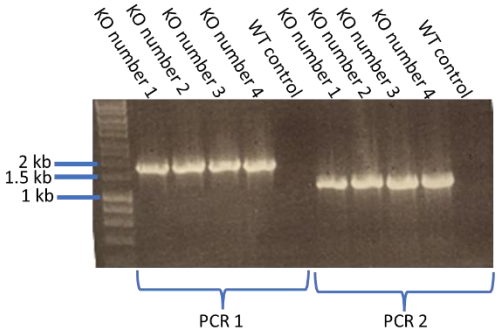
NPY1::*hygB*^{r} (in newly-generated *npy1Δ* cells), absence of *NPY1* ORF	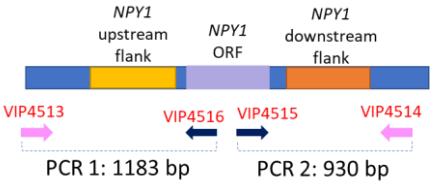	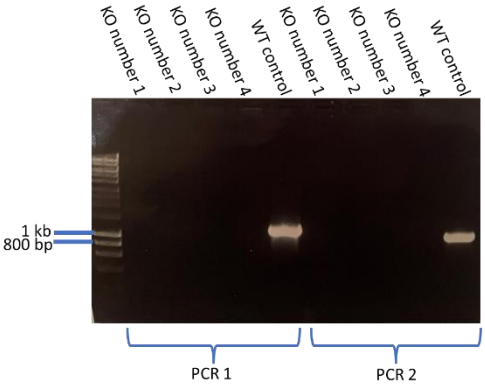

PMP47b::*G418*^{r} (in newly-generated *pmp47bΔ* cells), replacement of *PMP47b* ORF with *G418*^{r}	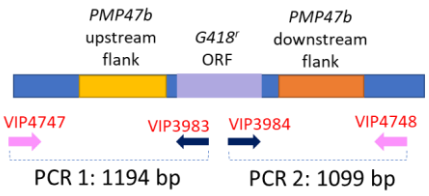	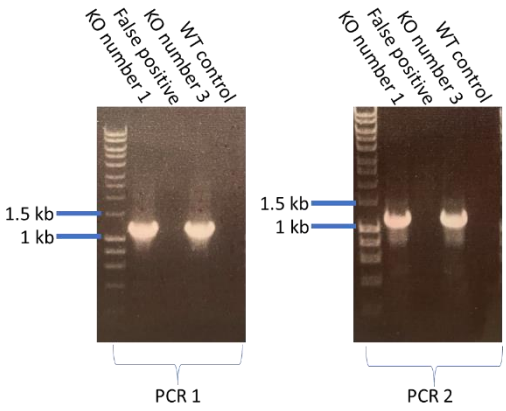
PMP47b::*G418*^{r} (in newly-generated *pmp47bΔ* cells), absence of *PMP47b* ORF	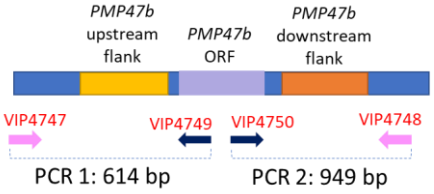	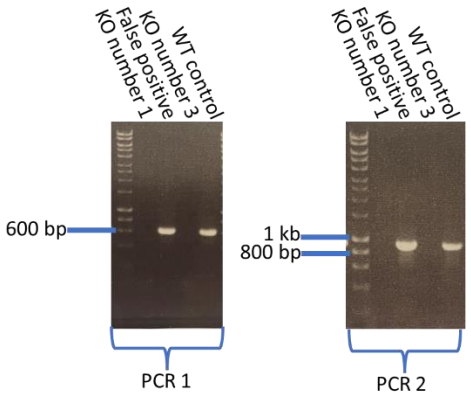
PMP47::*G418*^{r} (in newly-generated *gpd1/mdh3/pmp47Δ* cells), replacement of *PMP47* ORF with *G418*^{r}	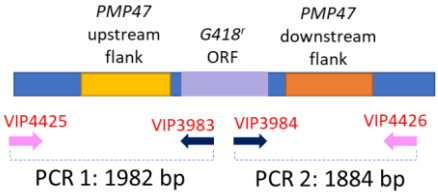	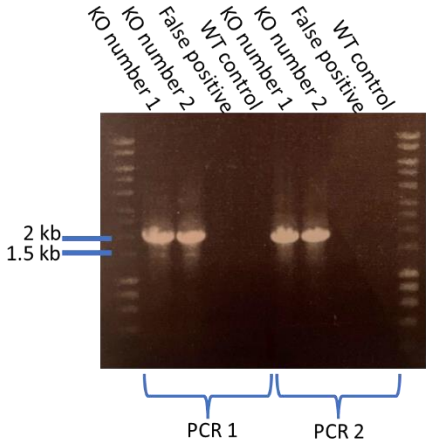
NPY1::*G418*^{r} (in newly-generated *gpd1/mdh3/npy1Δ* cells), replacement of *NPY1* ORF with *G418*^{r}	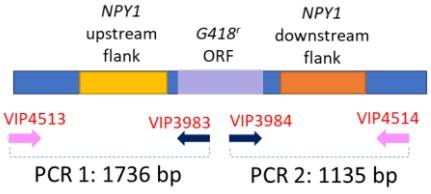	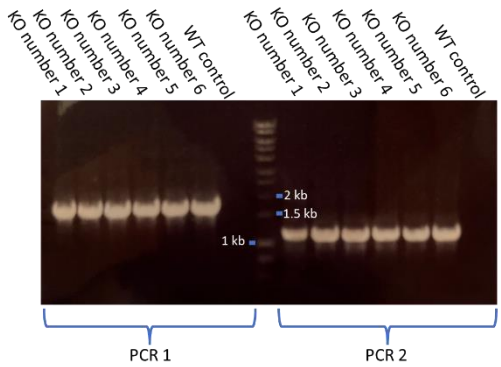

FOX2::hygB^r (in newly-generated *fox2Δ* cells), replacement of *FOX2* ORF *hygB*^{r}	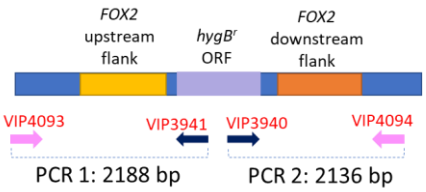	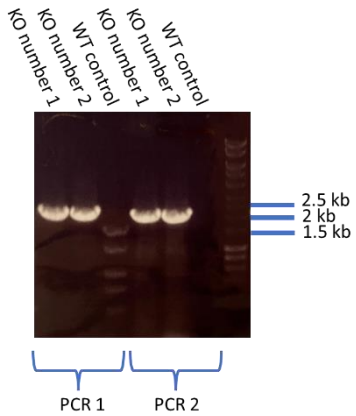
FOX2::hygB^r (in newly-generated *fox2Δ* cells), absence of *FOX2* ORF	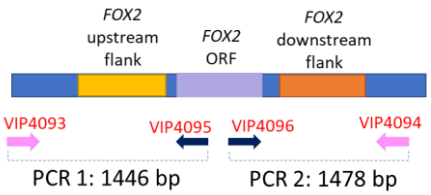	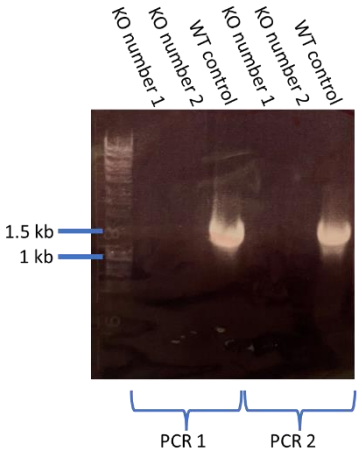

Appendix 5- The PCR verifications that show the integration of the tagging constructs in *D. hansenii* genome. As an example for the integration of the co-localization marker, the integration of the ''mCherry-SKL'' into Mdh3-tagged WT and *pex3Δ* genomes was shown only. The integration of the red marker into the genomes of both Gpd1-tagged and Pmp47-tagged cells were checked and confirmed in the same was as what was shown for Mdh3-tagged cells.

PCR check	Schematic representation & Gel Picture
Integration of ''GFP-*MDH3*'' construct into WT & *pex3Δ* genomes	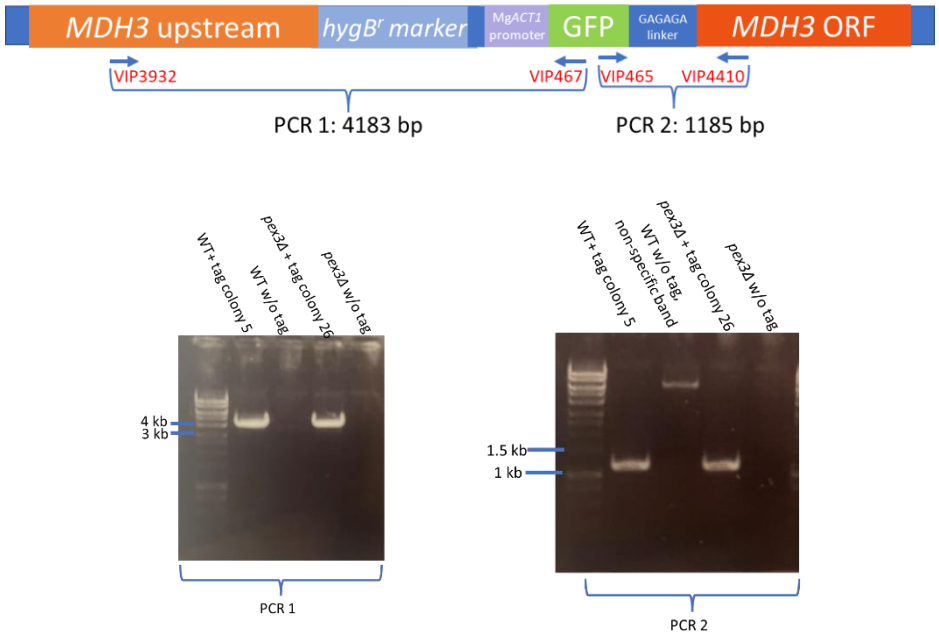
Integration of ''GFP-*NPY1*'' construct into WT & *pex3Δ* genomes	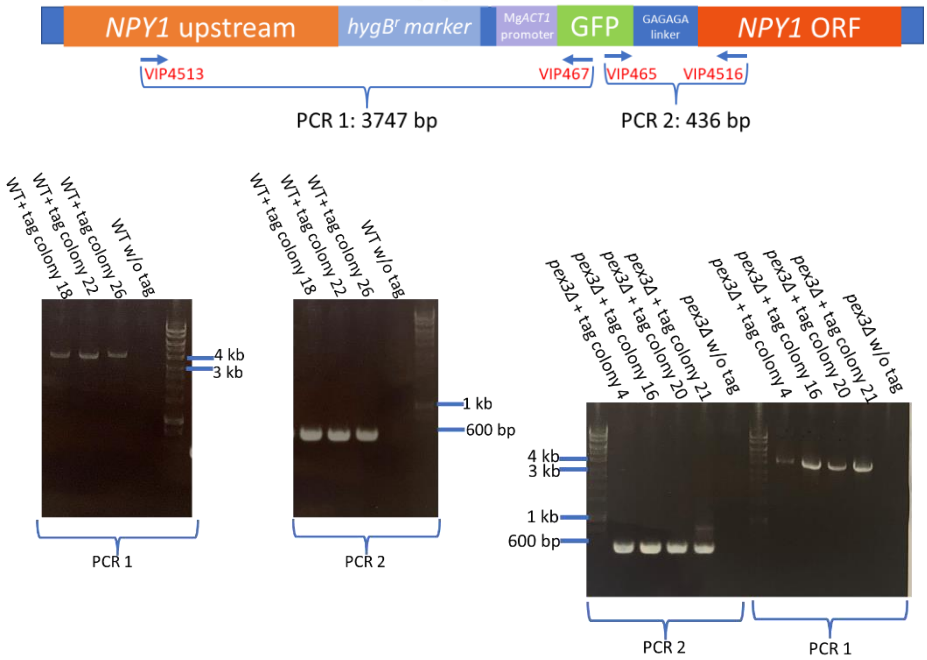

Integration of ''*GPD1*-GFP'' construct into WT & *pex3Δ* genomes	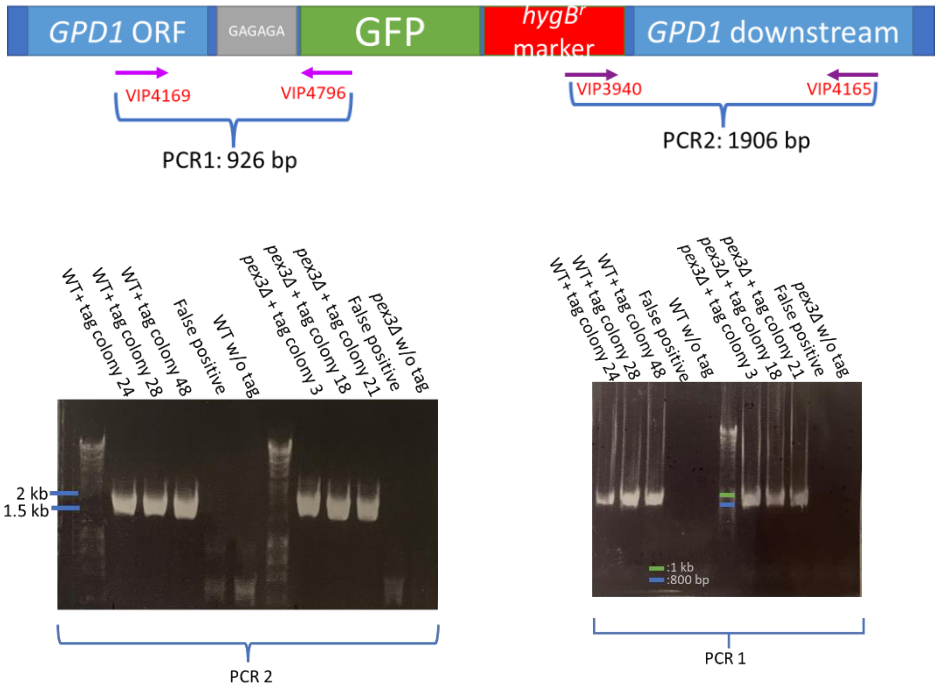
Integration of ''*PMP47*-GFP'' construct into WT genome	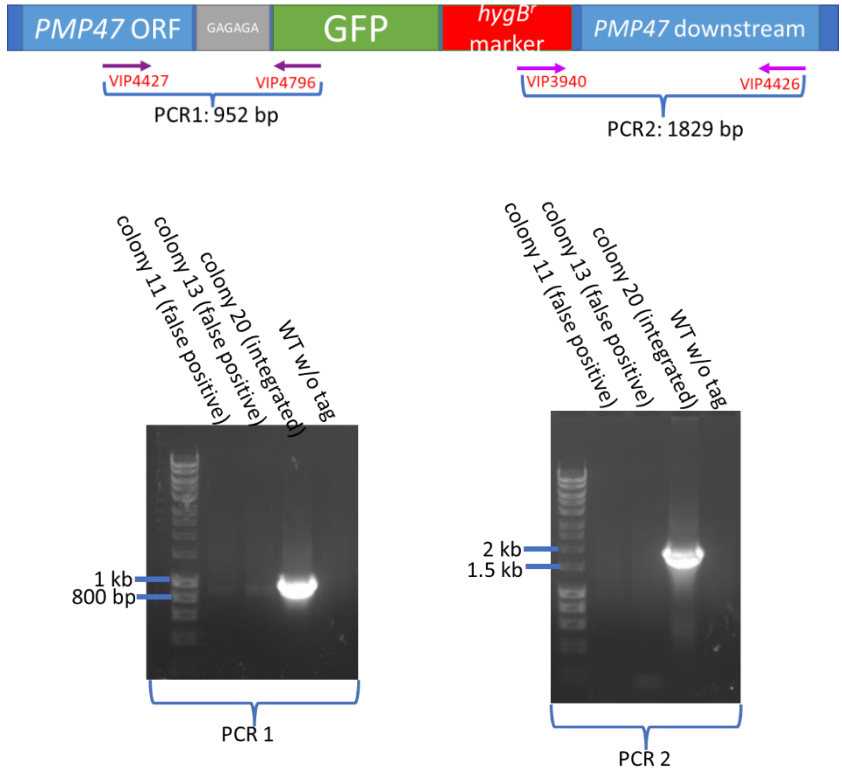

Integration of red marker ''mCherry-SKL'' into Mdh3-tagged WT & *pex3Δ* genomes	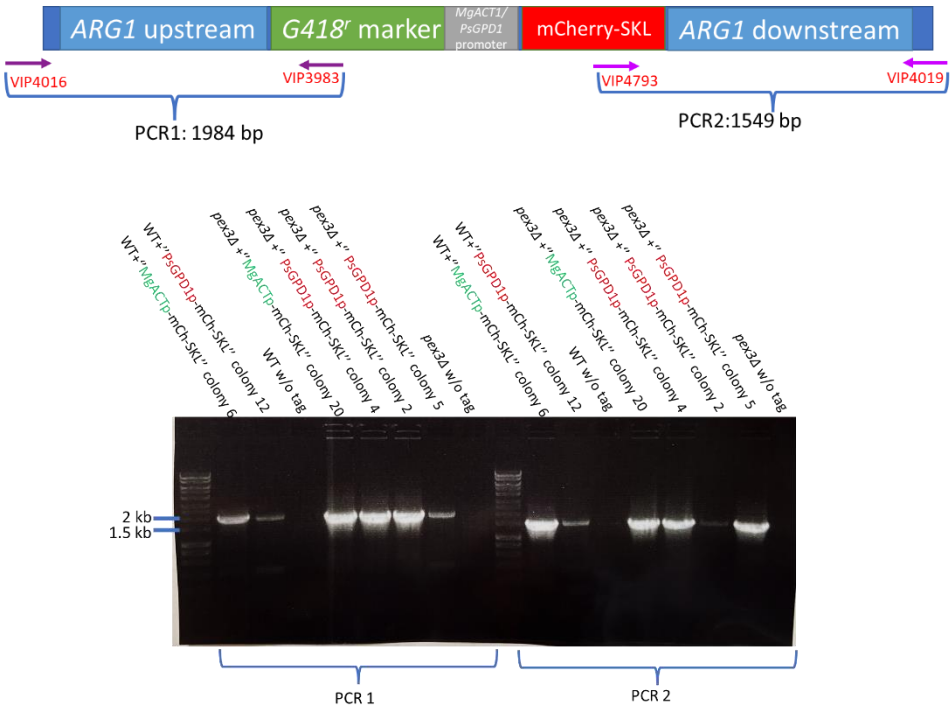

Appendix 6- Annealing sequences of the primers that were used in N-terminal and C-terminal tagging in *D. hansenii*.

Annealing sequence	In Forward/ Reverse primer?	Used for	Anneals to
CGAAGTTATGGAATGATCCAGAGG	Forward	N-terminal tagging of Mdh3 and Npy1	pSA5
TTTGTATAGTTCATCCATGCC	Reverse	N-terminal tagging of Mdh3 and Npy1	pSA5
GAATTCGAGCTCGGTACCCG	Forward	C-terminal tagging of Gpd1	pSLV38
GGATCCGGTGCAGGAGCTGGCGCAGTCGACCTCGAGATG	Forward	C-terminal tagging of Pmp47	pSLV38
CTCTAGAGTCGACCTGCAGG	Reverse	C-terminal tagging of Gpd1	pSLV38
CACCTCAGAAGATAGATTGGG	Reverse	C-terminal tagging of Pmp47	pSLV38

Appendix 7- The growth phenotype of *D. hansenii fox2Δ* cells on oleate and glucose based media. Prior to spotting, the cells were grown overnight in YM2 with 0.3% glucose and diluted in sterile water at OD=0.1 and 10 fold serial diluted 3 times. *pex3Δ* cells were included as a strain that cannot grow on oleate.

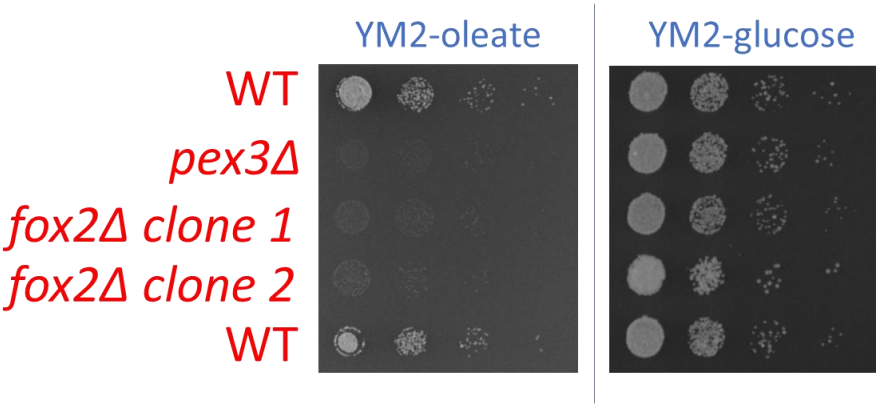

Appendix 8- N-terminal tagging of *Dh*ACAD11n in *S. cerevisiae*, that resulted in peroxisomal localization via PTS1-dependent pathway. The cells were grown logarithmically in minimal glucose media prior to analysis. Each cell wall is highlighted in blue. Scale bar is 5 µm.